AN INVESTIGATION OF THE ROLE OF TISSUE TRANSGLUTAMINASE IN PROGRAMMED CELL DEATH. (APOPTOSIS)

GRAHAM LLOYD THOMAS

A thesis submitted in partial fulfilment of the
requirements of The Nottingham Trent University
for degree of Doctor of Philosophy.

Biochemistry Research, Department of Life Sciences,
The Nottingham Trent University, Nottingham, England

This research programme was
carried out in collaboration with : -

The Samuel Roberts Noble Foundation,
Ardmore, Oklahoma, USA
&
The Noble Center for Biomedical Research,
Oklahoma Medical Research Foundation,
Oklahoma City, Oklahoma, USA

August 1998

Quoted below is a single sentence, written in 1931 by Aldous Huxley (1894 - 1963); it is taken from "Brave New World", and is spoken by "The Director of Hatcheries and Conditioning".

".... a brief description of the modern fertilizing process; spoke first, of course, of its surgical introduction - 'the operation undergone voluntarily for the good of Society, not to mention the fact that it carries a bonus amounting to six months' salary'; continued with some account of the technique for preserving the excised ovary alive and actively developing; passed on to a consideration of optimum temperature, salinity, viscosity; referred to the liquor in which the detached and ripened eggs were kept; and, leading his charges to the work tables, actually showed them how the liquor was drawn off from the test-tubes; how it was let out drop by drop on to the specially warmed slides of the microscopes; how the eggs which it contained were inspected for abnormalities, counted and transferred to a porous receptacle; how (and he now took them to watch the operation) this receptacle was immersed in a warm bouillon containing free-swimming spermatozoa - at a minimum concentration of one hundred thousand per cubic centimetre, he insisted; and how, after ten minutes, the container was lifted out of the liquor and its contents re-examined; how, if any of the eggs remained unfertilized, it was again immersed, and, if necessary, yet again; how the fertilized ova went back to the incubators; where the Alphas and Betas remained until definitely bottled; while the Gammas, Deltas and Epsilons were brought out again, after only thirty-six hours, to undergo Bokanovsky's Process".

For my Parents and Sister, who continually supported me throughout my studies.

Dedicated to

my Mother, Beryl

(6th. February 1933 to 26th. November 1998.)

"You will forever be in my thoughts

and I will miss you dearly.

Love always, Graham."

This thesis is, to the best of my knowledge, original except where due reference is made.

Graham L Thomas / August 1998

Acknowledgements

I would like to express my thanks to the following :-

Professor Martin Griffin, Director of Studies, for having continued confidence in my ability to carry out this work, for his help, advice and support.

Professor Paul Birckbichler, of Oklahoma University, Second Supervisor, for arranging all the details that allowed me to visit his laboratory at The Noble Centre for Biomedical Research part of Oklahoma Medical Research Foundation, Oklahoma, USA. This was a productive time, which I enjoyed tremendously, I would like to thank him for his unending support and friendship.

The Wellcome Trust for awarding me a Prize Studentship and the generous funding of this project.

Professor Trevor Palmer, Dean of the Faculty of Science, Mathematics and Operational Research, Nottingham Trent University, for allowing me to undertake my studies in the department of Life Science.

Dr. Manford K. "Bud" Patterson Jnr., for allowing me to use the facilities of the research laboratories of The Samuel Roberts Noble Foundation, Ardmore, USA. Firstly for making my visit there so enjoyable and secondly for his advice and support.

Mr. Alun Owen, Mr. Eifion Powell and Miss. Julian Jones, my secondary education biology teachers and Mr Keith Bowskill my chemistry teacher, for opening the world of science to me. " Everyone remembers a good teacher!"

All of my friends and colleagues in Nottingham, Ardmore, Oklahoma City and Sheffield, for their support, helpful advice and assistance. Thank you all for making my studies so enjoyable, all the laughter, beers, curries and chocolate. I would especially like to thank you all for listening to all my boring statistical scientific anecdotes.

NOTTINGHAM :- *Allister, Angela, Anne, Annette, Ben, Bernard, Brian, Chez, ClareG, ClareS, Daniel, Dave, Dave "Bill, Buffalo Bill", Debbie, Eli, Ellen, Hannah, Graham, Greg, James, Jane, Janet, Jean, Jill, KerryB, KerryD, Maggie, Mandy, Mark, Megan, Mick, Nigel, Pauline, Pete, PhilBo, PhilBa, Richard, Roger, Ros, Said, Sam, Steve "Ski" & Jo, TimJ, TimW, Tony, Trevor, Vicky & John and "The Plant Peolple".*

ARDMORE :- *Bassam, Becky, BobDO, BobK, Boyd, Bud, Charlie, Charlotte, Chip, David, Derek, Gene, Henry, Herb, Janet, Jay, Jeanie, Julie, Keith, Matt, Merle, Pam, Paul, Robert, Shellby-Sue, Shelly, Sidney, Tom and Yutaka.*

OKLAHOMA CITY :- *Animesh, Anna, Brian, Christie, Jackie, James, Jeff, Jin, Julie, Laura, PJ and Warren.*

SHEFFIELD :- *Abdulgarder, Bin, Chiwoneso, Denise, Eman, Faith, Gerry, Hayley, Helen, John, Julie, Lin, Megiud, Mohammed, Omkalthoun, Ougz, Sharah, Simon, Tarek, Tim, and Toru.*

Lastly, I would like to express my deepest thanks to my Parents, Beryl and Trevor and my Sister, Helen, for all their love and support. **GREY.**

Publications

Lee, K.N., **Thomas, G.L,** Arnold, S.A., Birckbichler, P.J., Patterson, M.K.Jnr., Conway, E., Maxwell, M.D. and Carter, H.A. (1992) Induction of tissue transglutaminase during retinoic acid-induced apoptosis of HT29 human colon cancer cells. Abstract # 1901, Molecular Biology of the Cell (Formerly Cell Regulation) vol. 3, pp 328a.

Thomas, G.L., Griffin, M.J., Henley, A. and Birckbichler, P.J. (1994) Induction of apoptosis and transglutaminase in transformed human lung fibroblasts following sodium butyrate treatment. Abstract. FASEB J., vol 8, No. 7, pp 1356.

Thomas, GL., Henley, A., Rowland, T., Sahai, A., Griffin, M. and Birckbichler, PJ. (1996) Enhanced apoptosis in tansformed human lung fibroblasts after exposure to sodium butyrate. In Vitro Dev. Cell Biol. - Animal 32 : 505-513.

CONTENTS

Abbreviations.

BHK-21	- baby Hamster kidney fibroblasts clone 21
CUB 74	- monoclonal antibody CUB 7402 raised to tTGase
CUB 11	- IgG γ 1 isotype control for CUB 74
DAB	- diaminobenzidine
DMEM	- Dulbecco's modified Earle's medium
DMSO	- dimethylsulphoxide
DNA	- deoxyribonucleic acid
DNAse I	- deoxyribonuclease I
DTT	- dithiothreitol
ECV304	- Human trachea endothelial cell line
EDTA	- ethylene diamine tetra acetic acid
EGTA	- ethylene glycol-bis(ß-aminoethyl ether) N,N,N',N'-tetra acetic acid
HEPES	- N-2-hydroxyethylpiperazine-N'-2-ethane sulphonic acid
HPLC	- high performance liquid chromatography
HRP	- horse-radish peroxidase
HT29	- Human epithelial colon carcinoma cell line
Mc.Coy's	- Mc.Coy's 5A tissue culture medium
MET B	- metastatic Hamster fibrosarcoma cell line
MET D	- metastatic Hamster fibrosarcoma cell line
MET E	- metastatic Hamster fibrosarcoma cell line
NaB	- n-butyric acid monosodium salt (sodium butyrate)
PAGE	- polyacrylamide gel electrophoresis
PARENT	- Parent cell line from which MET variants were cloned
PBS	- phosphate buffered saline
PMSF	- phenylmethylsulphonylfluoride
RA	- all trans retinoic acid
SDS	- sodium dodecyl sulphate
SV40	- simian virus 40
tTGase	- tissue transglutaminase
TGase	- transglutaminase
TBS	- TRIS buffered saline
TCA	- trichloroacetic acid
TEMED	- N,N,N',N'-tetramethylethylenediamine
TMB	- 3,3,5,5-tetramethyl benzidine
TRIS	- Tris(hydroxymethyl) aminomethane
tTGase	- tissue transglutaminase
WI38	- embryonic human lung cells
VA13a -	- SV40 transformed WI38

List of Plates.

List of Figures.

List of Tables.

The Role of Tissue Transglutaminase In Programmed Cell Death -Apoptosis.
Doctor of Philosophy Degree by Graham Lloyd Thomas

Abstract

The purpose of this study was to investigate the role of the tissue type II transglutaminase (tTGase) enzyme, (E.C. 2.3.2.13) in programmed cell death (apoptosis). tTGase is a member of a large family of enzymes which catalyse an irreversible crosslinking reaction between proteins, forming large insoluble polymeric complexes. Apoptosis is a form of cell death that is opposite to necrosis. Often referred to as "cell suicide", the cells shrink and break up forming small bodies which are the removed from healthy tissues by phagocytosis, with no resultant damaging immunological responses, as in necrosis. As homeostasis is maintained at all times during the apoptotic event it is thought to be a programmed or physiological form of cell death. Two, unique, polyclonal antisera, were raised against transglutaminase-mediated protein structures rich in the catalysis product of the ε (γ-glutamyl) lysine isodipeptide : i) a high molecular weight sodium dodecyl sulphate (SDS) / insoluble polymer and ii) the SDS / insoluble "apoptotic envelope".

Hepatocellular carcinomas, formed by induction-feeding with 2-acetylaminofluorene (2-AAF) in the diet of rats, when examined were found to contain time-dependent increasing amounts of both of the tTGase-mediated antigens. Conversely, three metastatic variants of a Hamster fibrosarcoma cell-line when resected *in vivo* produced tumour masses which showed both a decrease in tTGase catalytic activity and amounts of both tTGase-mediated antigens. This difference was concluded to be due to a cell type dilution effect, caused by the heterogenous hypercellularity found in the hepatocellular carcinoma.

In vitro studies showed that tTGase activity and antigen could be induced in a time- and dose-dependent manner in two neoplastic cell-lines, WI38 VA13a (an SV40 transformed Human lung fibroblast) and HT29 (an endothelial cell isolated from an Human colon carcinoma) by treatment with sodium butyrate (NaB, 1 - 5 mM over 1 - 5 days) and all-trans retinoic acid (R.A., 10 - 50 μM over 1 - 5 days) respectively. Detectable levels of apoptosis, shown by SDS-isolation and counting ELISA quantitation of "apoptotic envelopes" in both *in vitro* models did not match the increase in tTGase enzymatic induction. Furthermore, it was shown that NaB altered the normal cell cycle of WI38 VA13a to produce an anueploid sub-population of cells which evaded both mitosis and apoptosis. Morphological examination by confocal laser microscopy, showed the presence of small "apoptotic" light-refractive bodies (ARB's) in the HT29 / R.A. model. Characterisation of the ARB's by Normarski phase contrast microscopy showed them to be wholly intracellular fractions of the intact apoptotic cells. Numbers of apoptotic cells in both *in vitro* models was seen to be independent of the corresponding induction of tTGase. Finally, using a novel cell permeabilisation assay system, applied to the two tTGase induction models in WI38 VA13a and HT29, and to a third system on the Human umbilical vein cloned endothelial cell-line ECV 304, it was shown *in situ* that via the catalytic action of tTGase the biotinylated polyamine cadaverine can be specifically incorporated into a 42 KDa amine acceptor substrate. This acceptor protein was believed to be an essential extracellular matrix protein substrate of tTGase, crosslinked during the apoptotic event. Attempts were made to isolate and characterise this protein but amino acid sequence data could not be obtained.

The data in this thesis have shown that apoptosis can occur independently of tTGase activity; tTGase is therefore not an essential trigger for apoptosis initiation. However, tTGase has been shown to alter the biophysical nature of the apoptotic cell playing a fundamental role in formation of irreversible protein polymers in the apoptotic cell *in vivo* and stabilisation of the apoptotic envelope *in vitro*, via crosslinking of substrate proteins in the extracellular matrix.

1.0

Introduction.

1.1 Transglutaminases

Transglutaminases are a family of enzymes which catalyse post-translational modifications of proteins by transamidation of available glutamine residues. Transglutaminase-catalysed isopeptide crosslinks introduced into the protein are of great physiological importance; they are exceptionally stable and can be broken only by the total degradation of the two peptide chains. Transamidations (amine - γ- glutamyl transferase reaction) are reactions that lead to the formation of covalent; proteolysis resistant and degradation stable bonds, either within or between polypeptide chains. First reported during the 1950's by Sarkar *et al* (1957) who identified a guinea pig liver enzyme with transamidating activity. They proved that the activity of this enzyme was calcium dependent, as measured by the ability of the enzyme to catalyse the incorporation of a primary aliphatic amine into a substrate protein (Sarkar *et al* 1957, Clarke *et al* 1957, Niedle *et al* 1958, Clarke *et al* 1959, Mycek *et al* 1959).

The action of these enzymes results then in the formation of " irreversibly " crosslinked, often insoluble supramolecular structures. To date an enzyme specific for the cleavage of the transglutaminase-mediated crosslink product in proteins has not been isolated, however Baskova and her group working in Russia have claimed to isolate such an enzyme, "Destabilase" isolated from the saliva of the leech. Though, a degree of controversy surrounds this discovery, including the possibility that Destabilase is in fact a competitor inhibitor of transglutaminase and not cleavage enzyme. Therefore, the isodipeptide bond once formed is currently regarded as "irreversible".

In vertebrates, transglutaminases form a large protein family and have a widespread distribution in tissues and body fluids. Examples where the product has been derived via transglutaminase-mediated reactions are : fibrin clot formation during haemostats and wound healing; within the cell membrane of terminally differentiated erythrocytes; in extracellular matrices and in the cornified keratinocyte envelope of the epidermis.

Transglutaminases are well conserved within the genome and enzymes homologus to vertebrate transglutaminase have been found in invertebrates, plants, unicellular eukaryotes and in bacteria. While the physiological roles of the various isotypes of transglutaminase are not well understood, its catalytic reaction has been studied in detail. With distinct characteristics of the catalysis reaction of transglutaminase now being elucidated, the following criteria of this enzyme family could begin to be noted.

1.2 Definition of the catalytic reaction.

Enzymatic activity must be calcium dependent with an active site thiol; thus activity may be inhibited by divalent cation chelating agents or by thiol reactive compounds e.g. EDTA or iodoacetamide. A cysteine residue at position 277 in the active site is essential for catalytic activity (Lee *et al* 1993), the calcium is believed to help alignment at this position (Lee *et al* 1993, Wong *et al* 1991). The catalysis reaction is an acyl transfer between peptide bound glutamine residues and primary amine groups, This results in the post-translational modification of proteins, by either the specific incorporation of amines; or if the amine is the ε-amino group of protein bound lysine the formation of an isodipeptide crosslink ε(γ-

Glutamyl) lysine crosslink. The systematic name as given by the Enzyme Commission being, R-glutaminyl peptide: amine-γ-glutamyl transferases (E.C. 2.3.2.13).

The reaction is a multistep process, in which the active site cysteine reacts first with the g-carboxamide-group of a glutamine residue to form the acyl-enzyme intermediate with the release of ammonia. In a second step. the complex reacts with a primary amine to form an isopeptide bond and liberate the reactivated enzyme. The driving force for the reaction is supplied by the release of ammonia and its subsequent protonation, occurring readily under physiological conditions. The amine incorporation proceeds with a Michaelis-Menten type of saturation kinetics and should be strictly regarded as reversible.

transglutaminases also exhibit catalytic activity towards certain esters such as p-nitrophenyl-acetate and catalyse their hydrolysis by reaction with H_2O, at least under *in vitro* conditions (Folk *et al* 1967, 1977). However, reaction of H_2O or alcohols with the acyl-enzyme intermediate clearly occurs at a much slower rate than with primary amines.

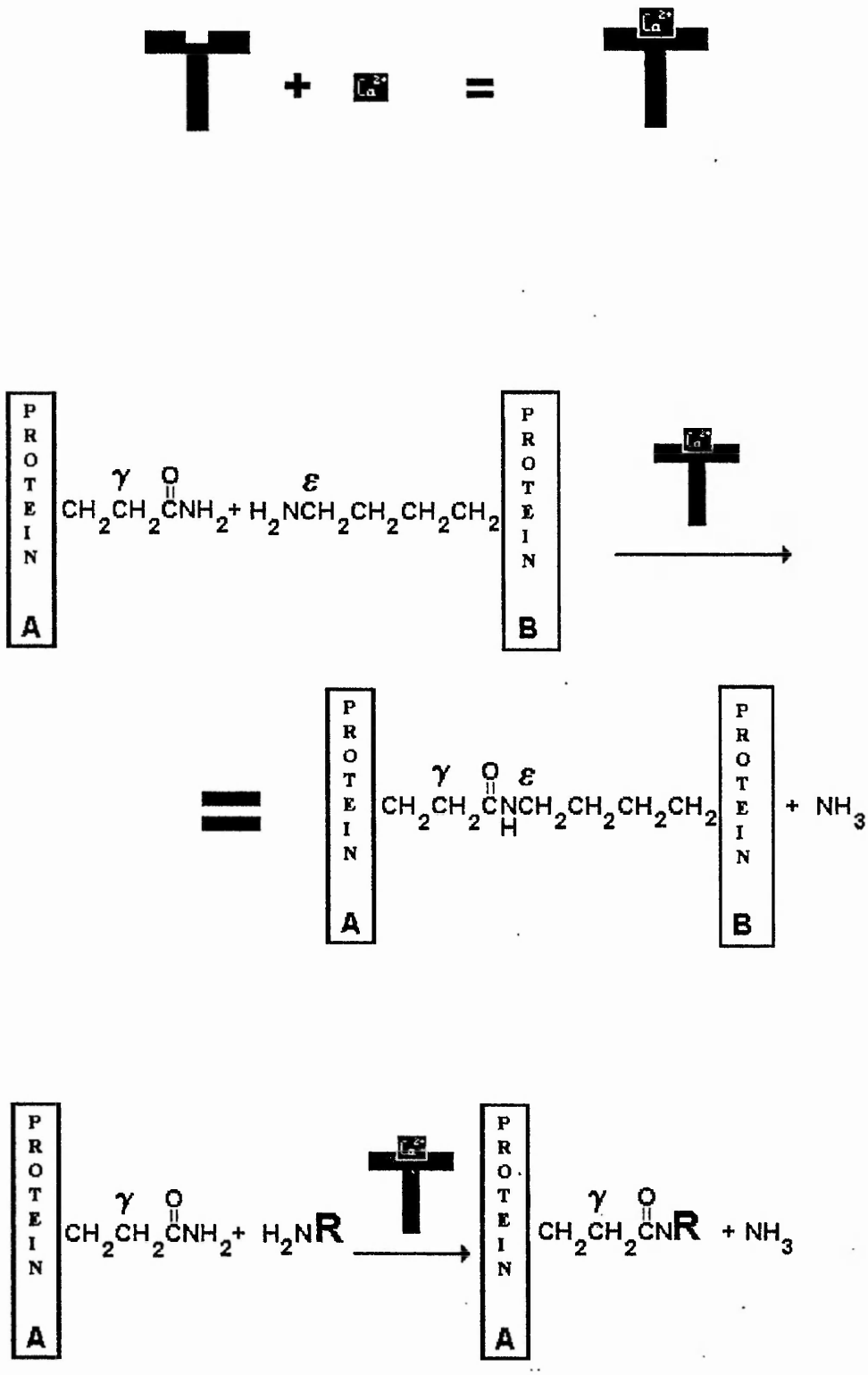

Protein (glutamine) γ (glutamyl) - R isopeptide

Figure 1.1 Schematic of Transglutaminase Catalytic reactions.

Different tissues and cell types express varying amounts of tTGase. For example using monoclonal antibodies specific to regions of the transglutaminase molecule, the constitutive expression of the enzyme protein has been detected in arteries, veins and capillaries. Several organ-specific cell types such as mesangial cells, reno-medullary intestinal cells and clonic pericryptal fibroblasts have been shown to express tTGase immunoreactivity (Aeschilmann and Paulson 1994). In the liver, the enzyme reactivity occurs along the border of the sinusoidal membrane, attributable to the expression by the sinusoidal endothelium. varying levels of transglutaminase mRNA have been observed in the lung, heart, kidney, liver, spleen and testes; whereas no detectable transcript has been detected in the brain or thymus (Aeschilmann and Paulson 1994). The figure below shows the structural and functional domains of the tTGase gene.

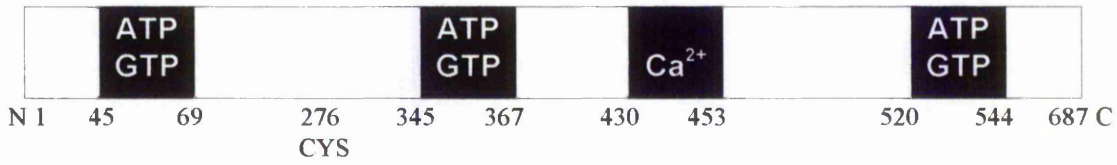

Figure 1.2 The Structural and functional; domains of the tTGase gene.

Tissue transglutaminase of human, bovine, mouse, guinea pig and chicken have been cloned and revealed good homology among species (88% from bovine to 65% from chicken) Aeschilmann and Paulson 1994. The enzyme from different species contains 685-691 amino acids with which encodes mRNA of 3.6 - 3.9kb and translated into for proteins of between 77-85 KDa molecular mass. The human tTGase gene has been mapped onto chromosome 20, within the band 20q12 (Gentile *et al* 1994). Though, there are potentially 6 N-linked glycosylation sites and 17 cysteine residues; the enzyme protein is neither gylcosylated or

contains disulphide linkages. The active cysteine residue is located at position 276 (Lee *et al* 1992) Although free nucleotide GTP has been shown to bind and inhibit tTGase activity, these regions are not homologus to GTP-binding proteins (Lee *et al* 1989). Similarly, the glutamine rich regions near amino acids 450 and 470 identified as potential Ca^{2+} biding sites have not been proven. Even, though the enzyme requires Ca^{2+} for its catalytic activity.

The number of proteins acting as glutaminyl substrates is restricted, as both primary-structure, (including charge) and conformation determine whether a glutamine residue is reactive or not (Folk *et al* 1977, Gorman and Folk 1981, Gorman and Folk 1984, Aeschilmann *et al* 1992). In contrast. the tolerance to structural differences in acyl-acceptors is considerable with preference for branched chain aliphatic amines with a methylene chain equal in length to the side chain of a lysine residue (Folk *et al* 1977, Lorand and Conrad 1984). Amino acid residues adjacent to the lysine do not have a pronounced influence on the substrate properties. Which explains why protein bound lysine residues and small primary amines serve equally well as amine donors. Thus. in a particular tissue only a small subset of proteins are glutaminyl substrates for the enzyme, whereas most proteins are able to contribute ε-amino groups of lysine residues to serve as acyl acceptors in the crosslinking reaction. Furthermore, the specificity for different glutaminyl substrates differs between transglutaminases, as shown by the structural difference in fibrin polymers formed by the action of tTGase and factor XIIIa (Shainoff *et al* 1991) and by the different affinities for amine incorporation by these enzymes into synthetic peptide variants of the amine acceptor site in β-casein (Gorman and Folk 1984). Distinct transglutaminases may recognise the same protein as substrate, but often with different affinity and / or with specificity for different glutamine residues.

1.3 Different types of Transglutaminases.

Identified now in mammalian, invertebrate, bacterial and plant systems the wide distribution of transglutaminases (Table 1.1) clearly show the diversity of its functions (Chung 1975, Mehta 1990, Nonaka 1992). Found both extra- and intra- cellular. For the purposes of the thesis I will concentrate on the mammalian forms.

1.3.1 Extracellular Transglutaminases.

1.3.1.1 Blood Plasma FactorXIIIa.

Plasma factor XIIIa, identified by Lorand *et al* in 1968, now known to be found in placenta, uterus, granulocytes, macrophages, megakaryocytes and monocytes. The enzyme plays an important role in the blood clotting cascade; by stabilising the fibrin clot. Unlike many other transglutaminases, plasma transglutaminase is an inactive zymogenic proenzyme; which needs to be activated by thrombin (FXIII converted to FXIIIa). In plasma, it is a tetrameter composed of two filamentous b-subunits and a dimer of non-covalently associated a-subunits and when occurring intracellularly, a dimer of only the a-subunit. It is the a-subunit which is cleaved during thrombin activation. The mature protein has a molecular mass of 83KDa (Takahashi *et al* 1986), the active site cysteine has been identified at position 314 (Ichinose *et al* 1986). The cDNA sequence does not contain a typical hydrophobic leader sequence for secretion; and is therefore an example of a typical cytoplasmic protein. Platelets, peripheral blood monocytes and the liver have been suggested as sites of Factor XIII synthesis (Weisberg *et al* 1987, Poon *et al* 1989)

Table 1.1 Different types of transglutaminase enzymes.

Descriptive Transglutaminase Name	*Alternative Names and Abbreviations*
EXTRACELLULAR	
Plasma	Factor XIII(a), fibrin stabilising factor, Laki-Lorand factor, fibrinoligase
Prostate	Seminal transglutaminase, dorsal prostate protein 1, major androgen-regulated secretory protein , vesiculase, TG_P
Erythrocyte Band 4.2	Erythrocyte membrane protein band 4.2
INTRACELLULAR	
Keratinocyte	Particulate-transglutaminase, transglutaminase type I, TG_K
Tissue	Cytosolic-, endothelial-, erythrocyte-, liver-transglutaminase, tTGase, , tissue transglutaminase analogues isolated from zebrafish and red sea bream, transglutaminase type II, TG_C
Epidermal	Bovine snout-, callus-, hair follicle-transglutaminase , transglutaminase type III, TG_E
NON-MAMMALIAN	
Hemocyte	*Limulus* transglutaminase, invertebrate analogous to factor XIII, TG_H
Invertebrate	Transglutaminase from filarial nematode *Brugia malayi, extracts of leech saliva analogous to both factor XIII and tTGase, Annulin analogue of keratinocyte transglutaminase*
Bacterial	Transglutaminase isolated from *Streptoverticillium sp.*
Plant	Non-calcium dependant transglutaminase isolated from plants during pollen grain emission and chloroplast proteins

After Aeschilmann and Paulsson (1996)

The sequence analysis of the b-subunit has shown it to be composed of 641 amino acids containing 8.5 % carbohydrate (Ichinose *et al* 1990). This gives a final molecular mass of 80KDa, this gene encodes a 20 amino acid leader sequence common to conventional secretory proteins.

1.3.1.2 Prostate / Seminal Transglutaminase.

Found in seminal plasma, this enzyme is involved in the formation of the nasal plug during parturition and the rodent copulatory plug; there are now thought to be two isotypes (Williams-Ashman *et al* 1979). Reported to be an homodimeric protein of 150KDa made of monomers each 71KDa as proved by SDS-PAGE (Wilson and French 1980, Ho *et al* 1992). Sequencing of cDNA clones encoding rat plasma TGase calculated a protein of 668 amino acids. However, this sequence was found to be N-terminally blocked, a typical feature of intracellular proteins. Its sequence contains a number of mannerly residues and a phosphatidylinositol anchor. Plasma TGase has been found absent from the ER and Golgi apparatus, suggesting that secretion does not occur via the usual mechanism. Moreover, it has been found in apocrine secretory vesicles that are pinched off from the plasma membrane into to the lumen where the contents are released following rupture; for this to occur the mature protein probably enters the vesicles directly from the cytoplasm (Seitz *et al* 1990, 1991)

1.3.2 Intracellular Transglutaminases.

1.3.2.1 Keratinocyte transglutaminase (Type I).

Required to cause skin protective calus and other protein crosslinked bonds in skin, hair and nails. Implicated in the formation of the cornified envelope during the terminal differentiation of keratinocytes (Rice and Green 1979). Cloning of keratinocyte

transglutaminase from both human and rat epidermal keratinocytes has identified two proteins with 92% sequence homology. The sequences encode for a protein 89-90KDa (Phillips *et al* 1990, Kim *et al* 1993). Peripherally associated with the cytoplasmic side of the plasma membrane through fatty acid acylation and thiolester linkages to plamitic and myristic acids. Anchorage has been conferred by a series of 5 cysteine residues at the n-terminus (Rice *et al* 1990, Kim *et al* 1993). During terminal differentiation of the keratinocyte *in vivo* proteolytic processing of this anchorage region results in a soluble form of the enzyme being created. Also found in the anchorage region of the molecule are a series of serine and arginine containing motifs similar to phosphorylation site of protein kinase C (Phillips *et al* 1990, Rice *et al* 1990). Phosphorylation might regulate the activity of the membrane bound enzyme via restricting substrate specificity.

1.3.2.2 Cellular/tissue transglutaminase (Type II).

Both cytosolic and membrane-bound forms of the enzyme have been found (Sarkar *et al* 1957, Chung 1972, Lorand and Stenberg 1976, Hand *et al* 1988, Griffin *et al* 1989). No specific function for this enzyme has yet been established; though the following have been reported. Transglutaminase involvement in erythrocyte rigidity (Lorand 1988) has been demonstrated and the enzyme has been implicated in control of growth and malignancy (Birckbichler *et al* 1976, 1977, 1978, Hand *et al* 1990), immunological activation (Leu *et al* 1982, Schroff *et al* 1981), and receptor-mediated endocytosis (Davies *et al* 1980). We have reported that tissue transglutaminase was low in malignant tissues and a variety of cells maintained in cell culture following viral or chemical transformation (Birckbichler *et al* 1976, 1977). An inverse relationship exists between metastatic spread and the level of tissue transglutaminase activity (Hand *et al* 1987). The enzyme has also been linked to non-

proliferative diseases, e.g., Alzheimer's disease (Selkoe *et al* 1982) and cataracts (Lorand 1988).

Early work by Bergamini *et al* in 1988 showed that binding of the nucleotide GTP to transglutaminase reduced the affinity of the enzyme to bind calcium resulting in conformational change of the enzyme structure. Lee *et al* in 1989 further showed the hydrolysis of GTP by guinea pig liver transglutaminase; indicating the second function of the enzyme of GTPase activity as well as the established crosslinking properties. This work has recently been confirmed by Nakaoka *et al* in 1994 reporting the existence of a GTP-binding protein with both transglutaminase activity and receptor signalling function. This new finding of receptor signalling ability of a transglutaminase has many implications in finally establishing a definitive function for the enzyme.

A further role of transglutaminase, is in the process of programmed cell death (apoptosis) (Schwartzman and Cidlowski 1993, Fesus *et al* 1987, 1989, Knight *et al* 1991, Piacentini *et al* 1991). Cells undergoing late stage apoptosis are stabilised by envelope formation through transglutaminase-mediated crosslinking and formation of the apoptotic envelope (Fesus *et al* 1987, 1989). It is this role of transglutaminase se in apoptosis which will be studied in this thesis.

Molecular cloning of tTGase of human (Gentile *et al* 1991), bovine (Nakanishi *et al* 1991), mouse (Gentile *et al* 1991), guinea pig (Ikura *et al* 1988) and chicken (Weraatchakul-Boonmark *et al* 1992) origin revealed a polypeptide of 685 691 amino acids with a molecular mass 77 KDa. The conservation between species is moderate 88% from bovine, 84% from mouse, 80% from guinea pig and 55% from chicken to human. The active site has been shown to involve cysteine 277 in the guinea pig enzyme (Ikura *et al* 1988, Folk

and Cole 1966, Lee *et al* 1992). The protein is not glycosylated (Folk *et al* 1977) nor disulphide bonded (Folk and Cole 1966, Boothe and Folk 1969), although it contains 17 cysteine residues and 5 potential sites for N-linked g1ycosylation. Consistent with these findings, tTGase lacks a hydrophobic leader sequence found in secreted proteins and the NH_2-terminus of tTGase is blocked by removal of the initiator methionine and subsequent acetylation of the penultimate alanine residue (Ikura *et al* 1989). The N^{α} acetyl group does not influence the catalytic activity of the enzyme (Ikura *et al* 1990) and might therefore have a different function. It has recently been suggested that N-acylation is a signal for "alternative" secretion of proteins (Muesch *et al* 1990). There is evidence for externalisation of tTGase in a variety of tissues (Aeschilmann *et al* 1991, 1993, Barsigian *et al* 1991, Kojima *et al* 1993) and this is likely to occur via an "alternative" secretory pathway.

A single transcript of 3.6-3.9 kb has been observed in varying amounts in different tissues: lung, heart, kidney, red blood cells, liver, spleen, testes; whereas it could not be detected in brain and thymus (Gentile *et al* 1991,Nakanishi *et al* 1991).

However, the relative amount of protein in these tissues differs from the mRNA levels, and the protein is most abundant in liver and spleen, followed by heart, kidney and lung (36). Relative specific activity (as % of activity in liver at 100%) in these tissues being - heart 32.2%, kidney 25.0%, lung 34.1% and spleen 51.8% (Aeschilmann and Paulsson 1996). It appears that tTGase expression in different tissues is regulated therefore, not only by transcription but also at the translational level or by the rate of protein turnover.

1.3.2.3 Epidermal hair follicle transglutaminase (Type III).

Abundant in the hair follicle of mammals; it is involved in the stabilisation of the hair fibre into the follicle pit (Peterson and Wuepper 1984). Epidermal transglutaminase is a proenzyme that requires proteolytic activation for catalytic activity; it is the least understood of the transglutaminase family on enzymes. The primary structure has recently established by cDNA cloning from human and mouse epidermis, this revealed a protein of 692 amino acids with a molecular mass of 77KDa. Homology of the sequence between mouse and human form is approximately 75%, which seems rather low (Kim *et al* 1993)

1.4 Programmed Cell Death -Apoptosis.

There are two distinct forms of cell death, necrosis and apoptosis (programmed cell death, PCD) (Kerr *et al* 1972, Wyllie *et al* 1980, Wyllie 1980, Wyllie 1981, Ellis *et al* 1986, Fesus *et al* 1987, 1989, Compton *et al* 1988, Mc Conkey *et al* 1989, Mc Conkey *et al* 1990, Knight *et al* 1991, Piacentini *et al* 1991, Schwartzman and Cidlowski 1993). Necrosis is the classical form of cell death (Summarised in Figure 1.1). It is induced by cytotoxic agents, thermal shock, oxygen debt or mechanical damage. Swelling of mitochondria, nuclear flocculation and dilation of the endoplasmic reticulum are observed. The cell usually dies due to membrane leakage and activation of intracellular enzymes (lysosymes and phospholipases). Once the cell membrane integrity has been compromised, its contents start to leak out and the fine intracellular homeostasis is lost. Metabolic reactions including ATP synthesis and production of membrane potentials no longer occur, the leaking contents of the cell begin to attack neighbouring cells . A localised and prolonged immune response is initiated, via the action of histamines, cytokines and prostaglandins (Fesus *et al* 1989).

Conversely if a cell dies by undergoing apoptosis, damage to the cell membrane is not observed. Those features of apoptosis that are now commonly used to characterise its process are : -Firstly, the apoptosing cell begins to shrink and separate from the neighbouring cells. The linker DNA (DNA that separates the histone chain beads of the double helix) is digested by the cells' endonuclease enzymes. This results in the internucleosomal cleavage of DNA, into nucleotides of 180 base pairs as seen by DNA "ladders" on agarose gel electrophoresis (Kerr *et al* 1972). Recent work by Peitsch *et al* in 1993 has characterised the endonuclease involved in apoptosis to be identical to the Ca^{2+} and Mg^{2+} dependent, DNAse I abundant in mammalian cells.

The inherent cell density of the apoptotic cells increase as the cell continues to shrink, nuclear chromatin condenses around the edge of the nucleus. The cell now has a characteristic pyknotic nucleus, (fragmented into many parts), the cell begins to break-up into small self-contained apoptotic bodies/envelopes. Glycoprotein receptors are believed to be expressed on the surface of these apoptotic cell bodies; which signal to neighbouring cells that this now "suicidal" cell is ready to be removed from the system by phagocytosis (Wyllie *et al* 1980, Wyllie 1980, Savill *et al* 1993). Throughout this process the integrity of the cell membrane is maintained, thus avoiding the loss of intracellular contents as observed in necrosis; resulting in the removal of the cell without the need for an immune response. Apoptosis is an energy requiring process which needs the expression of several genes- the so called "Death Genes" (Ellis and Horvitz 1986, Buttyan *et al* 1989, Buttyan *et al* 1988, Yuh *et al* 1989, Hockenberry *et al* 1990, 1991, Rubin *et al* 1991, Sentman *et al* 1991, Younish-Rouach *et al* 1991). Occurring at pre-determined point in the cells' proliferative cycle, the initiating signal for apoptosis is not understood.

Figure 1.3 Schematic summary of necrosis and apoptosis. (1) normal resting cell with sparse cytoplasm and heterogeneous nuclear chromatin. Cell volume normal. (2) Apoptosis - the cell has lost some volume and the cytoplasmic organelles are becoming tightly packed. There is clumping of the nuclear chromatin around the nuclear envelope. Membrane changes that can lead to phagocytosis are already present. (3) The cell shows definite signs of membrane blebbing in to apoptotic bodies. The chromatin has collapsed down in to crescents along the nuclear envelope. Cell volume is now markedly reduced. The nucleus has collapsed and apoptotic bodies are being formed of parts of the collapsed nucleus DNA and membrane fragments which are highly cross-linked. (4) the apoptotic bodies and the very small cell remnant are phagpcytosed. All the way through this process the membrane integrity has been preserved and no localised immune response is observed. (5) Necrosis - Focal chromatin margination. Mild mitochondrial swelling. rupture of cell membrane as the cell swells. (6) total loss of membrane integrity, cell contents lost localised immune response observed. High amplitude mitochondrial swelling, loss of organelle, rupture of endoplasmic reticulum nucleus and cell is destroyed..

Table 1.2 Differences between Necrosis and Apoptosis.

NECROSIS	*APOPTOSIS*
- Affects groups of cells	- Affects single cells
- Induced by cellular insult and trauma	- Probably induced by specific intracellular or endogenous signals
- Dilation of the E.R. - Swelling of mitochondria - Flocculation of nuclear chromatin	- Cell shrinkage by loss of water - Mitochondria, organelles and plasma membranes remain intact (in early stages): the nucleus begins to swell
Non-specific cleavage of DNA	- Specific cleavage of DNA by endonuclease activity leading to the typical DNA ladders
- Inflammatory response induced	- Cell fragmentation, crosslinked structures forming apoptotic envelopes are seen.
- Effect on neighbouring cells by release of destructive intracellular enzymes into the extracellular fluid.	- Phagocytosis by neighbouring cells and/or wandering macrophages, with no adverse effect on these cells

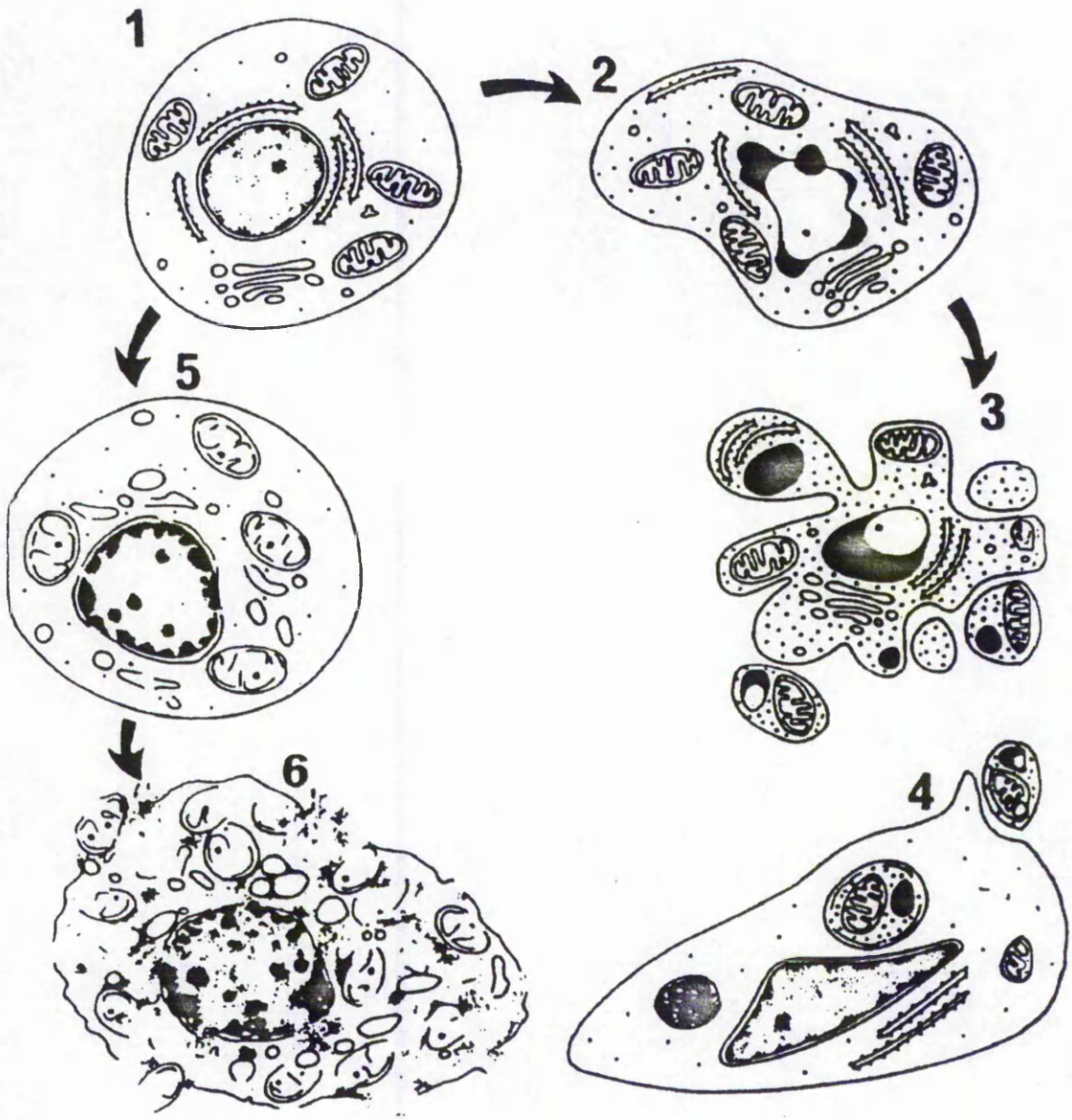

Figure 1.3 Schematic Summary of Necrosis and Apoptosis.

1.4.2 Genetic Control of Apoptosis

1.4.2.1 FAS/APO-1/CD95

Fas/APO-I was independently discovered by two laboratories using monoclonal antibodies cytolytic for a variety of human cell lines inducing a very distinct pattern of cell death (Trauth *et al* 1989, Yonehara *et al* 1989). The protein reactive with the antibodies was named Fas, which is a cell surface protein known to trigger apoptosis in a variety of cell types upon anti-Fas/APO-1 antibody binding or binding of the Fas ligand. This protein was also subsequently shown to be identical with the CD95 protein, a molecule involved in regulation of tissue development and homeostasis. Molecular cloning of Fas and APO-1 cDNA revealed that these two genes were identical (Itoh *et al* 1991, Oehm *et al* 1992). The Fas antigen is a 335 amino acid, cell surface protein with a molecular weight of 36 KDa, but with N-glycosylation has an apparent molecular weight of 43-44 KDa by SDS-PAGE (Itoh *et al* 1991). Analysis of Fas/APO-1 DNA indicates that Fas/APO-1 is a type I membrane protein belonging to the tumour necrosis factor/nerve growth factor receptor family. Mutational analysis of Fas/APO-1 and tumour necrosis factor receptor I (TNF-R1) demonstrates that the cytoplasmic domain (about 70 amino acids) conserved between Fas/APO-1 and TNF-R1 is necessary and sufficient for transduction of the apoptotic signal (Itoh and Nagata 1993, Tartaglia *et al* 1993). This domain was therefore designated a death domain. Northern blot hybridisation of mouse- tissue has indicated that Fas mRNA is expressed in the heart, kidney, thymus, liver, and ovary (Watanabe-Fukunaga *et al* 1992). Fas/APO-1 is expressed in almost all populations of mouse thymocytes except (CD4-CD8-) thymocytes (Ogasawara *et al* 1995). Recently, three functional soluble forms of Fas have been shown to be produced by alternative splicing (Cifone *et al* 1993, Cascino *et al* 1995).

1.4.2.2 FAS Ligand

The ligand for Fas/APO-1/CD95 was identified in a cytotoxic T cell hybridoma that could lyse cells expressing Fas/APO-1 but not cells lacking this receptor (Rouvier *et al* 1993) The gene displays homology with TNF and other related factors and encodes a 40 KDa cell surface protein (Tanaka *et al* 1995). Fas/APO-1 ligand has no signal sequence at the N-terminus, but has a domain of hydrophobic amino acids in the center of the molecule, indicating that it is a type II membrane protein with the C-terminal region oriented on the extracellular side of the cell membrane. Approximately 150 ammo acids in the extracellular region of Fas/APO-1 ligand have significant homology with members of the TNF family (Suda *et al* 1993). The ligand for Fas/APO-1 is expressed predominantly in activated T cells and plays a major role in cytotoxicity. Recombinant Fas ligand expressed on the surface of COS cells can induce apoptosis in Fas-expressing cells, indicating that Fas/APO-1 ligand is a death factor and that Fas/APO-1 is its receptor. Genetic analysis of the mouse gld (generalised lyrnphoproliferative disease) gene reveals that it is the Fas/APO-I gene with a point mutation in the C- terminal portion of the gene (Takakashi *et al* 1994, Lynch *et al* 1994). This mutation abolishes the ability of Fas/APO-1 ligand to bind to Fas (Takakashi *et al* 1994). Fas ligand is detected in a soluble form resulting from cleavage at the cell membrane by a metalloproteinase (Tanaka *et al* 1995). Thus, Fas/APO-1 and its ligand are needed for the apoptotic process that occurs during T cell maturation.

1.4.2.3 Interleukin-1β-converting Enzyme (ice)

Much of the knowledge of apoptosis has been derived from studies in the nematode *Caenorhabditis elegans* (*C. elegans*) (Ellis *et al* 1991). A series of genes that control various elements of cell death have been identified. Two genes, ced-3 and ced-4, are key

apoptotic genes in *C. elegans*. ced-3 encodes a cysteine protease that exhibits substantial homology to mammalian interleukin-1β-convertmg enzyme (ICE) (Yuan *et al* 1993). ICE converts the 33 KDa protease form of IL-1β to the active 17.5 KDa form with cleavage specificity after aspartic acid residues (Thornberry *et al* 1992, Cerretti *et al* 1992). Mutations of ced-3 prevent apoptotic death in cells and transfection of ced-3 and ICE into a number of cell types induces apoptosis (Miura *et al* 1993, Gagliardini *et al* 1994). A potential substrate for ICE/ced-3 proteases during apoptosis is poly (ADP-ribose] polymerase (PARP), an enzyme involved in DNA repair and genomic integrity (Kaufmann *et al* 1993, Lazebnik *et al* 1994). PARP is proteolytically cleaved at the onset of apoptosis by an ICE-like enzyme which prevents PARP from participating in DNA repair. In addition, the Ca^{2+}/Mg^{2+}-dependent nucleases involved in internucleosomal DNA cleavage, a hallmark of apoptosis are regulated by PARP (Yoshihara *et al* 1975, Tanaka *et al* 1984). The cow pox virus gene crmA encodes a 38 KDa protein that can inhibit ICE (Wang *et al* 1994). Recently, a family of ICE/ced-3 cysteine proteases have been identified which include ICE rel-II, ICE rel-III, Nedd-2/lCH-1 and CPP-32 (Kumar *et al* 1994, Wang *et al* 1994, Fernandes-Alnemri 1994, Munday *et al* 1995). All of these proteases have a conserved pentameric peptide, QACRG, surrounding the active site. Overexpression of each of these proteases in a variety of cell types results in apoptosis.

1.4.2.4 bcl-2

The bc1-2 proto-oncogene is encoded by a gene 230 kb in size that gives rise to a 24-26 KDa protein which has been localised to the mitochondrial membrane (Hockenberry *et al* 1991, Reed *et al* 1991, Silverman *et al* 1993). Although data exists for implicating bc1-2 as a novel GTP-binding protein, the major function of bc1-2 appears to be an inhibitor of apoptosis by an as yet undefined mechanism (Reed *et al* 1991, Vaux *et al* 1993, Kozopas *et*

al 1993, Wagner *et al* 1993). It is well documented that bcl-2 becomes deregulated in tumour cells as a result of translocation into the immunoglobulin heavy-chain locus and is therefore constitutively activated in B cell malignancies (i.e. follicular lymphoma and chronic lymphocytic leukaemia (Silverman *et al* 1993, Larsen *et al* 1993, Nunez *et al* 1989). In addition, bcl-2 has also been shown to protect mammalian cells from DNA, RNA, and protein-synthesis inhibitors, as well as from sodium azide, colchicine, steroids, heat shock and irradiation treatments (Vaux *et al* 1993). bcl-2 can inhibit apoptosis caused by a variety of physiological and pathological stimuli (Pezzella *et al* 1990, Tsujimoto 1989, Hawkins and Vaux 1994). Although it has been shown that the phosphorylation state of bcl-2 is critical to its ability to inhibit apoptosis, the exact mechanism of action through which bcl-2 exerts its effects is largely unknown. One intriguing observation is that bcl-2 may function as a pro-oxidant regulating levels of reactive oxygen intermediates and controlling early entry into apoptosis (Haldar *et al* 1995, Steinman 1995).

1.4.2.5 bax

bax is a 21 KDa protein with extensive amino acid homology with bcl-2 (Oltvai *et al* 1993, Hanada *et al* 1995). The protein is encoded by six exons and has been shown to undergo alternative splicing leading to at least two cytoplasmic forms (Oltvai *et al* 1993), Bargou *et al* 1995). bax has been shown to form heterodimers with bcl-2 and the ratio of bcl-2/bax determines the survival or death of cells following an apoptotic stimulus such as removal of growth factor (Oltvai *et al* 1993, Korsmeyer *et al* 1993). Stimulation of bax synthesis also appears to be a result of wild type but not mutant p53 activity based on the observation the bax gene promoter region contains 4 motifs showing consensus p53 binding sites (Miyashita and Reed 1995). bax binds the C-terminal domain of bcl-2 around amino acids 197-218, the failure to do so results in onset of apoptosis, as does the formation of bax homodimers

(Oltvai *et al* 1993, Hanada *et al* 1995). Although the formation of the bcl-2/bax heterodimer appears to promote cell survival this may not be absolutely sufficient for the anti-cell death function (Hanada *et al* 1995). More recently it has been suggested that dysregulation of apoptosis due to imbalances in bax/bcl-2 levels may contribute to the pathogenesis of breast cancer (Bargou *et al* 1995).

1.4.2.6 bcl-x

bcl-x is a bc1-2 related gene that can function as a regulator of programmed cell death independent of bc1-2. Alternative splicing results in two distinct bcl-x mRNAs. The larger mRNA gives rise to a protein product, bcl-x_L, which is similar in size and predicted structure to bc1-2 (Boise *et al* 1993). bcl-x immunoreactivity has been detected in a wide variety of cell types and similar to bc1-2, the protein is typically localised in the cytosol in association with the mitochondrial periphery (Krajewski *et al* 1994, Gonzalez-Garcia *et al* 1994). Alternative splicing results in two distinct bcl-x mRNAs. bcl-xL is similar in size and structure to bc1-2, contains BH1 and BH2 domains, and is expressed in long lived tissues such as the brain (Boise *et al* 1993). The smaller form, bcl-x_S, lacks the BH1 and BH2 domains, and is expressed in cells that undergo a high turnover such as immature (CD4+ CD8+) thymocytes (Boise *et al* 1993). It most likely differs from bc1-2 in its regulatory activity on cell differentiation through controlled tissue expression (Boise *et al* 1993, Gonzalez-Garcia *et al* 1994). Like its homologue bc1-2, the mechanism and extent of bcl-x's function are still increasing. Bcl-x_L has been shown to modify the cell's response to oxidants as well as to participate in resistance to chemotherapeutic agents and radiation (Fang *et al* 1995, Datta *et al* 1995).

1.4.2.7 bak

Bak (for bc1-2 homologous antagonist/killer) is a gene that exhibits structural similarity to bc1-2 and other members of the family in the BH1 and BH2 domains (Chittenden *et al* 1995, Farrow *et al* 1995, Kiefer *et al* 1995). bak is 25, 22 and 19% identical to bc1-2, bcl-x_L and bax, respectively. The bak gene encodes a 211 amino acid protein with a molecular weight of 23 KDa. Northern hybridisation studies have shown that bak is expressed in a wide variety of tissues including heart, spleen, thymus, ovary, testis, colon, prostate and peripheral blood lymphocytes (Farrow *et al* 1995). Over-expression of bak in sympathetic neurones deprived of NGF accelerates apoptosis and blocks the protective effect of adenovirus 2 EIB 19kDa, known to block cell death induced by Fas and TNFα (Kiefer *et al* 1995, Gooding *et al* 1991). bak is thought to induce apoptosis by abolishing the protective function of bc1-2 and bcl-x_L (Chittenden *et al* 1995, Kiefer *et al* 1995). *In vitro* studies have shown that bak protein interacts with bc1-2, and more strongly with bcl-x_L, but not with bcl-x_S (Chittenden *et al* 1995).

1.4.2.7 myc Oncogene Family.

The v-myc oncogene, initially identified in the MC29 avian retrovirus, causes myelocytomas, carcinomas, sarcomas and lymphomas (Cole *et al* 1986), and belongs to a family of oncogenes conserved throughout evolution. In humans the family consists of five genes: c-myc, N-myc, R-myc, L-myc, and B-myc (Le Gouy *et al* 1987). Amplification of the c-myc gene has been found in several types of human tumours including lung, breast and colon carcinomas (Alitalo *et al* 1983), while the N-myc gene has been found amplified in neuroblastomas, small cell lung carcinomas and Wilms tumours (Nisen *et al* 1986). L-myc is amplified in small cell lung cancer (Nau *et al* 1985). Immunological studies have shown

that the human c-myc gene gives rise to at least two nuclear phosphoproteins of 64 KDa and 67 KDa (Persson *et al* 1984) that exhibit relatively short (30 minutes) half lives *in vivo* and exhibit DNA binding properties *in vitro*.

Expression of myc may be necessary for activation-induced death (Evan *et al* 1992). Deregulated c-myc expression is a potent inducer of apoptosis when combined with a block to cell proliferation, most notably following deprivation of growth factors (serum) or forcible arrest with cytostatic drugs (Evan *et al* 1994). The induction of apoptosis by c-myc requires the presence of the myc partner, max, as well as the presence of a functional p53 protein, thus p53 may mediate apoptosis as a safeguard mechanism to prevent cell proliferation induced by oncogene activation. Expression of the c-myc gene is induced rapidly upon addition of serum to quiescent cells, and its expression is followed by mitosis. However, overexpression of c-myc in quiescent cells maintained without serum leads to apoptosis (Evan *et al* 1992). This is most likely due to regulation of gene transcription by the myc-max heterodimer (Evan *et al* 1994, Bissonnette *et al* 1994). Thus, the induction of c-myc in cells grown in the presence of appropriate growth factors or co-expression of other survival genes, such as bcl-2, causes cell proliferation. In the absence of these factors, c-myc expression causes cell death.

1.4.2.8 fos

The proto-oncogene fos has been implicated in cell growth, differentiation and development (Verma 1986, Verma and Graham 1987, Muller (1986). fos is induced by a large number of stimuli ranging from mitogens, differentiation-specific agents, pharmacological agents, etc. (Greenberg and Ziff 1984, Verma and Sassone-Corsi 1987). Induction of the 62 KDa fos protein is rapid but transient and represents about 0.1% of the total cellular protein

(Greenberg and Ziff 1984). The fos protein is associated with a 39 KDa protein which has been identified as the protein product of the jun proto-oncogene (c-jun) (Rauscher III *et al* 1988). The fos/jun protein complex binds specifically to a sequence element in DNA referred to as the AP-1 binding site (Sassone-Corsi *et al* 1988, Rauscher III *et al* 1988).

1.4.2.9 c-jun/AP-1

The jun gene is a cell-derived sequence that has been identified as the presumed oncogene of avian sarcoma virus 17, which induces fibrosarcomas in chickens (Cavaleri *et al* 1985). v-jun shares homology with the DNA binding domain of yeast transcription factor GCN4 (Arndt *et al* 1986, Vogt *et al* 1987). Cloning of the proto-oncogene c-jun, the cellular homologue of the viral sequence, demonstrated that it encoded a DNA binding protein of 39 KDa with structural and functional properties of transcription factor AP-1 (Bohmann *et al* 1987, Angel *et al* 1988). The protein product of c-jun is a 39 KDa protein that associates with the oncogene protein product of fos (Sassone-Corsi *et al* 1988, Rauscher III *et al* 1988). The fos/jun protein complex binds specifically to a sequence element in DNA referred to as the AP- 1 binding site (Volm *et al* 1993). In some studies, overexpression of the jun protein has been correlated with increased metastatic potential. More recently, jun has been shown to be involved in the onset of programmed cell death, particularly in the area of neuronal differentiation and neuronal plasticity. A causal role for cjun in programmed neuronal death has also been directly demonstrated (Schlingensiepen 1994,, Estus *et al* 1994).

1.4.210 SV40 T Antigen

The large T antigen of SV40 binds DNA and complexes with wild type p53 to initiate viral DNA replication during lytic cell growth (Carroll *et al* 1974, Lane and Crawford 1979). By binding and sequestering p53, SV40 T antigen prevents p53 from exerting its ability to take part in the apoptotic process (Sheng *et al* 1994). This process may involve repression of a cell survival gene or genes by the free wild type p53 (Caelles *et al* 1994). In addition, large T antigen binds DNA polymerase, the AP-2 transcription factor, and the retinoblastoma (Rb) protein (Mitchell *et al* 1987, De Caprio *et al* 1988).

1.4.2.11 p53

The p53 tumour suppressor gene is necessary for some, but not all forms of apoptosis (Clarke *et al* 1994, Strasser *et al* 1994, Gotz and Montenarh 1995). p53 exerts a significant and dose-dependent effect in the initiation of apoptosis, but only when it is induced by agents that cause DNA-strand breakage. The p53-dependent induction of apoptosis appears to be composed of two components. The first is the requirement for p53 transactivation of target genes through sequence-specific DNA binding; while the second is an apparent transactivation-independent pathway that by passes p53 target genes (Caelles *et al* 1994, Haupt *et al* 1995). The growth-suppressive role of p53 occurs by activating the expression of the WAF1 gene, also known p21Cipl, which is a potent inhibitor of GI and G2 cyclin dependent kinases (cdk) (El-Deiry *et al* 1993, Harper *et al* 1993, Xiong *et al* 1993). Activated cdks phosphorylate and inactivate the Rb protein. Induction of WAF1 by p53 results in inactivation of cdks leading to a failure to phosphorylate Rb and subsequent cell cycle arrest. Both G1 and G2 arrest and apoptosis occur in response to p53-dependent

induction of WAFI (El-Deiry *et al* 1994, Argarwal *et al* 1995). Inability to induce WAFI precludes p53 dependent arrest (Waldman *et al* 1995), while abrogation of p53-dependent growth arrest and apoptosis can occur through either mutational inactivation of p53 (Fan *et al* 1994) or by aberrant expression of MDM2 (Chen *et al* 1994). These findings fit well with the current model of p53 function in which p53 somehow senses DNA damage and arrests the cell cycle in either G1 or G2 allow DNA repair to take place. If repair is not successful, p53 may promote cell death by apoptosis, thereby preventing the propagation of genetic defects to successive generations of cells. p53 has also been shown to have a direct effect on apoptosis by down regulating bc1-2 expression and up-regulating bax expression (Miyashita *et al* 1994).

The role of transglutaminase in this process of apoptosis is not fully established but investigation into the apoptotic bodies/envelopes has shown them to be rich in the transglutaminase-mediated product of ε(γ-glutamyl) lysine isodipeptide crosslinks. The crosslink is chemically stable to digestion by detergents and other chaotrophic agents. Thus by monitoring the formation of transglutaminase-mediated products, it is possible to assess the degree of endogenous apoptosis in both cells and tissues; *in vivo* and *in vitro*. (Fesus *et al* 1987, 1989, Knight *et al* 1991, Piacentini *et al* 1991)

1.5. Significance of apoptosis in cellular homeostasis.

Programmed cell death is now a recognised feature of homeostasis of cells and tissues, there exists a fine balance between cell proliferation, necrosis and apoptosis which maintains the numbers of cells in a tissue or organ. If this balance is lost then uncontrolled proliferation, synonymous with neoplastic or malignant hyperplasic growth may exist to the detriment of the organism as a whole. Furthermore, apoptosis plays an important role in body growth and development; during early embryogenesis to specialisation of limbs, control of adult organ size (Wyllie *et al* 1980).

In 1972 Kerr, Wyllie and Currie (Kerr *et al* 1972) were the first authors to propose apoptosis as a distinct and separate mode of cell death different to necrosis. Since this time a vast amount of research has been targeted to the understanding of apoptosis, especially its controlling mechanisms. It is now strongly believed that apoptosis is controlled by specific gene expression e.g. c-myc and p53 (Wyllie 1981, Compton *et al* 1990, Mc Conkey *et al* 1989, Mc Conkey 1990, Ellis and Horovitz 1986, Buttyan *et al* 1988 and 1989, Yuh and Thompson 1989, Hockenberry *et al* 1990, Rubin *et al* 1991, Sentman *et al* 1991, Younish-Rouach *et al* 1991). During such work two genes have been found which appear to protect against apoptosis during certain circumstances, bcl-2 and the sequence homologue BHRF1 gene of the Epstein-Barr virus.

Calcium ionophores, glucocorticoid hormones, steroids, retinoids and certain monoclonal antibodies have been shown to induce apoptosis; both *in vivo* and *in vitro*. Experiments with these substances have suggested that an increase in intracellular cytosolic calcium levels acts as a trigger for apoptosis. The increase in calcium appears to stimulate the activation of the endonucleases and is essential for the catalytic activity of transglutaminase.

The complex nature of calcium inside the cell will have many other effects, which could benefit to an efficient process of apoptosis; or conversely interfere with the mechanism. This information has led to the hypothesis that there needs to be a multi-stimulus response controlling the apoptotic event. Such signals, may involve the new synthesis of the death gene proteins which help organise the process of apoptosis into this rapid and controlled mechanism.

The therapeutic applications of apoptosis have become very evident. With increased knowledge of the controlling mechanisms for apoptosis; it may lead to new treatments of apoptosis induction in malignant and disease states. The most obvious condition being that of cancer. In a malignant neoplastic state the balance between proliferation and apoptosis has been lost, the result being the unchecked progression and invasiveness of tumours. Through, genetic manipulation of the death genes and/or inconjunction with topical pharmacological agents the induction and increased incidence of apoptosis in neoplastic growth may lead to reduction in tumour growth and ultimately to tumour regression. Similarly, specific targeting of pathogenic organisms which are causing disease and removal of them by inducing them to undergo apoptosis; could provide a whole new branch of medicine.

1.6 Aims of this study.

To investigate the role of tissue (Type II) transglutaminase in programmed cell death (apoptosis). In order to carry out this investigation it will be necessary to develop a number of *in vivo* and *in vitro* models in which the levels of transglutaminase may be closely monitored and controlled. Furthermore, at each stage of the model the level of apoptosis will then have to be determined.

Four models of significant neoplastic importance have thus far been established to help elucidate the role of transglutaminase in programmed cell death. It is these four models which will be discussed in this thesis; they are :-

I). Rat liver *in vivo* hepatocarcinogenesis model, induced by the oral administration of 2-acetly-aminofluorene.

II). Hamster metastatic fibrosarcoma model, both *in vitro* and *in vivo* passage of the tumours.

III). Pharmacological induction of transglutaminase and apoptosis following *in vitro* treatment of a human lung fibrosarcoma model with sodium butyrate.

IV). Pharmacological induction of transglutaminase and apoptosis following *in vitro* treatment of a human colorectal carcinoma model with retinoic acid

2.0 Materials and Methods.

2.1 Abbreviations.

2.2 Listing of Specific Chemicals and Equipment Suppliers.

2.3 Specific Methods Used.

2.3.1 Tissue Cell Culture.

2.3.1.1 Culture Media for Specific Cell Lines.

2.3.1.1.1 Metastatic Variants of Hamster Fibrosarcoma.

2.3.1.1.2 WI38 VA13a (VA13a) human embryonic lung fibroblasts

2.3.1.1.3 HT29 Human Colon Cancer Cells (Retinoic Acid Stimulation).

2.3.1.1.4. ECV304 Human Umbilical-vein Cloned Endothelial Cell Line.

2.3.1.2 Splitting Cells.

2.3.1.3 Counting and Viability of Cells

2.3.1.4 Freezing Down Cells.

2.3.1.5 Thawing Out Frozen Cells.

2.3.2 Tumour Propagation *in vivo*.

2.3.2.1 Propagation of Metastatic Fibrosarcoma in Hamsters via *in vivo* Passage of Cell Cultures.

2.3.2.2 Propagation of Rat Hepatocellular Carcinomas via 2-AAF Acetylaminofluorene (2-AAF) administration in the diet.

2.3.2.3 Transplantation of Tumours.

2.3.2.4 Harvesting of tumour tissue.

2.3.2.5 Tumour Resection.

2.3.3 Tissue Homogenisation.

2.3.4 Cell Sonication.

2.3.5 DNA Extraction / Assay.

2.3.5.1 DNA Assay (after BURTON)

2.3.5.2 DNA Assay -Diphenylamine Reaction.

2.3.5.3 Hoefer DNA Quantitation Assay.

2.3.6 Protein Assays.

2.3.6.1 BioRad DC Protein Assay Kit.

2.3.6.2 Lowry Protein Assay.

2.3.7 Tissue Transglutaminase Activity Assay.

2.3.7.1 Nottingham Trent University Method.

2.3.7.2 Oklahoma Medical Research Foundation Method.

5.3.7.3 Transglutaminase Activity Assay / NCBR-OMRF ver.2

2.3.8 Tissue Transglutaminase Antigen Assay by ELISA Methods.

2.3.8.1 Tissue Transglutaminase Antigen Assay by DIRECT ELISA

2.3.8.2 Tissue Transglutaminase Antigen Quantitation by INHIBITION ELISA.

2.3.8.2.1 Preparation of the Exogenous Reaction Tubes : -

2.3.24.1 DEPC Treatment.

2.3.24.2 Extraction of total RNA from Tissue Using TRIZOL™ Reagent

2.3.24.3 RNA Denaturing Agarose Gel Electrophoresis.

2.3.24.4 Capillary Transfer Of RNA From Agarose Gels To Nylon Membranes

2.3.25 DNA Analysis.

2.3.25.1 Extraction of DNA from Cells for Endonucleased DNA Ladders.

2.3.25.2 Production of cDNA Probes

2.3.25.3 Isolation of the 2.6 Kbp EcoRI/Hind III Human Tissue Transglutaminase Fragment from hTG1

2.3.25.4 Isolation of the cDNA Probe Template from the Restriction Digest

2.3.25.5 Agarose Gel Electrophoresis of DNA

2.3.25.5.1 Isolation of DNA from Agarose Gels

2.3.25.5.2 Production of Radiolabelled cDNA Probes

2.1.25.6 Hybridisation of Radiolabelled cDNA Probes to RNA Attached to Nylon Membranes (Northern Blotting).

2.0 Materials and Methods.

2.1 Abbreviations.

BHK-21	- baby Hamster kidney fibroblasts clone 21
CUB 74	- monoclonal antibody CUB 7402 raised to tissue transglutaminase
CUB 11	- IgG γ 1 isotype control for CUB 74
DAB	- diaminobenzidine
DMEM	- Dulbecco's modified Earle's medium
DMSO	- dimethylsulphoxide
DNA	- deoxyribonucleic acid
DNAse I	- deoxyribonuclease I
DTT	- dithiothreitol
ECV304	- Human trachea endothelial cell line
EDTA	- ethylene diamine tetra acetic acid
EGTA	- ethylene glycol-bis(ß-aminoethyl ether) N,N,N',N'-tetra acetic acid
HEPES	- N-2-hydroxyethylpiperazine-N'-2-ethane sulphonic acid
HPLC	- high performance liquid chromatography
HRP	- horse-radish peroxidase
HT29	- Human epithelial colon carcinoma cell line
Mc.Coy's	- Mc.Coy's 5A tissue culture medium
MET B	- metastatic Hamster fibrosarcoma cell line
MET D	- metastatic Hamster fibrosarcoma cell line
MET E	- metastatic Hamster fibrosarcoma cell line
NaB	- n-butyric acid monosodium salt (sodium butyrate)
PAGE	- polyacrylamide gel electrophoresis
PARENT	- Parent cell line from which MET variants were cloned
PBS	- phosphate buffered saline
PMSF	- phenylmethylsulphonylfluoride
RA	- all trans retinoic acid
SDS	- sodium dodecyl sulphate
SV40	- simian virus 40
tTGase	- tissue transglutaminase
TGase	- transglutaminase

TBS	- TRIS buffered saline
TCA	- trichloroacetic acid
TEMED	- N,N,N',N'-tetramethylethylenediamine
TMB	- 3,3,5,5-tetramethyl benzidine
TRIS	- Tris(hydroxymethyl) aminomethane
tTGase	- tissue transglutaminase
WI38	- embryonic human lung cells
VA13a-	- SV40 transformed WI38

2.2 Listing of Specific Chemicals and Equipment Suppliers.

All other chemicals not stated were obtained, in the highest purity possible form Sigma Chemical Company.

Affinity Research Products LTD., GBT Business Park, Technology Drive, Nottingham. NG9 2ND : - Biotinylated lysine probe, 5 mg of 95% pure polypeptide synthesised, sequence $^{+}$H- Thr*-Val-Gln-Gln-Glu-Leu-OH free acid (* biotinylated).

Amersham International Plc., Life Sciences Div., P.O. Box 929, Slough. SL1 4YW : - All radionuclides, [1,4-^{14}C] Putrescine dihydrochloride, Rainbow markers for SDS-PAGE high range.

Aldrich Chemical Co., The Old Brickyard, New Road, Gillingham, Dorset. SP8 4JL : - n-butyric acid monosodium salt.

Amicon LTD., Upper Mills, Stonehouse, Gloucestershire. GL10 2BJ : - 50,000 Da cut-off filters (#XM50) for the 8050 ultrafiltration unit, Micropure 0.22µm filters and vials, Microcon 50,000 Da cut-off inserts.

Anachem, Anachem House, 20 Charles Street, Luton. LU2 0EB : - Gilson pipettes and tips.

Beckman Instruments (U.K.) LTD., Progress Road, Sands Industrial Estate, High Wycombe. HP12 4JL : - Polycarbonate centrifuge bottles and tops (26 ml) for 70Ti rotor.

BioRad Laboratories LTD., BioRad House, Maylands Avenue, Hemel Hempstead. HP2 7TD : - Biotinylated SDS-PAGE markers low range, Protein assay kit DC (Lowry), Protein standard kit, Protein assay kit DL (Bradford), Bio-Lyte pH 3-10 ampholyte,

British Drug House Merck LTD. (BDH), Hunter Boulevard, Magna Park, Lutterworth, Leicester. LE17 4XN : - sodium hydroxide.

Cambridge Bioscience, 25 Signet Court, Stourbridge Centre, Swanns Road, Cambridge. CB5 8LA : - Biotin-X-cadaverine (biotinylated pentylamine) # B1596.

Gelman Sciences, Brackmills Business Park, Caswell Road, Northampton. NN$ 0E7 : - nitro-cellulose sheets

Guildhay LTD., 6 Riverside Business Centre, Walnut Tree Close, Guilford, Surrey. GU1 4UG : - Universal polyclonal antibody purification kit EZE-SEP.

Imperial Laboratories (Europe) LTD., West Portway, Andover, Hampshire. SP10 3LF : - Mc.Coy's 5A, BHK-21 baby hamster kidney cell line, HT29 human colorectal tumour cell line.

Life Technology, P.O. Box 35, Trident House, Renfrew Road, Paisley, Scotland. PA3 4EF : - Gentecin, neomycin sulphate G418, Cryovials, Nunc 4 & 8 well chamber slides.

Millipore (U.K.) LTD., The Boulevard, Ascot Road, Croxley Green, Watford. WD! 8YW : - Immobilon P^{sq} sequencing membranes.

Pharmacia LKB Biotechnology Div., Dray Avenue, Knowlhill, Milton Keynes. MK5 8PH : - Protein A sepharose 4 fast flow, Percoll density separation medium.

Richardson's of Leicester, Evington Valley Road, Leicester. LE5 5LJ : - Laboratory plastic ware, surgical equipment and disposable syringes/needles.

Sarstedt LTD., 68 Boston Road, Beaumont Leys, Leicester. LE4 1AW : - Laboratory plastics and disposables.

Sartorius, Longmead Business Centre, Blenheim Road, Epsom, Surrey. KT19 9QN : - Sterile syringe filters 0.22µm.

Sigma Chemical Co., Fancy Road, Poole, Dorset. BH17 7 NH : - All chemicals each at Anarlar grade or highest available purity : - acrylamide/bis-acrylamide liquid (37.5:1) #A3699, ammonium persulphate capsules #A2301, ammonium sulphate #A4418, Anti-mouse IgG biotin # B6649, Anti-mouse IgG FITC #F0257, Anti-rabbit IgG Biotin # 8895, Anti-rabbit IgG FITC # F9887, carboxypeptidase Y # C3888, 4-chloro-1-napthol tablets #C6788, collagenase type VII # C0773, cyanogen bromide activated sepharose 4B #C9142,

dansyl chloride #D2625, dithiothreitol #D0632, DMSO vials #D1234, Extr-Avidin alkaline phosphatase #E2636, ExtrAvidin-Peroxidase #E2886, Freund's complete adjuvant #F4258, Freund's incomplete adjuvant #F5506, leucine aminopeptidase cytosolic form type III # L9876, PBS packets #P3813, PBS/Tween-20 packets #P3563, poly-l-lysine solution #P8920, prestained SDS-PAGE molecular weight markers (27,000-180,000 Da) #SDS-6H, prolidase (pfs) #P6675, protease type XIV bacterial pronase E # P5147, proteinase K #P6556, TEMED #T9281, trichloroacetic acid # T4885, Tris/glycine blot buffer X10 #T4904, Tris/glycine SDS-PAGE buffer X10 #T7777, trypsin insoluble on agarose # T1763.

2.3 Specific Methods Used.

2.3.1 Tissue Cell Culture.

All cell lines were grown under sterile conditions and incubated in an atmosphere of 5% (v/v) carbon dioxide at 37°C. Following initial flask seeding or subculture the cells were allowed to establish a normal growth pattern, only those cultures which were in the exponential phase of growth were used for experimentation. Stock cultures were maintained and subcultured when numbers reached 80% confluency. Portions of all cell lines were removed, prior to passage two and stored frozen in liquid nitrogen. experimental cultures were not allowed to progress further than passage five, at this time they were destroyed and replaced with cells from the liquid nitrogen stocks.

2.3.1.1 Culture Media for Specific Cell Lines.

2.3.1.1.1 Metastatic Variants of Hamster Fibrosarcoma.

The parent (HSV-2-333-2-26) (metastatic index (6/19) - **low**) and two cloned sublines, MET E (metastatic index (19/20) - **high**) and MET D (metastatic index (1/20) - **no/low**) were grown in vitro according to the method in section 2.3.1.1.

Briefly, cells were cultured to sub-confluence in Dulbecco's Modified Eagles Medium (DMEM). Supplemented with 5% (v/v) horse serum. L-glutamine (574 mg per litre) (make up in Milli-Q pure water, and filter sterilise into medium) once added, medium must be used within 2 - 3 weeks, as L- glutamine breaks down in dilute solution. Penicillin & Streptomycin (Pen. & Strep.) 0.5 ml/l, but only if needed.

To harvest the cells for *in vivo* passage the cells were, maintained for 2 h in serum-free DMEM then harvested by gentle agitation in 5 mM Tris, 2 mM EDTA (pH 7.4) (TE) and washed twice in TE. Cell viability and total counts was assessed using the trypan blue vital dye exclusion method (2.3.1.3). Dilutions made in serum free DMEM to give an homogenous cell suspension of 1 x 10^5 viable cells per 100 µl of medium.

2.3.1.1.2 WI-38 VA13a (VA13A) human embryonic lung fibroblasts

WI-38 VA13A (VA13A) human embryonic lung fibroblasts, a gift from Dr. V. J. Cristafalo of University of Pennsylvania, Philadelphia, PA., were maintained in T-75 flasks (Corning Glassworks) and grown in Mc.Coy's 5a medium supplemented with 10% foetal bovine serum (Intergen Corporation). The flasks were initially seeded at a cell density of 35,000 cells per square centimetre and the cells were maintained at 37°C and subcultured weekly. Where appropriate, two days after subculture when the cells had established exponential growth phase, the culture medium was replaced with fresh medium containing sodium butyrate (1 mM and 2 mM). Control cultures received fresh medium without sodium butyrate. Cell numbers were determined daily using the citric acid-crystal violet method for nuclei (2.3.1.3). Cultures were maintained for an additional period of 5-7 days with the medium being changed every 48 h.

2.3.1.1.3 HT29 Human Colon Cancer Cells (Retinoic Acid Stimulation).

HT29 human colon cancer cells (a gift from Dr. Bernard Weinstein, Columbia University) were maintained in T-75 flasks (Corning Glassworks) and grown in Mc.Coy's 5a medium supplemented with 10% foetal bovine serum (Rehesis), penicillin (50 μg / ml) and streptomycin (100 μg/ml). The cells were maintained at 37°C and subcultured weekly. Where appropriate, all-trans-retinoic acid (10 μM and 50 μM) was added to cultures 48 hr after subculture. The flasks were wrapped in aluminium foil, placed at 37°C and incubated for an additional 5 days with complete medium changes every 48 h. Control cultures received an equivalent amount of 100% ethanol. At the end of the 5 day exposure period, cell number was enumerated using the citric acid-crystal violet method for nuclei (2.3.1.3).

Retinoic Acid Stimulation :

1. Seed cells into T75 or T150 flasks at $5x10^5$ and 10^6 cells per flask respectively (or so as to produce a flask at ~80% confluency).
2. Filter sterilise 0.67 mM all-Trans retinoic acid (RA) (made up in ethanol : sterile water (1:1)).

3. Add 15 µl of RA to 10 ml of medium on a settled flask of cells. (To give final conc. of RA of 1 µM.)
4. Incubate cells for 15 hours.
5. After 15 hours remove the RA containing medium.
6. Wash cells twice with serum free DMEM and harvest with TE.

2.3.1.1.4. ECV304 Human Umbilical-vein Cloned Endothelial Cell Line.

The ECV-304 cell line was obtained from the European Collection of Animal Cell Cultures (Porton Down, Wilts., U.K.). The cells were grown at 37°C with air / carbon dioxide (19:1) in growth medium, consisting of DMEM supplemented with 10 % (v/v) foetal bovine serum. The cells were trypsin-treated before each experiment by using 0.05 % (v/v) trypsin in serum-free DMEM; the trypsin was decanted by centrifugation at 2000 g for 2 min and the cells were resuspended in growth medium containing serum. The cell suspension was then ready for electropermeabilisation (2.3.16).

2.3.1.2 Splitting Cells.

Cells should be split when approximately 80-90% confluent.

1. Pour off medium.
2. Add 2 ml of warm (37°C) Trypsin/EDTA to a T75 flask, 4 ml to a T150. Ensure that the whole growing surface of the flask is wetted with the Trypsin/EDTA.
3. Incubate at 37°C for 5 min.
4. Tap the flask to ensure that all cells are loose.
5. Decant cell suspension into a sterile centrifuge tube.
6. Add 5 ml of warm (37°C) medium drop-wise to the cell suspension.
7. Spin down cells for 5 min at 1500 rpm (400g) in a MSE bench top centrifuge.
8. Pour of supernatant.
9. Gently resuspend cells in the dregs by tapping the centrifuge tube on the floor of the hood.
10. Add 5 ml of warm (37°C) medium to the cells, and gently resuspend the cells by pulling the solution up and down the pipette twice, to give a single cell suspension.
11. Remove 10 µl (using a sterile pipette tip) and place in a microfuge tube. To this add 10µl of trypan blue and count the number of viable cells.
12. Seed the cells into new flasks :-

for T75 flasks	4×10^6 per flask for confluency next day
	4×10^5 per flask for use in 2 - 3 days
	2×10^5 per flask for use in 3 - 4 days
for T150 flasks	8×10^6 per flask for confluency next day
	4×10^5 per flask for use in 2 - 3 days
	2×10^5 per flask for use in 3 - 4 days

13. Add warm (37°C)medium to the flasks, 10 - 15 ml to a T75, 20 - 30 ml to a T150 flask.
14. Tighten flask lids to hand tight and then loosed half a turn so as to allow air to circulate. For vented flask lids, tighten to hand tight only.
15. Incubate at 37°C in a humid, 5% (v/v) CO_2, atmosphere. Check that the incubator water tray contains water (Add copper sulphate (2 % (w/v)) to the water to prevent

fungal growth). Check level of CO_2 cylinder regularly, and replace cylinder when necessary.

2.3.1.3 Counting and Viability of Cells

Vital dye exclusion, using Trypan blue :

1. Harvest cells to a single cell suspension as described in section 2.3.1.2.
2. Add 0.2% (w/v) Trypan blue in PBS.
3. Add 4 parts Trypan blue to 1 part saline (4.5 % (w/v)). (Ready diluted dye may be available ready diluted from Sigma).
4. Add Trypan blue solution to cells, to give a final ratio of 1:1. Incubate cells at 37°C for 5 min.
5. Count the two subsets of cells in a heamocytometer (blue ones are non-viable, clear ones are viable). Remember 1:1 dilution when calculating viable cells per ml.

Crystal Violet cell nuclei method :

1. Remove the growth medium and replace with 1 ml of 0.1 M citric acid leave flask to incubate for 2h at 37°C or overnight at 4°C.
2. After incubation the removed 100 µl of the cell suspension and add it to 900 µl of 0.1 M citric acid, mix by gentle inversion.
3. To the diluted cell suspension add 1 ml of 0.1 % (w/v) crystal violet in 0.1 M citric acid, mix well by gentle inversion.
4. Count multiple portions of the stained suspension in a heamocytometer, all cell nuclei will stain light purple.

2.3.1.4 Freezing Down Cells.

1. Harvest with 0.2 % (w/v) trypsin / 0.1 M EDTA
2. Spin down at 1500 rpm (MSE bench top centrifuge, 400 g) for 5 min and remove supernatant.
3. Resuspend in cold freezing mixture (10^7 cells per ml).
4. Place in cryogen ampoules, 1 ml per ampoule.
5. Freeze at -70°C o/n and then transfer to liquid nitrogen store.

Freezing mixture (STERILE) 95% (v/v) serum, 5% (v/v) DMSO. Store in foil covered bottle at 4°C long term, room temperature very short term.

Storage time for frozen cells : -70°C for up to 6 months; liquid nitrogen for years!

2.3.1.5 Thawing Out Frozen Cells.

1. Remove cells from storage, using appropriate protection.
2. Place in a plastic Mc.Cartney bottle and place in incubator until thawed (thaw as quickly as possible).
3. Transfer cells to a sterile centrifuge tube, add medium drop-wise (Hanks balanced salt solution (HBSS) or serum free DMEM) so as to dilute the DMSO slowly.
4. Centrifuge at 1500 rpm (bench-top centrifuge) for 5 min and remove supernatant.
5. Repeat the washing as above.
6. Resuspend in medium and plate out into one T75 flask.
7. Incubate at 37°C
8. Change medium next day and split if required.

2.3.2 Tumour Propagation *in vivo*.

2.3.2.1 Propagation of Metastatic Fibrosarcoma in Hamsters via *in vivo* Passage of Cell Cultures.

Five hamster fibrosarcomas, whose origins and characteristics have been described (Walker *et al*, 1982; Teale and Rees, 1987) are available. In brief, their origins are as follows :-

Parent Inactive HSV-2-333-2 induced 'in vitro' transformation of hamster embryo fibroblasts.

Met B

Met C

Met D Derived from lung nodules of animals whose primary Met E parent tumour load had been resected.

Met F

1. Cultured cells from the required cell line are harvested following trypsinisation of confluent monolayers, in the usual manner.
2. Wash three times in Hanks balanced salt solution (HBSS) and resuspended in HBSS at 10^5 cells per ml.
3. Assess viability of cell suspensions by trypan blue exclusion, and only use preparations of more than 90% viability.
4. Inject subcutaneously 0.1 ml of a 10^5 cells / ml cell suspension (10^4 cells) into the right flank of Syrian golden hamsters.
5. Fill in a cage label, according to Home Office guide lines.
6. Check animals for tumour growth at regular intervals, by palpitation of right flank and sacrifice before they became distressed.

2.3.2.2 Propagation of Rat Hepatocellular Carcinomas via 2-AAF Acetylaminofluorene (2-AAF) administration in the diet.

The model used may be summarised as follows. Male Sprague-Dawley rats (200-250 g) were purchased from Sasco Inc., Omaha, NE. A modified version of the Teebor and Becker method (Teebor and Becker 1971) of cyclic feeding of 2-AAF was used to produce 2-AAF-mediated hepatocarcinogenesis. Rats were administered an 2-AAF diet comprised of a semi-synthetic control diet containing 0.05% 2-AAF (Ringer *et al* 1983) for 3 weeks followed with 1 week on control diet. This cyclic regimen was repeated from 2 to 5 times depending on the experiment. Control animals were fed the semi-synthetic control diet (Purina Rodent Laboratory Chow No. 5001) continuously during the period that experimental animals were in cyclic feeding regimens. Rats that were to be maintained for a period of time beyond a particular cyclic feeding protocol were placed on control diet until used. The results in this chapter refer to a basal control group at week 1, four groups all fed 2-AAF and exposed for 1, 2, 3 and 4 cycles of diet respectively and a basal control group aged matched to the oldest group of experimental animals (4 cycles of 2-AAF)

2.3.2.3 Transplantation of Tumours.

Propagation of hamster fibrosarcomas by the subcutaneous implantation of freshly excised, non-necrotic, tumour tissue into male Syrian hamsters.

1. Kill a tumour bearing hamster by overdose of gaseous anaesthesia..
2. Open the tumour with a single incision across the middle.
3. In the non-necrotic outer region of the tumour, cut blocks of tissue approx. 2 mm^3, but do not remove from the tumour.
4. Anaesthetise the new host hamster with ether.
5. Pluck or shave a patch on the right flank (15 mm x 15 mm) and sterilised with Dispray 1 if available (Stuart Pharmaceuticals Ltd.).
6. Make a small incision through the hairless skin being careful not to cut into the muscular tissue.
7. Make a subcutaneous pocket (approx. 10 mm x 3 mm) by inserting the closed points of a pair of scissors into the incision and then opening them and pulling them out.
8. Insert a freshly excised, non-necrotic, cube of tumour tissue into this pocket.
9. Close the incision with a stainless steel wound clip (Clay-Adams).
10. Repeat the transplant into another animal in case the first transplant does not 'take'.
11. Fill in a cage label.

All instruments should be sterilised in Hibitain solution, and wiped before use. Check animals for tumour growth at regular intervals, and sacrifice before, or in the case of time courses, at the first signs of, distress.

2.3.2.4 Harvesting of Tumour Tissue.

1. Sacrifice animals by cervical dislocation.
2. Remove non-necrotic tumour tissue and place on ice.
3. Small cubes of tissue (approx. 5 mm^3) may be placed into cryostat tubes and stored in liquid nitrogen for transplantation. (Store for up to 6 months).

2.3.2.5 Tumour Resection.

Developing tumours of 5 - 10 mm diameter, approx. 12 days after transplantation, are suitable for resection.

1. Anaesthetise the animal with ether.
2. Pluck the hair away from the skin covering and around the tumour mass.
3. Open the skin around the tumour mass and cut out the tumour, removing as little skin as possible.
4. Loosen the skin around the excision from the underlying musculature with the use of scissors (using scissors points it is possible to 'peel' the skin away from the muscular tissue).
5. Close the wound with several stainless steel wound clips (9 mm).
6. Monitor the animals closely post-resection, those showing signs of respiratory distress or illness should be sacrificed and examined for secondary tumours.
7. All surviving animals should be sacrificed at 7 - 8 weeks post-resection and examined for signs of metastatic spread.
8. Remove metastatic nodules from the lungs, kidneys, body wall etc. and either place on ice for analysis or place in cryostat tubes and store in liquid nitrogen.

All instruments should be sterilised in Hibitain solution, and wiped before use.

2.3.3 Tissue Homogenisation.

1. Keep tissue on ice before, during and after homogenisation.
2. Make tissue homogenates up to 20% (w/v) after homogenisation.

For normal liver; hamster and rat tumours :-

1. Weigh non-necrotic tissue and then wash in cold Buffer A (5 mM Tris-HCl pH 7.4, 2 mM EDTA).
2. Mince tissue in two volumes of cold homogenising buffer (0.25M sucrose, 5 mM Tris-HCl pH 7.4, 2 mM EDTA, 1 mM DTT, 5 mM benzamidine, 1 mM PMSF in DMSO to 1% (v/v) final volume) by use of a variable speed Ultra-Turrax with 1 x 30 sec burst at low speed (pre-cool the blade to 4^{o}C in ice cold Buffer A).
3. Add another two volumes of cold homogenising buffer, and further homogenise with five passes of a close fitting (clearance 0.25 - 0.30 mm) glass/teflon Potter-Elvehjem homogeniser or with the Ultra-Turrax.

For human tumours :-

1. Thaw tissue on ice, weigh and wash in cold Buffer A.
2. Homogenise samples (50 - 200 mg) in two volumes of cold homogenising buffer containing 1% (w/v) lubrol-PX, 1 µg/ml leupeptin and 1 µg/ml pepstatin, using five passes of a microhomogeniser (homogenise in a Category I cabinet).

For cultured cells :-

1. Harvest cells using HEPES:EDTA (5 mM : 2 mM), not trypsin.
2. Pellet the cells at 400g (1500 rpm in bench top centrifuge).
3. Wash cell pellet twice with cold Buffer A.
4. Resuspend to 10^7 cells / 300 µl in cold homogenising buffer containing 1% (w/v) lubrol-PX, and homogenise using five passes of a microhomogeniser.

Fractionation into cytosol and 71,000g pellet.

1. Centrifuge tissue homogenate at 71,000g for 45 min at 4°C (33,000 rpm in 8x25 ml 70TI Beckman rotor).
2. Decant the cytosolic supernatant.
3. Resuspend the pellet in an equivalent volume of cold homogenising buffer using the Ultra-Turrax.

Previously weighed one gram samples of control and experimental tissues were homogenised as follows; by using six slow passes of a Potter-Elvehjem homogeniser in four volumes of homogenising buffer. (10 mM Tris-HCl, pH 7.4 containing 0.25 M sucrose, 1 mM EDTA, 5 mM benzamidine and 1 mM phenylmethylsulfonyl fluoride (PMSF)). Thus preparing a 20 % (v/v) homogenate (This procedure is carried out at 4°C, all tissues, solutions and equipment are kept on ice, prior to and during the sample preparation).

2.3.4 Cell Sonication.

For cultured cells :-

1. Harvest cells using HEPES:EDTA (5 mM : 2 mM), not trypsin.
2. Pellet the cells at 400g (1500 rpm in bench top centrifuge).
3. Wash cell pellet twice with ice-cold homogenising buffer (0.25M sucrose, 5 mM Tris-HCl pH 7.4, 2 mM EDTA, 1 mM DTT, 5 mM benzamidine, 1 mM PMSF in DMSO to 1% (v/v) final volume)
4. Resuspend to 10^7 cells / 300 µl in cold homogenising buffer containing 1% (w/v) lubrol-PX, then were exposed to five pulses (each 0.1 - 0.2 ms) of an electric field of 1.0 kV/cm from a capacitance of 3 µF, in a 0.4 cm-wide cuvette n a Gene Pulser apparatus (BioRad, Hemel Hempstead, U.K.).

2.3.5 DNA Extraction / Assay.

2.3.5.1 DNA Assay (after BURTON)

1. Add 2.6 ml ice-cold TCA (10% w/v) to 0.4 ml of homogenate (20% w/v).
2. Centrifuge for 10 min at 2000 g (bench top centrifuge).
3. Resuspend pellet in 3 ml TCA (10% w/v) and re-centrifuge.
4. Wash x 2 with 95% ethanol (centrifuging as above).
5. Drain final pellet thoroughly (do not use oven).
6. Hydrolyse DNA by adding 3 ml TCA (5% w/v) and incubating at 90°C for 10 min.
7. Centrifuge to clarify lysate. Adjust volume to 3 ml with TCA (5% w/v).
8. Add 1 ml of lysate to 2 ml of freshly prepared diphenylamine reagent in glass tubes (acid washed).
9. Vortex the tubes and leave o/n at room temperature, and in the dark, for the colour to develop.
10. Read absorbance at 600 nm.
11. Standard curve 10 - 100 µg / ml DNA.

Diphenylamine reagent :

1.5 g diphenylamine

100 ml Analar glacial acetic acid

1.5 ml concentrated H_2SO_4

0.5 ml acetaldehyde (16 mg / ml)

DNA standard : Calf thymus DNA 1 mg/ml in 5% (w/v) TCA (378 µl calf thymus DNA in 622 µl 8% (w/v) TCA). [N.B. ACID WASH ALL GLASSWARE BEFORE USE.]

Mix 2 ml of a 20 % (v/v) liver homogenate with 6 ml cold 10 % trichloroacetic acid (TCA). Allow to stand for 5 min in ice-water. Centrifuge for 5 min at 0°C. Discard the supernatant containing the acid-soluble nucleotides. Wash the pellet of nucleic acid / protein by resuspending it in 5 ml cold 10 % TCA. This must be done thoroughly by grinding the pellet to a fine suspension with 0.25 ml 10 % TCA, taken from the 5 ml volume. Sediment again by centrifugation. Up to this point the tubes must be kept cold to prevent breakdown of the nucleic acid into further acid-soluble fragments.

The insoluble residue is suspended in 5 ml 5 % TCA and the nucleic acids are then hydrolysed by heating for 20 min at 90°C. Attempt to keep the temperature at precisely 90°C for this period. A longer incubation will be required if the temperature falls below 90°C. Cool tubes and centrifuge to remove the insoluble proteins and retain the supernatant which contains the degraded nucleic acids and pyrimidine nucleotides, purine bases, ribose and deoxyribose both free and as phosphate esters. This supernatant ("extract") was used to estimate the amount of DNA in 1 g of liver by the following method.

2.3.5.2 DNA Assay -Diphenylamine Reaction.

Five ml of fresh diphenylamine reagent (1 g diphenylamine in 98 ml glacial acetic acid and 2 ml concentrated sulphuric acid) was added to 2 ml of neat extract. The tubes were mixed then heated at 100°C for 40 minutes. Then cooled rapidly and the optical density read at 600 nm. The amount of DNA in each sample was determined by reading from a calibration curve of DNA standards (DNA standards over the range of 0 - 320 μg were prepared this calibration graph can be seen in the results section 2.4.5).

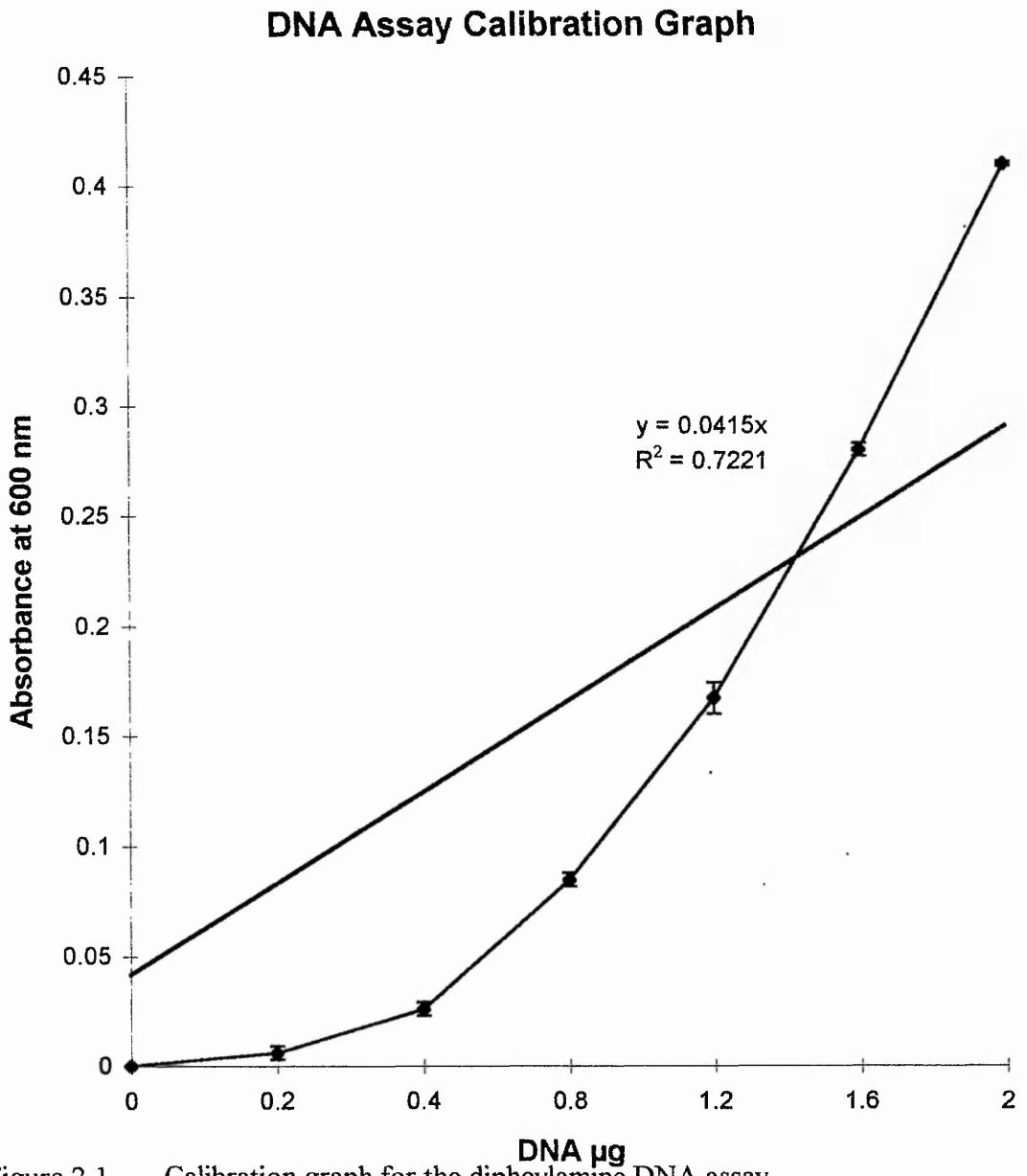

Figure 2.1 Calibration graph for the dipheylamine DNA assay.

2.3.5.3 Hoefer DNA Quantitation Assay.

Hoefer DNA Assay Kit (TKO 102) for Use with the TKO-100 Minifluorimeter

The TKO-102 standards kit includes calf thymus DNA standard (250 µl of 1 mg / ml in 10 mM Tris-HCl, 50 mM EDTA, pH 8.0) used for calibration and DNA standard curve. DNA measurements are based on the binding of Hoechst 33258 (H32258), a fluorescent dye, to DNA. The fluorescence of H32258 dye depends in part on the AT content of the DNA. The calf thymus DNA provided in the kit is 60% GC : 40% AT, which is comparable to most animal and plant DNA. It is double stranded and highly polymerised. {In the presence of single stranded DNA H32258 will an emitted fluorescence of half that produced for double stranded genomic DNA. Single stranded oligonucleotides will not however cause H32258 to fluoresce}.

Materials :

10X TNE Buffer (100 mM Tris-HCl, 10 mM EDTA, 2.0 M NaCl, pH 7.4)

Into 800 ml of distilled water, mix

Trizma base	12.1 g
EDTA-NA_2	3.7 g
NaCl	58.4 g

pH to 7.4 with concentrated HCl, adjust volume to 1 L. Filter through 0.22 µm filter and store at 4°C.

Note, the 1x TNE buffer is a common DNA storage buffer modified slightly for the fluorescence assay. The salt concentration has been increased to 0.1 M to enhance the stability of the DNA/Dye complex and the pH adjusted to 7.4 for optimum fluorescent enhancement. For crude extracts, a higher concentration of salt will aid in dissociating proteins from the DNA and enhance the fluorescent signal.

Hoechst stock solution	1.0 mg / ml
(in distilled water store 4°C in dark for 6 months)	

Working dye solution A : 0.1 µg / ml H33258 in 1X TNE. For measuring samples between 10-500 ng /ml final concentration.

Hoechst stock solution	10.0 µl
10X TNE	10.0 µl
Filtered distilled water	90.0 µl

Prepare fresh daily, keep at room temperature.

Working dye solution B : 1.0 µg / ml H33258 in 1X TNE. For measuring samples between 100-2000 ng /ml final concentration.

Hoechst stock solution	100.0 µl
10X TNE	10.0 µl
Filtered distilled water	90.0 µl

Prepare fresh daily, keep at room temperature.

Procedure :

1. Turn the TKO 100 on at least 15 minutes before use
2. Prepare a 1:10 dilution of the calf thymus DNA stock standard (100 µl DNA, 100 µl 10X TNE buffer and 800 µl water) keep at 4°C for upto six months.
3. Fill the TKO 105 glass fluorimetry cuvette with 2 ml of working dye solution. Wipe sides clean, then place into the sample chamber. Orienting the cuvette with the letter "G" forward each time.
4. Close the lid and adjust the "ZERO" control knob until the display reads "000". Initially start with the scale knob adjusted to 50% sensitivity.

5. Thoroughly mix the 1:10 dilution of calf thymus DNA (100 µg / ml), deliver 2µl of the DNA into the 2 ml of dye solution in the cuvette (to give a final concentration of 100 ng / ml DNA). Mix by pipetting up and down with a disposable pipette, using care not to introduce bubbles into the solution.
6. Close the cuvette chamber and adjust the "SCALE" knob until the display reads "100" indicating 100 ng / ml. Fluorescence readings will be linear over the range 100-500 ng / ml DNA.
7. Repeat steps 3 -6 a number of times until the reference standard read as "100" reproducibly. Between samples empty the cuvette, then drain it by blotting onto a paper towel. Alternatively, to set the range between 100 µg / ml and 2000 µg / ml, deliver 2 µl of the DNA standard (1.0 mg / ml) at step 5. Then at step 6 adjust the "SCALE" knob to "1000" indicating 1000 ng /ml; for this use working H33258 solution B. The fluorescence readings will be linear over the range 100-2000 ng / ml DNA.

Once calibrated DO NOT ADJUST THE SCALE KNOB FURTHER.

8. Measure the samples in the same manner using units of ng / ml. Blank each sample by adjusting the "ZERO" knob to "000" each time the fresh 2 ml of dye is added to the cuvette.

2.3.6 Protein Assays.

2.3.6.1 BioRad DC Protein Assay Kit.

The BioRad DC Protein Assay is a colourimetric assay for protein concentration following detergent solubilisation. The reaction is Similar to the well-documented Lowry assay. The reaction reaches 90% of its maximum colour development within 15 minutes and the colour changes not more than 5% in 1 hour after the addition of reagents. The assay is based on the reaction of protein with an alkaline copper tartrate solution and Folin reagent. There are two phases, the reaction between protein and copper in an alkaline medium and the subsequent reduction of Folin reagent by the copper-treated protein. Proteins effect a reduction of the Folin reagent by loss of 1, 2 or 3 oxygen atoms, thereby producing one or more reduced species which have a characteristics blue colour. Colour development is monitored colourimetrically with maximal absorbance at 750 nm and minimal absorbance at 405 nm. Procedure for microplate assay :

1. Preparation of working reagent. Add 20 µl of reagent S to each ml of reagent A that will be needed for the run. (This working reagent A' is stable for 1 week even though a precipitate will form after 1 day. If precipitate forms, warm the solution and vortex. Do not pipette the undissolved precipitate as this will likely plug the pipette tip). If samples do not contain detergent you may omit step #1 and use reagent A as supplied.
2. Prepare 3 - 5 dilutions of protein standard containing from 0.2 mg/ml to 1.5 mg/ml protein. Standards supplied are bovine serum albumin and bovine gamma globulin. A standard curve should be prepared each time the assay is performed. Foe best results the standard should be diluted in the same buffer as the samples.
3. Pipette 5 µl of standards and samples into a clean, dry microtiter plate.
4. Add 25 µl of reagent A' or reagent A into each well.
5. Add 200 µl of reagent B into each well. Gently agitate the plate to mix the reagents. Incubate at 37°C for 15 minutes.
6. After 15 minutes absorbances can be read at 750 nm.

Reagents : A An alkaline copper tartrate solution

B A dilute Folin solution

S A concentrated SDS solution.

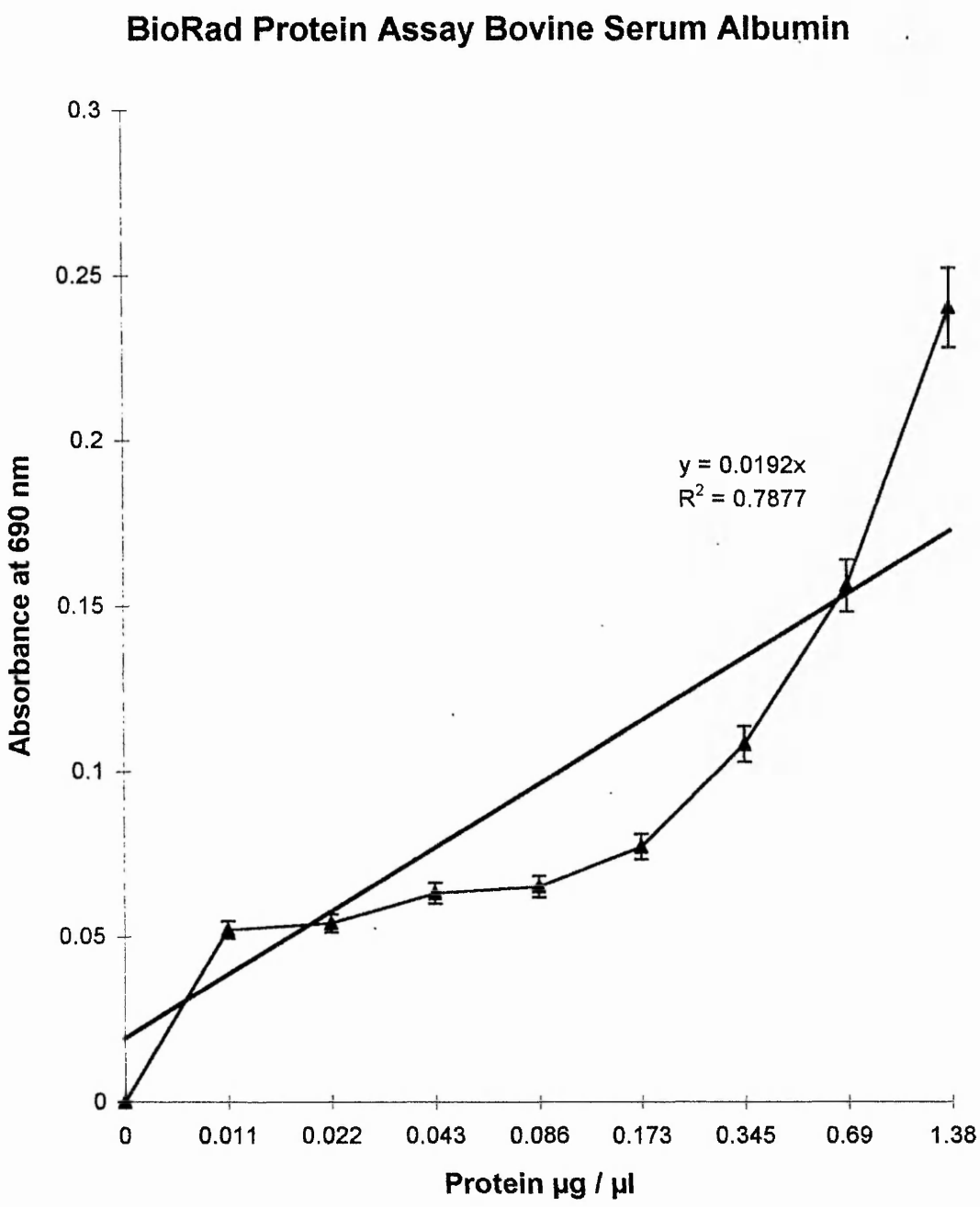

Figure 2.2 Calibration graph for the BioRad DC Protein assay using Bovine Serum Albumin.

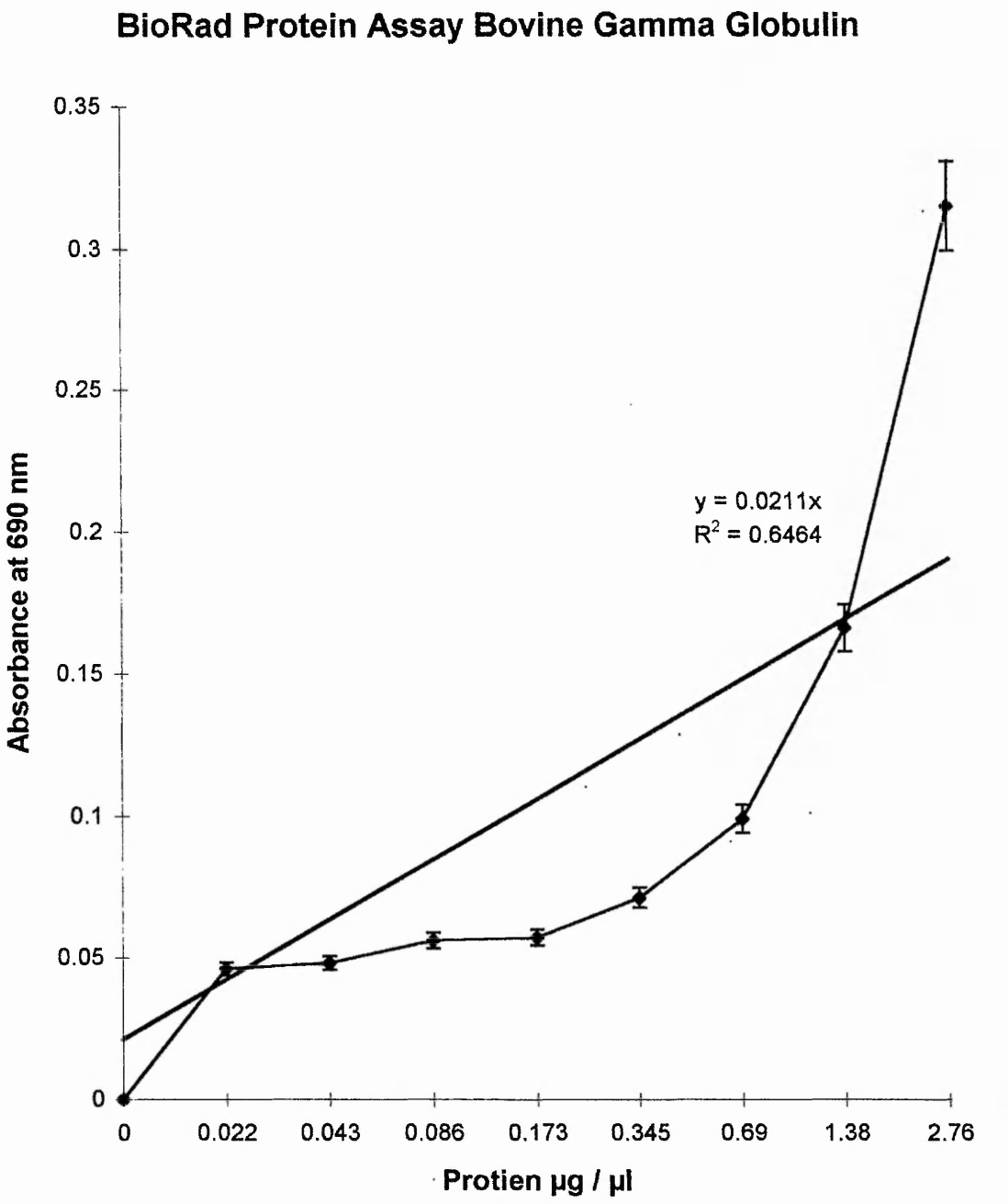

Figure 2.3 Calibration graph for the BioRad DC Protein assay using Bovine Gamma Globulin.

2.3.6.2 Lowry Protein Assay.

Protein concentration is estimated using a modification of the method of Lowry *et al* (1951). To ensure solubilisation of the samples, determinations are carried out in the presence of SDS.

1. Mix 100 µl of sample with 100 µl of 2% (w/v) SDS.
2. Add 1 ml of Folin's solution (49 parts A, 1 part B), with vortexing.
3. Leave for 20 min.
4. Add 100 µl of Folin's-Ciocolteau (1 : 1 with H_2O) (vortex gently whilst adding).
5. Leave for 20 min.
6. Read absorbance at 750 nm.
7. Standard curve 100 - 600 µg BSA in PBS (remember to add SDS), using just PBS in the assay to give a blank.

Solution A : 0.4% (w/v) NaOH
2.0% (w/v) Na_2CO_3
0.02% (w/v) Na Tartarate

Solution B : 0.5% (w/v) $CuSO_4$

Folin's Solution : 49 parts Solution A to 1 part Solution B

Folin's-Ciocolteau : 1:1 dilution with distilled water

Protein in samples of SDS-insoluble polymer was determined by a modification of the method of Lowry *et al* 1951 (14), after partial digestion of the polymeric material with proteinase K (0.15 mg / ml of polymer in 0.15 M PBS, pH 7.4, 0.1 % SDS) incubated at 37° Centigrade for 12 h, then boiled to inactivate. After digestion, samples were made 1 % (w/v) with respect to SDS, before being assayed.

2.3.7 Tissue Transglutaminase Activity Assay.

The principle of the transglutaminase activity assay relies on the ability of the enzyme to catalyse the incorporation of a radiolabelled primary amine into a protein acceptor substrate (Lorand *et al* 1972).

2.3.7.1 Nottingham Trent University Method.

[^{14}C]-Putrescine Assay:-

1. Reactions are carried out at 37°C in 0.5 ml microfuge tubes.
2. Reaction vials contain the following in a total volume of 100 µl:-

Tris-HCl	10 µl of 50 mM pH 7.4
DTT	10 µl of 38.5 mM
$CaCl_2$	5 µl of 50 mM in 50 mM Tris
[1,4-^{14}C]-Putrescine	10 µl of 12 mM stock
N,N'-dimethylcasein	20 µl of 25 mg/ml in 50 mM Tris
Sample	45 µl

3. At 2, 5 and 10 minutes after initiation of the reaction (by addition of the sample), remove duplicate 10 µl aliquots and spot onto 10 mm^2 filter paper squares then place in ice-cold 10 % (v/v) TCA for at least 10 min.
4. Wash filter papers, at the end of an assay, as follows:-

1 x 10% TCA (w/v) ice-cold	10 min.
3 x 5% TCA (w/v) ice-cold	5 min.
1 x 1:1 acetone : ethanol	5 min.
1 x acetone	5 min.

5. Dry filter papers (o/n in fume cupboard).
6. Place filter papers in 2 ml of Optiphase High Safe liquid scintillant for counting in the Packard Liquid Scintillator.

7. At the end of the assay, 10 µl aliquots from each vial are spotted onto filter paper squares and allowed to air dry; these are used as a measurement of total counts in the assay in order to estimate counting efficiency.
8. Control incubations are carried out with 10 mM EDTA (5 ml of 200 mM in Tris) substituted for $CaCl_2$. Background levels of 60 - 100 cpm occur in these controls.

Filter papers are pre-soaked in 100 mM EDTA with 1% (w/v) methylamine, dried in an oven before use, and marked with a 2H pencil. (1% methylamine may be added to the washing solutions, this prevents non-specific binding of radiolabelled putrescine to the filter papers).

12 mM [^{14}-C]-putrescine stock :

Add 50 µl of 243 mM cold putrescine to 1 ml of [^{14}- C]-putrescine (250 µCi./ ml)

N,N'-dimethylcasein stock :

25 mg/ml N,N'-dimethylcasein in 50 mM Tris-HCl pH 7.4, needs to be left stirring o/n in cold room to dissolve thoroughly. Freeze 500 µl aliquots in microfuge tubes.

2.3.7.2 Oklahoma Medical Research Foundation Method.

Cells were harvested and washed three times with calcium- free Earle's solution (116 mM NaCl, 5.4 mM KCl, 1 mM NaH_2PO_4, 0.8 mM $MgSO_4$, 26 mM $NaHCO_3$, pH 7.4), scraped lightly into homogenisation buffer (150 mM NaCl, 40 mM Tris-HCl, pH 7.4,) and sonicated for 10 sec to disrupt the cells. Protein was determined using the BioRad kit (BioRad Laboratories, 2000 Alfred Nobel Drive, Hercules, CA 94547). Transglutaminase activity was determined by measuring the amount of 0.5 mM [1,4- ^{14}C]putrescine (1 µCi/µmol, Amersham Corporation, 2636 South Clearbrook Drive, Arlington Heights, IL 60005) which was incorporated into N,N'-dimethylcasein (DMC) in a 200 µl reaction mixture containing 10 mg/ml DMC, 150 mM NaCl, 40 mM dithiothreitol (DTT), 40 mM Tris-HCl, pH 7.4). After a 20 min incubation at 37°C, the reaction was stopped by the addition of 7.5% trichloroacetic acid (TCA) and the resulting precipitate collected on Whatman GF/A filter, washed four times with 5% TCA and then the radioactivity bound to the filter paper counted by liquid scintillation spectrometry. One unit of transglutaminase activity is expressed as one nmol putrescine incorporated per hour. Specific activity is expressed as units/mg protein.

5.3.7.3 Transglutaminase Activity Assay / NCBR-OMRF ver.2

Transglutaminase activity was measured by the incorporation of [1,4- ^{14}C] putrescine into N,N'-dimethylcasein. Briefly, cells were harvested and washed three times with calcium free Earle's solution (116 mM NaCl, 5.4 mM KCl, 1 mM NaH_2PO_4 , 0.8 mM $MgSO_4$, 26 mM $NaHCO_3$, pH 7.4), scraped lightly into homogenisation buffer (150 mM NaCl, 40 mM Tris-HCl, pH 7.4,) and sonicated for 10s to disrupt the cells. Protein was be determined using the BioRad kit (BioRad Laboratories, 2000 Alfred Nobel Drive, Hercules, CA 94547). Transglutaminase activity was determined by measuring the amount of 0.5 mM [1,4- ^{14}C]putrescine (1 µCi/µmol, Amersham Corporation, 2636 South Clearbrook Drive, Arlington Heights, IL 60005) which was incorporated into N,N'-dimethylcasein (DMC) in a 200 µl reaction mixture containing 10 mg/ml DMC, 150 mM NaCl, 40 mM dithiothreitol (DTT), 40 mM Tris-HCl, pH 7.4). After a 20 min incubation at 37°C, the reaction was stopped by the addition of 7.5% trichloroacetic acid (TCA) and the resulting precipitate collected on Whatman GF/A filter, washed four times with 5% TCA and then the

radioactivity counted by liquid scintillation spectrometry. One unit of transglutaminase activity is expressed as one nmol putrescine incorporated per hour. Specific activity is expressed as units/mg protein.

2.3.8 Tissue Transglutaminase Antigen Assay by ELISA Methods.

By raising both polyclonal and monoclonal antibodies to tissue transglutaminase antigen (Extracted and purified from Sigma Guinea Pig Liver (GLP)). It has been possible to quantitate the amount of transcribed and translated tTGase protein found within tissue and cellular homogenates or sonicates. Inconjunction, these antibodies have also been used in conventional immunohistochemistry procedures to visualise the *in situ* localisation on tissue sections and cell monolayers.

2.3.8.1 Tissue Transglutaminase Antigen Assay by DIRECT ELISA

1. Coat wells of ELISA plate with a 1/4000 dilution of goat anti-transglutaminase (50 µl per well) and leave overnight at 4°C.
2. Wash plate x3 with PBS.
3. Block remaining binding sites with 2% w/v Marvel or BSA in PBS (250 µl per well) and leave for two hours at 37°C.
4. Wash plate x3 with PBS - 0.05% (v/v) Tween.
5. Add 50 µl of sample to each well as required and leave for two hours at 37°C
6. Wash x3 with PBS.
7. Add 50 µl per well of a 1/1000 dilution of rabbit anti-transglutaminase (diluted in PBS : Marvel) and leave overnight at 4°C.
8. Wash plate x3 with PBS : Tween.
9. Add 50 µl per well of anti-rabbit HRP conjugate, diluted 1/1000 in PBS : Marvel, and leave for 2 hours at 37°C.
10. Wash plate x3 with PBS : Tween, then x2 with distilled water.
11. Add 100 ml of HRP substrate per well and leave at room temperature for 20 min.
12. Stop the reaction with 50 µl per well of 2.5 M H_2SO_4.
13. Read at 450nm.

Standard Curve : 200, 100, 80, 60, 40, 20, 10 5 ng GPL tTGase per well

Controls : Pre-immune serum for goat and rabbit anti-TG, PBS for sample.

2.3.8.2 Tissue Transglutaminase Antigen Quantitation by INHIBITION ELISA.

This procedure is used to quantitate the amount of transglutaminase antigen present in a biological sample. It relies on the ability of the antigen present to combine with transglutaminase antibody. This binding effectively reduces the amount of antibody which can subsequently bind to transglutaminase which is attached to a 96-well microtitre plate. Hence, when this antigen-bound anti-transglutaminase is added to the 96-well plate, less of it is able to react with the transglutaminase attached to the plate; thus less colour is produced. Thus, the name INHIBITION ELISA is used as there will be an inhibition of the colour produced.

2.3.8.2.1 Preparation of the Exogenous Reaction Tubes : -

Dilute tissue culture hybridoma fluid CUB 7402 with Mc.Coy's 5a (CM5a) tissue culture media + 10% (v/v) foetal calf serum. Place 200µl of this diluted solution to a sterile capped tube (Falcon 2054). Add a known volume of sample to the tube, which has previously been estimated for protein concentration. Dilution of the sample (in PBS) may be necessary to find the effective range. Add CM5a + 10% (v/v) serum to a final volume of 1000µl. Prepare control samples in the same manner using an equal volume of sample buffer. Incubate tubes (capped - to avoid loss of CO_2, thereby maintaining constant pH) for 2 h with agitation, at 37°C. Place tubes in cold room overnight.

For the standard curve, add 25-1000 ng purified Guinea-pig liver tissue transglutaminase to a series of tubes in place of sample as described above. Remove duplicate 100µl aliquots and add them to a 96-well plate previously coated with 100 ng tissue transglutaminase / well. Quantitate by standard ELISA (See section 2.3.8.3).

2.3.8.3 Procedure for the Standard ELISA, using Biotin/Strept-Avidin Peroxidase Conjugates.

Coat plate with 100 ng tissue transglutaminase / well (50 µl volumes). Leave at 37°C for 1 hr, or in the cold room over night. Drain plate by inversion, blot dry on paper towel. Block each well with 250 µl of 3% (w/v) BSA in Solution A, leave at 37°C for 1 h. Aspirate all liquid from each well, wash plate X3 with 250 µl per well Solution A. Add 100 µl of sample or primary antibody to wells according to the "plate map". Incubate at 37°C for 3 h. Aspirate all liquid from each well, wash plate X3 with 250 µl per well Solution A. Add 100 µl per well of the secondary antibody. Rabbit-anti-Mouse Biotin diluted 1:50,000 in 1% (w/v) BSA in Solution A. Incubate at 37°C for 1 h. Aspirate all liquid from each well, wash plate X2 with 250 µl per well Solution A. Aspirate all liquid from each well, wash plate X2 with 250 µl per well PBS. Add 100 µl per well of a commercial Strept-Avidin Peroxidase conjugate diluted as recommended in PBS. Incubate at 37°C for 30 minutes. Aspirate all liquid from each well, wash plate X2 with 250 µl per well PBS-Tween. Aspirate all liquid from each well, wash plate X2 with 250 µl per well with distilled water. Add 100 µl per well of peroxidase substrate of your choice two possibles are : -

I) ABTS ready-to-use from gives a green-blue colour after 30 minutes incubation; stopped by adding 50 µl per well of 1% (w/v) SDS and read at 405-410 nm.

II) TMB (Tetramethylbenzidine) activated with hydrogen peroxide. This gives a blue colour after 5 minutes of incubation; stopped with 50 µl per well 2.5M sulphuric acid and read at 455 nm. (To make see 2.3.9.4).

Determine the amount of transglutaminase in the sample by comparing the colour development; ether directly or for the inhibition ELISA with comparison to the standard curve.

2.3.8.4 Procedure for the SANDWICH ELISA, using Biotin/Strept-Avidin Peroxidase Conjugates.

1. Coat plate with 50 µl per well with Polyclonal antiserum raised against transglutaminase in Rabbit(Capture antibody). Leave at 37°C for 1 h, or in the cold room over night.
2. Drain plate by inversion, blot dry on paper towel.
3. Block each well with 250 µl of 3%(w/v) BSA in Solution A. leave at 37°C for 1 h.
4. Aspirate all liquid from each well, wash plate X3 with 250 µl per well Solution A.
5. Add 100 µl of sample or primary antibody (Monoclonal raised to transglutaminase in mouse) to wells according to the "plate map". Incubate at 37°C for 3 h.
6. Aspirate all liquid from each well, wash plate X3 with 250 µl per well Solution A.
7. Add 100 µl per well of the secondary antibody. Pierce Rabbit-anti-Mouse Biotin diluted 1:50,000 in 1% (w/v) BSA in Solution A. Incubate at 37°C for 1 h.
8. Aspirate all liquid from each well, wash plate X2 with 250 µl per well Solution A.
9. Aspirate all liquid from each well, wash plate X2 with 250 µl per well PBS.
10. Add 100 µl per well of a commercial Strept-Avidin Peroxidase conjugate diluted as recommended in PBS. Incubate at 37°C for 30 minutes.
11. Aspirate all liquid from each well, wash plate X2 with 250 µl per well PBS-Tween 20.
12. Aspirate all liquid from each well, wash plate X2 with 250 µl per well with distilled water.
13. Add 100 µl per well of peroxidase substrate of your choice two possibles are : -

    I) ABTS ready-to-use from Pierce gives a green-blue colour after 30 minutes incubation; stopped by adding 50 µl per well of 1% (w/v) SDS and read at 405-410 nm.

    II) TMB (Tetramethylbenzidine) activated with hydrogen peroxide. This gives a blue colour after 5 minutes of incubation; stopped with 50 µl per well 2.5M sulphuric acid and read at 455 nm. (To make see below).
14. Determine the amount of transglutaminase in the sample by comparing the colour development.

NOTES :-

The primary antibody should also be raised against transglutaminase; but must be from a different host animal species used to produce the capture antibody coated on the plate. Ideally the secondary antibody-conjugate will be raised to immunoglobulins of the primary antibody host species and made in the same host animal species as the capture antibody, in the example above

Rabbit anti-Mouse. This will minimise the non-specific cross-reaction; to the capture antibody on the plate.

2.3.8.5 Solutions for ELISA Procedures.

PBS :

120 mM NaCl

2.7 mM KCl

10 mM phosphate, pH 7.4

PBS-Tween 20 :

PBS plus 0.01 % (v/v) Tween 20

Solution A :

PBS

1.5 mM magnesium chloride

0.05 % (v/v) Tween 20

0.01 5 (w/v) sodium azide

TMB Substrate :

20 ml 0.1 M sodium citrate, in water, pH 6.0

150 µl TMB (10 mg/ ml) in DMSO

25 µl 3 % (v/v) hydrogen peroxide in water

2.3.9 ε–(γ) Glutamyl Lysine Crosslink Quantitation by Reversed Phase HPLC.

This is a modification of the method of Griffin and Wilson (1984).

All solutions MUST be made up with Milli-Q water in ACID WASHED glassware. Use HPLC grade reagents only. All buffers must be filtered through 0.22μm Durapore filters (Waters Associates) before use.

Column - Nova-Pak C18 (Millipore / Waters). HPLC system - either the Beckman System Gold set-up or a model 6000 and a model 510 pump, controlled by a model 660 gradient programmer (Millipore / Waters), with a data acquisition system consisting of a Nelson Analytical 900 series interface box and a Walters IBM compatible personal computer using Nelson Analytical software. Fluorescence detection - Perkin-Elmer LS-1 fluorimeter (excitation = 340 nm, emission = 455 nm).

1. Equilibrate column for 30 min in 80% A : 20% B (or until base line is steady)
2. Derivitise samples with OPA reagent at room temperature for 1.5 min (30 sec with vortexing).
3. Apply 20 μl to the column.
4. Elution is effected at a constant flow rate of 1.5 ml/min. The gradient programme for elution is as follows :-

Time (min)	**%A**	**%B**
Initial	80	20
35	20	80
40	0	100
45	0	100
55	80	20

The solutions used are detailed below :-

Buffer A :	20 mM potassium acetate pH 5.6
	1% (v/v) tetrahydrofuran
Buffer B :	Methanol (HPLC grade)
	1% (v/v) tetrahydrofuran
OPA reagent :	100 mg OPA
	5 ml 0.4 M potassium borate buffer, pH 10.4
	5 ml methanol (HPLC grade)
Derivatisation mix :	50 µl OPA reagent
	5 ml 2-mercaptoethanol
	20 µl sample

2.3.9.1 Proteolytic Digestion of SDS-Insoluble Polymer for ε (γ -Glutamyl) Lysine Crosslink Analysis.

1. Precipitate the protein from a homogenate sample by the addition of TCA to a final concentration of 10% (w/v) (aim to precipitate approximately 10 mg of protein). (Use 1.2 ml microfuge tubes).
2. Centrifuge for 30 sec in a microcentrifuge (13,500 rpm pulse).
3. Wash the resultant pellet as follows :- (spin down in the microcentrifuge between washes) :-

1 x 10% (w/v) TCA	5 min
3 x diethylether : ethanol 1 : 1	5 min
3 x diethylether	5 min

4. Dry the final pellet thoroughly and rehydrate in 50 µl H_2O, 950 ml 0.1 M $(NH_4)_2CO_3$ pH 8.0 at 32°C (add 1 crystal of thymol to each sample to prevent bacterial decay).
5. Various proteolytic enzymes are then added sequentially, as in the following protocol :-

   i) 0.1 mg subtilisin, incubate at 32°C for 12 h with gentle shaking, repeated twice at 10 h intervals

   ii) 0.15 mg pronase, incubate at 32°C for 12 h with gentle shaking, then at 100°C 15 min to inactivate pronase

   iii) 90 ml of activated leucine aminopeptidase, 75 µl of activated prolidase and $MgCl_2$ to a final concentration of 5 mM, incubate at 37°C for 10 h, repeated once

Adjust digest to pH 6.75 - 7.00

   iv) 0.2 mg carboxypeptidase Y, incubate at 30°C for 12h.

6. Leave digested samples overnight in a dessicator, under vacuum, containing one beaker of 0.5N NaOH and one beaker of 1.0 M H_2SO_4, to remove $(NH_4)_2CO_3$.

Activation of leucine amino peptidase (LAP) :-

10 µl 50 mM $MnCl_2$

90 µl 10 mM Tris-HCl pH 8

100 µl LAP (22.75U)

Incubate at 37°C for 2 - 3 h.

Activation of prolidase :-

20 µl 50 mM $MnCl_2$

80 µl 10 mM Tris-HCl pH 8.0

80 µl distilled water

20 µl prolidase (38.6 Units)

Incubate at 37°C for 2 - 3 h.

2.3.9.2 Proteolytic Digestion of SDS-Insoluble Apoptotic Envelopes ε (γ - Glutamyl) Lysine Crosslink Analysis.

1. Wash isolated apoptotic bodies in 0.1 M $(NH_4)_2CO_3$ pH 8.0. (Only wash once so as not to remove all the SDS as Proteinase K works better in the presence of a small amount of SDS.)
2. Resuspend in 950 µl of 0.1 M $(NH_4)_2CO_3$ pH 8 and 50 µl of water.
3. Various proteolytic enzymes are then added sequentially, as in the following protocol :-

   i) 0.15 mg of Proteinase K (15 µl of 10 mg / ml), incubate at 37°C for 12 h, then boil to inactivate.

   ii) 0.15 mg pronase, incubate at 32°C for 12 h with gentle shaking, then at 100°C 15 min to inactivate pronase

   iii) 90 µl of activated leucine aminopeptidase, 75 µl of activated prolidase and $MgCl_2$ to a final concentration of 5 mM, incubate at 37°C for 10 h, repeated once

Adjust digest to pH 6.75 - 7.00

   iv) 0.2 mg carboxypeptidase Y, incubate at 30°C for 12h.

6. Leave digested samples overnight in a dessicator, under vacuum, containing one beaker of 0.5 N NaOH and one beaker of 0.5 N H_2SO_4, to remove $(NH_4)_2CO_3$.

Activation of leucine amino peptidase (LAP) :-

10 µl 50 mM $MnCl_2$

90 µl 10 mM Tris-HCl pH 8.0

100 µl LAP (22.75 Units)

Incubate at 37°C for 2 - 3 h.

Activation of prolidase :-

20 µl 50 mM $MnCl_2$

80 µl 10 mM Tris-HCl pH 8.0

80 µl distilled water

20 µl prolidase (38.6 Units)

Incubate at 37°C for 2 - 3 h.

2.3.9.3 Quantitation of ε (γ-glutamyl)lysine.

Quantitate isodipeptide using reverse phase HPLC and verify on random samples, using the amino acid analyser method. Verify peaks as being ε(γ -glutamyl) lysine by the addition of known amounts of ε(γ-glutamyl) lysine (Serva) (i.e.. spiking the sample). Quantitate by the subtraction of unspiked peak from spiked peak, and by reference to the peak heights of known amounts of ε(γ -glutamyl) lysine (Serva).

Measurement of the ε(γ-glutamyl)lysine isopeptide was performed following exhaustive proteolytic digestion by modification of our previously published method (9). All enzymatic incubations were carried out at 37°C on an orbital shaker (200 rpm). Samples were resuspended in 200 µl 0.2 M N-ethylmorpholine acetate, pH 8.1 containing 0.02% sodium azide, and pronase (20 µl = 1 µg = 124 units) added. The samples were incubated for 18-24 h, heated in boiling water for 5 min, cooled, and fresh pronase added. After an additional 48 hr incubation, the samples were boiled in water for 5 min, cooled, leucineaminopeptidase (50 µl = 100 µg = 27 units) added. After an additional 96 hr incubation, the samples were heated in boiling water for 5 min, cooled and carboxypeptidase A (5 µl = 100 µg = 6 units), carboxypeptidase B (10 µl = 100 µg = 10 units), carboxypeptidase Y (10 µl = 100 µg = 2 units) were added. The samples were desalted, and processed for isopeptide using reverse phase HPLC and pre-column derivatisation with phenylisothiocyanate (PITC) essentially according to the method of Fesus *et al* (1989). Presence of the isopeptide was confirmed by the detection of lysine following treatment of a portion of the purified material with γ-glutaminylcycloaminotransferase, an enzyme specific for γ-glutaminyl isopeptides. Fibrin was run as a positive control to ensure digestion and chromatography conditions were operating properly.

2.3.10 Preparation / Purification of SDS- Insoluble Polymer from liver.

1. Kill animals by exposure to Fluothane.
2. Exsanguinate the liver via the heart.
3. Cut a block of liver, 1.5 - 2 cm.
4. Cut 5 µm tissue sections (50 -100 mg) using a Mc.Ilwain tissue chopper.
5. Homogenise tissue slices with 6 slow passes of a Potter-Elvehjem homogeniser in 4 volumes of ice-cold 10 mM Tris-HCl (pH 7.4) containing 0.25 M sucrose, 1 mM EDTA, 5 mM benzamidine and 1 mM PMSF.
6. Mix with an equal volume of 2% (w/v) SDS, 10% (v/v) 2-mercaptoethanol and boil for 10 min.
7. Cool to room temperature, and dialyse against 100 volumes of buffer A for 4h
8. Layer samples onto a linear gradient (in sealable centrifuge tubes) of 5 - 15 % (w/v) sucrose in buffer A, with an underlying cushion of 60% (w/v) sucrose in buffer A.
9. Centrifuge at 20°C for 12 h at 71,000 gmax using the Beckman 70Ti.
10. Collect fractions 800 µl .
11. SDS-insoluble polymer is located in the high density sucrose fractions.
12. Clean up the polymer by repeating the sucrose gradient but using 0.5% (w/v) Lubrol-PX (buffer B) instead of the SDS.
13. Dialyse the polymer against buffer B.

Buffer A : 10 mM Tris-HCl (pH 7.4) containing 1% (w/v) SDS, 1 mM EDTA and 2 mM DTT.

Buffer B : 10 mM Tris-HCl (pH 7.4) containing 0.5% (w/v) Lubrol-PX, 1 mM EDTA and 2 mM DTT.

Placed onto a hard wax disc was 1g of liver, this was chopped finely (1µm) with a Mc.Ilwain Tissue Chopper. Then chopped again at 90° to the first cut. The chopped tissue was then digested with 2 ml of collagenase type VII (Sigma C0773) at 500 units/ml made-up in homogenising buffer (10 mM HEPES, pH 7.4 containing 142 mM NaCl, 66 mM KCl and 1 mM EGTA.) The samples were incubated for 3 h, submersed at 37°C in a shaking water bath. After incubation the samples were filtered through a fine mesh of 150 µm into

clean 50 ml tubes. Following digestion the samples were then solubilised with the addition of 10 ml SDS (5 mg / ml) and 5 ml DTT (6.25 mg / ml) and boiled for 5 minutes. The samples were allowed to cool, then centrifuged at 2,000 rpm for 5 min in a bench-top centrifuge. The supernatant and any fibrin, which appears as a black precipitate on top of the white pellet of polymer was removed. The polymer was cleaned by washing and re-centrifugation in Tris/EDTA/Sucrose buffer containing 1 mg / ml DNAse I to prevent the polymer clumping; finally the polymer was resuspended in 1 ml of PBS pH 7.4. The total protein concentration was determined as described earlier (2.3.2).

2.3.10.1 Isolation of SDS-Insoluble/Apoptotic Polymer from Tumour Tissue :

Placed onto a hard wax disc was 1g of non-necrotic tumour tissue, this was chopped finely (1 μm) with a Mc.Ilwain Tissue Chopper. Then chopped again at 90° to the first cut. The chopped tissue was then digested with 2 ml of collagenase type VII (Sigma C0773) at 500 units / ml made-up in homogenising buffer (10 mM HEPES, pH 7.4 containing 142 mM NaCl, 66 mM KCl and 1 mM EGTA). The samples were incubated for 3 h, submersed at 37°C in a shaking water bath. After incubation the samples were then solubilised with the addition of 10 ml SDS (5 mg / ml) and 5 ml DTT (6.25 mg / ml) and boiled for 5 minutes. All samples were allowed to cool, then centrifuged at 2,000 rpm for 5 minutes in a bench-top centrifuge. The supernatant and any fibrin, which appears as a black precipitate on top of the white pellet of insoluble polymer, was removed. The polymer was cleaned by washing and re-centrifugation in TRIS/EDTA/Sucrose buffer containing 1 μg / ml DNAse I to prevent the polymer clumping; finally the polymer was resuspended in 1 ml of PBS. The total protein concentration was determined as described earlier.

2.3.11 Isolation of Apoptotic Envelopes from Cell Cultures.

This is a modification of the method of Schmidt *et al*, 1989.

1. Harvest those cells in the culture medium and those that are attached to the flask.
2. Resuspend cell pellet in DMEM to give 10^7 cells per 500 ml .
3. Add 50 µl of 20% (w/v) SDS, containing 50 µg DTT, to the single cell suspension.
4. Boil for 5 min.
5. Allow to cool then add 10 µg of DNAse 1 per 500 µl to prevent clumping of the apoptotic envelopes.
6. Spin down the envelopes for 5 min at 13,000 rpm in a microfuge.
7. Wash the apoptotic envelopes twice in TE containing 2% (w/v) SDS and 1 mg/ml DNAse 1, before being counted in a heamocytometer.

Isolation of apoptotic envelopes from cultured cells was performed using the method previously described by Knight *et al* (1991); involving the digestion of harvested cells with 20% (w/v) sodium dodecyl sulphate (SDS)and 100 mM dithiothreitol (DTT). Once isolated the envelopes were immunohistochemically stained by incubation with 500 ml of the relevant primary antisera (Anti-SDS-Insoluble Polymer, Anti-Apoptotic Envelope or Monoclonal to ε (γ glutamyl) lysine dipeptide (81d1c2) a kind gift of Dr. S. El-Alaoui) at 37°C for two hours. Centrifuged at 13,500 rpm, washed in 0.01M phosphate buffered saline (PBS) and blocked out with 3% (w/v) bovine serum albumin (BSA fraction V) diluted in PBS for 30 minutes. Secondary, antibody staining with anti-primary host, specific FITC conjugates diluted in block buffer was achieved after 45 minutes incubation at 37°C. Stained envelopes were examined using a fluorescent microscope.

2.3.12 Polyclonal Antibody Production to Raise Antibodies to Transglutaminase Mediated Cell Products.

1. Acquire New Zealand White rabbits and allow to settle in the animal house for a few days.
2. Mix equal volumes of Freund's Complete adjuvant with antigen solution (vortex the adjuvant while adding the protein solution).
3. Ensure that the emulsion will pass through a suitable needle.
4. Before immunising the rabbits, take a test bleed from an ear vein *.
5. Inject each animal subcutaneously in 3 sites, left front shoulder, right front shoulder, and rear flank (wipe injection sites well with alcohol before injecting). Immunise each animal with between 100 and 500 µg antigen.
6. Take an ear vein test bleed 10 days after immunising and assess the titre.
7. Give booster injections at 3 week intervals until the titre no longer rises (three boosts); i.e.. repeat stages 2, 3, 5 and 6.
8. 10 - 12 days after the final boost, bleed the rabbit out by cardiac puncture **.

* - Ear vein bleeds :-

1. Soak some cotton wool in hand hot water.
2. Using the cotton wool, gently warm the ear so as to enlarge the lateral peripheral vein.
3. Carefully insert an orange needle into the enlarged vein and slowly draw out between 500 - 1000 µl of blood into a sterile syringe.
4. Leave the blood to coagulate overnight in the fridge.
5. Spin down the serum and store.
6. After the 3 booster test bleed has been taken, assay all the bleeds for their titre against the immunogen.

** - Cardiac puncture :-

1. Switch on the table heater so that the table is warm but not hot (setting 1 - 1.5).
2. Administer a dose of Hypnoval (2 mg/kg) IP.
3. Leave animal for 10 - 30 mins.
4. Give an IV (ear vein) injection of Hypnorm (0.4 ml/kg).
5. When the animal no longer gives eye responses, insert a green needle (attached to a 20 - 30 ml syringe) into the heart and gently withdraw blood. Release the pressure on the heart from the syringe every so often so that the heart does not collapse.

6. Collect the blood into clean large centrifuge tubes suitable either for the MSE-21 or MSE-24.
7. Leave blood to clot overnight in the fridge.
8. Spin down the clot and collect the serum.

Fresh antigen was prepared using the above two methods. Three sub-cutaneous injections (1 ml total volume) of antigen mixed in equal ratio with Freund's Complete (first injection) and Freund's Incomplete Adjuvant (second and third injections) were given to New Zealand White rabbits over a period of five months. Analysis of the ear vein bleeds at 21 days following injection showed increase in the IgG titre. The animals were humanely sacrificed 28 days after the final injection by cardiac puncture and the serum collected. Control animals were used as a source of non-immune serum.

2.3.12.1 Purification of IgG by Ammonium Sulphate Precipitation.

1. Precipitate protein by the addition of ammonium sulphate to the serum, slowly (over a 30 min period) whilst stirring and over ice. Add sufficient salt to give a final concentration of 50% saturation : i.e. 29.1g salt per 100 ml.
2. Centrifuge serum preps. to pellet the precipitated protein, using MSE-21 at 10,000 rpm for 30 min.
3. Wash the pellet with 50% saturated ammonium sulphate and re-spin as above until pellet is devoid of red cells. (Depending on the size of the pellet, use a few ml each time (i.e. 10 ml) and spin down the cleaned pellet.)
4. Dissolve the pellet in half the original serum volume of 10 mM potassium phosphate pH 8 buffer using a glass rod to aid dissolving.
5. Dialyse o/n against 1l of H_2O per serum prep. at 4°C.
6. Dialyse again o/n against 1l 20 mM potassium phosphate buffer pH 8 at 4°C.
7. Centrifuge in MSE-21 at 10,000 rpm for 30 min to remove lipoprotein.
8. Retain supernatant, aliquot and store at -20°C.

50% saturated ammonium sulphate :-

58.2g $(NH_4)_2SO_4$ in 200 ml H_2O.

20 mM potassium phosphate buffer, pH 8 :-

A - 0.2M KH_2PO_4 (5.44g in 200 ml)

B - 0.2M Na_2HPO_4 (28.39g in 1l)

21.2 ml A + 379.8 ml B, make up to 4l and check pH.

2.3.12.2 Immunoaffinity Chromatography To Purify IgG Fractions.

Coupling of antibody to CNBr activated Protein A Sepharose.

1. Swell cyanogen bromide activated Sepharose (2g) at room temperature for 15 min in 1 mM HCl.
2. Wash with 400 ml 1 mM HCl using a glass sinter funnel.
3. Collect the 'dry' Sepharose by centrifugation at 2000 rpm in a bench top centrifuge (MSE Centaur 1).
4. Resuspend the Sepharose in 0.1M $NaHCO_3$ pH 9, 0.5M NaCl (10 ml).
5. Add serum to the gel (1 ml serum per 3 ml of gel).
6. Check the pH and readjust to 9 if necessary.
7. Rotate the gel end over end at 4^oC over night.
8. Collect the Sepharose by filtering on a glass sinter funnel and wash with 0.25M $NaHCO_3$ pH 9 until no protein is present in the eluent.
9. To block unbound sites on the Sepharose, add 20 ml 1M ethanolamine-HCl pH 9 and rotate the gel end over end for 2h at room temperature.
10. Wash the gel with 50 ml 0.5M $NaHCO_3$ pH 9, followed by 50 ml 0.1M Borate + 1M NaCl pH 4.1 and finally with 50 ml double distilled water.
11. Store the gel at 4^oC in 0.02% (w/v) sodium azide and washed thoroughly with distilled water before use.

2.3.13 ELISA Quantitation of Apoptotic Envelopes and SDS-Insoluble Polymer.

1. Coat ELISA plate with 50 µl per well of 1 mg/ml poly-l-lysine in PBS at room temperature for 1 h .
2. Wash plates x3 with PBS.
3. Add 50 µl sample per well and leave at room temperature for 30 min.
4. Add 50 µl of ice cold glutaraldehyde (0.5% (v/v) in PBS) to each well (DO NOT wash the plate before the addition of the glutaraldehyde), and leave for a further 60 min at room temperature.
5. Wash plates x3 with PBS.
6. Block plates for 1h at room temperature with 250 µl per well of PBS containing 2% (w/v) dried milk powder and 100 mM glycine.
7. Wash plates x3 with PBS.
8. Block plate for a further 30 min at room temperature with 250 µl per well of PBS containing 2% (w/v) dried milk powder.
9. Wash x3 with PBS 0.05% v/v Tween (washing buffer).
10. Add 50 µl per well of rabbit anti-transglutaminase (diluted 1/1000 in PBS if using old batch of serum, 1/200 in PBS if using new batch of serum.)
11. Incubate the plates overnight at 4^{o}C.
12. Wash plate x3 with washing buffer.
13. Add 50 µl per well of anti-rabbit HRP conjugate, diluted 1/5000 in PBS : Marvel, and leave for 2 hours at 37^{o}C.
14. Wash plate x3 with washing buffer, then x2 with distilled water.
15. Add 100 µl of HRP substrate per well and leave at room temperature for 20 min.
16. Stop the reaction with 50 µl per well of 2.5 M H_2SO_4 .
17. Read at 450nm.

Standard Curve : Lanes A - C

200, 100, 80, 60, 40, 20, 10 5 ng GPL tTGase per well

Controls : Pre-immune serum for rabbit anti-TG, PBS for sample.

Solutions :-

PBS (0.15M pH 7.4)	8.00 g	NaCl
	0.20 g	KCl
	1.15 g	Na_2HPO_4
	0.20 g	KH_2PO_4
	1.00 L	distilled water
Washing buffer	0.05% (v/v)	Tween-80 in PBS
HRP substrate	20 ml 0.1M	sodium acetate-acetic acid pH 6.0
	150 µl	TMB (10 mg/ml in DMSO)
	25 µl 3% (v/v)	H_2O_2

Microtitre ELISA plates were coated with 50 µl per well of poly-l-lysine and left shaking at 27°C for 1 h. The plates were washed four times with 200 µl per well of Solution A (10 mM PBS, pH 7.4 containing 1.5 mM magnesium chloride, 2.0 mM 2-mercaptoethanol, 0.05 % (v/v) Tween-20 and 0.02 % (w/v) sodium azide.) The plates then coated with 50 µl per well with polymer samples at various dilutions such that the protein concentration per well was known; the plates left shaking at room temperature for 2 hours or at 37°C overnight. Plates again washed four times with solution A. Blocking of empty binding sites in each well was achieved by adding 200 µl per well of 3 % (w/v) bovine serum albumin made-up in solution A and the plates left shaking at room temperature for 1 h. Plates again washed four times with solution A.

To each well 100 µl of the primary antiserum was added - either the anti-SDS-insoluble polymer antisera or the anti-apoptotic antisera. These were added at a range of dilutions made in blocking buffer. The primary antisera was left on shaking for 3 h at room temperature. Plates again washed four times with solution A.

Development of the assay was achieved by adding 100 µl per well of a secondary antibody raised against the primary antibody and conjugated to Biotin (Anti-rabbit IgG Biotin diluted at 1:2500 in PBS and 1 % (w/v) BSA) this was left shaking for 1 h at room temperature. Plates washed four times with PBS pH 7.4. To amplify the signal 100 µl of ExtrAvidin-Peroxidase was added to each well at a dilution of 1:5000 in PBS. This was left at 37°C for 45 minutes.

Prior to visualisation the plates were washed twice in PBS then twice in distilled water. The visualisation step was carried out by adding 100 µl per well of peroxidase substrate (tetramethyl benzoate TMB : - 150 µL of TMB (10 mg/ml in DMSO) added to 20 ml of 0.1 M sodium citrate buffer pH 6.0 and 20 µl of 3 % (v/v) hydrogen peroxide. The reaction was allowed to proceed shaking in the dark at room temperature of 5 minutes. The reaction was stopped by addition of 50 µl per well of 2.5 M sulphuric acid. Absorbances were read at 450 nm in an automated ELISA plate reader.

2.3.13.1 ELISA for Polymer Quantitation :

Microtitre ELISA plates were coated with 50 µl per well of poly-l-lysine hydrochloride (optional depending on the binding capacity of the ELISA plates used) and left shaking at 27°C for 1h. The plates were washed four times with 200 µl per of Solution A (10 mM PBS, pH 7.4 containing 1.5 mM magnesium chloride, 2.0 mM 2-mercaptoethanol, 0.05% (v/v) Tween-20 and 0.02% (w/v) sodium azide). The plates were then coated with 50 ml per well with the polymer samples at various dilutions, such that the protein concentration per well was known; the plates left shaking at room temperature for 2 hours or at 37°C overnight. A standard curve of polymer extracted from rat liver, obtained as described previously for tumour tissue was set-up on each plate. Following this antigen coating the plates were washed three times with solution A. Blocking of empty binding sites in order to reduce non-specific background was achieved by adding 200 µl per well of 3% (w/v) BSA diluted in solution A to each well. Plates were left shaking at room temperature for 1h. Non-bound BSA was removed by washing three times with solution A. To each well 100 ml of the primary antisera was added, at a range of dilutions made-up in blocking buffer. The primary antisera was left on the plates for 3h at 37°C, after which time the unbound antibodies were removed by washing the plate three times in solution A.

Development of the assay was achieved by adding 100 ml per well of a secondary antibody conjugated to Biotin raised against the host species IgG of the primary antisera (Anti-rabbit IgG Biotin diluted at 1:2,500 in PBS with 1 % (w/v) BSA). The secondary antibody was incubated on the plate for 1h at 37°C. The plates were then washed four times with PBS pH 7.4 prior to the addition of 100 ml per well of ExtrAvidin-Peroxidase diluted 1:5,000 in PBS. The peroxidase was left to bind to the biotin by incubation at 37°C for 45 minutes; unbound peroxidase was removed by two washes of PBS followed by two washes of distilled water. Visualisation of the reaction was carried out by adding 100 µl per well of peroxidase substrate (tetramethyl benzidine-TMB): - 150 µl TMB (10 mg/ml in DMSO) added to 20 ml of 0.1 M sodium citrate buffer pH 6.0 and 20 ml of 3% (v/v) hydrogen peroxide. The reaction was allowed to proceed shaking in the dark at room temperature for 5 minutes; colour development was finalised by addition of 50 ml per well of 2.5 M sulphuric acid; absorbances were read at 450nm.

2.3.14 Immunohistochemistry.

Standard Immuno-peroxidase, alkaline phosphatase, FITC staining methods for tissues, cells, envelopes were used.

2.3.14.1 Neutral Buffered Formal Saline Tissue Fixation.

40 % (v/v) Formalin	10 ml
60 mM Na_2HPO_4	30.5 ml
60 mM KH_2PO_4	19.5 ml
0.85 % (w/v) Saline	40 ml

2.3.14.2 Immunohistochemical Staining of Tumour Tissue Sections :

Staining of the metastatic variants of the hamster fibrosarcoma, the method used was as recommended with the Biomen Supersensitive Multilink Kit (Biomen Limited, Tripod House, 105-107 Lansdowne Rd., Croydon, England). The primary anti-apoptotic envelope antiserum was diluted 1:50 and incubated on the sections for 2h at 37°C. Non-specific binding was reduced by diluting all antisera and conjugates in 10% (v/v) filtered non-immune sheep serum. Substrate aqueous fast red, counter stained with haematoxylin.

2.3.14.3 Indirect Immunofluorescence Studies on Cell Monolayers

1. Wash cells in PBS.
2. Fix cells in 4% paraformaldehyde in PBS for 10 - 15 min.
3. Wash cells in PBS.
4. Permeabilise cells (and block endogenous peroxidase activity) with 0.5% H_2O_2 in methanol for 30 min.
5. Wash in PBS.
6. Block background binding by incubating cells for 10 - 30 min with non-immune serum from animal species from which secondary antibody comes.
7. Blot away excess fluid and apply primary antibody diluted in non-immune secondary antibody serum (e.g. goat anti-TGase diluted 1/20 in normal rabbit serum).
8. Leave overnight in a humidity chamber.
9. Wash 3 times in PBS.
10. Add secondary antibody (e.g. biotinylated anti-goat) diluted in normal rabbit serum as per manufacturers instructions.
11. Leave for 45 min.
12. Wash 3 times in PBS.
13. Apply streptavidin-HRP conjugate at appropriate dilution and leave for 30 min.
14. Wash 3 times in PBS.
15. Develop colour using Diaminobenzidine or Diaminobenzidine tetrachloride (5 mg/10 ml) in buffer containing 5 µl H_2O_2.

Four-well chamber slides (Nunc) were set-up at the same cell density as described earlier and maintained in a similar fashion as for the T-75 flasks. For processing, the medium was removed and the monolayers washed twice with PBS. Paraformaldehyde 4% (w/v) was added and allowed to incubate on the cells for 15 min at room temperature. Following cell fixation, the paraformaldehyde was removed and the cells were washed twice with PBS, this washing procedure was carried out between all stages of the cell staining. Permeabilisation of the cells was achieved by incubating the fixed cells with absolute methanol for 30 min at -20°C . The primary antisera was then added to appropriate wells and allowed to bind at 4°C overnight. After the overnight incubation with antisera, the cell layers were again washed to remove unbound antibodies. Development and enhancement of the

fluorochrome staining used the principle of anti-primary host species, biotin secondary antibodies followed by streptavidin-FITC conjugates (Calbiochem) as per the manufacturer's instructions. Examination of the slides was carried out on a Leitz Ortholux II ultraviolet microscope fitted with Olympus camera attachments.

2.3.15 Microscopy.

2.3.15.1 Examination of Sodium Butyrate Treated Cells by Light Microscopy

On each day of the experiment, the cells were examined on an Olympus CK-2 inverted microscope for changes in morphology and toxic effects of the butyrate treatment. Photomicrographs were taken of those cultures which showed altered morphology.

2.3.15.2 Normarski Diffraction Interference Phase Contrast Microscopy.

Samples of the cell populations prepared above were concentrated onto microscope slides using a cytospin centrifuge (Shanddon Scientific). Aqueous non-permanent mounts were made and the slides examined under a conventional light microscope fitted with Normarski phase contrast optics (Nikon). Photomicrographs were taken of normal and apoptotic cells; the latter cells clearly show the presence of ARB's.

2.3.15.3 Confocal Laser Microscopy.

Following examination of the preparations by conventional light microscopy, the slides were re-examined on an argon laser confocal microscope/cytometer (Meridian ACAS). The pulsed argon laser was set to scan each field for auto-fluorescence and to capture a computer enhanced image of the field. Corresponding images were made of the same field scanning for merge/phase image. Resultant pairs of scans for numerous fields were obtained, each showing the total auto-fluorescent score per field and a computer generated image of all cells per field. It was possible to analyse the data from these scans to obtain correlations for total fluorescent score per field and numbers of apoptosing cells per field.

Using the confocal feature of the microscope, an individual apoptotic cell obtained from a 5 day 50 μM RA-treated culture was subjected to laser scanning at 0.4 μm intervals in the Z axis. The resultant auto-fluorescent scans obtained showed that the ARB's were the source of the light refractiveness/auto-fluorescence and confirmed that they were spherical intracellular bodies.

2.3.16 Electropermeabilisation of Single Cell Suspensions.

Batches of up to 10^7 cells were collected into a Microfuge tube and pelletted by centrifugation in a Microfuge (Jouan A40) at 2000g for 2 min at room temperature. The supernatant was replaced with ice-cold 'poration buffer', containing 140 mM potassium glutamate, 7 mM $MgSO_4$, I mM EGTA, 0.5 mg / ml BSA (A-7030; Sigma), with $CaCl_2$ added to give a Ca^{2+} concentration of 10 nM. The cells were washed three times in this buffer, by resuspension and centrifugation, and then were exposed to five pulses (each 0.1 - 0.2 ms) of an electric field of 1.0 kV/cm from a capacitance of 3 μF, in a 0.4 cm-wide cuvette n a Gene Pulser apparatus (BioRad, Hemel Hempstead, U.K.).

2.3.17 Incorporation of Biotinylated Polyamine Probes.

After electropermeabilisation (Section 2.3.16), the cells were washed once more in poration buffer and placed into microfuge tubes in batches of 2 x 10^5 cells. These constituted individual determinations in the assays. The cells were pelletted 2000g for 2 min and placed on ice. To start the 5 min pre-incubation, the supernatant was replaced with buffer (50 - 100 µl) containing different concentrations of biotinylated cadaverine (BTC) and tTGase inhibitors. The cells were then transferred from ice to a water bath at 37 °C, together with the addition of $CaCl_2$ or water to give the various Ca^{2+} levels used. Reactions were stopped by addition of 500 µl of PBS containing 100 µM iodoacetamide and mixing. The cells were then centrifuged at 13,000g for 2 min at room temperature and the supernatants discarded. The pellets were then stored at -20°C before assay or were treated for SDS/PAGE as described in section 2.3.22.

Before SDS/PAGE (Section 2.3.22), permeabilised cells were washed once in 0.25 M sucrose, 5 mM Tris / 2 mM EDTA, pH 7.4, before being resuspended in Laemmli sample buffer, Consisting of 62.5 mM Tris, 2 % (w/v) SDS, 5 % (v/v) 2-mercaptoethanol, 10 % (v/v) glycerol and 0.01 % (w/v) Bromophenol Blue. The samples were then sonicated (Section 2.3.4)on ice with 3 x 5 s pulses, with 5 s gaps, at 5 µm peak width using a fine probe (Soniprep; M. S. E. Loughborough, U.K.), and then incubated at 90-100°C for 5 min before loading on gels. SDS/PAGE was conducted by using a 3 % stacking and a 10 % resolving gel on a Mini-Protean system (BioRad), by the method of Laemmli (1970). Electroblotting (Section 2.3.23.1) was conducted with a semi-dry system (LKB Multiphor Pharmacia-LKB, Uppsala, Sweden) with a continuous transfer buffer as described by Harlow and Lane (1988, pp. 488-489). The blot was then incubated in 1 % (w/v) BSA in PBS. pH 7.4. overnight at 4°C, followed by a wash in PBS containing 0.05 % (v/v) Tween-

20, pH 7.4 (PBS-T), for 10 min. Incubation of the blot was then in PBS-T containing 1% (v/v) BSA and Extr-Avidin peroxidase (1/2000) for 60 min, with shaking. The blot was then washed for 2 x 10 min in PBS-T, followed by a rinse in deionized water. The blot was then incubated in substrate buffer containing 4 chloro-1-naphthol, until labelled proteins were detected (Section 2.3.23.2), whereupon the blot was transferred to water and subsequently photographed.

2.3.18 Percoll Density Gradient Centrifugation Separation Of Apoptosing And Non-Apoptosing Cell Populations.

1. Layer sequentially into a 2 ml microfuge tube the following densities of Percoll :-

1.080 g/ml	150 µl	(956.6 µl/ml)
1.078 g/ml	300 µl	(954.8 µl/ml)
1.076 g/ml	300 µl	(953.0 µl/ml)
1.074 g/ml	300 µl	(951.3 µl/ml)
1.072 g/ml	300 µl	(949.5 µl/ml)
1.070 g/ml	300 µl	(947.7 µl/ml)

2. Resuspend cells in 1.06 g/ml Percoll (938.9 µl/ml) made iso-osmotic with 0.15M NaCl. (Do not try to spin cells down in this solution, it is too dense for a successful sedimentation.)
3. Layer 150 µl of cell suspension on to the top of the Percoll step gradient.
4. Place microfuge tube carefully into a scintillation vial insert and then centrifuge in a swing out rotor for 30 min at 400g (1500 rpm in a MSE bench top centrifuge).
5. Non-viable cells will float on the top of the gradient;
   Viable non-apoptosing cells will form a band in the 1.07 - 1.06 interface;
   Apoptosing cells form a pellet at the bottom of the tube.
6. Carefully remove the separated cell populations.

A modification of the method of Cotter *et al* (1990) was utilised (60). An iso-osmotic Percoll (Pharmacia) density gradient was set-up in a 2 ml centrifuge tube as follows: 150 µl of 1.080 g/ml, 300 µl 1.078 g/ml, 300 µl 1.076 g/ml, 300 µl 1.074 g/ml, 300 µl 1.072 g/ml and 300 µl 1.070 g/ml Percoll, respectively. Cells from a T-75 flask were gently scrapped into the culture medium, transferred to a 50 ml centrifuge tube and pelletted by centrifugation. The cell pellet was washed 3-times with Tris buffer (10 mM Tris-HCl, pH 7.4) and finally resuspended in 150 µl of 1.060 g/ml Percoll. The suspension was carefully layered atop of the prepared Percoll Gradient. The gradient was centrifuged in a rotor name swing out rotor for 30 min at 400g. Non-viable cells float on the top of the gradient; viable non-apoptosing cells form a band at the interface of the 1.070-1.060 g/ml Percoll and apoptosing cells form a pellet at the bottom of the tube. After centrifugation, the individual cell populations were carefully removed from the gradient and washed in PBS.

2.3.19 Flow Cytometry.

Cells were processed by washing twice with calcium-free Earle's solution, incubated in 10 ml of 10 mM EDTA for 1 hr at 37°C, and detached from the flask by shaking. The resultant cell suspension was made homogenous by aspiration 5 times with a 10 ml pipette. The cells were pelletted by centrifugation at 2,000 rpm for 5 min and resuspended in 0.4 ml calcium-free Earle's solution to which 1 ml of 70% (v/v) ethanol was added drop-wise as a fixative. The cell suspensions were stored at 4°C until propidium iodide staining was performed. On the day that flow cytometry analysis was performed, all cell preparations were centrifuged and resuspended as single cells in 1.0 ml of calcium- free Earle's solution. To remove contaminating RNA, 5 µl of a 5 mg/ml stock solution of RNAse I was added and the mixture was incubated for 30 min at 37°C. The cell suspension was treated with 2 µl of propidium iodide (1.8 mg/ml made in calcium-free Earle's solution), and allowed to stand on ice for 5 min prior to analysis. Analysis was carried out on a Becton Dickinson FACS Scan flow cytometer. A total of 20,000 excitation events were monitored and the data recorded. Post-run analyses were carried out using the CellFIT Cell-Cycle Program from Becton Dickinson Version 2.01.2. Cell cycle distribution histograms of the control populations and populations treated with the sodium butyrate were compared. A portion of the cells was visualised by examination on the fluorescent microscope.

2.3.20 Tritiated Thymidine Incorporation Assay.

Cells were incubated with ^{3}H-methyl-thymidine (100 Ci/mmole, Amersham Corporation) for 1 hr. After the incubation, the culture medium was removed and an aliquot kept for counting. The cell layer was washed three times with PBS containing 4 mM unlabelled thymidine. Proteins and DNA were precipitated by incubation with 10% (v/v) TCA and left for 1 hr at room temperature. The TCA was decanted and a second incubation with 10% TCA was performed for 1 hr at 4^{o}C. The TCA was removed and the contents of the flask were solubilised in 0.5 N NaOH by incubation at 37^{o}C for 2 hr. Finally, aliquots of the solubilised material were taken for liquid scintillation counting. Protein estimations were carried out as described earlier. Preparation of cellular DNA was performed on duplicate flasks using the method of the Stratagene DNA extraction kit (Stratagene, 11011 North Torrey Pines Road, La Jolla, CA 92037). Once isolated, the total cellular DNA was quantitated using the method for the Hoefer TKO 100 minifluorimeter, (Hoefer Scientific Instruments, 654 Minnesota Street, San Francisco, CA 94107).

Labelling:

1. Dilute (^{3}H)methyl-thymidine (50-100 Ci/mmole)with distilled water (1 µl / 100 µl)
2. Filter sterilise if incubation will be longer than 6-8 hr
3. Dilute 100x with medium (10 µl / ml medium).
4. Incubate 37°C.

Processing:

1. Remove liquid from cell monolayer
2. Wash 3x with PBS + 4 mM thymidine (96 mg / 100 ml). Make fresh.
3. Add 10% TCA. Incubate RT 30-60 min.
4. Remove liquid.
5. Add 10% TCA. Incubate 4°, 60 min.
6. Remove liquid.

7. Add 0. 5 M NaOH. Incubate 37°C, 120 min. Shake occasionally.

8. Remove aliquots for protein and liquid scintillation counting.

Processing Step	Sample	Recommended Volume / ml
2,3,5	T-25	5*
	T-75	10*
	Coverslip	100
7	T-25	2
	T-75	5
	Coverslip	Omit this step
8 (Scintillation Counting)	T-25	0.2
	T-75	0.2
	Coverslip	Entire coverslip

* If radioactivity is to be determined in the TCA washes the volumes for steps 3 & 5 may be reduced to 2 ml for T-25 and 5 ml for T-75 flasks.

2.3.21 Bromodeoxyuridine (BrdU) Cell Proliferation Assay.

Incorporation of Bromodeoxyuridine

The tritiated thymidine method assumes that the synthesis of new DNA and hence cellular proliferation is distributed evenly in all cells. This may not be the case. Therefore, it was necessary to know how many of the cells in the population were behaving normally. The Amersham cell proliferation assay kit (Amersham Corporation) provides a means of testing this question in situ. The principle of the kit is to immunohistochemically stain those cells which are incorporating a thymidine analogue, 5-bromo-2'- deoxyuridine (BrdU) into replicating DNA. We identified those cells which were proliferating by examination of cell monolayers following staining with the cell proliferation assay kit by light microscopy.

1. Add 100 µl of cell suspension to each well of 96 well, tissue culture grade microtitre plate. Cells should be passaged and cultured under the conditions routinely employed for the cell line being used for the assay. Where possible avoid the use of media containing thymidine. Media may be used with or without serum supplementation as appropriate to the experiment. Use cells at 1000 - 10,000 cells / well depending on the duration of the experiment.
2. Incubate plate in tissue culture incubator until cells have attached to the plate.
3. Add agent(s) under study and incubate as usual. Agent(s) should be added in such a way as to leave 100 µl of medium in all wells after additions have been made. For example where doubling dilutions are required add 100 µl of reagent at twice the highest concentration to one or more wells. mix by pipetting up and down and then transfer 100 µl to the next well. Continue this procedure until the required concentration range is obtained, discarding the 100 µl from the last well.
4. Prepare labelling medium by diluting 1;500 with complete tissue culture medium. Warm to 37°C before use. Use the same tissue culture medium as used for the cell culture. Prepare only sufficient labelling medium required for each experiment. Discard any unused labelling medium.
5. Add 100 µl to experimental wells, add 100 µl culture medium to "Blank" wells. Incubate at 37°C for 2 hours.

6. Drain plate by inversion. Wash plate with PBS by flooding each well for 30.sec. Then drain by inversion.
7. Fix cells by adding 200 µ of fixative to each well for 30 minutes at room temperature. (Fixative glacial acetic acid 50 ml. ethanol 900 ml and water 50 ml).
8. Wash plate wells thoroughly by flooding wells three times with PBS + 0.1 % (v/v) Tween 20. The washing step is important and should be carried out thoroughly.
9. Block wells with 100 µl of 3 % (w/v) BSA in PBS/Tween for 15 minutes at room temperature. Drain by inversion.
10. Add 50 µl of reconstituted nuclease / anti-5-bromo-2'-deoxyuridine to all wells and incubate at room temperature for 1 hour.
11. Wash plate with PBS/Tween as in step 8
12. Add 50 µl of diluted peroxidase anti-mouse IgG to all wells and incubate at room temperature for 30 minutes.
13. Wash plate with PBS/Tween as in step 8
14. Add 100 µl of peroxidase colour development solution to all wells and incubate at room temperature until the required colour intensity has developed.
15. Stop colour development with 50 µl stop reagent to all wells and measure the absorbance of each well at 410 nm.
16. If required the plate may be developed with an insoluble peroxidase substrate for microscopical identification of positive cells.

Reagent Composition ;

Labelling Reagent. 5-bromo-2'-deoxyuridine and 5-fluoro-2'-deoxyuridine (10 :1 ratio) Supplied as a concentrated solution diluted 1: 500 in tissue culture medium before use. Store at 2-8°C, do not freeze

Anti-5-bromo-2'-deoxyuridine antibody. The monoclonal antibody supplied in Tris, BSA, magnesium chloride and preservative. this must be diluted with reconstituted nuclease solution before use. Store at 4°C

Nuclease. Nuclease for DNA degradation supplied lyophilised and must be reconstituted with water before adding to antibody solution.

2.3.22 Polyacrylamide Gel Electrophoresis (PAGE).

SDS PAGE : 2 - 20 % (w/v acrylamide) gradient.	**2%**	**20%**
30% (w/v) acrylamide	2 ml	20 ml
1% (w/v) bis-acrylamide	10.1 ml	2 ml
1.5 M Tris pH 8.8	7.5 ml	7.5 ml
water	10 ml	0.1 ml
10% (w/v) SDS	300 µl	300 µl
10% (w/v) fresh $(NH_4)_2S_2O_8$	100 µl	100 µl
TEMED (keep at 4°C)	10 µl	10 µl

Pour gradient such that 20% becomes the bottom of the gel.

SDS PAGE Non-gradient Resolving gel	**15%**	**10%**	**6.5%**
30% (w/v) acrylamide	15 ml	10 ml	6.5 ml
1% (w/v) bis-acrylamide	2.6 ml	1.7 ml	1.2 ml
1.5 M Tris pH 8.8	11.2 ml	11.2 ml	11.2 ml
water	1.2 ml	6.9 ml	11 ml
10% (w/v) SDS	300 µl	300 µl	300 µl
10% (w/v) fresh $(NH_4)_2S_2O_8$	100 µl	100 µl	100 µl
TEMED (keep at 4°C)	10 µl	10 µl	10 µl

Stacking gel :	**4%**
30% (w/v) acrylamide	3 ml
1% (w/v) bis-acrylamide	2 ml
1.5 M Tris pH 6.8	2.5 ml
water	11.2 ml
10% (w/v) SDS	200 µl
10% (w/v) fresh $(NH_4)_2S_2O_8$	100 µl
TEMED (keep at 4°C)	10 µl

Degas before the addition of SDS, $(NH_4)_2S_2O_8$ and TEMED.

Sample buffer :

10 mM Tris pH 6.8

2.5% (w/v) SDS

10% (v/v) glycerol

5% (v/v) 2-mercaptoethanol

0.02% (w/v) bromophenol blue

Running buffer (5x conc.)

Glycine	144 g/l
Tris pH 8.5	30 g/l
10% (w/v) SDS	50 ml/l

2.3.22.1 Gel Staining

Stain and Fix :

Methanol	200 ml
Acetic acid	40 ml
Water	200 ml
Commassie blue	440 mg

Destain :

Methanol	50 ml
Acetic acid	70 ml
Water	880 ml

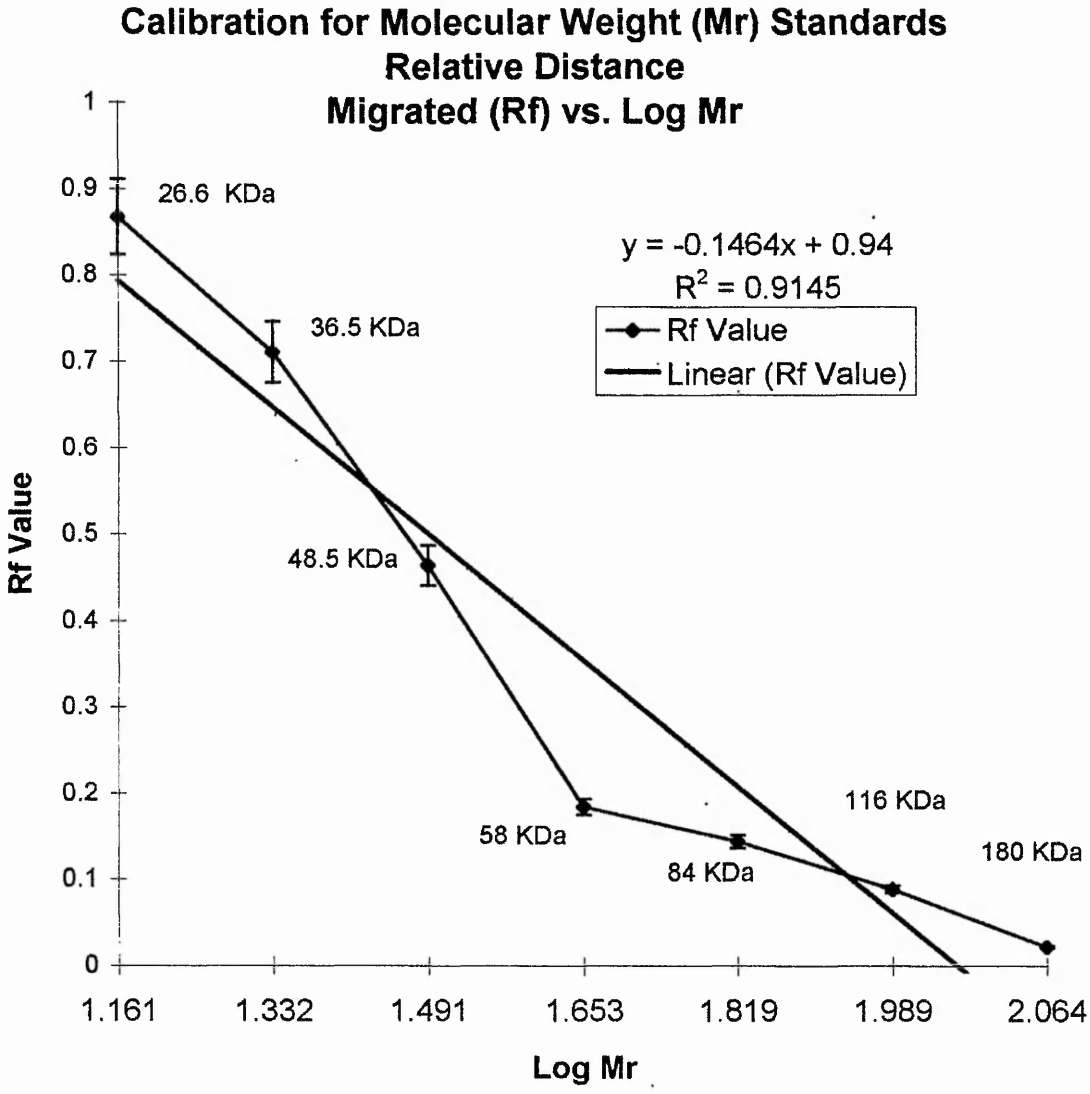

Figure 2.4 Calibration graph for Molecular Weight (Mr) standards, Relative Distance migrated (Rf) vs. Log Mr.

2.3.22.3 Isoelectric Focusing In Rod Gels.

Acrylamide Gel Solution:

30% (w/v) acrylamide	6 ml
H_2O	19 ml
Ampholines (BioRad 3-10)	1.5 ml
1% (w/v) $(NH_4)_2S_2O_8$	1.25 ml

Add up to 2 mg sample protein to 2 ml of gel and pour onto rod.

Electrophorese as follows :-

200V for 15 min

300V for 15 min

400V for 30 min

500V for 30 min

400V for 30 min

Top tank buffer : 0.01 M H_3PO_4 (250 ml) - acidic, pH 3.0

Bottom tank buffer : 0.02 M NaOH (2.5 L) - alkali, pH 10.0

2.3.23 Electroblotting of Protein to Membranes.

USING LKB MULTIPHOR 2 DRY BLOTTER (Pharmacia UK)

1: Saturate the graphite anode and cathode with distilled water. Remove excess with tissue.

2: Cut 6 pieces of filter paper to gel size and soak in either:-

a) discontinuous anode buffer 1

b) continuous buffer

Avoid trapping air bubbles between the papers, by wetting via capillary action. Place on anode plate.

3: Cut 3 pieces of filter paper to gel size and soak in either:-

a) discontinuous anode buffer 2

b) continuous buffer

Avoid air bubbles. Place on anode filter papers.

4: Cut a piece of nitro-cellulose to gel size and soak in either:-

a) discontinuous anode buffer 2

b) continuous buffer

Place on top of filter papers.

5: Soak SDS PAGE in buffer (either discontinuous anode 2 or continuous)and place carefully on nitro-cellulose. To remove air bubbles, wet the gel with buffer and ease the bubbles out.

6: Cut 9 pieces of filter paper to gel size and soak in either:-

a) discontinuous cathode buffer b) continuous buffer

Place on top of SDS PAGE.

7: Place cathode plate on top and connect anode and cathode plate to the electrode pins.

8: Run the blot for 1 hr. at 0.75 mA/cm^2 and then for 20 mins. at 0.6 mA/cm^2.

CONTINUOUS BUFFER:-

Glycine	39 mM
TRIS pH 6.6	48 mM
SDS	0.0375 % (w/v)
Methanol	20% (v/v)

DISCONTINUOUS BUFFER:-

Anode 1		
TRIS	0.3 M	pH 10.4
Anode 2		
TRIS	25 mM	pH 10.4
Cathode		
6-amino-n-hexanoic acid	40 mM	pH 7.6

2.3.23.1 Staining of Protein Membranes

Method 1:-

Stain n/c in amido black solution for 0.5 - 1 min.. Destain to clear background.

Method 2:-

Stain n/c in ponceau red solution for 1 - 5 mins.. Destain to clear background in water. To destain completely wash in TBS with 0.1% Tween.

Amido black:- 0.2g in 200 ml destain.

Destain:-

Methanol	900 ml
Glacial acetic acid	200 ml
Distilled water	900 ml

Ponceau red:- 0.4g in 200 ml water.

2.3.23.2 Immunodevelopment Protocol For Blots - Western Blot

1. After blotting, block remaining protein-binding sites on n/c with solution A at RT. for 60 mins. or overnight at 4°C.
2. Rinse in solution B.
3. Incubate with primary antibody (1/1000 in solution A) overnight at 4°C or for 2 hrs. at 37°C.
4. Wash in solution B for 3x10 mins..
5. Incubate with anti species IgG biotin conjugate (1/1000 in solution B+1% marvel) for 2 hrs. at RT. with gentle shaking.
6. Wash in solution B for 3x10 mins..
7. Incubate with peroxidase labelled streptavidin (1/500 in solution B) for 30 mins. at RT. with gentle shaking.
8. Wash in solution B for 3x10 mins..
9. Rinse in distilled water and then equilibrate in PBS.
10. Incubate with chloronapthol reagent at RT. until colour development (brown, mauve or purple, depending on the state of your colour vision!) - about 15 mins..
11. Stop reaction by washing with distilled water.

SOLUTION A:-

TRIS	100 mM, pH 9.0
NaCl	150 mM
Tween-80	0.05 % (v/v)
Marvel	1 % (w/v)

SOLUTION B:-

TRIS	50 mM, pH 7.4
NaCl	200 mM
Tween-80	0.1 % (v/v)

CHLORONAPTHOL REAGENT:-

4-chloro-1-napthol	20 mg
DMSO	2.5 ml

Add drop-wise to 47.5 ml PBS with constant stirring.

Add 25 µl 3 % (v/v) H_2O_2,use IMMEDIATELY.

2.3.24 RNA Analysis.

During all work with RNA, several practices were maintained in order to protect the samples from contamination and degradation by nuclease enzymes. All glassware was washed and rinsed thoroughly in Ultrapure water (Elga Maxima Ultrapure water, 18.2 MΩ) and then baked and stored at 250°C until required. All plastic-ware used was taken from unopened stocks and autoclaved (121°C, 15 psi, 15 minutes) before use. All chemicals used were obtained nuclease free. Solutions were made up using DEPC (diethylpyrocarbonate) treated autoclaved water (0.001% (v/v) DEPC, 121°C, 15 psi, 15 minutes). Where possible, these solutions were themselves DEPC treated and autoclaved before use (See 2.3.2). Disposable gloves were worn at all times when working with RNA.

2.3.24.1 DEPC Treatment.

Before doing any RNA work, ALL plastic-ware, glassware, and solutions must be treated with DEPC (diethylpyrocarbonate).

To make up DEPC water, add 8 drops DEPC to 1 litre of water, leave overnight in the fume cupboard (with any lids loose), and autoclave.

Soak tips, centrifuge tubes, Eppendorf's, etc. overnight in DEPC + water (8 drops/l) in the fume cupboard. Autoclave.

Always wear gloves when handling DEPC treated items, or those items about to be treated.

2.3.24.2 Extraction of Total RNA from Tissue Using TRIZOL™ Reagent

Total RNA was extracted from tissue samples using TRIZOL™ Reagent (Total RNA Isolation Reagent - Life Technologies). This is a monophasic solution of phenol and guanidine isothiocyanate which allows isolation of total RNA in a single step as modified from Chomczynski and Sacchi (1987).

Tissue sections used for northern analysis were immediately snap frozen and stored in liquid nitrogen on collection. Typically, total RNA was extracted from tissue sections of 150-200 mg. A volume of 1 ml of TRIZOL™ Reagent was used per 50-100 mg of tissue and the amounts of subsequent reagents used were determined according to the initial volume of TRIZOL™ Reagent.

A single frozen tissue sample was placed in a sterile, disposable tube, containing the appropriate amount of TRIZOL™ Reagent and homogenised completely (Ultra Turrax T25 homogeniser, 24000 min^{-1}, 3 x 5 second bursts). The homogenate was incubated for 5 minutes at room temperature to allow complete dissociation of nucleoprotein complexes.

200 µl of chloroform per 1 ml TRIZOL™ Reagent used initially was added to produce dissociation of the phenol and aqueous phases. The sample was shaken vigorously by hand for 15 seconds, incubated at room temperature for a further 3 minutes, and then centrifuged at 12000 x g for 15 minutes at 4°C (Jouan MR22*i*, 6 x 50 ml rotor pre-cooled to 4°C). This separated the sample into two distinct phases; an upper, aqueous, RNA-containing phase, an interface containing DNA and denatured proteins, and a lower, phenol-chloroform organic phase containing protein.

The upper aqueous phase was transferred to a fresh tube and 500 µl of propan-2-ol (isopropanol) per 1 ml TRIZOL™ Reagent used in the initial homogenisation was added to this and mixed well to induce precipitation of the RNA. The samples were incubated for 10 minutes at room temperature, or more preferably, for 45 minutes at 4°C, to allow complete precipitation of the RNA.

The precipitate was harvested by centrifugation at 12000 x g for 10 minutes at 4°C (Jouan MR22*i*, 6 x 50 ml rotor pre-cooled to 4°C). The resulting RNA pellets were washed with 1

ml 70% ethanol per 1 ml of TRIZOL™ Reagent and allowed to partially dry before being re-dissolved in DEPC treated water. The pellets were not allowed to dry totally as this resulted in a significant reduction in the solubility of the RNA, making re-dissolving the samples very difficult. The samples were incubated for 5 minutes at 65°C to ensure complete re-dissolution and were then stored at -80°C until required.

The optical density of the RNA samples at 260 nm and 280 nm (corresponding to the peak absorbance wavelengths for RNA and protein respectively) was used as an assessment of their concentration and purity. Samples were diluted 1 in 100 in DEPC treated water and the absorbance of each was read at 260 nm and 280 nm (scanning spectrophotometer). On a 1 cm light path:

The A_{260nm} of a 50 μg/ml RNA sample = 1 unit

RNA concentration (μg/ml) = A_{260nm} x 50

$$\text{RNA concentration } (\mu g/\mu l) = \frac{A_{260nm} \times 50}{1000}$$

$$\text{RNA concentration } (\mu g/\mu l) \text{ of a sample diluted 1 in 100} = \frac{A_{260nm} \times 50 \times 100}{1000}$$

$$= A_{260nm} \times 5.$$

The A_{260nm} : A_{280nm} ratio provides information on the purity of the RNA sample, where a ratio of > 1.9 indicates pure RNA and a ratio of < 1.9 indicates some degree of contamination with protein/phenol.

2.3.24.3 RNA Denaturing Agarose Gel Electrophoresis.

The Hoefer (Hoefer Scientific Instruments, 654 Minnesota Street, San Francisco, CA 94107) large horizontal gel system, having a 20 cm x 20 cm gel bed were used for the electrophoresis of RNA. All apparatus was washed using RNAse AWAY™ (Molecular Bio Products) and rinsed thoroughly with DEPC treated water to ensure it was free from endonucleases.

Gels of 300 ml and 400 ml volumes were used consisting of 1% (w/v) agarose, 1X MOPS buffer (diluted from a 10X stock ; 200 mM MOPS, 50 mM sodium acetate, 10 mM EDTA) and 2% (v/v) formaldehyde (diluted from a 37% stock). The agarose and MOPS were mixed, heated to boiling point and allowed to simmer until the agarose had completely dissolved. This was then heat-cooled to 50°C, at which point the formaldehyde was added. The gel was poured and allowed to harden for 1 hour. 2 L of 1X MOPS buffer was used as the electrophoresis running buffer.

RNA samples of typically 25 µg were prepared in DEPC treated water ideally within a volume of 5 -10 µl and not exceeding 20 µl. To each sample, 35 µl of sample buffer (0.005% (w/v) ethidium bromide, 50% (v/v) deionised formamide, 1X MOPS buffer, 6% (v/v) formaldehyde, 3.6% (w/v) Ficoll, 1.25 mM EDTA, 0.006% (w/v) bromophenol blue) was added. The samples were then incubated at 65°C for 15 minutes to abolish any secondary structure of the RNA before being loaded into the gel wells and electrophoresed at a constant voltage, typically 95 V. The current was maintained below 2.5 mA per cm^3 to avoid the gel overheating which would result in breakdown of the gel matrix and poor resolution of the RNA samples.

When the gel had run the required distance, approximately 1 cm short of the edge of the gel as indicated by the bromophenol blue front, it was viewed and photographed on a UV transilluminator (UVP). The 28s and 18s rRNA subunits were visible as intense, discreet bands approximately in a ratio of 2:1, at 5 kb and 2 kb respectively,. The mRNA was seen as a feint smear along the entire length of each lane.

2.3.24.4 Capillary Transfer Of RNA From Agarose Gels To Nylon Membranes

The RNA was transferred to Hybond-N nylon membranes (Amersham Life Sciences) by capillary blotting, using the assembly as illustrated in figure 2.1.3.1. The gel was rinsed in 20X SSC (3.0 M NaCl, 0.3 M sodium citrate, pH 7.0) and inverted onto a Whatman 3 MM filter paper wick, pre-wetted with 20X SSC. This wick was supplied with transfer buffer from a 1.5 - 2 L reservoir of 20X SSC. The gel was surrounded completely with cling film to prevent the flow of buffer short-circuiting the gel and passing directly to the absorbent material above, and therefore reducing the transfer of RNA from the gel to the nylon. A Hybond-N nylon membrane was placed on top of the gel, followed by a double thickness of Whatman 3 MM filter paper, all of which were pre-wetted with 2X SSC. This was followed by a stack of dry paper towels and an evenly distributed weight of 0.5-1 kg to aid the capillary action.

The transfer was left to proceed overnight, after which the gel and nylon membrane were viewed under UV light to ensure complete transfer had occurred. The banding pattern originally seen on the gel was transferred to the nylon membrane, and the gel now showed no fluorescence below 15 kb.

The nylon membrane was dried by baking at 80°C for 10 minutes and the RNA was crosslinked to the nylon membrane by 700 000 Joules ultraviolet irradiation (Amersham Life Science Ultraviolet Crosslinker). The membranes were then either probed immediately, or stored at room temperature in clean Whatman 3 MM filter paper until required.

2.3.25 DNA Analysis.

Preparations of cellular DNA were prepared to confirm the presence of apoptosis. DNA was extracted using the Stratagene DNA extraction kit (Stratagene, 11011 North Torrey Pines Road, La Jolla, CA 92037). The total cellular DNA was quantitated using the method for the Hoefer TKO 100 minifluorimeter, (Hoefer Scientific Instruments, 654 Minnesota Street, San Francisco, CA 94107) to ensure loading of equal amounts of DNA. Samples of the DNA were subjected to standard agarose electrophoresis and the DNA visualised by ethidium bromide staining (59).

2.3.25.1 Extraction of DNA from Cells for Endonucleased DNA Ladders.

After the method of Stratagene DNA Extraction Kit (Cat # 200600) Stratagene, 11011 North Torrey Pines Road, La Jolla, CA 92037).

Sample size : 1 X 10^8 cells per extraction, to yield 600 - 1000 µg DNA

1. Harvest cells from cell culture vessel
2. Pellet cells at 350g (1500 rpm with a Sorvall JS5.2 rotor) at 4°C for 15 minutes.
3. Discard supernatant and resuspend cells in 2 ml PBS
4. Repeat step 2
5. Sonicate in 1 ml of Solution 1, then make-up volume to 11 ml
6. Add Pronase to the sonicated pellet to yield a final concentration of 100 µg / ml
7. Incubate at 60°C with shaking for 1 h, or at 37°C overnight
8. Chill on ice for 10 min
9. Add 4 ml of Solution 2, Invert several times to mix
10. Sit on ice for 5 min
11. Pellet the precipitate at 2000g (3400 rpm with a Sorvall JS5.2 rotor) at 4°C for 15 minutes
12. Transfer supernatant using a large bore pipette to a sterile 50 ml conical tube

13. Add RNAse A to supernatant to yield a final concentration of 20 µg / ml
14. Incubate at 37°C for 15 min
15. Precipitate DNA by adding 2 volumes of 100 % ethanol to supernatant. Invert gently until the DNA precipitates (a "hair ball" will form).
16. Remove DNA by spooling out with a clean glass rod
17. Rinse DNA on rod with 70 % ethanol. Dry by briefly touching with a tissue
18. Resuspend the DNA in 500 µl of Tris-EDTA buffer. [10 mM Tris, 0.1 mM EDTA pH 8.0]. Mix sample by gentle inversion, do not vortex or pipette sample, store at 4°C.

Notes:

To avoid shearing genomic DNA during transfer, use wide-bore tips at all times. Transfer of DNA in step 12 should be done trying to avoid carry-over of any contaminating material which will contain protein contaminants. If DNA does not visibly ppt. in step 15, place tube at -20°C for a minimum of 2 h or overnight. Pellet DNA by spinning at 2000g for 20 minutes.

Reagent Composition;

Solution 1	50 mM Tris-HCl, pH 8.0
	20 mM EDTA, pH 8.0
	2 % (w/v) SDS
Solution 2	Saturated NaCl
RNAse A	10 mg/ ml stock
Pronase	225 mg / ml stock

Store solutions 1 and 2 at room temperature, aliquot enzymes and store at -20°C.

2.3.25.2 Production of cDNA Probes

cDNA probe templates were cut from the appropriate plasmid vector by restriction enzyme digestion, in the presence of the optimum buffer from Appligene's 5-Buffer System. Digests were allowed to proceed for 2 hours at 37°C.

2.3.25.3 Isolation of the 2.6 Kbp EcoRI/Hind III Human Tissue Transglutaminase Fragment from hTG1

The digest contained 30 µg of the plasmid hTG1, 100 units of EcoRI and 60 units of Hind III in 1X Appligene Buffer # II (10 mM Tris-HCl, 50 mM NaCl, 10 mM $MgCl_2$, 10 mM 2-Mercaptoethanol, 0.1 mg/ml BSA, pH 8.0). The digest yielded a 2.8 Kbp fragment of human tissue TGase cDNA obtained by digestion of the TGase clone hTG1, a full-length clone isolated from human endothelial cell library (57).

2.3.25.4 Isolation of the cDNA Probe Template from the Restriction Digest

Agarose gel electrophoresis was used to separate the cDNA probe template from the digest and this was subsequently isolated from the gel using the Promega BandPrep kit.

2.3.25.5 Agarose Gel Electrophoresis of DNA

The BioRad Minigel Submarine System was used for the electrophoresis of DNA. A 1% (w/v) agarose, 1X TAE (diluted from a 50X TAE stock containing 2 M Trizma base, 5% (v/v) Glacial acetic acid, 0.05 M EDTA, pH 8.0) was prepared, to which ethidium bromide was added to a final concentration of 0.5 µg/ml prior to pouring. The running buffer was 1X TAE, 0.5 µg/ml ethidium bromide. 30 µl of 6X blue/orange DNA loading dye (10% (w/v) Ficoll 400, 0.25% (w/v) bromophenol blue, 0.25% (v/v) xylene cyanol FF, 0.4% (w/v) orange G, 10 mM Tris-HCl (pH 7.5), 50 mM EDTA) (Promega) was added to the digest and this mixture was loaded, 30 µl per well, onto the gel. [6 µl of (ϕX174RFDNA/HaeIII fragments) were used. as DNA molecular weight markers (Promega)] The gel was electrophoresed at a constant voltage of 80 V until the bromophenol blue front had run to approximately 1 cm short of the edge of the gel. The gel was then viewed on a UV transilluminator to confirm that digestion had occurred, in which case distinct bands were seen at appropriate weights, representing the cDNA insert and the cut plasmid.

2.3.25.5.1 Isolation of DNA from Agarose Gels

The required band was cut from the gel using a sterile scalpel blade and the DNA was extracted from the gel using the Sephaglas™ BandPrep kit (Pharmacia Biotech.). This kit uses a glass matrix, Sephaglas BP, and sodium iodide based on the method described by Marko, M.A., et al., (1982).

The agarose containing the DNA was dissolved by incubation at 60°C for 5-10 minutes in 1 µl of Gel Solubilizer (6 M NaI, 50 mM Tris-HCl (pH 8.0), 0.05% (v/v) Na_2SO_3, 10 mM EDTA) per mg of gel. 5 µl of a uniform suspension of Sephaglas BP (20% (w/v) Sephaglas BP suspended in 6 M NaI, 50 mM Tris-HCl (pH 8.0), 0.05% (v/v) Na_2SO_3, 10 mM EDTA) was added per µg of DNA present. This was incubated for 5 minutes at room temperature to allow the DNA to bind to the Sephaglas BP, mixing every minute to resuspend the Sephaglas BP. The Sephaglas BP matrix bound DNA was then collected by pulse centrifugation at 1260 x g (MSE Micro Centaur, 5000 rpm, 12 x 1.5 ml rotor) and the supernatant containing the dissolved gel and Gel Solubilizer was discarded. The DNA containing pellet was washed twice with Wash Buffer (20 mM Tris-HCl (pH 8.0), 1 mM EDTA, 0.1 mM NaCl, 60% (v/v) ethanol) where 8 x the volume of Sephaglas was used, to remove any gel contaminants. This was then allowed to air dry before the DNA was retrieved with Elution Buffer (10 mM Tris-HCl (pH 8.0), 1 mM EDTA), using 2 x the Sephaglas BP volume. The pellet was mixed with the Elution Buffer, incubated for 5 minutes at room temperature with periodic agitation, and then centrifuged at 7571 x g for 1 minute (MSE Micro Centaur, 13000 rpm, 12 x 1.5 ml rotor). The DNA containing supernatant was removed and the elution procedure was repeated on the pellet. A second TAE gel was run using a 5 µl sample of the purified cDNA to check the quality and estimate the quantity of DNA present. The DNA was stored at -20° until required.

2.3.25.5.2 Production of Radiolabelled cDNA Probes

[α-^{32}P]dCTP labelled probes, with specific activities of 1.0 to 1.8 x 10^9 cpm/µg, were synthesised using the Promega Prime-a-Gene® Labelling System. The method uses a mixture of random hexa-nucleotides to prime DNA synthesis from a linear double stranded DNA template (Feinberg, AP, Vogelstein, B., 1983).

A sample containing 25 ng of the cDNA template in 25 µl of Labelling Buffer giving a final concentration in the complete reaction mixture of 1X (diluted from a stock of 5X Labelling buffer: 250 mM Tris-HCl (pH 8.0), 25 mM $MgCl_2$, 10 mM DTT, 1 M HEPES (pH 6.6), 26 $Absorbance_{260\ nm}$ units/ml Random Hexa-deoxyribonucleotides) was prepared, to which was added the non-labelled nucleotides dATP, dGTP and dTTP to a final concentration of 20 mM each. The template was denatured by boiling for 3 minutes and then cooling rapidly on ice. Following denaturation, nuclease free BSA was added to a final concentration of 400 µg/ml. Klenow, the large fragment of DNA polymerase I containing exonuclease, but lacking endonuclease activity, was added to a final concentration of 100 units/ml. 25 µCi of [α-^{32}P]dCTP was added, giving a final CTP concentration of at least 333 nM. The reaction was allowed to proceed for 1-3 hours, after which little further probe was synthesised. Any un-incorporated labelled nucleotides were removed by size occlusion chromatography using Sephadex® G-50 NICK™ columns (Pharmacia Biotech) to minimise problems of non-specific binding during probing. The column was rinsed out and equilibrated with TE (10 mM Tris, 1 mM EDTA). The reaction mixture was pipetted onto and allowed to enter the gel bed and was then washed in with 400 µl TE. The labelled probe was then eluted with a second 400 µl volume of TE.. The 400 µl of probe collected was then ready for use in a hybridisation reaction.

2.1.25.6 Hybridisation of Radiolabelled cDNA Probes to RNA Attached to Nylon Membranes (Northern Blotting).

Hybridisation reactions were performed using a thermostatically controlled laboratory oven. Nylon membranes were pre-hybridised at 42°C for 1 hour in rotating hybridisation chambers containing 10 ml of 50 % (v/v) deionised formamide, 5X SSPE (diluted from a 20X SSPE stock containing 3.6 M NaCl, 0.2 M NaH_2PO_4, 0.02 M EDTA, pH 7.4), 1 % (w/v) SDS (sodium dodecylsulphate diluted from a 20 % stock), 5X Denhardt's Reagent (diluted from a 100X stock containing 2 % (w/v) Ficoll, 2 % (w/v) polyvinylpyrolidine, 2 % (w/v) BSA), to which was also added 200 µl of denatured, sonicated herring sperm DNA.

Following pre-hybridisation, the solution in the chambers was replaced with the complete hybridisation buffer. This contained all the components of the pre-hybridisation buffer with the addition of the radiolabelled cDNA probe which had been denatured by boiling for 3 minutes and immediately cooling on ice. Hybridisation was allowed to proceed overnight at 37 or 42°C, dependent on the probe being used.

The optimum hybridisation temperature was that which resulted in maximal specific binding of the probe to its target , while maintaining minimal binding of the probe to non-specific sites. This was dictated by properties of the individual probes, such as size and the degree of sequence homology between the probe and its target. In general, for large or highly homologous probes it was possible to hybridise at a higher temperature than for shorter or less homologous probes.

Following hybridisation, the membranes were washed twice in 2X SSPE, 0.2 % (w/v) SDS at room temperature for 10 minutes. Two further 30 minute washes were carried out at a stringency optimum for each probe, where wash stringency is increased with increasing temperature and decreasing SSPE concentration.

Following washing, the membranes were removed from the hybridisation chambers and placed between clean Whatman 3 MM paper to remove any excess moisture. The membranes were sealed in cling film to prevent complete dehydration and exposed to Kodak X OMAT AR and LS, or Kodak Biomax MS film in autoradiography cassettes fitted

Provided the membrane was not allowed to dry out completely, it was possible to strip a particular membrane of its bound probe and re-use that membrane in a further hybridisation reaction. Stripping was done by the addition of a boiling solution of 0.1% (w/v) SDS to the membrane which was then allowed to cool with gentle agitation (IKA Labortechnik KS250 Basic, 50-100 rpm.).

3.0 Investigation of the Relationship Between The Amount of Apoptotic SDS / Insoluble Polymer Found in Rat Liver and the Stage of Hepatocarcinoma as Induced by a Diet of 2-Acetylaminofluorene (2-AAF).

3.1 Introduction.

3.2 Results.

- 3.2.1 Production of antibodies to tTGase-mediated products.
- 3.2.2 Standardisation of the anti-apoptotic envelope antibody.
- 3.2.3 Standardisation of the anti-SDS/insoluble antibody.
- 3.2.4 Calibration of quantitative ELISA for tTGase-mediated products.
- 3.2.5 Propagation of rat hepatocellular carcinomas using the 2-AAF model.
- 3.2.6 DNA analysis of tumour homogenates.
- 3.2.7 Quantitation of apoptotic tTGase-mediated products using anti-envelope antibody ELISA.
- 3.2.8 Quantitation of SDS/insoluble tTGase-mediated polymer using anti-polymer antibody ELISA.
- 3.2.9 In situ localisation of tTGase-mediated products with rat hepatocellular carcinoma samples via immunohistochemistry.

3.3 Discussion.

3.1 Introduction.

It is now evident that the major reason for the paradoxically slow growth of many tumours is the high rate of cell loss (Moore 1987). This is contrary to the original perception of Iverson in 1967, who suggested that although cancer is perceived as a tissue that grows faster than its tissue of origin; it should be more correct to think of a malignant tumour as a tissue that has a slight cell loss. Thus it is conceivable that many tumours survive not simply because of a particularly high rate of cell proliferation, but rather because of a precarious balance in the processes of production and loss. Therefore, it is acceptable to evaluate the malignancy of tumours by analysis of rate of cell proliferation balanced against the rate of cell loss.

Neoplastic growth is balanced by rates of cellular differentiation, migration., mitosis and cell removal via either necrosis (death) or apoptosis (programmed cell death), Wyllie (1981). Such cell removal in a tumour has been shown to be induced by increasing the amount of apoptosis. This has been achieved in a number of neoplastic cells for example hormone-responsive tumours which undergo apoptosis *in vivo* with the appropriate stimulus. An example being the glucocorticoid-induced death of chronic B lymphocytic leukaemia cells (Mc.Conkey *et al* 1991). So that by increasing the rate of cell loss, one may cause a tumour to regress.

Electron microscopy studies have shown that apoptotic bodies from tumour cells are the same in structure as those cell fragmentation bodies derived from non-neoplastic cells; also that the majority of these bodies are rapidly taken up by the phagocytosis action of neighbouring cells (Kerr *et al* 1972).

Tissue transglutaminase expression has been shown to be involved in apoptosis by the action of crosslinking protein substrates into an SDS-insoluble envelope - the "apoptotic body". These envelopes have been characterised as having a high concentration of ε(γ-glutamyl) lysine isodipeptide crosslinks (Piacentini *et al* 1991, Knight *et al* 1991). A further transglutaminase-mediated product that can be isolated from tissue is a large, highly crosslinked, fibrous polymeric version of these apoptotic envelopes (Hand *et al* 1988, Knight *et al* 1993). In mammalian systems, an increased expression of hepatic transglutaminase mRNA has been associated with the occurrence of apoptosis during regression of liver hyperplasia (Fesus *et al* 1987). The finding of increased expression of proto-oncogenes or cell-cycle related genes during cell death by apoptosis supports the concept that cell death is an active process that requires cell proliferation.

The work of Ledda-Columbano *et al* (1989) has suggested that it would be of interest to investigate whether hepatic necrosis could be discriminated from apoptosis on the basis of the levels of serum transaminases e.g. transglutaminase..

Previous work from this laboratory (Barnes *et al* 1985, Hand *et al* 1987,1988) have used models of hepatocarcinogenesis to investigate the role of tTGase in tumour malignancy and metastasis. Their findings show the existence of two compartmentalised forms of the enzyme subsequently termed the cytosolic fraction and the nuclear membrane-bound or particulate fraction. Activity levels were found to be reduced by 65% in hepatocellular carcinomas when compared to normal liver, of the activity remaining the particulate form of the enzyme represented 95% of total activity. This finding has since been linked to the metastatic potential of solid tumours, where an inverse relationship exists between the levels of tTGase activity and the ability of a primary tumour to metastasise (Knight *et al* 1993).

A link between tTGase , tumour metastases and apoptosis having been postulated by the work of this laboratory and that of Fesus and Piacentini; it was therefore hypothesised that the lowering of tTGase in the tumour could cause a resultant drop in apoptosis which creates an imbalance in the proliferation / death ratio. An imbalance which may favour the progressive growth of the neoplasm, enhancing the risk of metastases.

This study aims to investigates the degree of apoptosis produced and its localisation within the neoplasms produced in the rat liver after the chronic administration of the carcinogen 2-acetylaminofluorene (2-AAF). It also examines if a link exists between apoptosis and levels of tTGase activity which could influence the proliferation / death ratio in favour of tumour progression.

3.2 Results.

3.2.1 Production of antibodies to tTGase-mediated products.

In order to evaluate the 2-AAF model of rat hepatocarcinogenesis it was first necessary to produce two antibodies raised to tTGase-mediated products, which could then be used for immunological quantitation via ELISA and *in situ* detection via immunohistochemistry. As described previously transglutaminase catalyses a reaction which produces an insoluble isodipeptide linkage - ε(γ-glutamyl) lysine which leads to the stabilisation of multimeric aggregates. Significant levels of this crosslink have been found in apoptotic envelopes isolated from cell culture (Fesus *et al* 1990) and in an SDS-insoluble polymer isolated from tissue samples (Hand *et al* 1991). Thus, these two structures have been deemed to be formed by transglutaminase-mediated processes, hence they were chosen as markers for transglutaminase activity in this study. The two antibodies used were coded as follows :-

i) Anti-apoptotic envelope antibody, raised to SDS-insoluble apoptotic envelopes isolated form BHK-21 fibroblasts grown in culture, as described in section (2.3.2.1). Referred to henceforth as the **"envelope"** antibody.

ii) Anti-SDS/Insoluble polymer antibody, raised to the large (2×10^6 KDa) polymeric material isolated from normal rat liver, as described in section (2.3.10). Referred to henceforth as the **"polymer"** antibody.

The methods of production and purification of both antigens and antibodies are described in sections 2.3.9 to 2.3.12 inclusive.

3.2.2 Standardisation of the anti-apoptotic envelope antibody.

An immortalised normal fibroblastic cell lineage, isolated from the kidneys of 21 day old baby hamsters (BHK-21) was grown as described in section 2.3.1.1. The method of Schmitz *et al* 1987 (2.3.11) was used to isolate apoptotic envelopes from sub-confluent cultures (80% confluency) of BHK-21. The isolation principle relies on the following fact; the presence of a high density of ε(γ-glutamyl) lysine dipeptide bonds within proteinous structures, renders them insoluble in chaotrophic agents such as reducing SDS and

Thus this level of fluorescence is in close agreement to published data and confirms the belief that formation of such apoptotic envelopes involves a tTGase-mediated catalytic reaction.

3.2.3 Standardisation of the anti-SDS/insoluble antibody.

The high molecular weight SDS/insoluble polymer was extracted and purified according to the method set out in section 2.3.10.1 This antibody was prepared in our laboratory by Dr. CRL Knight, its specificity has previously been shown to the SDS/insoluble polymer (Maxwell *et al* 1991, Knight *et al* 1993). Confirmation of this is shown in chapter 7 (section 7.2.2) where Western blot immunological probing of rat liver homogenates is described. The size of the polymer prevents it entering the resolving gel during PAGE, experiments using a calcium ionophore A23187 show a time- and dose-dependent accumulation of the polymer from rat liver following incubation with, biotin-cadaverine, an amine substrate donor of transglutaminase (section 7.2.2).

Plate 3.2. parts 1-6 show light micrographs of extracted polymer from rat liver (X200 magnification). Due to the complex nature of the polymer it was necessary to characterise its component parts. Thus, immunofluorescent staining was carried out as described in section 2.3.14, using a number of monoclonal antibodies raised to cytoskeletal proteins. Plate 3.2 part 1 shows a phase contrast image of unstained polymer. Non-specific binding of the FITC conjugates and antibodies was assessed using the IgG_1 isotype control antibody CUB11, the level of background staining can be seen in plate 3.2 part 2. The reactivity of the polymer to actin, alpha tubulin, cytokeratin and fibronectin are shown in plates 3.2 parts 3-6 respectively; from the pattern of staining it is evident that each of these structural proteins are components found within the polymer. This finding supports the work of Aeschilmann and Paulson (1994) who found that each of these proteins when tested individually are substrates of tissue transglutaminase.

3.2.4 Calibration of quantitative ELISA for tTGase-mediated products.

A standard ELISA protocol was developed (2.3.13) using the envelope and polymer antibodies to quantitate the amount of each found in samples of tissues extracted from rats in which hepatocellular carcinoma has been induced after oral administration of 2-acetyl aminofluorene (2-AAF). Each of the test bleeds and final bleed for the anti-envelope serum were screened in the ELISA method against constant protein loading of apoptotic envelope

Plate 3.1 Morphology and immunohistochemical staining of isolated apoptotic envelopes from BHK-21.

1. An unstained envelope, viewed by bright field light microscopy, isolated via the SDS/DTT boiling method (section 2.3.11); the bar is 8μm in length and indicates the average size of an envelope.

2. An envelope, viewed by epifluorescence that has been stained with non-immune rabbit serum with FITC secondary antibody as a control of non-specific binding in the assay (method 2.3.14.3).

3. An apoptotic envelope positively stained with the anti-apoptotic envelope antisera.

4. An envelope that has been stained with a monoclonal antibody raised to the transglutaminase-mediated crosslink, ε(γ-glutamyl)lysine. A kind gift from Dr. Said El-Alaoui.

The reactivity, and specificity of the anti-envelope antisera has been proved for the isolated envelopes raised *in vitro*. Furthermore, the good degree of staining by the monoclonal antibody to the transglutaminase-mediated product, gives strong evidence for the envelopes themselves being formed by the action of transglutaminase. All photographs are at a magnification of X400 and have been exposed for a period of 2 minutes under the ultraviolet light-source of the Leitz Dialux microscope. The filter cube fitted allowed the FITC to absorb light at 488 nm and emits light at 517 nm.

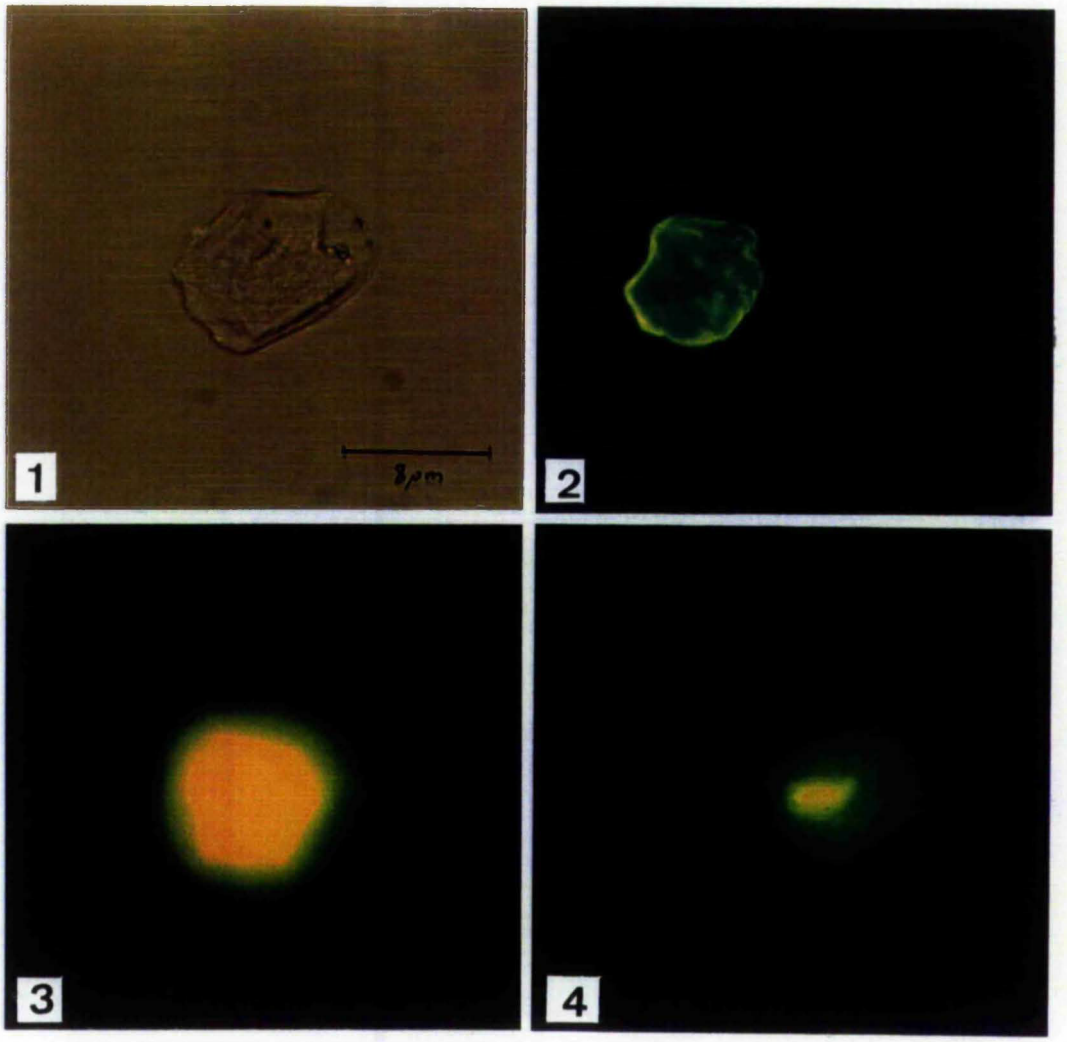
1
8 µm
2
3
4

guanidine hydrochloride; by applying this principle apoptotic envelopes (which are known to be rich in these bonds) were isolated.

Plate 3.1 (1-4) shows a light micrograph of an isolated apoptotic envelope (x400 magnification) During isolation DNA extracted from the previously intact cell and cause the envelopes to clump, thus to maintain an homogenous preparation for immunisation, DNAse I is added to the preparation during isolation. Boiling of the preparation denatures the DNAse I while leaving the envelopes intact. Comprehensive, sequential proteolytic digestion of isolated apoptotic envelopes (section 2.3.9.1) may then be performed prior to quantitation of the ε(γ-glutamyl) lysine content by either amino acid analysis or reversed phase HPLC (section 2.3.9.3). Following proteolytic digestion the total protein content may be determined by standard Biuret and Lowry techniques (sections 2.3.6.1 & 2).

Having isolated and purified a large number of apoptotic envelopes from sister cultures of BHK-21, these were used to raise a polyclonal antibody in New Zealand white rabbits (2.3.12). After recovery of the rabbit serum via cardiac puncture, the IgG fraction was purified by a combination of ammonium sulphate precipitation (2.3.12.1) and immunoaffinity chromatography (2.3.12.2).

To confirm the reactivity of the IgG fraction, immunofluorescence staining was carried out against an aliquot of envelopes used for immunisation. Plate 3.1 part 2 and 3.1 part 3 show the reactive epifluorescence obtained following staining of envelopes according to the method set out in 2.3.14.3. Plate 3.1 part 2 shows the background signal obtained through non-specific binding of the FITC-conjugated reagents, the outline of an intact apoptotic envelope can clearly be seen. Plate 3.1 part 3 has an apoptotic envelope staining positively with the anti-envelope antibody, strong epifluorescence masks the outline of the envelope.

Further immunological confirmation was carried out by repeating the fluorescent staining replacing the anti-envelope antibody with a monoclonal antibody which react with to tTGase-mediated ε(γ-glutamyl) lysine dipeptide (Mab 81d1c2 a kind gift of Dr. S. El-Alaoui). Plate 3.4 shows positive reactivity of the monoclonal antibody raised to the dipeptide; the fluorescence produced is confined to a small area of the apoptotic envelope this result is in agreement with the observations of Fesus and Tarsca 1989 who found 1 nmol / 2 x 10^7 in digested envelopes from Chinese hamster ovary cells to be ε(γ-glutamyl) lysine. Due to the "small" size of the dipeptide and taking into account that the envelope is still intact the numbers of "immunologically visible" epitopes for this monoclonal antibody will be low.

Plate 3.2 Physical appearance and characterisation of the high molecular weight SDS / insoluble polymer isolated from rat liver samples.

1. Unstained polymer isolated by the method of 2.3.10.1, viewed by phase contrast light microscopy, photographed under a wet mount at a magnification of X200.

2. Polymer stained with monoclonal antibody CUB 11, a non-reactive isotype control (dilution 1:5) followed by anti-mouse FITC secondary antibody (method 2.3.14.3) as a control of non-specific binding, photographed at a magnification of x200.

3. Polymer stained with monoclonal antibody raised against actin (dilution 1:5) followed by anti-mouse FITC secondary antibody (method 2.3.14.3) photographed at a magnification of x400.

4. Polymer stained with monoclonal antibody raised against alpha tubulin (dilution 1:10) followed by anti-mouse FITC secondary antibody (method 2.3.14.3) photographed at a magnification of x400.

5. Polymer stained with monoclonal antibody raised against cytokeratin (dilution 1:10) followed by anti-mouse FITC secondary antibody (method 2.3.14.3) photographed at a magnification of x400.

6. Polymer stained with monoclonal antibody raised against fibronectin (dilution 1:5) followed by anti-mouse FITC secondary antibody (method 2.3.14.3) photographed at a magnification of x400.

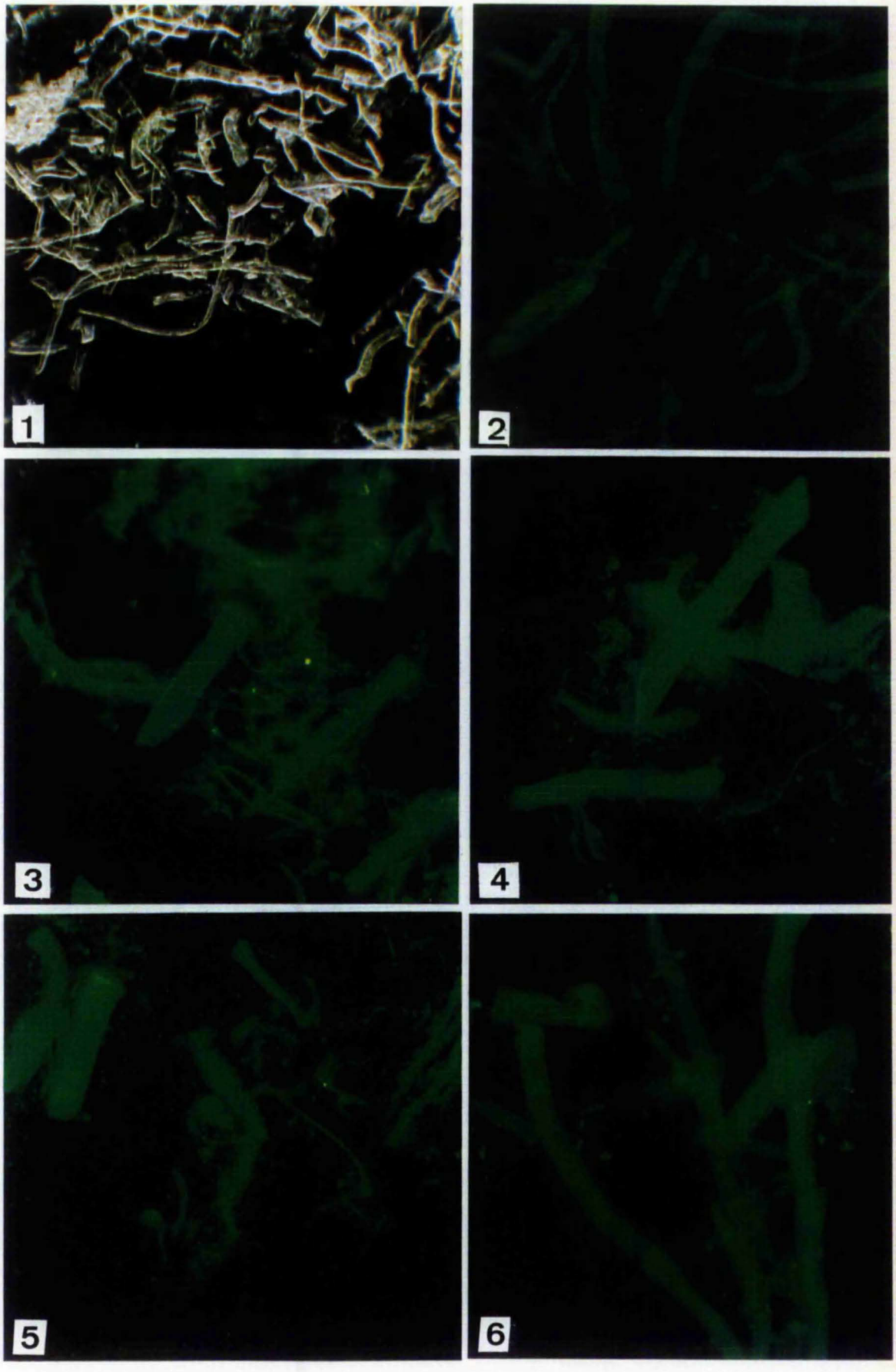
1
2
3
4
5
6

antigen (100 ng / well). Figure 3.1 shows the reactivity of the test bleeds, in absorbance units at 450 nm. The bleeds were taken six weeks apart, a gradual increase in the titre of reactive antibodies can be seen as the immunisation progressed. Also titration of reactivity can be seen as the dilution of antibody is tested from 1:10 to 1:100,000. From this figure the dilution of 1:1000 was selected for all further ELISA analyses.

Having now established that both the anti-envelope and anti-polymer antisera were reactive to their specific antigens namely, isolated apoptotic envelopes from BHK-21 in cell culture and extracted SDS/Insoluble polymer from rat liver. It was necessary to test the cross-reactivity of the antibodies to samples of the tTGase-mediated products to which they were not initially raised. Figure 3.2 shows the cross-reactivity of both the anti-envelope and anti-polymer antisera at dilutions of 1:1000 against a titration of antigen coating the wells (3.7 ng / well to 10 µg / well). From this figure it can be seen that both anti-sera cross-react with the two antigens. Thus, inferring that both the polymer and envelope are composed of similar protein structural components. Indeed when analysed for amino acid composition the two antigens show 85% homology for amino acid content (Hand *et al* 1994). What is also evident from the graph shown in Figure 3.2 is the degree of sensitivity of each antibody. The envelopes being relatively large intact structures, it conceivable that many of the epitopes, which are reactive to the anti-polymer are stearically hidden; similarly if you think of the polymer as the building-block components of an envelope prior to construction when reacted with the anti-envelope antibody the reactivity is reduced.

Having now determined the reactivity, cross-reactivity and specificity of the two antisera it was necessary to construct calibration graphs in order to quantitate the amount of each antigen detected in the tissue homogenates. Figure 3.3 shows the calibration graph for the anti-envelope antibody to SDS/insoluble rat liver polymer and Figure 3.4 shows a similar calibration graph for the anti-polymer antibody. Using these two graphs it was possible to determine the amounts of each tTGase-mediated product found in the experimental rat liver samples.

Figure 3.1 Titration of the serum collected from test bleeds and final bleed of the New Zealand white rabbit immunised with isolated apoptotic envelopes from BHK-21 fibroblast grown in cell culture (Sections 2.3.11, 2.3.12) Each test bleed was taken six weeks following sub-cutaneous injection of the antigen. Dilution of the sera was over the range 1:10 to 1:100,000 in PBS. 50µl volumes of each dilutions were screened using the ELISA method set out in 2.3.13 against 10µg / well of isolated apoptotic envelopes, a clear increase in antibody titre can be seen with progression of the immunisation schedule.

Screen of Test Bleeds vs. Apoptotic Envelopes

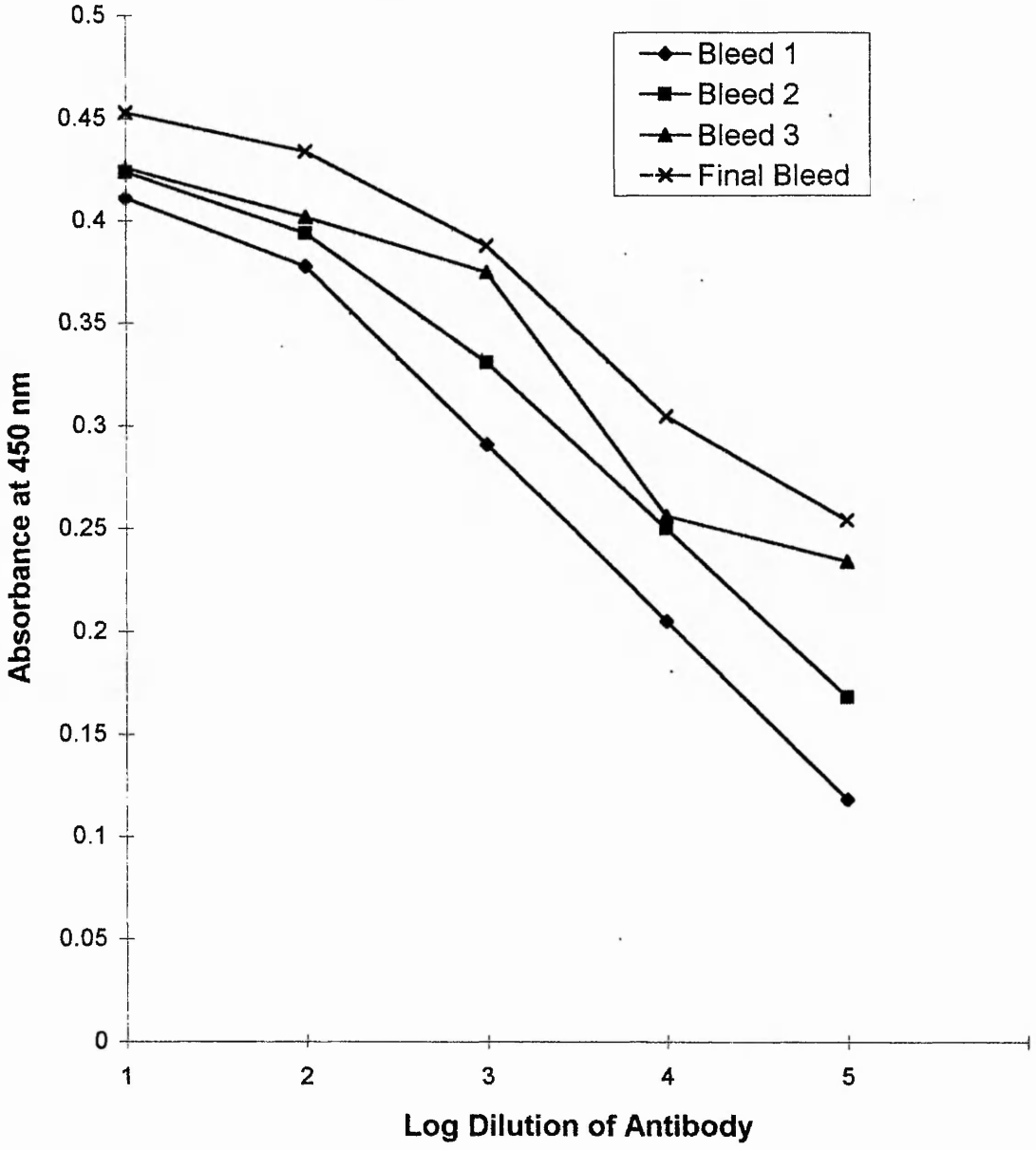

Figure 3.2 Analysis of the cross-reactivity of the anti-envelope antibody and anti-polymer antibody to their correct and incorrect antigens. The ELISA method of 2.3.13 was used to screen 1:1000 dilutions of both antisera against an increasing amount per well of the two tTGase- mediated products apoptotic envelopes and SDS/insoluble polymer respectively. Cross-reactivity of both antisera can be seen to both antigens, as would be expected. The degree of sensitivity being reduced markedly when the "incorrect" antigen of challenge is screened. This is probably due to stearic hindrance and masking of the reactive epitopes, leaving them invisible to the antibodies.

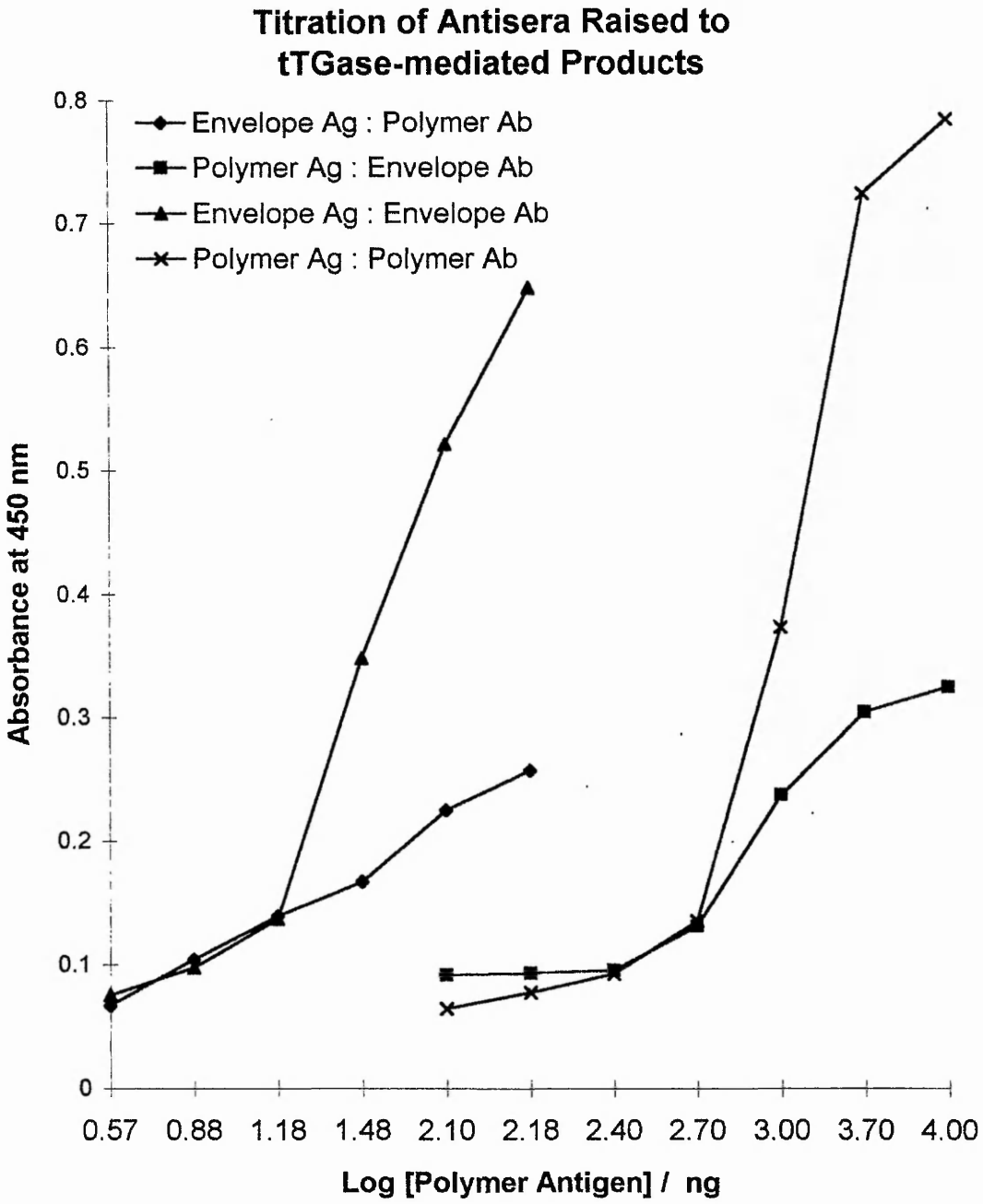
Titration of Antisera Raised to tTGase-mediated Products
Envelope Ag : Polymer Ab
Polymer Ag : Envelope Ab
Envelope Ag : Envelope Ab
Polymer Ag : Polymer Ab
Absorbance at 450 nm
0.8
0.7
0.6
0.5
0.4
0.3
0.2
0.1
0
0.57
0.88
1.18
1.48
2.10
2.18
2.40
2.70
3.00
3.70
4.00
Log [Polymer Antigen] / ng

Figure 3.3 Calibration graph for the indirect quantitative ELISA testing anti-envelope antibody versus isolated apoptotic envelopes from BHK-21 fibroblasts, according to the method described in 2.3.13. 50µl per well of 1:1000 dilution of the primary antibody was reacted against increasing protein loading per well of the antigen. The plotted values have been corrected for the background absorbance readings at 450 nm, using an immunoperoxidase conjugated system and TMB substrate, reactions stop with sulphuric acid after 5 minutes.

Anti-Envelope vs. SDS-Insoluble Liver Polymer

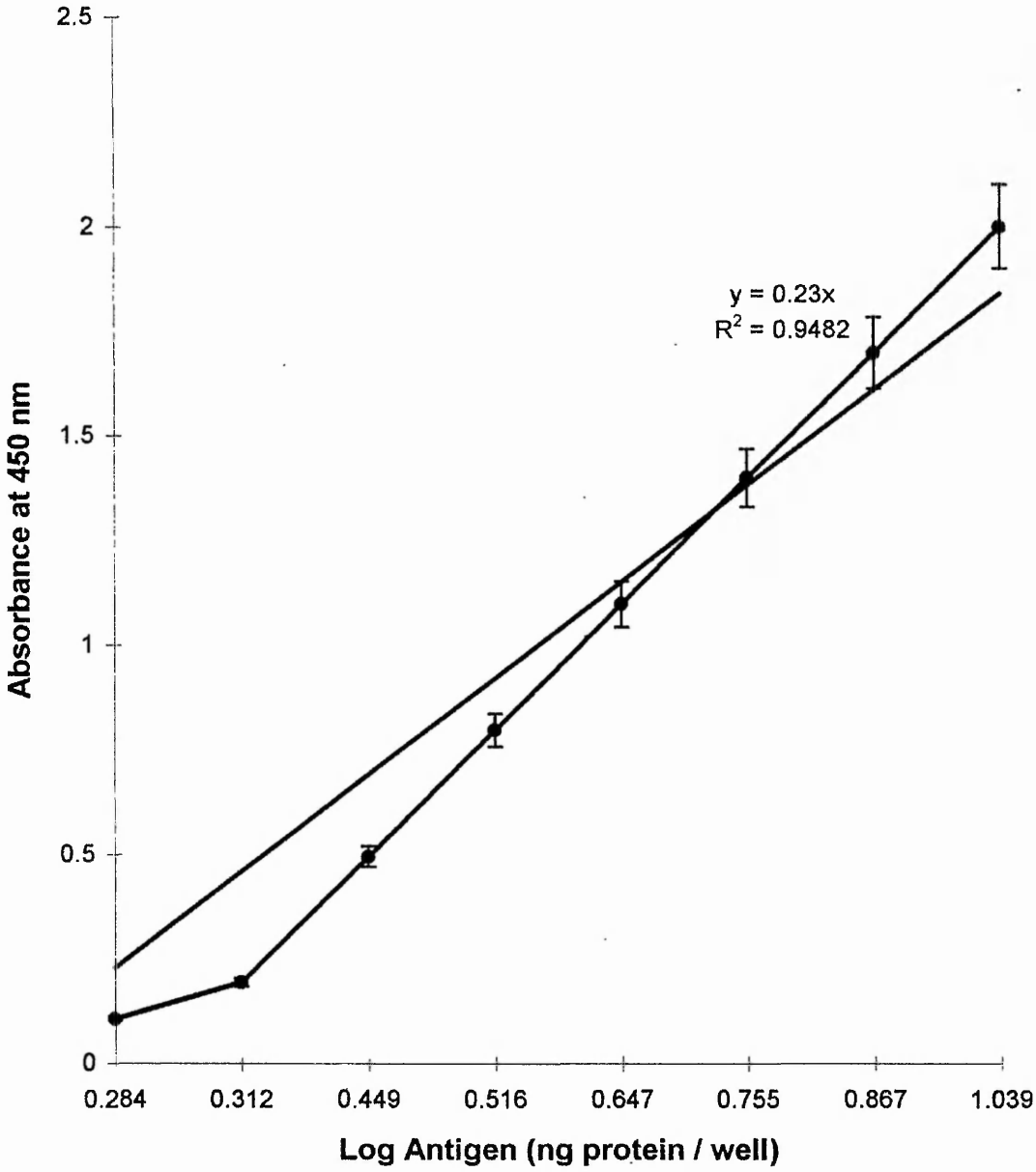

Figure 3.4 Calibration graph for the indirect quantitative ELISA testing anti-SDS/insoluble antibody versus isolated SDS/insoluble polymer from rat liver, according to the method described in 2.3.13. 50µl per well of 1:1000 dilution of the primary antibody was reacted against increasing protein loading per well of the antigen. The plotted values have been corrected for the background absorbance readings at 450 nm, using an immunoperoxidase conjugated system and TMB substrate, reactions stop with sulphuric acid after 5 minutes.

Anti-Polymer vs. SDS Insoluble Liver Polymer

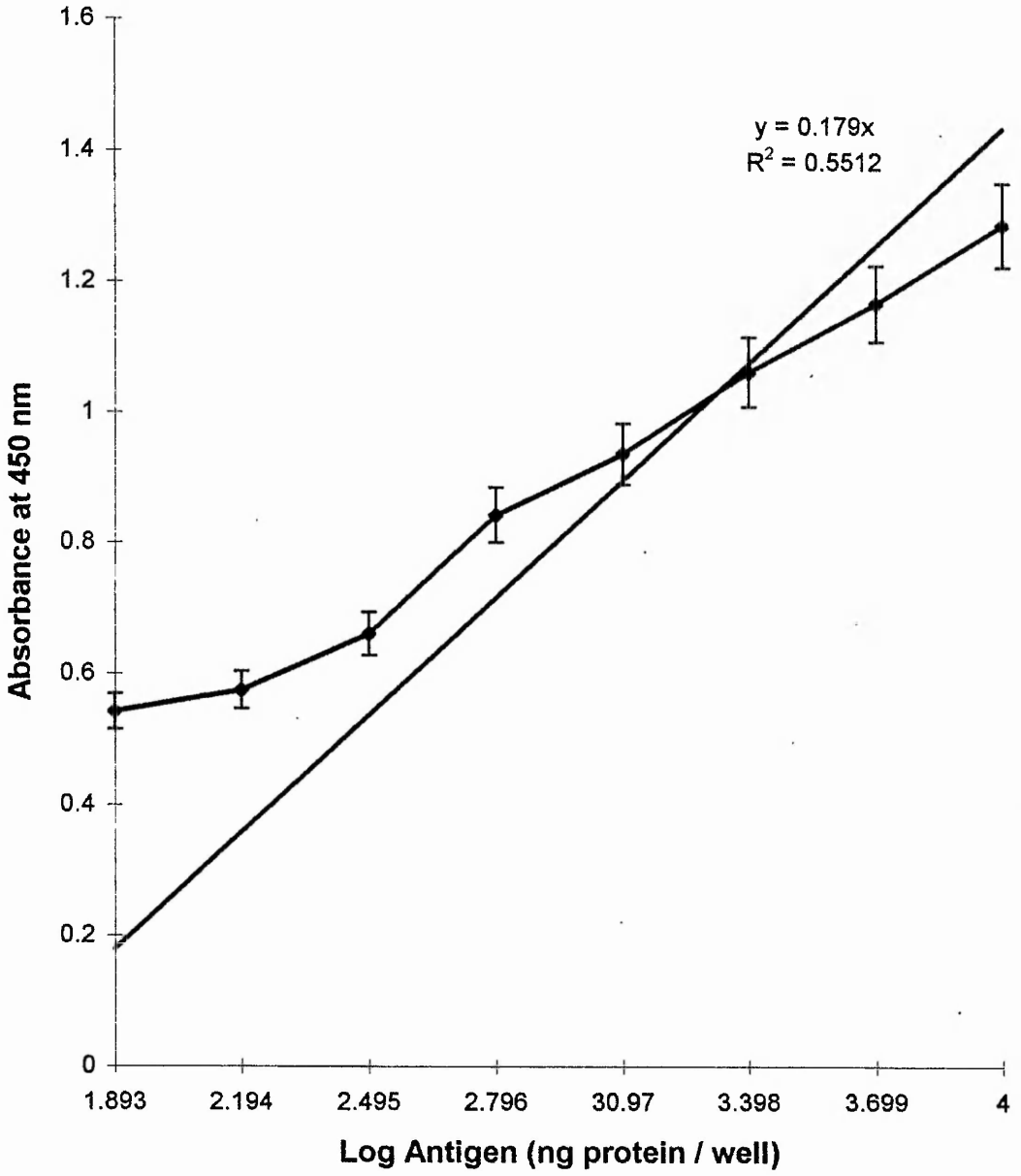

3.2.5 Propagation of rat hepatocellular carcinomas using the 2-AAF model.

The model used may be summarised as follows. Male Sprague-Dawley rats (200-250 g) were purchased from Sasco Inc., Omaha, NE. A modified version of the Teebor and Becker method (Teebor and Becker 1971) of cyclic feeding of 2-AAF was used to produce 2-AAF-mediated hepatocarcinogenesis. Rats were administered an 2-AAF diet comprised of a semi-synthetic control diet containing 0.05% 2-AAF (Ringer *et al* 1983) for 3 weeks followed with 1 week on control diet. This cyclic regimen was repeated from 2 to 5 times depending on the experiment. Control animals were fed the semi-synthetic control diet (Purina Rodent Laboratory Chow No. 5001) continuously during the period that experimental animals were in cyclic feeding regimens. Rats that were to be maintained for a period of time beyond a particular cyclic feeding protocol were placed on control diet until used. The results in this chapter refer to a basal control group at week1, four groups all fed 2-AAF and exposed for 1,2,3 and 4 cycles of diet respectively and a basal control group aged matched to the oldest group of experimental animals (4 cycles of 2-AAF)

At sacrifice 1g (wet weight) samples of liver tissue were excised and homogenised according to the method in section 2.3.3. At this point in the study there was no difference apparent from gross physical examination of the homogenates. Portions of each homogenate were taken for DNA analysis (section 3.6). The remaining volume of homogenate was then subjected to SDS treatment followed by sucrose gradient centrifugation and lubrol-Px dialysis as described in section 2.3.10.1. After the treatment of the homogenates by boiling in the presence of SDS and DTT an obvious difference in the physical appearance of the samples became apparent. Plates 3.3 show the gross physical appearance of the SDS preparations for each of the experimental groups. The colour of both the 1 cycle basal and 4 cycle basal groups are constant within the group and comparative to each other. However, when you examine the experimental groups the colour of the samples becomes progressively lighter with continued administration of 2-AAF, also the variation of colour within each group becomes more pronounced.

3.2.6 DNA analysis of tumour homogenates

The physical change in appearance of the samples noted at this stage, was thought to e due to the numbers of cells present within the 1g tissue samples. If as predicted by the model those animals exposed to greater numbers of 2-AAF diet cycles would have greater

Plate 3.3 Physical appearance of digested liver homogenates from the AAF hepatocarcinogenesis model.

1. Digested liver homogenates from rats fed 1 cycle of AAF diet.

2. Digested liver homogenates from rats fed 2 cycles of AAF diet.

3. Digested liver homogenates from rats fed 3 cycles of AAF diet.

4. Digested liver homogenates from rats fed 4 cycles of AAF diet.

A. Digested liver homogenates from rats fed 1 cycle of control diet.

B. Digested liver homogenates from rats fed 4 cycles of control diet

These pictures show the AAF liver samples following the digestion with collagenase type VII (methods 2.3.9) and prior to the isolation of SDS / insoluble polymer (methods 2.3.10). It is clearly seen that there is a decrease in the amount of cellular material obtained from the one equal gram starting weights; as the amount of AAF administered increases. Note the age matched controls (A and B) which appear unchanged. This observation of the change in cellular material has been confirmed by DNA analysis (Figures 3.5 and 3.6).

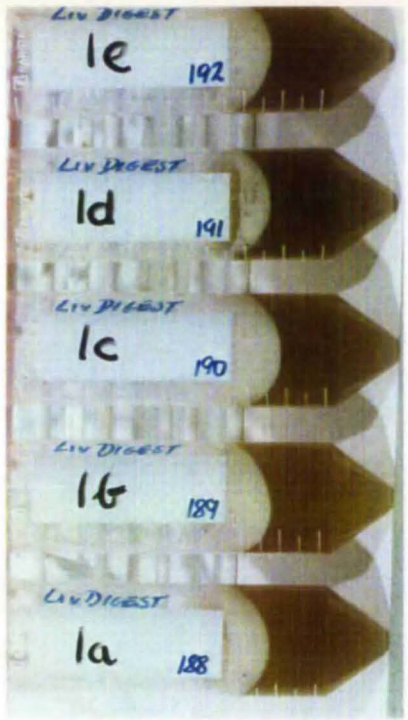
1
LIV DIGEST 1e 192
LIV DIGEST 1d 191
LIV DIGEST 1c 190
LIV DIGEST 1b 189
LIV DIGEST 1a 188

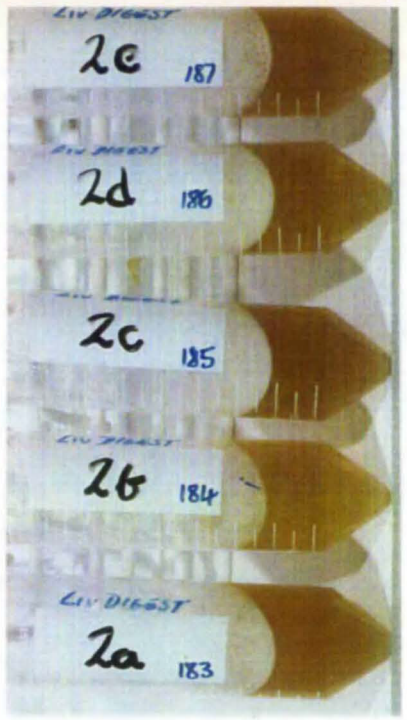
2
LIV DIGEST 2e 187
LIV DIGEST 2d 186
LIV DIGEST 2c 185
LIV DIGEST 2b 184
LIV DIGEST 2a 183


3
LIV DIGEST 3e 180
LIV DIGEST 3d 179
LIV DIGEST 3c 178
LIV DIGEST 3b 177
LIV DIGEST 3a 176


4
4e 175
LIV DIGEST 4d 174
LIV DIGEST 4c 173
LIV DIGEST 4b 172
LIV DIGEST 4a 171


A
LIV DIGEST c1d 202
LIV DIGEST c1c 201
LIV DIGEST c1b 200
LIV DIGEST c1a 199


B
C4d 206
LIV DIGEST C4C 205
LIV DIGEST C4b 204
LIV DIGEST C4a 203

numbers of both neoplastic and necrotic cells compared to healthy hepatocytes with large areas of hypertrophy and vacuolation. Thus in order to standardise the parameters being measured DNA analysis was performed on portions of all extracts. The diphenylamine method used is described in section 2.3.5.2, Figure 3.5 shows the DNA assay calibration graph. Figure 3.6 shows the amount of DNA (mg) found within 1g of tissue sample for the assays. Clearly evident is the significantly high level of DNA ($P < 0.01$) seen in the 2 cycle 2-AAF animals, compared to the basal animals. This is due to the resultant hyperplasia produced as the active metabolites of 2-AAF accumulate in the liver during the induction phase of carcinogenesis. In those animals exposed to 4 cycles of 2-AAF the levels of DNA had significantly fallen with respect to the control ($P< 0.025$) by this time the level of damage seen in the histological sections of excised liver tissue are very marked (see section 3.2.9). The changes in the profile of DNA content within a standard sampling weight of tissue reflects the numbers of cells present and closely correlate to the numbers of 2-AAF diet cycles fed to the animals and the progressive nature of the hepatocellular carcinogenesis.

Figure 3.5 Calibration graph for the diphenylamine DNA assay (section 2.3.5.2). 2ml volumes of calf thymus DNA standard were reacted with diphenylamine according to the above method, prior to colourimetric analysis at 600 nm.

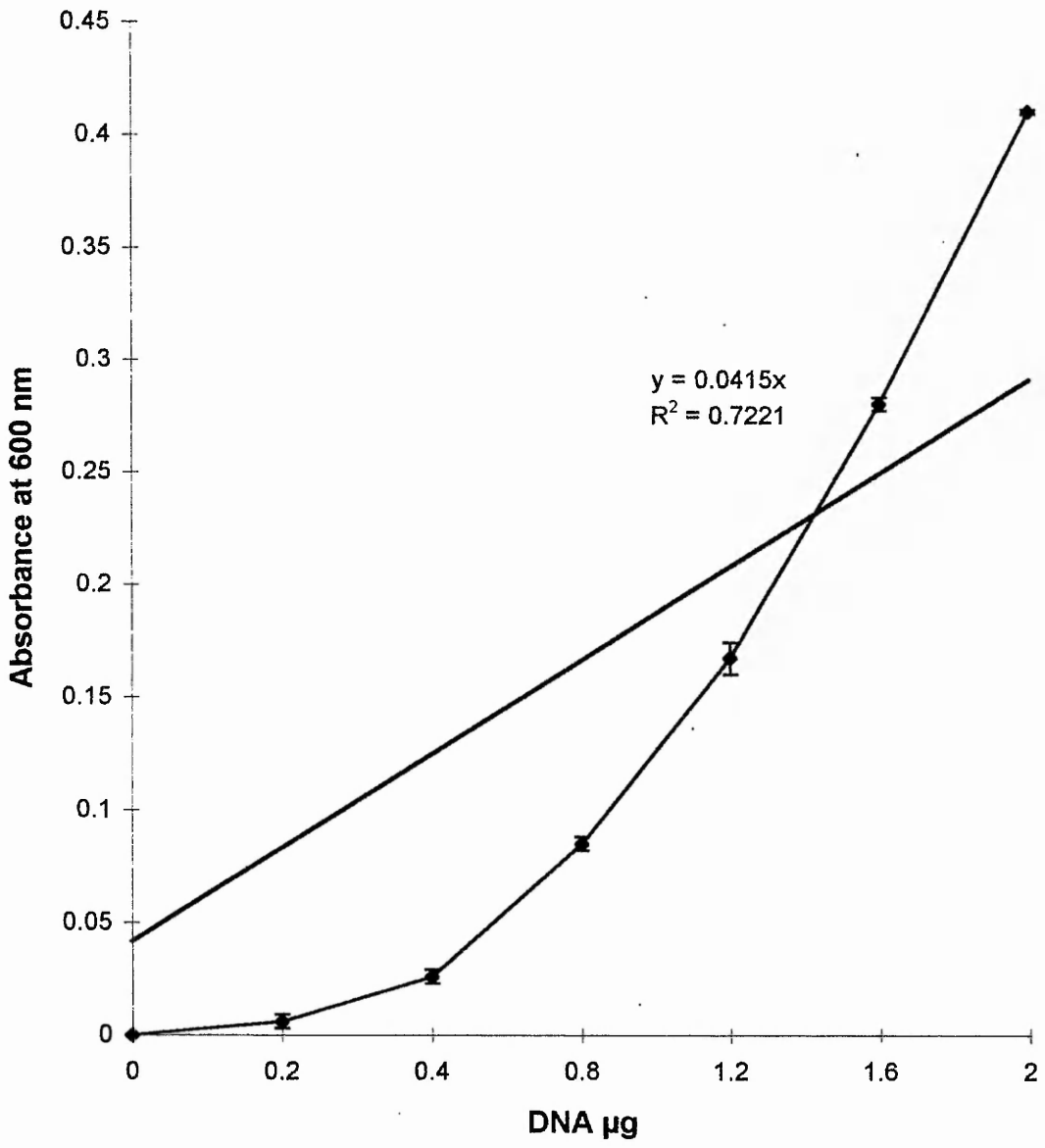
DNA Assay Calibration Graph
Absorbance at 600 nm
0.45
0.4
0.35
0.3
0.25
0.2
0.15
0.1
0.05
0
y = 0.0415x
R2 = 0.7221
0
0.2
0.4
0.8
1.2
1.6
2
DNA µg

Figure 3.6 Quantitation of the DNA content found in basal and 2-AAF treated rat liver samples. 2ml aliquots of 20% (v/v) homogenates prepared according to the method of 2.3.3 were tested using the diphenylamine method of 2.3.5.2 prior to colourimetric analysis at 600 nm. From the graph the peak of DNA content can be seen in the 2 cycle 2-AAF samples, corresponding to responsive hyperplasia in the animals during the induction phase of neoplasia ($P < 0.01$). As the progressive feeding of 2-AAF continues the DNA content of the samples falls, until at 4 cycles 2-AAF it has dropped significantly to the controls ($P < 0.025$) as the livers are at this time showing signs of hepatocellular carcinomas, vacuolation atrophy and necrosis. ($n = 5 \pm$ S.D.)

DNA Analysis of AAF Livers

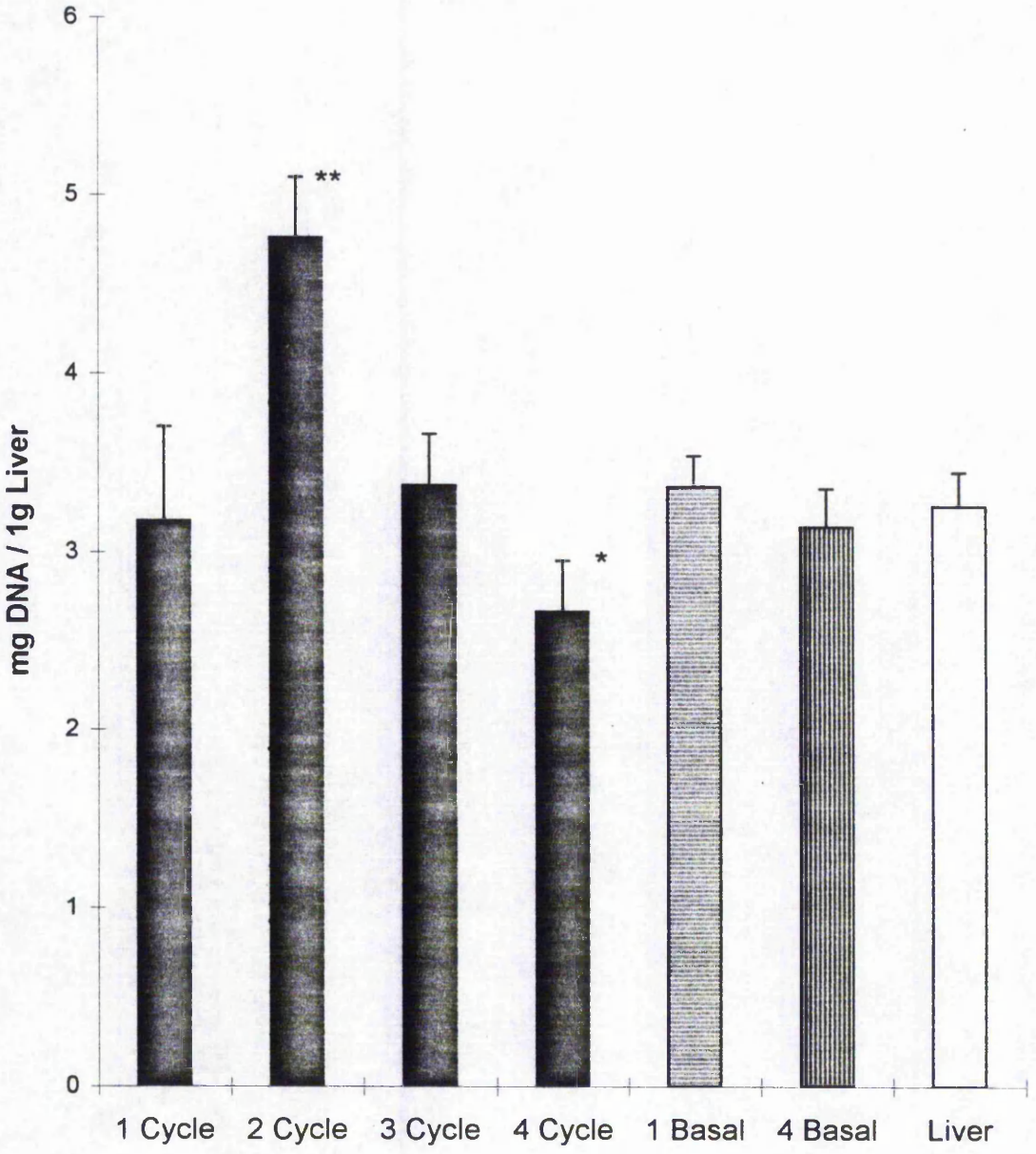

3.2.7 Quantitation of apoptotic tTGase-mediated products using anti-envelope antibody ELISA

Using the indirect ELISA method discussed earlier the amount of apoptotic tTGase-mediated products, within the SDS/insoluble extract of tissue samples, were quantitated using anti-envelope antibody ELISA. Figure 3.7 shows the background corrected absorbance values for 50µl volumes of SDS/ insoluble extract. After 3 cycles of 2-AAF diet the levels rise but not significantly from the basal samples. Rat liver polymer was used as a positive control. Extrapolation from the calibration graph (Figure 3.3) allows the amount of apoptotic tTGase-mediated product to be expressed as mg protein / 1g tissue, these results and those of total SDS/insoluble polymer are shown in Figure 3.9 which follows.

3.2.8 Quantitation of SDS/insoluble tTGase-mediated polymer using anti-polymer antibody ELISA

Using the indirect ELISA method discussed earlier the amount of total SDS/insoluble tTGase-mediated polymeric product, within the SDS/insoluble extract of tissue samples, were quantitated using anti-polymer antibody ELISA. Figure 3.8 shows the background corrected absorbance values for 50µl volumes of SDS/ insoluble extract. After 3 cycles of 2-AAF diet the levels rise, such that the 4 cycle animals have a level significantly different from the basal samples ($P < 0.025$). Rat liver polymer was used as a positive control. Extrapolation from the calibration graph (Figure 3.4) allows the amount of apoptotic tTGase-mediated product to be expressed as mg protein / 1g tissue, these results and those of total SDS/insoluble polymer are shown in Figure 3.9. which follows.

By extrapolation from the corresponding calibration graph the level of each polymer can be expressed as mg protein / 1g tissue; this is shown for all samples ($n = 6 \pm$ S.D.) in Figure 3.9. The amount of total tTGase-mediated SDS/insoluble polymer is seen to rise with continued exposure of the xenobiotic diet 2-AAF, and becomes significantly different from the controls after 4 cycles of diet administration ($P < 0.025$). By further standardising the data for the amount of DNA present in the standard weight of tissue sample (Figure 3.10) both the 3 and 4 cycle animals show significant differences from the control ($P < 0.05$) however, the standard deviation within each group is very high.

Figure 3.7 Quantitation of the apoptotic fraction of the SDS/insoluble polymer isolated from the tissue samples reacted with the anti-envelope antibody according to the ELISA method of 2.3.13. The absorbance data for each of the 4 cycles of 2-AAF diet are compared to age-matched basal diet animals, normal rat liver extract and purified SDS/insoluble polymer from rat liver. (n=5 ± S.D.)

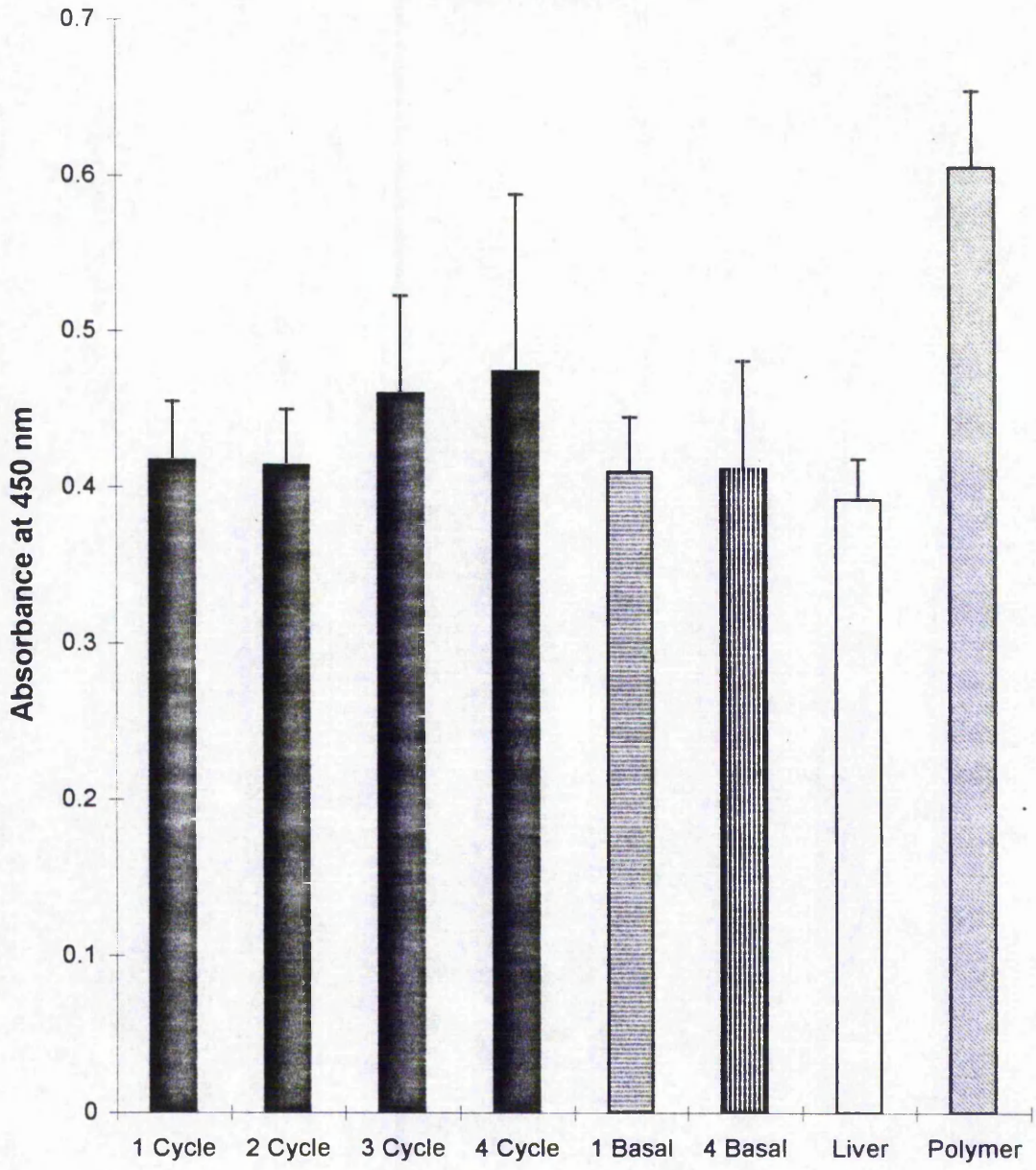
Apoptotic SDS-Insoluble Polymer
in AAF Livers
Absorbance at 450 nm
0.7
0.6
0.5
0.4
0.3
0.2
0.1
0
1 Cycle
2 Cycle
3 Cycle
4 Cycle
1 Basal
4 Basal
Liver
Polymer

Figure 3.8 Quantitation of the total SDS/insoluble polymer isolated from the tissue samples reacted with the anti-polymer antibody according to the ELISA method of 2.3.13. The absorbance data for each of the 4 cycles of 2-AAF diet are compared to age-matched basal diet animals, normal rat liver extract and purified SDS/insoluble polymer from rat liver. (n=5 ± S.D.)

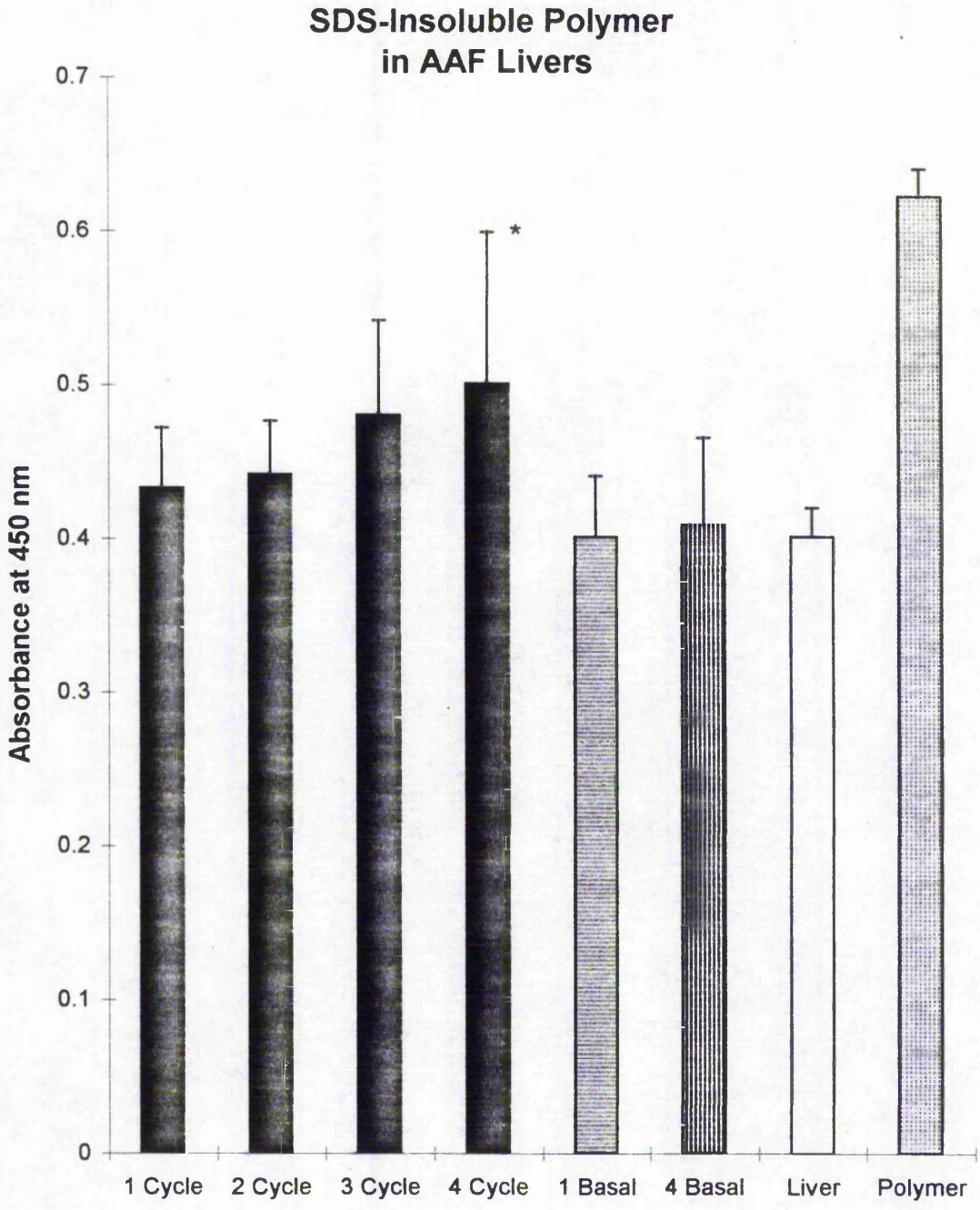
SDS-Insoluble Polymer
in AAF Livers
Absorbance at 450 nm
0.7
0.6
0.5
0.4
0.3
0.2
0.1
0
*
1 Cycle
2 Cycle
3 Cycle
4 Cycle
1 Basal
4 Basal
Liver
Polymer

Figure 3.9 The absorbance data shown in figures 3.7 and 3.8 were extrapolated onto the calibration graphs for the anti-envelope antibody and anti-polymer antibody respectively (Figure 3.3 and 3.4) from this the amount of each tTGase-mediated product could then be expressed as mg protein / 1g of tissue tested. The pattern of distribution for both apoptotic and SDS/insoluble polymers are very similar, with the amounts of apoptotic product being 3 to 4 fold lower than that of the SDS/insoluble polymer. Levels in the control and basal samples remained constant while there was a steady increase seen in the livers of those animals fed the 2-AAF diet with time. (n=5 ±S.D.)

SDS-Insoluble Polymer vs. Apoptotic Polymer Isolated from 1g of AAF Liver

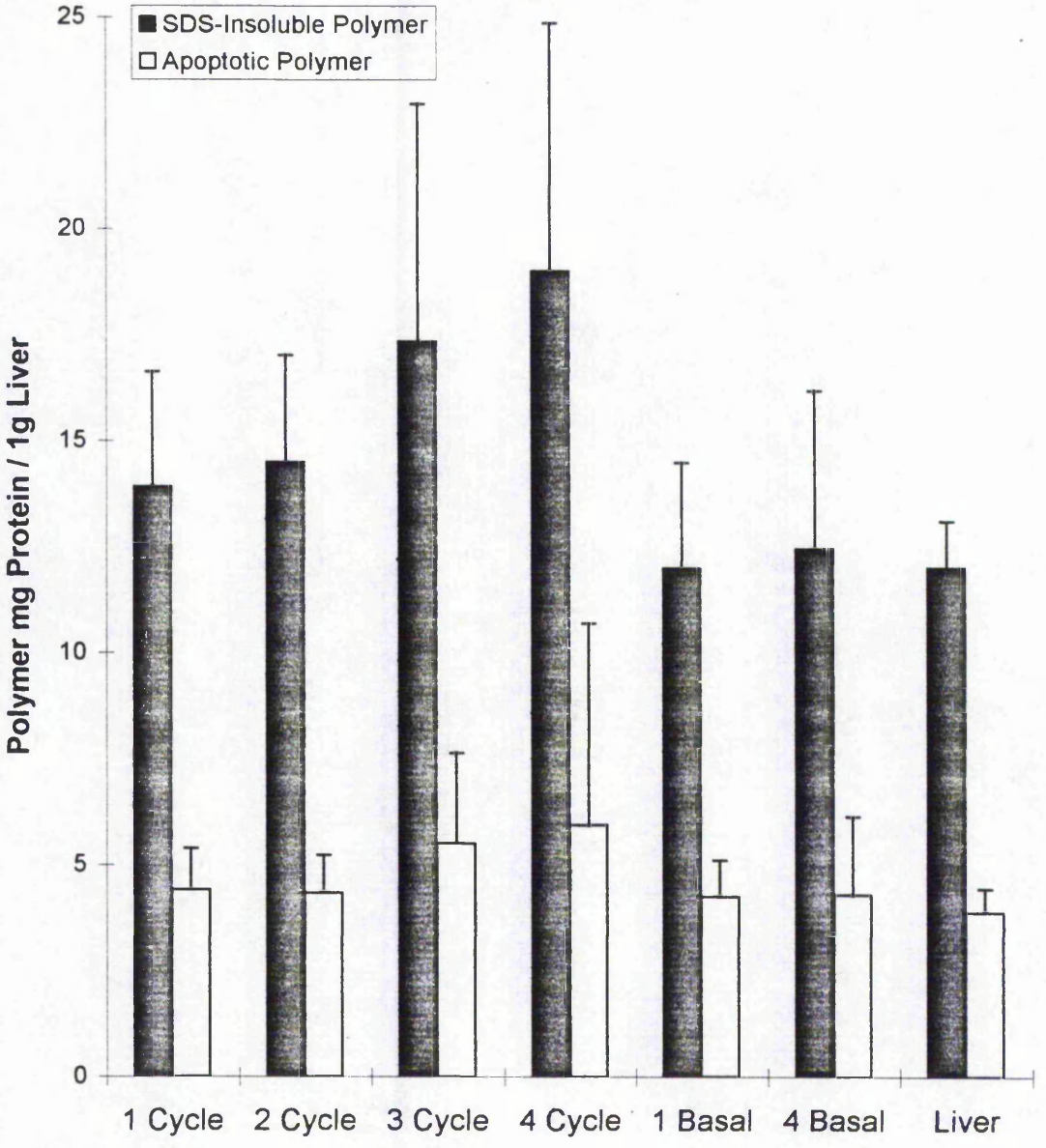

Figure 3.10 Summary graph showing the amount of both tTGase-mediated apoptotic and SDS/insoluble products from basal, 3 cycle and 4 cycle 2-AAF treated rat livers. The quantitation has been standardised and the amounts of product are expressed as mg protein / mg DNA / 1g of tissue, this takes into account the drop in cell number associated with the progression of neoplasia in this model. Both 3 and 4 cycle samples had levels of Total polymer significantly higher than the basal control ($P < 0.025$). Though it must be noted that there was a large variation within the groups tested, possibly due to the randomicity of tissue sampling.

tTGase-mediated Products in Rat Hepatocellular Carcinoma

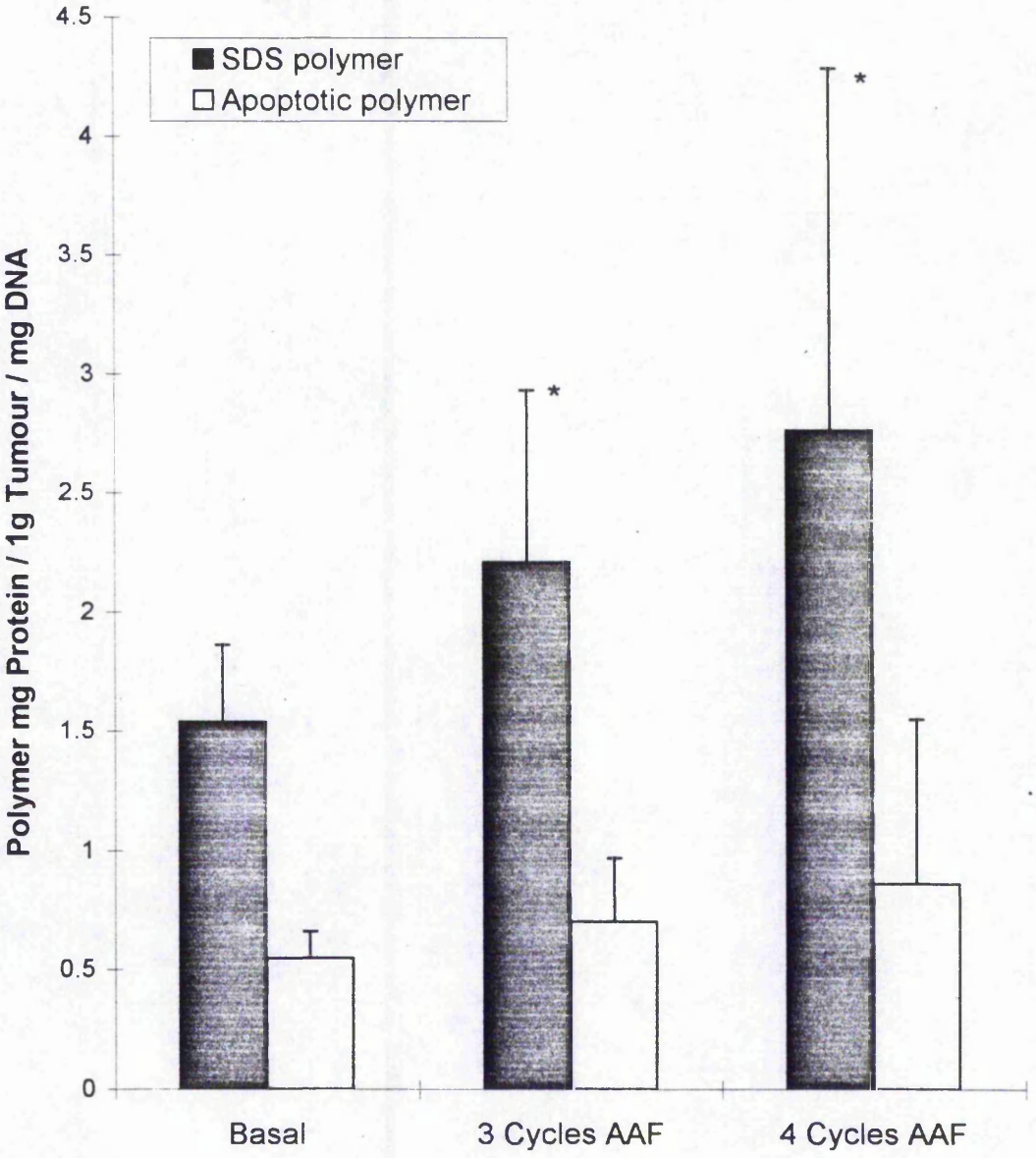

3.2.9 In situ localisation of tTGase-mediated products with rat hepatocellular carcinoma samples via immunohistochemistry.

The ELISA quantitation has shown the progressive increase of the tTGase-mediated apoptotic and SDS/insoluble polymers from the experimental samples of 2-AAF treated rat livers. The availability of serial histological sections taken from the remaining rat livers made it possible to visualise the localisation of this reactive material *in situ*. The initial hypothesis linked the lack of tTGase to subsequent lowering of apoptosis and the progression of neoplasia, thus the paraffin embedded fixed sections of liver were stained with the anti-envelope antibody. The immunohistochemical staining protocol is given in section 2.3.14.2.

From the quantitative evidence it is only the livers from those animals subjected to 2 cycles of 2-AAF or greater which have significant amounts of detectable polymer thus the immunohistological study will be limited to looking at the staining patterns in these tissues. Plate 3.4.A & B test for non-specific binding of non-immune antibody and anti-envelope antibody on basal tissues respectively, no staining is evident. Plates 3.4 C & D show the non-immune staining and anti-envelope antibody staining on serial sections of a 3 cycle 2-AAF liver, definite positive staining can be seen with the anti-envelope antibody. Plates 3.4 D & E show similar staining on serial sections from a 4 cycle 2-AAF liver, it is evident that the degree of positive staining has increased and corresponds to the findings of the ELISA quantitation.

Providing confirmatory evidence that the apoptotic polymer detected via ELISA can also be visualised *in situ* The significance of this was further examined by staining of experimental sections from animals which had received 3 or 4 cycles of 2-AAF then removed from the xenobiotic diet and fed standard diet for a further six weeks, thus allowing a period of recovery and tissue regeneration.

Plate 3.4 Immunohistochemical staining of serial sections of paraffin embedded rat liver taken from the 2-AAF hepatocarcinogenesis model.

A. This liver has come from an animal that has received three cycles of basal / control diet only.. Stained with a 1:100 dilution of non-immune rabbit serum, magnification X40.

B. This liver has come from an animal that has received three cycles of basal/control diet only. Stained with 1:100 dilution of the anti-apoptotic envelope antisera, magnification X40. Photographs A and B serve as a test for the degree of non-specific binding. In both photographs the structure of healthy liver lobules can be seen, those vascolated areas are from the blood vessels and bile caniculii; no areas of necrosis are visible.

C. This liver has come from an animal that has received three cycles of 2-AAF diet only stained with a 1:100 dilution of non-immune rabbit serum, magnification X100.

D. This liver has come from an animal that has received three cycles of basal/control diet only has been stained with a 1:100 dilution of the anti-apoptotic envelope antisera, magnification X100.

E. The rat liver seen in these photographs has come from an animal fed four cycles of 2-AAF diet, stained with a 1:100 dilution of non-immune rabbit serum, magnification X100.

F. The rat liver seen in these photographs has come from an animal fed four cycles of 2-AAF diet, stained with a 1:100 dilution of the anti-apoptotic envelope antisera, magnification X100.

The arrows in plates D and F highlight those cells of typical apoptotic appearance which have stained positively with the anti-apoptotic envelope antisera, while plates 3 and 5 have stained negative for the antibody. With the progression of the xenobiotic in the animal it is also evident that there is more intense staining with the anti-apoptotic envelope antisera, indicating that the amount of apoptosis in the liver is increasing; confirming the data observed for the levels of apoptotic polymer as detected with the same antibody by ELISA (Figures 3.7 and 3.8).

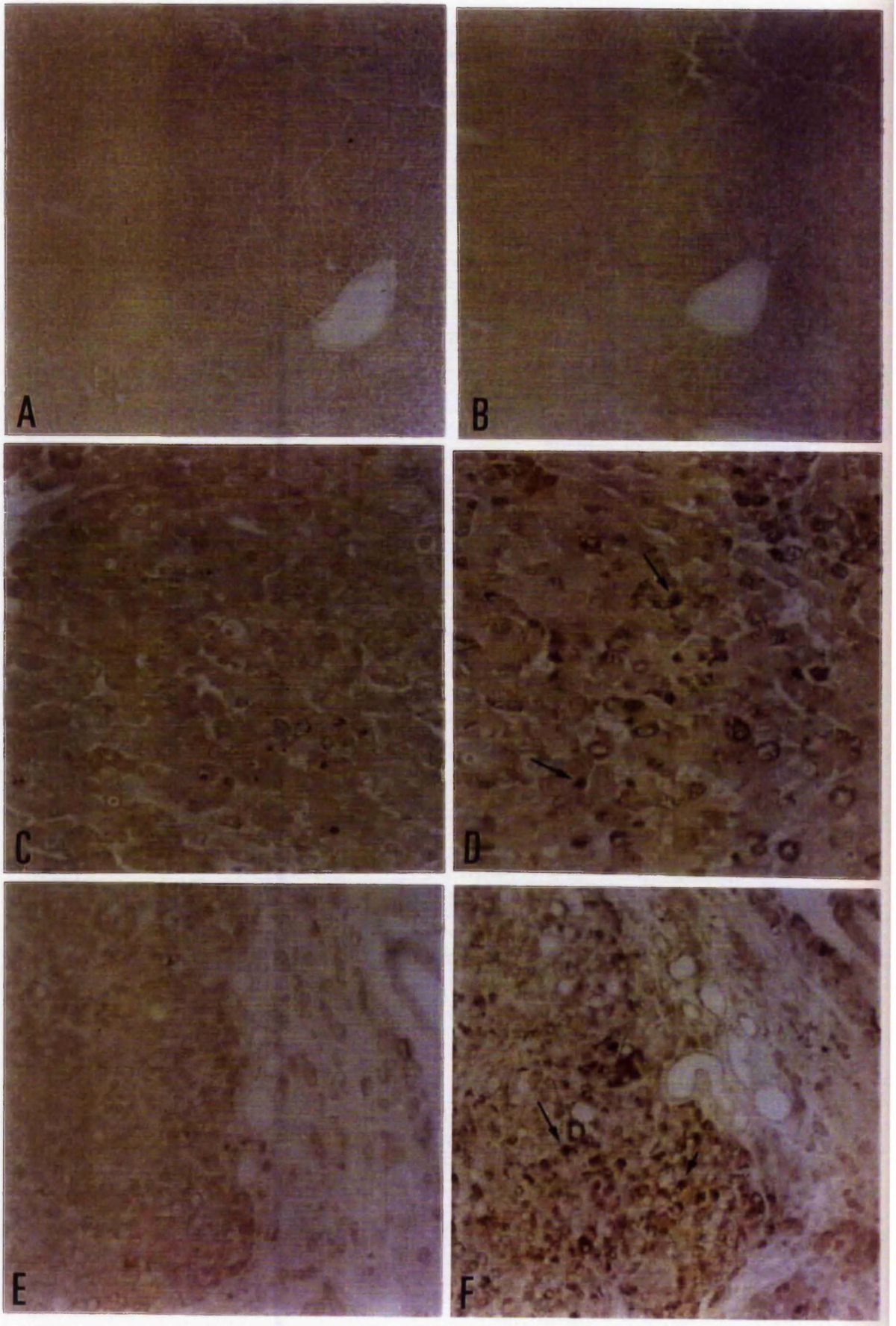
A
B
C
D
E
F

Plate 3.5 Immunohistochemical staining of serial sections of paraffin embedded rat liver taken from the 2-AAF hepatocarcinogenesis model. Investigation of the effects of recovery and tumour progression.

A. A four cycle dosed liver stained with 1:100 dilution of the anti-apoptotic envelope antisera, photographed at a magnification of X40. The four cycle liver (plate A) shows the predominate staining throughout the whole of the liver, a node of neoplastic growth (N) which can be clearly visualised.

B. Section liver from animals fed three cycles of AAF followed by six weeks of recovery, stained with a 1:100 dilution of non-immune rabbit serum, magnification X100.

C. An age-matched liver that has come from an animal dosed with three cycles of 2-AAF; then removed from the diet and allowed to recover for six weeks. Stained with 1:100 dilution of the anti-apoptotic envelope antiserum. This liver which has been allowed to undergo recovery also has a very marked neoplastic node (N), the boxed region will be shown at a higher magnification in (plate D).

D. A X100 magnification of the boxed region of node (N) seen in (plate C) stained with 1:100 dilution of the anti-apoptotic envelope antisera. This shows two distinct regions of staining (AR), is an apoptotic region around the margins of the neoplastic node, towards the center of the node a recovery region (RR) with much reduced incidence of positive staining for apoptosis can be seen. Cells with typical apoptotic motifs are marked with arrowheads.

This series of photographs give evidence that apoptosis may be part of the mechanism for invasion and progression of solid tumours into healthy tissues; by the deletion and remodelling of the neoplastic nodules.

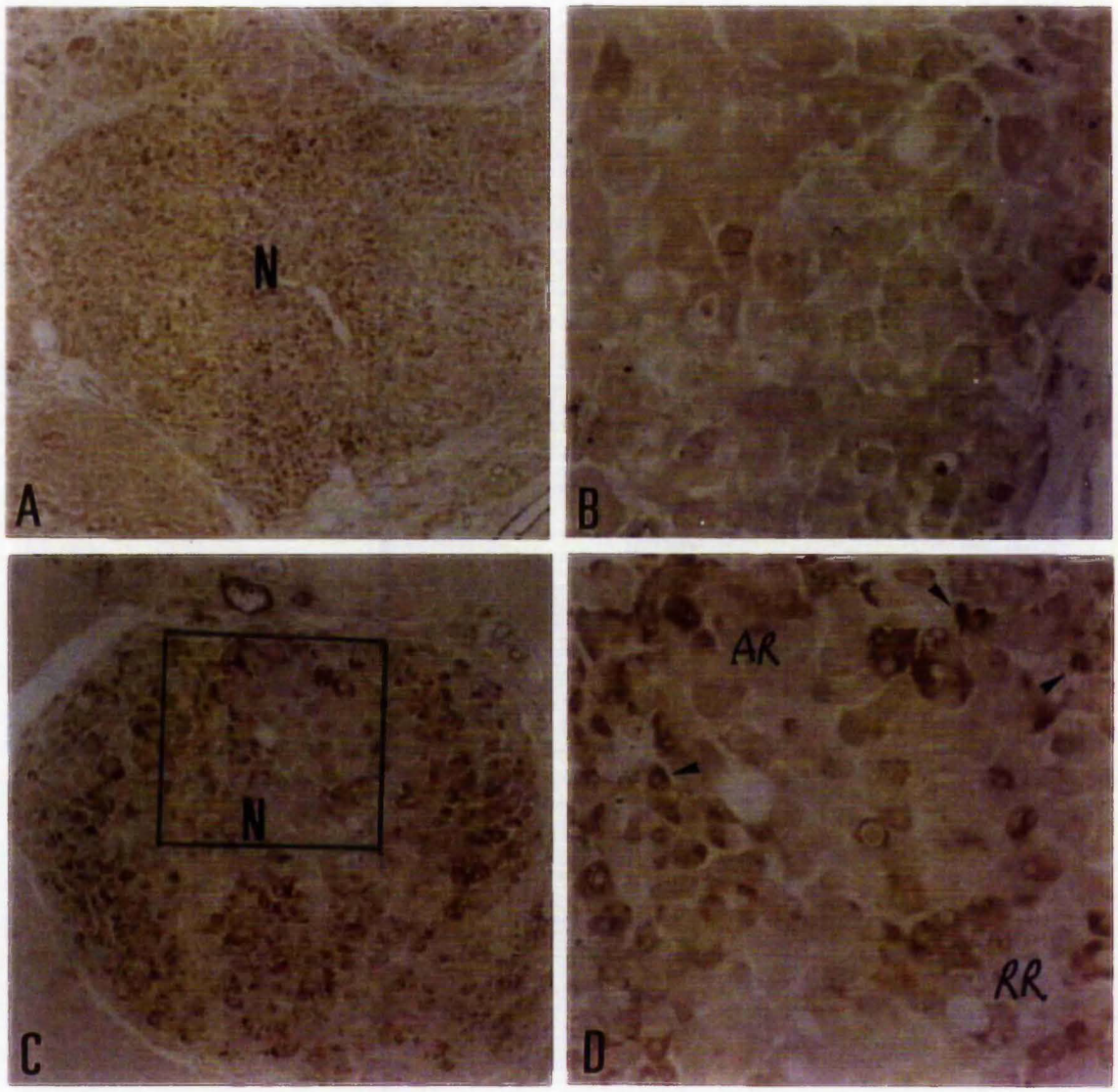
N
A
B
N
C
AR
RR
D

Shown in Plate 3.5 part A an anti-envelope antibody, positively staining nodule of neoplastic cells, taken from an animal fed 4 cycles of 2-AAF with a six week recovery period, the intensity of staining is markedly reduced from that of a similar non-recovery animal plate 3.4.E. Plate 3.4 part B anti-envelope antibody staining in a liver following 3 cycles of 2-AAF plus six week of recovery, clearly now there is very little positive staining, especially when compared to a similar non-recovery animal plate 3.4.D.

Similarly, shown in Plate 3.5 part C is a positively staining neoplastic nodule from the liver of an animal fed 4 cycles of 2-AAF then allowed six weeks recovery; positive staining being confined to the nodule. Plate 3.5.D is an enlargement of the boxed area shown in plate 3.5.C here cells with the morphological appearance of apoptosis are indicted.

3.3 Discussion.

Statistical analysis was performed on the final results for each of the polymers as determined for each of the AAF cycles. These calculations showed statistical significance in the maintained rise in total SDS-insoluble polymer for 3 and 4 cycle samples ($P < 0.05$). This statistical difference is very low and strongly reflects the high degree of variation within the samples of each group. From the *in situ* staining of liver sections from animals treated with 2-AAF the degree of destruction that can be caused following 3 and 4 cycle administration of the diet produced samples of marked variation in overall morphology. These livers were grossly vacuolated and severely damaged, such that a one gram wet weight of tissue may well have a much reduced cell number. Of those cells remaining many may be necrotic and the bulk of the remainder neoplastic at the margins of growth. There may be little healthy proliferative tissue, undergoing normal levels of apoptosis.

What was evident in the staining patterns with antisera raised to transglutaminase-mediated products was the high intensity of staining near the edges of expanding nodules as healthy tissue was replaced by neoplastic. This tTGase activity could be resulting in the formation of polymer hence, for those livers which have many small developing nodules surrounded by the normal tissue which is to be destroyed you would expect to find an increase in polymer up until the point at which neoplastic cells far out number normal hepatocytes.

In sampling the 2-AAF livers for this study the one gram wet weights of tissue were taken randomly from each of the provided samples. This randomicity was first noted in the range of appearance of the samples following the initial digestion. It would therefore be expected to have a random number of neoplastic nodules in each of the samples as too there would be a random number of normal cells.

On reflection the results obtained have shown this to be true. It also suggest that the degree of destruction in the samples has not yet reached the point where neoplastic cells predominated. Due to the large standard deviation in the 3 and 4 cycle samples this however can not be assumed one hundred percent. A larger population number would confirm this.

In comparison to other studies carried out here in Nottingham my results show an opposite picture with an increase in polymers rather than a decrease as observed by Knight *et al*

(1991, 1993). This can be explained by examining the nature of their samples; in both papers the neoplastic tissue study was biased i.e. whole tumours only, were removed and used for estimations. Hence, the samples were pre-selected for neoplastic tissue and would have no or little contamination by healthy cells which would have surrounded the tumours. A marked difference in the mixed cell populations I would have obtained by the random sample of one gram weights.

If this method of quantitation were to be used on biopsy samples, I feel that my method of tissue sampling is more realistic and non-biasing. As normal biopsy procedures will undoubtedly remove the bulk of the cells thought to be neoplastic at the same time as removing some of the healthy cells into which the neoplasms had been invading, thereby creating a natural dilution effect.

The anti-polymer antiserum used in this study was raised against SDS-insoluble polymer from rat liver that was prepared via a lengthy method of sucrose/SDS density gradient centrifugation. While the anti-envelope antiserum was raised against intact apoptotic envelopes prepared from Hamster fibroblasts in culture. Thus the possibility of both these antibodies to react well with samples of SDS-insoluble polymer did not carry equal favourability.

It was hoped that this study would highlight a correlation between the degree of 2-AAF administration, neoplastic state of the liver and amount of SDS/apoptotic polymer present. No distinct link has been found. However, the observation of net increase in both polymers in samples of tissue in conjunction with prolonged dosage of 2-AAF has been shown to be significant when examined along side the *in situ* staining, as the positive staining was closely confined to only the neoplastic regions of the tissues.

This may reflect the role of apoptosis when taking into account the extent of neoplastic invasiveness into healthy tissues and hence be useful as a diagnostic method in screening biopsy material. Those cells which are weak being eliminated in favour of the proliferatively aggressive malignant neoplastic cells.

If a series of biopsy samples show an increase in the apoptotic and total tTGase-mediated SDS-insoluble polymers, this may be an indication of higher level of invasiveness and rate of progression of a neoplasm; as seen for the 3 and 4 cycle 2-AAF treated rat livers. A

corresponding decrease being complementary to regression of the neoplasm resulting in hyperplasia and proliferation of the host tissue as seen in the 2 cycle samples and those which had been subjected to a recovery period after initial induction phase of neoplasia.

In conclusion, this study has shown that the large molecular weight polymer produced in rat liver as a result of the enzyme transglutaminase appears to increase in amount in livers which have been induced into neoplasia by 2-AAF. As both the anti-polymer and anti-apoptotic envelope antiserum crossreacted with the polymer isolated by the SDS digestion method it can be inferred that there was also an increase in the apoptotic index of these tissues with increasing exposure to 2-AAF.

This last finding does not hold with current opinion which finds a drop in apoptotic index with tumour progression, but can be explained in this study by looking at the randomicity of sample taking. In contrast to the previous work carried out by Professor Griffin's team I took both damaged and healthy tissue for examination, both in unknown amounts. The finding of an increase in apoptotic index may then be a reflection of the changes proceeding in the healthy tissues surrounding invasive neoplasms within the liver; as opposed to a drop seen in transglutaminase activity of to 65% of normal liver values (Hand *et al* 1987); and hence apoptotic index when only tumour tissue is examined.

Due to the fact that the data obtained in the chapter was from the analysis of archive tumour tissue prepared in the laboratories of Dr. Ringer (The Samuel Roberts Noble Foundation, Ardmore, USA) processing of the tissue for catalytic tTGase activity was not possible, hence the examination for products shown to be tTGase-mediated. The possible sampling error which may have occurred by taking random 1g weights of tissue not confined solely to the area of neoplasia has also further complicated the interpretation of these results.

Hence, a second model of progressive neoplastic growth has been investigated, this centers around the induction of a non-invasive metastatic fibrosarcomas in Hamsters and will be discussed in the following chapter.

4.0 Analysis of tTGase-Mediated Catalytic Products and the Correlation with Apoptosis from a Series of Hamsters Metastatic Fibrosarcomas..

4.1 Introduction.

4.2 Results.

4.2.1 Propagation of metastatic hamster fibrosarcomas.

4.2.2 PARENT - Low incidence-metastatic hamster fibrosarcoma.

4.2.3 MET D - -Low/no incidence - metastatic hamster fibrosarcoma.

4.2.4 MET E - High incidence - metastatic hamster fibrosarcoma.

4.3 Discussion.

4.1 Introduction.

In the previous chapter the 2-AAF model of heptocarcinogenesis was used to look for any relationship between the catalytic action of tTGase and the progression of neoplasia. Knowing that one of the parameters used for investigation of the model was analysis of two proteinous structures. Namely, the apoptotic envelope and the high molecular weight SDS-insoluble polymer each with 85% homology in amino acid content. Both are rendered insoluble in chaotrophic agents, by the presence of the specific catalytic product of tTGase , namely the ε(γ-glutamyl) lysine dipeptide, they can be regarded as tTGase-mediated products.

It was found that the amounts of both the apoptotic envelope and the high molecular weight SDS-insoluble polymer increased in parallel with the continued administration of the causative agent and subsequent progression of disease. Removal of the causative agent in the early stages of the time-course (cycles 1, 2 and 3 of 2-AAF) resulted in a reversal of the staining pattern for the anti-envelope antibody, and resulted in a full recovery in the pathology of the previously diseased tissues. However, if the administration program of the causative agent 2-AAF was allowed to proceed to 4 cycles removal of the diet did not see reversal of the disease condition and these animals would proceed to develop hepatomas and die of liver failure.

Some of the data found in the 2-AAF model did not correspond to previously published data from this laboratory (Barnes *et al* 1985, Hand *et al* 1986, 1987). Namely, as was previously reported data indicated that tTGase activity levels fell by 65% in the hepatocellular carcinoma tissue. Thus it would follow that levels of any catalytic products would remain constant at the level of endogenous product, (matching that of control animals) formed prior to administration of causative agent; as there is as yet no known mammalian enzyme identified which can cleave the ε(γ-glutamyl) lysine dipeptide. Whereas, it was found that there occurred a small increase in the level of both the apoptotic reactive product and the total SDS/ insoluble polymer. This can possibly be explained by the sampling method used.

The make-up of the 1g tissue samples taken for analysis in the 2-AAF model was not assessed thus tumour tissue was sampled with normal tissue in unknown amounts, therefore

the rise in parameters measured could have been due to a contamination effect of the normal tissue which still had high levels of transglutaminase.

In order to clarify the importance of tTGase in carcinogenesis and assess the possible effects of normal / tumour tissue contamination a second model of tumourigenesis was studied. In this chapter the relationship between the same two transglutaminase-mediated products, the apoptotic envelope and the high molecular weight SDS / insoluble polymer is studied in solid transplantable Hamster fibrosarcomas. The two antibodies described in the previous chapter are used to measure tTGase products inconjunction with an assay for the catalytic transglutaminase activity. The model of tumourigenesis applied was that of *in vivo* passage of a series of metastatic hamster fibrosarcomas. The HSV-2-333-2-26 cell line (parent) was originally obtained by *in vitro* transformation of hamster embryo fibroblasts with inactivated HSV-2; this cell line was kindly provided by Dr. F. Rapp (Department of Micro-biology, Pennsylvania State University, Hershey, PA, U.S.A.). Sublines were derived from metastatic lung nodules in hamsters whose primary load had previously been resected; following *in vivo* passage, in vitro cultures were established Teal and Rees (1987). The metastatic potential of each variant cell line was assessed as the number of animals, whose primary tumour load had been resected, that developed metastases out of the number of animals in which the tumours had been propagated and this figure is shown in parentheses throughout the text.

Cell cultures of each metastatic variant were grown *in vitro* then a 100µl bolus of viable cells was implanted sub-cutaneously in Syrian Golden hamsters and tumours allowed to develop.

In contrast to the model of 2-AAF administration where the active metabolites of the causative agent accumulated in the liver and induced neoplastic cell growth in the previously normal hepatocytes, this second model will allow the growth of an homogenous population of already neoplastic cells. The fibrosarcomas are quick growing forming large, highly vascularised, encapsulated, solid tumour masses under the skin; unlike the hepatocellular carcinomas they are made up of a predominantly homogenous cell type invaded not by the cells of the surrounding tissues but those of the haemopoetic and immune systems.

Thus, when sampling the tissue of the fibrosarcomas it was possible to select those parts of the tissue which were mainly composed of proliferating neoplastic cells, any areas of

necrosis (often found to the center of the tumours) could be dissected away at the time of tissue collection. The possibility of major contamination by otherwise normal, non-neoplastic cells was therefore greatly reduced.

This study enabled the utilisation of a second model of tumourigenesis, in order to study the relative presence of tTGase-mediated apoptotic and SDS/insoluble cell products. The scheme of analyses is the same as for the 2-AAF model of heptocellular carcinogenesis. A major change in the type of tumour chosen will, by virtue of the way in which it grows, will allow the tissue samples to be collected in a more controlled fashion. Areas of non-neoplastic or necrotic tissue will not be incorporated into the evaluations, thus the investigate aims to account for the influence of contaminating non-neoplastic cells within the tumour tissue samples taken in the 2-AAF model. The tumour lines chosen being of different metastatic potential, will capitalise on the known relationship of an inverse correlation between transglutaminase activity and metastatic spread. Thus, if a clear correlation between crosslinked apoptotic protein products and transglutaminase is observed, it may help to explain the spread of metastases.

4.2 Results.

4.2.1 Propagation of metastatic hamster fibrosarcomas.

The parent (HSV-2-333-2-26) (metastatic index (6/19) - **low**) and two cloned sublines, MET E (metastatic index (19/20) - **high**) and MET D (metastatic index (1/20) - **very low**) were grown *in vitro* according to the method in section 2.3.1.1. Briefly, cells were cultured to sub-confluence in Dulbecco's modified essential medium (DMEM) with 5% (v/v) foetal calf serum, maintained overnight in serum-free DMEM then harvested by gentle agitation in 5 mM Tris, 2 mM EDTA (pH 7.4) (TE) and washed twice in TE. Cell viability and total counts was assessed using the trypan blue vital dye exclusion method (2.3.1.3). Dilutions made in serum free DMEM to give an homogenous cell suspension of 1 x 10^5 viable cells per 100 µl of medium.

Tumours were passaged *in vivo* by a single sub-cutaneous injection of a 100 µl bolus of the respective cell suspensions, into the right flank of 2 month old Syrian hamsters. Control animals received a bolus containing serum free DMEM only, these animals did not form tumours. The animals were maintained with *ad libitum* access to food and water, 7 days post inoculation a small tumour mass could be detected by palpitation of the skin on the right flank. Animals were sacrificed on days 32, 38 and 46 post inoculation, this was sufficient time for the tumour masses to grow to an excess of 4 cm in diameter, but not sufficient time for the secondary lung metastases which form with these tumours to become life threatening.

At sacrifice portions of non-necrotic tumour tissue were snap frozen for cryostat sectioning and immunohistochemical staining with the anti-envelope antibody, a second portion was prepared for SDS/insoluble polymer analysis using the ELISA method (2.3.13) and the third portion immediately homogenised (2.3.3) and assayed for transglutaminase catalytic activity (2.3.7.1). The series of figures that follow will summarise the results of each of these assays, through the time course, for the three different hamster tumours.

To correlate this second model with the first, all ELISA procedures were standardised using the same positive control polymer, isolated from basal rat liver. All dilutions of primary antisera were kept at 1:1000 and the calibration graphs for both anti-envelope antibody and anti-polymer antibody (Figures 3.2.3 and 3.2.4) incorporate standard curve data from the

ELISA plates used in this study. Extracts of the SDS/insoluble polymers isolated from the MET tumour series were examined by light microscopy (2.3.15.1) (not shown) to compare its appearance to the polymers isolated from rat liver and the 2-AAF hepatocellular carcinoma model. The extracted polymers were of identical physical appearance to those previously isolated see Plate 3.2.1 for comparison.

4.2.2 PARENT - Low incidence-metastatic hamster fibrosarcoma.

Figure 4.1 shows a combination of the ELISA quantitation results for both tTGase-mediated products (Y1) and tTGase activity (Y2) found in Parent tumours. The corresponding age-matched levels of SDS/insoluble polymer and apoptotic polymer, fail to match each other very well. The maximum level of total polymer being very high at 50.57 mg protein/ 1 g tissue/ mg DNA achieved on day 32. The maximum level of apoptotic polymer at 6.39 mg protein/ 1 g tissue/ mg DNA seen on day 38, similar to that found for MET D (Figure 4.2). The transglutaminase activity again did not correlate well to the amounts of both polymers maximising on day 32 of growth was a very high level of 3282.4 nmol putrescine/ h / 1 g tissue; which continued to drop rapidly to a low on day 46 of 145.2 nmol putrescine/ h / 1 g tissue. With time the tTGase activity continued to drop while the level of SDS/insoluble polymer remained constant from day 38 to day 46.

Plate 4.1 shows the immunophosphatase staining (section 2.3.14.2) of non-immune (A inset) and anti-envelope antibody (B main picture) of 4 µm cryostat section of Parent tumour. The fast red TR/napthol substrate of alkaline phosphatase has positively stained a number of individual cells, some of which are small and condensed with a morphological appearance of apoptosis. The non-immune sections were negative.

Plate 4.1 Immunohistochemical staining of Parent low incidence hamster fibrosarcoma, cryostat section taken at day 32 of growth.

A. Inset, control stained with non-immune rabbit serum diluted to give the same protein concentration as the dilution of antibody used in A, followed by anti-rabbit alkaline phosphatase secondary antibody (diluted 1:300). Substrate aqueous fast red, counter stained with heamatoxylin. Photographed at a magnification of X250.

B. Stained with 1:100 dilution of the anti-apoptotic envelope antisera, followed by anti-rabbit alkaline phosphatase secondary antibody (diluted 1:300). Substrate aqueous fast red, counter stained with heamatoxylin. Photographed at a magnification of X250.

A small cluster of positively stained cells (arrowhead) can be seen, in the non-necrotic part of the tumour. The non-immune serum, gives a low level of staining and adds validity to the positive serum.

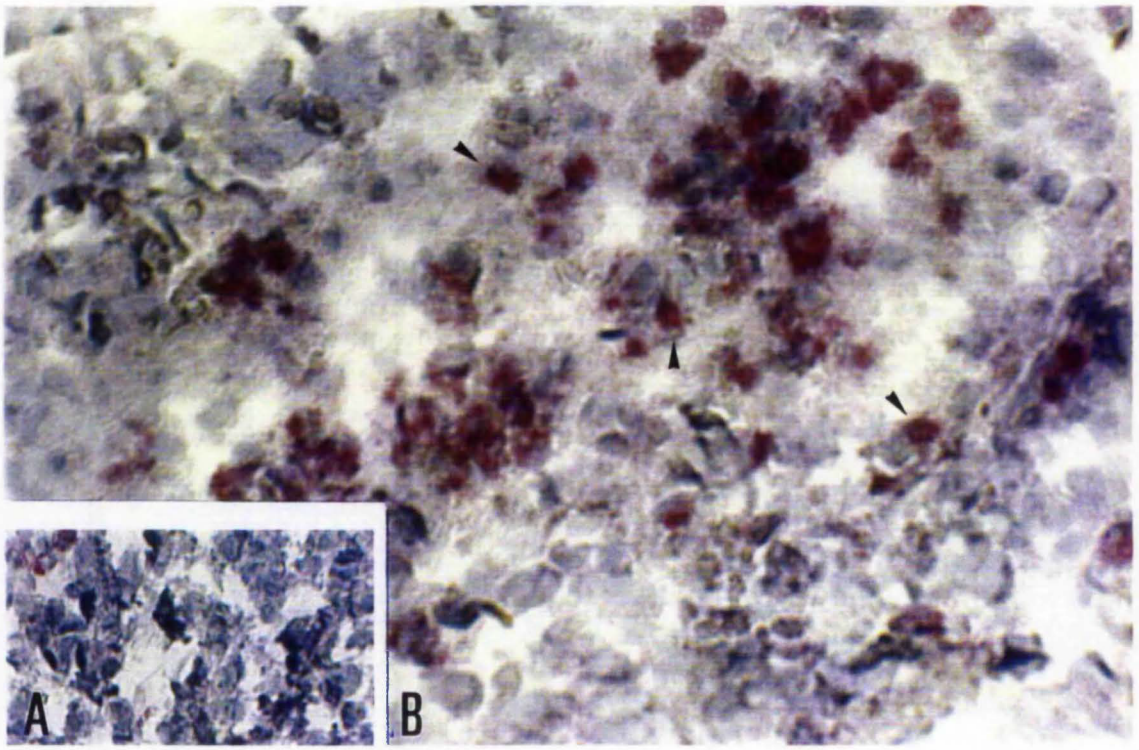
A
B

Figure 4.1 Quantitation of apoptotic and total SDS/insoluble polymer from Parent tumours removed from hamsters at different time points were analysed by ELISA (section 2.3.13) are shown on Y1 and tTGase activity within the tumours as measured by radiolabelled putrescine incorporation (section 2.3.7.2) shown on Y2. The mean data for groups of tumours, n=6 ± S.D. are shown.

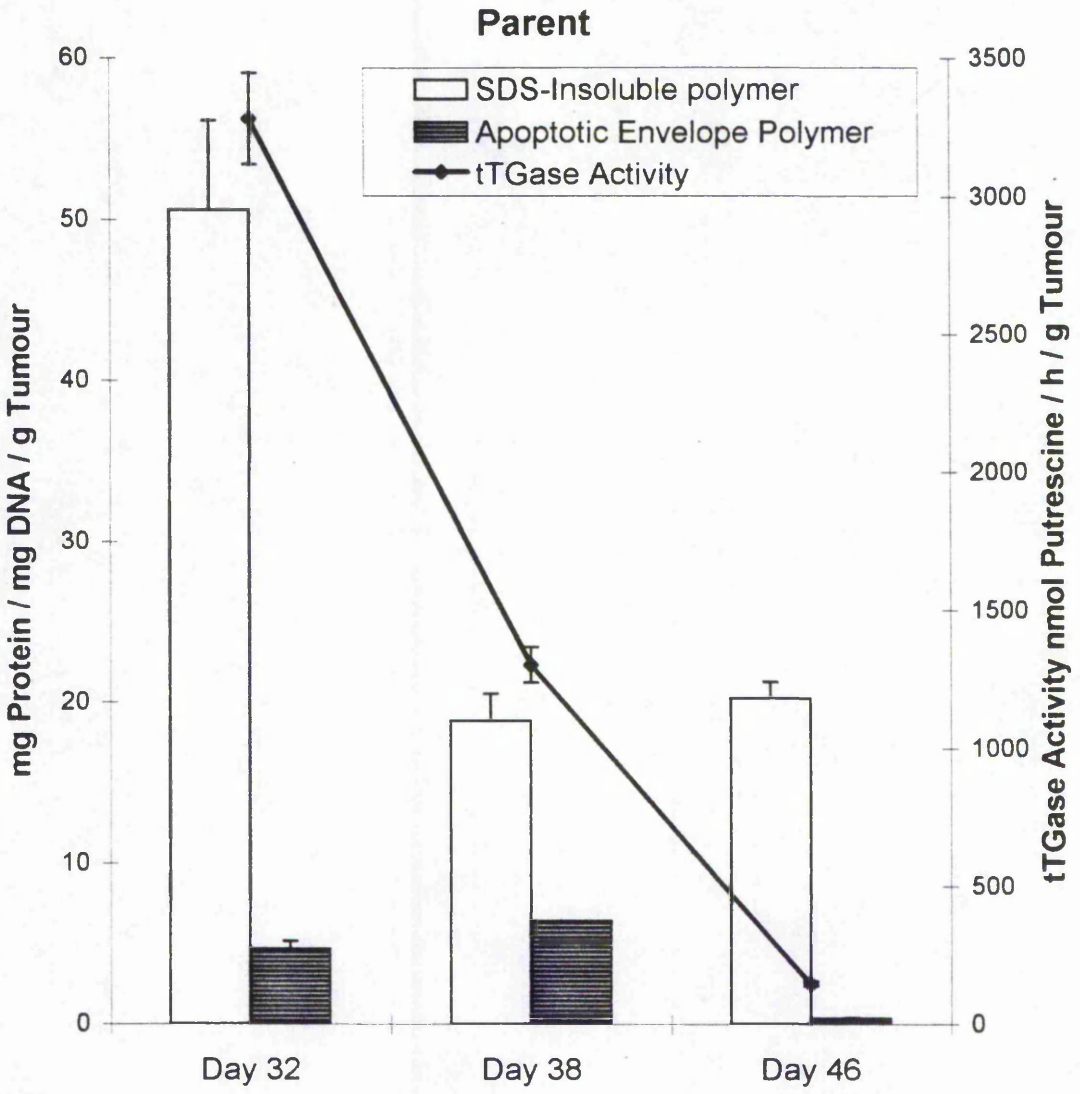
Parent
SDS-Insoluble polymer
Apoptotic Envelope Polymer
tTGase Activity
mg Protein / mg DNA / g Tumour
tTGase Activity nmol Putrescine / h / g Tumour
60
50
40
30
20
10
0
3500
3000
2500
2000
1500
1000
500
0
Day 32
Day 38
Day 46

4.2.3 MET D - -Low or no incidence - metastatic hamster fibrosarcoma.

Figure 4.2 shows a combination of the ELISA quantitation results for both tTGase-mediated products (Y1) and tTGase activity (Y2) found in MET D tumours. The corresponding age-matched levels of SDS/insoluble polymer and apoptotic polymer, match each other very well. The maximum level of total polymer being 35.98 mg protein / mg DNA (isolated from 1 g of tumour tissue), achieved on day 38. This time point also produced the maximum level of apoptotic polymer at 14.13 mg protein / mg DNA / 1 g tissue. This level of apoptotic polymer is 55 times that seen in the Parent tumour. The transglutaminase activity again correlated well to the amounts of both polymers maximising on day 38 of growth was 867.1 nmol putrescine/ h / 1 g tissue. The mean tTGase activity over the tested time course was 500 U / 1g tissue.

Plate 4.2 shows the immunophosphatase staining (section 2.3.14.2) of non-immune (A inset) and anti-envelope antibody (B main picture) of 4 µm cryostat section of MET D tumour. The fast red TR/napthol substrate of alkaline phosphatase has positively stained a number of individual cells, some of which are small and condensed with a morphological appearance of apoptosis. The staining pattern and distribution of positively staining cells was very similar to that seen for the Parent tumour (Plate 4.2 B). The non-immune sections were negative.

Plate 4.2 Immunohistochemical staining of MET D low/no incidence hamster fibrosarcoma, cryostat section taken at day 32 of growth.

A. Inset, control stained with non-immune rabbit serum diluted to give the same protein concentration as the dilution of antibody used in A, followed by anti-rabbit alkaline phosphatase secondary antibody (diluted 1:300). Substrate aqueous fast red, counter stained with heamatoxylin. Photographed at a magnification of X250.

B. Stained with 1:100 dilution of the anti-apoptotic envelope antisera, followed by anti-rabbit alkaline phosphatase secondary antibody (diluted 1:300). Substrate aqueous fast red, counter stained with heamatoxylin. Photographed at a magnification of X250.

A small cluster of positively stained apoptotic cells (arrowhead) can be seen, in the non-necrotic part of the tumour. The non-immune serum, gives a low level of staining and adds validity to the positive serum.

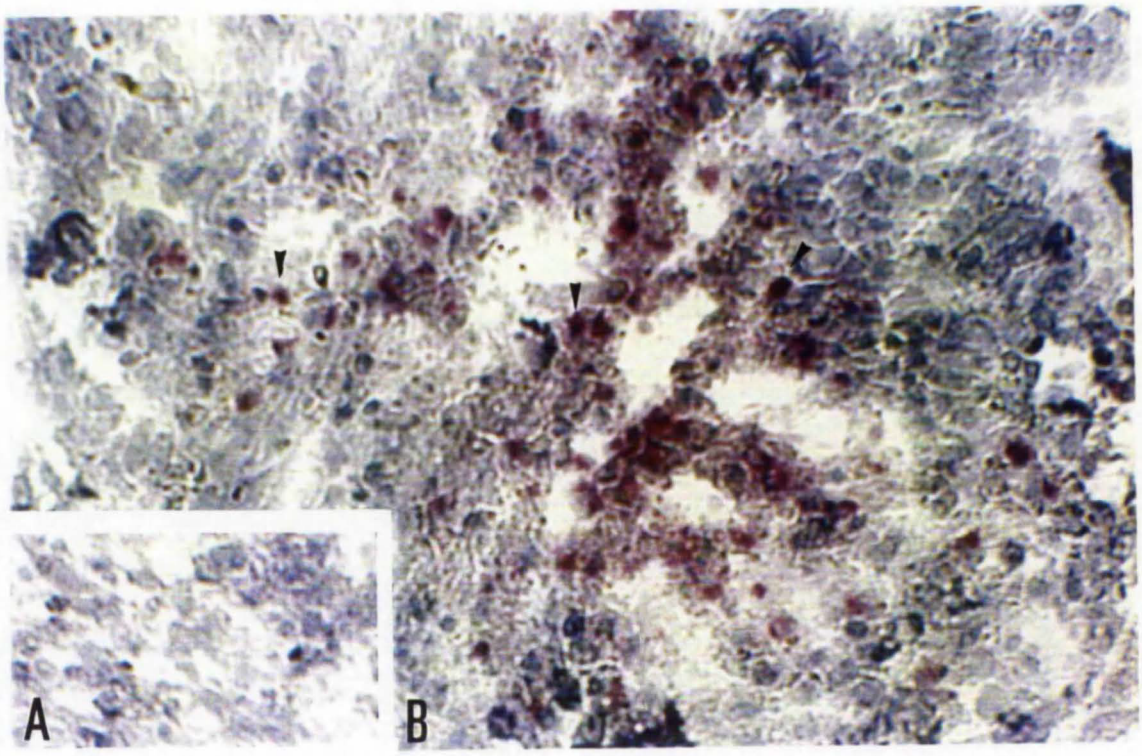
A
B

Figure 4.2 Quantitation of apoptotic and total SDS/insoluble polymer from MET D tumours removed from hamsters at different time points were analysed by ELISA (section 2.3.13) are shown on Y1 and tTGase activity within the tumours as measured by radiolabelled putrescine incorporation (section 2.3.7.2) shown on Y2. The mean data for groups of tumours, n=6 ± S.D. are shown.

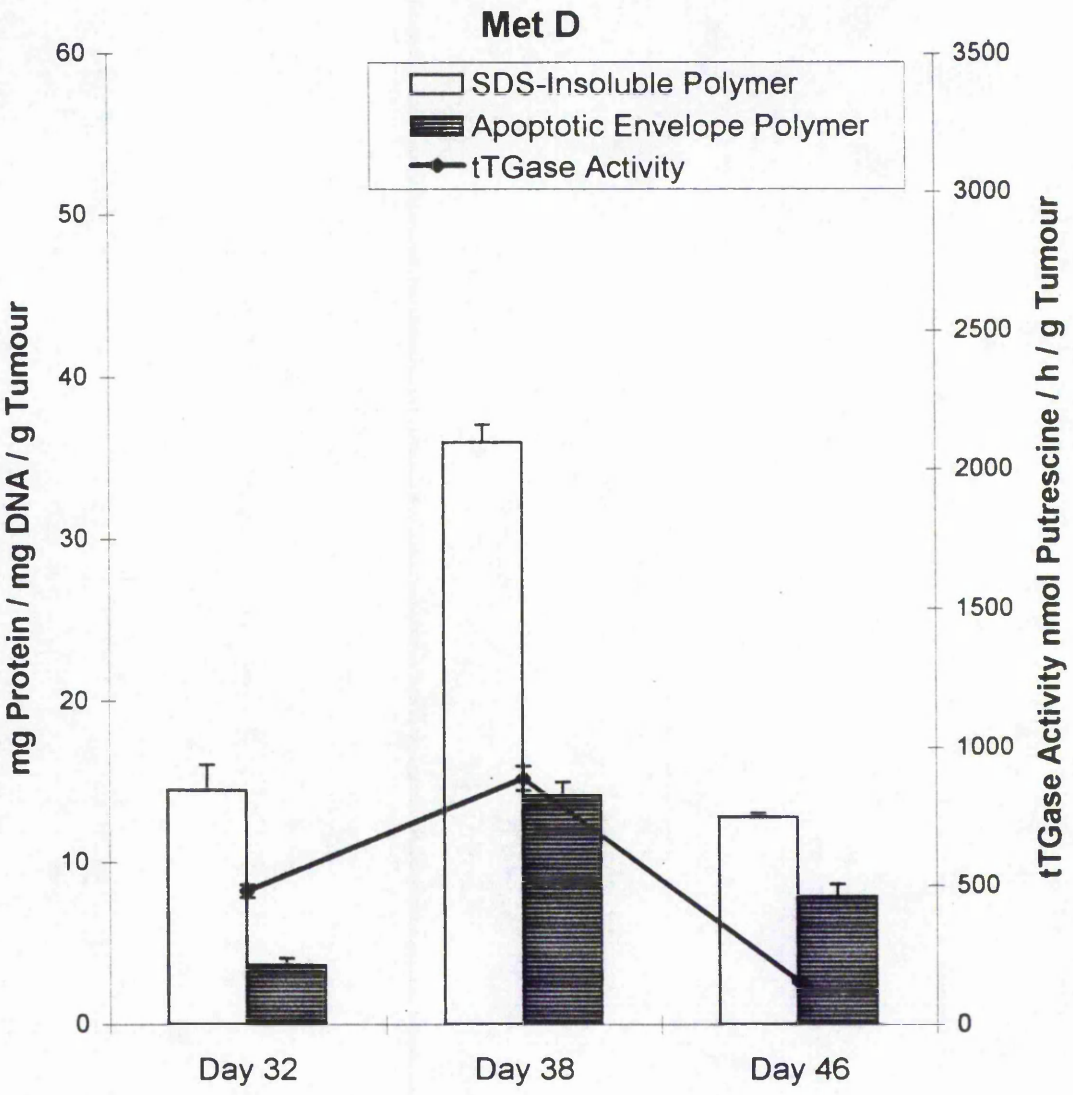
Met D
SDS-Insoluble Polymer
Apoptotic Envelope Polymer
tTGase Activity
mg Protein / mg DNA / g Tumour
tTGase Activity nmol Putrescine / h / g Tumour
60
50
40
30
20
10
0
3500
3000
2500
2000
1500
1000
500
0
Day 32
Day 38
Day 46

4.2.4 MET E - High incidence - metastatic hamster fibrosarcoma

Figure 4.3 shows a combination of the ELISA quantitation results for both tTGase-mediated products (Y1) and tTGase activity (Y2) found in MET E tumours. The corresponding age-matched levels of SDS/insoluble polymer and apoptotic polymer, match each other very well. The maximum level of total polymer being 36.63 mg protein/ 1 g tissue/ mg DNA achieved on day 32. This time point also produced the maximum level of apoptotic polymer at 5.17 mg protein/ 1 g tissue/ mg DNA. The transglutaminase activity again correlated well to the amounts of both polymers maximising on day 32 of growth was 886.7 nmol putrescine/ h / 1 g tissue. The overall drop in both polymers during the proliferation of the tumour and matched drop in transglutaminase activity may be linked to its metastatic behaviour.

Plate 4.3 shows the immunophosphatase staining (2.3.14.2) of non-immune (A inset) and anti-envelope antibody (B main picture) of 4 μm cryostat section of MET E tumour. The fast red TR/napthol substrate of alkaline phosphatase has positively stained a number of individual cells, some of which are small and condensed with a morphological appearance of apoptosis. The staining pattern and distribution of positively staining cells was very similar to that seen for that of both the Parent and MET D tumours (Plate 4.1 B & 4.2 B). The non-immune sections were negative.

Plate 4.3 Immunohistochemical staining of MET E high incidence hamster fibrosarcoma, cryostat section taken at day 32 of growth.

A. Inset, control stained with non-immune rabbit serum diluted to give the same protein concentration as the dilution of antibody used in A, followed by anti-rabbit alkaline phosphatase secondary antibody (diluted 1:300). Substrate aqueous fast red, counter stained with heamatoxylin. Photographed at a magnification of X250.

B. Stained with 1:100 dilution of the anti-apoptotic envelope antisera, followed by anti-rabbit alkaline phosphatase secondary antibody (diluted 1:300). Substrate aqueous fast red, counter stained with heamatoxylin. Photographed at a magnification of X250.

A small cluster of positively stained cells (arrowhead) can be seen, in the non-necrotic part of the tumour. The non-immune serum, gives a low level of staining and adds validity to the positive serum.

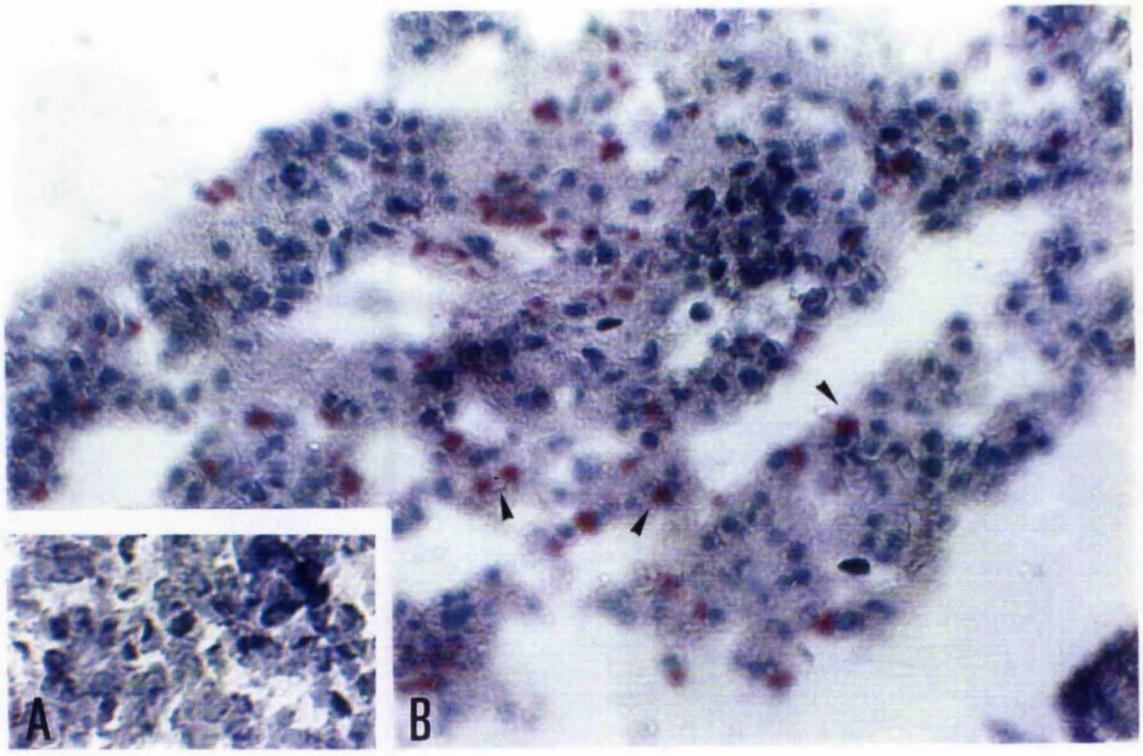
A
B

Figure 4.3 Quantitation of apoptotic and total SDS/insoluble polymer from MET E tumours removed from hamsters at different time points were analysed by ELISA (section 2.3.13) are shown on Y1 and tTGase activity within the tumours as measured by radiolabelled putrescine incorporation (section 2.3.7.2) shown on Y2. The mean data for groups of tumours, n=6 ± S.D. are shown.

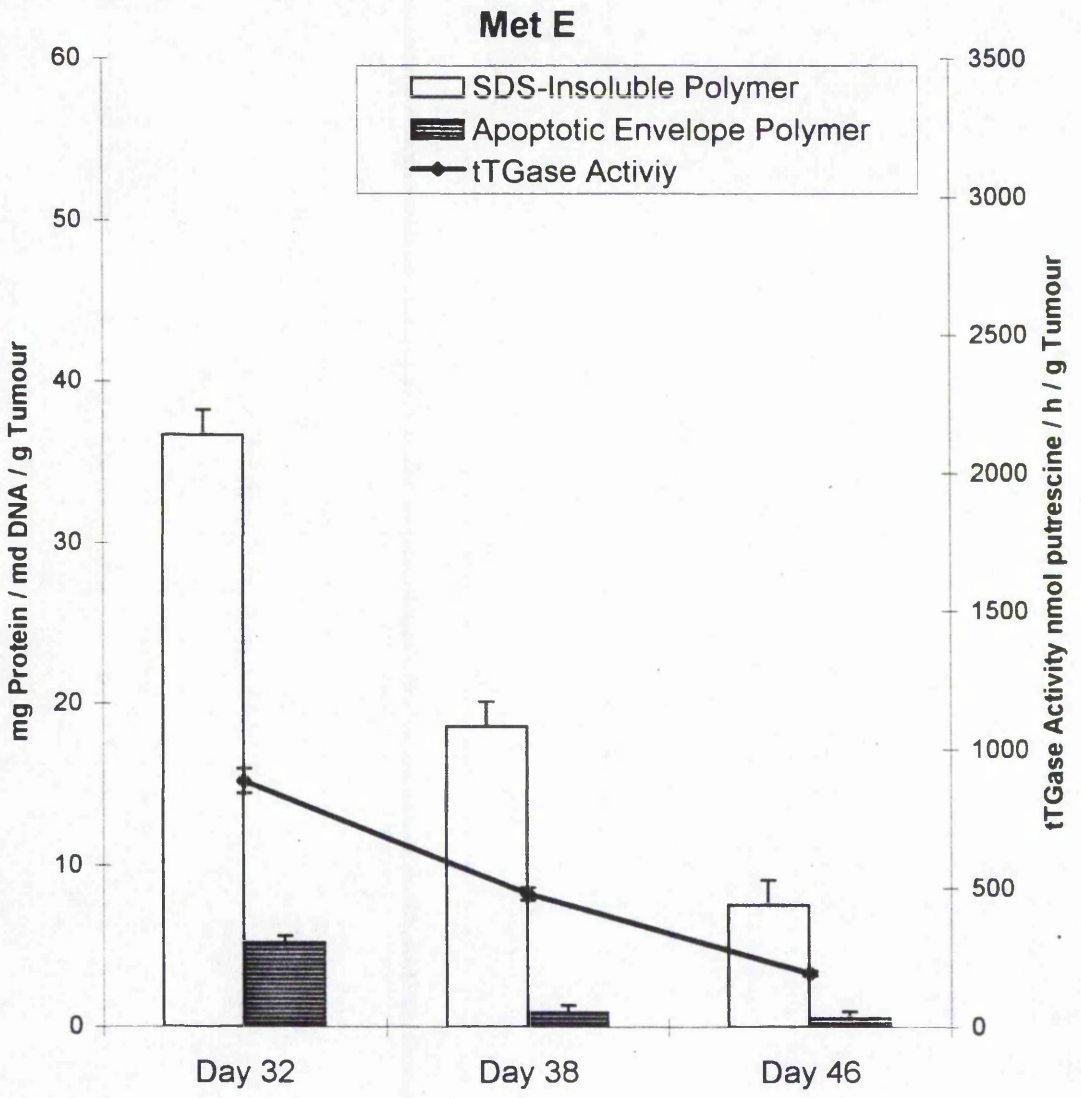
Met E
SDS-Insoluble Polymer
Apoptotic Envelope Polymer
tTGase Activiy
mg Protein / md DNA / g Tumour
tTGase Activity nmol putrescine / h / g Tumour
60
50
40
30
20
10
0
3500
3000
2500
2000
1500
1000
500
0
Day 32
Day 38
Day 46

4.3 Discussion.

Analysis of the three types of metastatic tumour in this section and the hepatocellular carcinoma from section 3, have shown that there generally exists a good correlation between the transglutaminase activity of the tumour mass and the amount of SDS/insoluble and apoptotic polymers that can be isolated from it. The hamster fibrosarcomas represent relatively homogenous populations of neoplastic cells growing in an exponential manner sub-cutaneously. Compared to the heterogeneous nature of the 2-AAF induced rat hepatocellular carcinoma; which invades into the surrounding hepatic tissue resulting in increased hyperplasia, cellular differentiation, proliferation and as indicated apoptosis. The staining patterns for the fibrosarcomas were all very similar (Plates 4.1 B, 4.2 B and 4.3 B).

However, the ELISA method utilising the same antibody is more sensitive and reveals the differences in each of the tumour types with tumour age. The tables shown below, tabulates and summarize the raw data expressed in the preceding figures.

Sample day	*MET E*	*S.D. +/-*	*MET D*	*S.D. +/-*	*PARENT*	*S.D. +/-*
32	36.63	1.83	18.55	1.58	50.57	5.56
38	18.55	0.93	35.98	1.08	18.86	1.86
46	7.49	0.45	12.76	0.25	20.22	1.02

Table 4.2.1 : ANALYSIS OF SDS-INSOLUBLE POLYMER (mg / g tissue / mg DNA)

Sample day	*MET E*	*S.D. +/-*	*MET D*	*S.D. +/-*	*PARENT*	*S.D. +/-*
32	5.17	0.26	3.63	0.44	4.67	0.47
38	0.90	0.04	14.13	0.85	6.39	0.45
46	0.52	0.04	7.87	0.79	0.36	0.05

Table 4.2.2 : ANALYSIS OF APOPTOTIC POLYMER (mg / g tissue / mg DNA)

Sample day	*MET E*	*S.D. +/-*	*MET D*	*S.D. +/-*	*PARENT*	*S.D. +/-*
32	886.7	47.3	478.9	26.4	3282.4	187.6
38	479.0	26.4	867.1	46.2	1301.3	81.4
46	193.2	23.4	154.9	20.4	145.2	12.7

Table 4.2.3 : TRANSGLUTAMINASE ACTIVITY (nmol Putrescine incorp / h / g tissue)

This study inconjunction with the previous study has shown that the anti-apoptotic envelope antisera has good specificity for crosslinked protein envelopes thought to be markers apoptotic cells death. Both as the fully stable crosslinked apoptotic envelopes isolated from cells grown in culture; but also for apoptotic cells found within neoplastic growths of two kinds. The invasive model of rat liver hepatocarcinogenesis and the transplanted model of the metastatic hamster

fibrosarcomas. In both cases the degree of apoptosis as measured by the indirect ELISA for transglutaminase-mediated apoptotic polymers has tried to be correlated to the transglutaminase activity; either through immunohistochemical staining (2-AAF model)or by the radiolabelled putrescine incorporation assay of tTGase activity (MET tumours).

The data of this section is in agreement with the work of Knight *et al* (1990) who found an inverse relationship between tTGase activity in the MET tumours when passaged *in vivo* and the cell lines when grown *in vitro* to the known metastatic potential of the cell lines. Thus, as tTGase activity fell metastatic potential of the tumours increased. Also, the level of tTGase activity was noted to fall with the age of the tumour, a finding repeated in this study. Knight carried out isolation and counting of apoptotic envelopes from cell cultures of the MET variants and found the apoptotic indices (apoptotic envelopes / 100 cells) to be lower in the MET cell lines when compared to controls (BHK-21 0.0480 apoptotic envelopes / 100 cells) but no correlation was found to exist with metastatic potential (Parent 0.0178 apoptotic envelopes / 100 cells; MET D 0.0252 apoptotic envelopes / 100 cells); MET E 0.0109 apoptotic envelopes / 100 cells). This finding is similar to the pattern of both immunohistochemical staining, which appeared the same for all tumour types and the levels of apoptotic polymer quantitated for each tumour.

The major finding of the data in this study is that the overall levels of both polymers fell with the progressive growth of the tumours, irrespective of metastatic potential and that this fall in tTGase-mediated products was matched by a fall in tTGase activity. These findings are in agreement with the general rule that tTGase activity is low in tumours and that cell death (apoptosis) is correspondingly decreased (Fesus *et al* 1989, Ledda-Columbano *et al* 1992). Thus it can be inferred that the unexpected results found in the 2-AAF model could well be due to a contamination effect of the neoplastic tissue with "normal" non-neoplastic tissue taken when sampling.

To conclude no simple correlation has been found to exist between the tissue transglutaminase activity and the degree of cell death via apoptosis seen in either the 2-AAF model of tumourigenesis or the MET fibrosarcoma model.

However, both studies do at times highlight the definite link between the two parameters. Tissue transglutaminase though not controlling apoptosis does appear to play a role in the

physical alteration of those cells subjected to its catalytic action by formation of ε(γ-glutamyl) lysine dipeptide bonds during apoptotic envelope production.

The two models studied thus far have relied on the endogenous levels of tTGase activity and levels of production of tTGase-mediated products to investigate the role of tTGase in programmed cell death. Tumourigenesis models were chosen as these have been well studied and provided reproducible experimental samples. Though, it has become evident that the type of tumour studied will influence the outcome of the experiment.

The availability of a number of established cell lines has made it possible to study the pharmacological action of many topically applied agents on the levels of tTGase activity. Mammalian cell culture of both normal and neoplastic cell lines therefore has many advantages over *in vivo* passage of tumour cells, not least the lack of need for animal experimentation. Having examined how tTGase activity is related to cell death (apoptosis) during tumour progression the following two sections will look at this relationship in two different cell culture models.

5.0 Evaluation of Sodium Butyrate as an Anti-Neoplastic Agent :Induction of Apoptosis and Transglutaminase in Transformed Human Lung Fibroblasts.

5.1 Introduction.

5.2 Results.

5.2.1 Cell Culture.

5.2.2 Examination of Sodium Butyrate Treated Cells by Light Microscopy.

5.2.3 Assay for Cellular Proliferation by Tritiated Thymidine Uptake.

5.2.4 Incorporation of Bromodeoxyuridine.

5.2.5 Transglutaminase Activity Assay.

5.2.6 Transglutaminase Quantitation by Inhibition ELISA.

5.2.7 Isolation and Quantitation of Apoptotic Envelopes.

5.2.8 Indirect Immunofluorescence Studies on Cell Monolayers.

5.2.9 Effect of Sodium Butyrate on Cell Cycle Kinetics.

5.3 Discussion.

5.1 Introduction

In 1977 Birckbichler *et al* showed that the immortalised embryonic lung fibroblast WI38 had significant tissue transglutaminase enzymic activity and antigen. The characteristics of this cell line allowed it to grow into smooth multi-cell-thick layers of elongated fibroblasts forming "sheet-like layers of skin", the cells showed no contact inhibition and would remain viable for upto 7 days. After 7 days the total cell number in a single flask would exceed the limiting factor of nutrients available in the medium and the cells would begin to die, via necrosis, large areas of cell layers, sloughing-off from the bottom of the flask. This cell model proved useful for the study of wound healing as shown in the work of Upchurch *et al* in 1992. When cell monolayers were wounded a high degree of cellular migration into the wound site would occur, tTGase activity increased and the wound site would eventually overgrow with new cells and repair.

When transformed with the SV40 virus (Girardi *et al* 1966) to produce the daughter cell-line WI38 VA13a (subsequently referred to as VA13a) the cell line now showed no or little tissue transglutaminase activity or antigen; its growth pattern and morphology had also changed. VA13a though still fibroblastic, shows a high degree of contact inhibition in culture, the cells are more irregular in shape with multiple foot processes. Cell adherance to various basal lamina (e.g. fibronectin) had become weakened (Girardi *et al* 1966) and the cell line now shows signs that it has lost the ability for cellular migration and wound repair.

Further investigations by Birckbichler *et al* (1983) showed that the topical application of sodium butyrate to cell cultures of VA13a caused the stimulation of a dose and time-dependant induction of tissue transglutaminase activity and antigen. Concomitantly, with the return of tTGase activity in the culture, cell morphology changed and a non-cytotoxic selection process occurred which resulted in a cell population being left which now showed signs of terminal differentiation (Birckbichler *et al* 1983).

Many reports are available in the literature of the action of sodium butyrate to terminally differentiate various cell types (see discussion at end of this chapter), resulting in cell cycle arrest and reduction of cell population number in many diseased states. Observation of VA13a culture when grown in the presence of sodium butyrate showed signs of cells, both floating in the culture medium and adhered to the flask bottom, of a morphology typical of apoptosis.

Given these observations it was thought that the mode of action of sodium butyrate on VA13a was through the induction of tTGase- which in turn caused the reduction in cell number through its possible involvement in programmed cell death (apoptosis).

The objective of the work discussed in this chapter was to investigate the topical action of sodium butyrate on VA13a, analysing the induction of tTGase activity and antigen. This could then be correlated with respect to changes in cell number, levels of apoptosis as determined by cell morphology and the production of tTGase-mediated apoptotic envelopes; and changes in the cell cycle kinetic of the total cell population.

5.2 Results

5.2.1 Cell Culture in the Presence of Sodium Butyrate

VA13a cells were grown and treated topically with sodium butyrate as described in section 2.3.1.1.4. Cell numbers were determined using the citric acid nuclei counting method (section 2.3.1.3.) cell sonicates were prepared as described in section 2.3.4 protein content of sonicates was determined using the BioRad DC Protein Assay Kit (section 2.3.6.1).

Sodium butyrate had a dose-dependent effect on the cell density of VA13a cells (Figure 5.1). Significant differences in cell numbers between sodium butyrate-treated cells and control cells were seen two days after the addition of sodium butyrate and differences remained throughout the course of the experiment. Cultures exposed to 2 mM sodium butyrate for 7 days had final cell populations which were double the initial seeding density but only 23% of those seen in the control populations not exposed to sodium butyrate for the same time period. Cultures exposed to 1 mM sodium butyrate had cell numbers 5 times higher than the initial seeding density, but the cell number was still only about 56% of the number of cells seen in the control populations.

5.2.2 Examination of Sodium Butyrate Treated Cells by Light Microscopy

Examination of the cell cultures by light microscopy were made daily during the course of the experiment following the methodology set out in section 2.3.15.1. Photomicrographs were taken of those cultures which showed altered morphology.

Significant morphological differences were evident in both 1 mM and 2 mM sodium butyrate cultures within 1 day after the addition of butyrate when compared to control cultures (Plate 5.1 b-d). A similar pattern was observed for the amount of transglutaminase which was detected with a monoclonal antibody to transglutaminase although the differences were not evident until 2 days following butyrate addition (Figure 5.4). The presence of enlarged cells with elongated foot processes was noted, as was the high degree of cellular debris and apparently dead cells now floating in the culture medium.

Figure 5.1 Effect of sodium butyrate on cell growth density of VA13a. Cultures were inoculated at 30-40,000 cells/cm^2 and 48 h later exposed to various concentrations of sodium butyrate as described in section 2.3.1.1.4. The cultures were maintained on the appropriate media for various time periods with complete medium changes every 48 h. At the indicated times, cells were harvested for cell counts using the citric acid method 2.3.1.3. Data represents the mean of 6 experiments, error bars mean ± standard error of mean..

Effect of Sodium Butyrate on Growth of VA13a

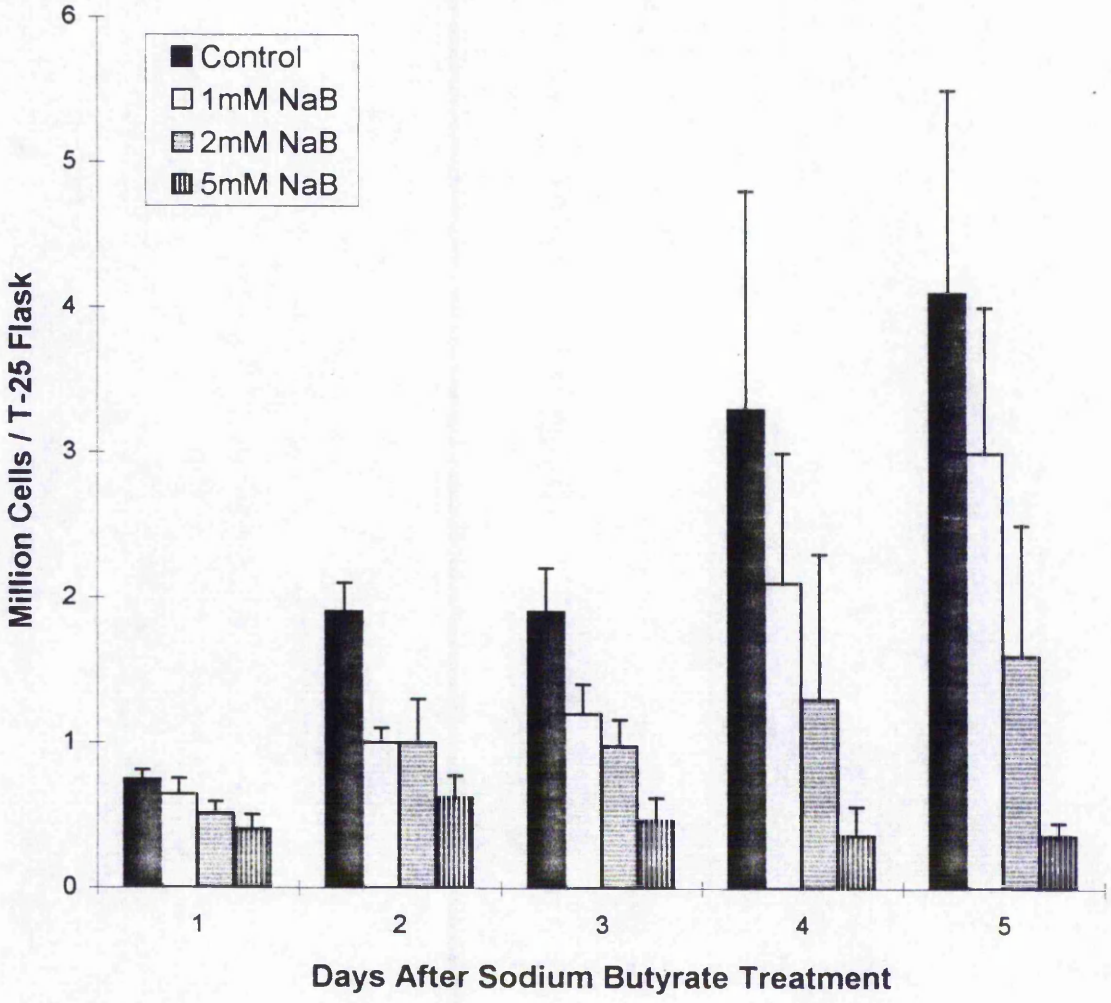

Plate 5.1 Effect of sodium butyrate on cell growth morphology of VA13a.

Cultures were inoculated at 30-40,000 cells/cm^2 and 48 h later exposed to various concentrations of sodium butyrate. The cultures were maintained on the appropriate media for various time periods with complete medium changes every 48 h. At the indicated times, cells were photographed on an Olympus CK-2 inverted microscope. Shown are the light micrographs of cell cultures (control (B), 1mM NaB (C), 2mm NaB (D); inset plate (A) shows effect of NaB on VA13a growth curves, shown in figure 5.3.1). Note the elongated appearance of the sodium butyrate treated cultures (C & D). Data represents the mean of 6 experiments, error bars mean ± standard error of mean. Magnification X 62.5 in all plates.

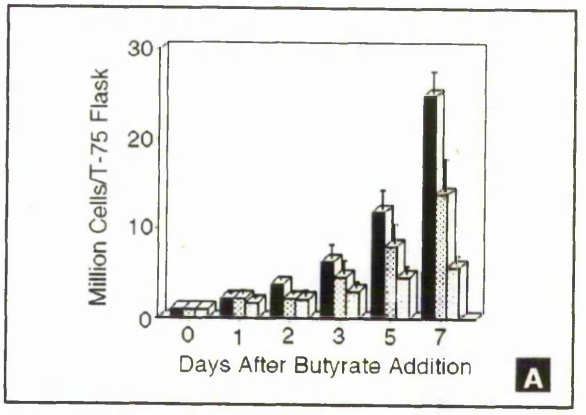
Million Cells/T-75 Flask
30
20
10
0
0 1 2 3 5 7
Days After Butyrate Addition
A

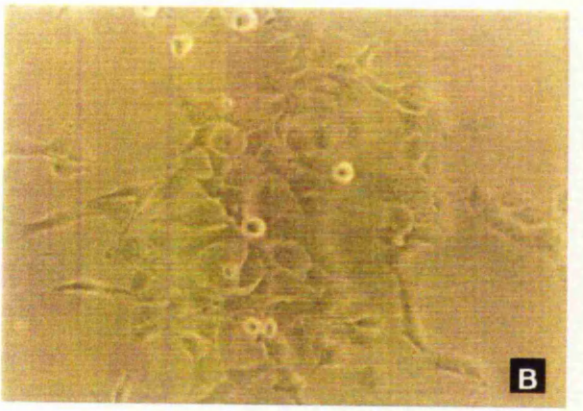
B

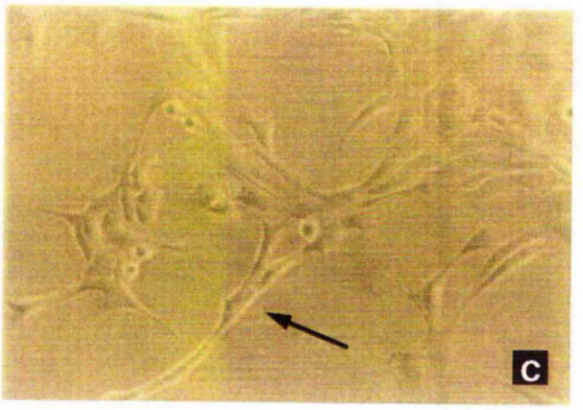
C

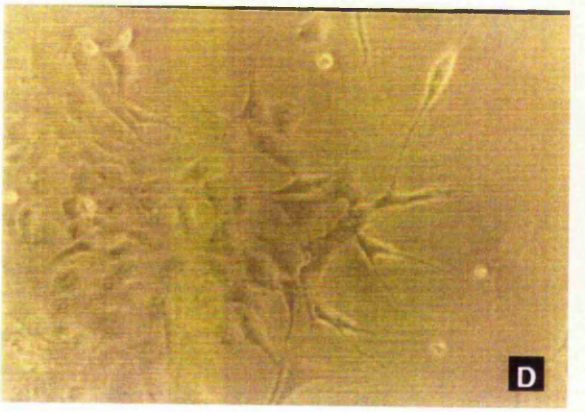
D

5.2.3 Assay for Cellular Proliferation

In order to assess the possible cytotoxic effects of sodium butyrate (NaB) on VA13a cell proliferation was monitored by using the established technique of ^{3}H-methylthymidine incorporation into cells which were being treated with NaB, the method used is set out in section 2.3.20. Figure 5.2 shows the continued incorporation of the thymidine with time, until such time that the population has departed from the exponential phase of growth.

Tritiated thymidine incorporation studies showed the cultures were actively synthesising DNA and thus ruled out that these differences were a consequence of cytotoxicity by sodium butyrate (Figure 5.2).

5.2.4 Incorporation of Bromodeoxyuridine

The tritiated thymidine method assumes that the synthesis of new DNA and hence cellular proliferation is distributed evenly in all cells. This may not be the case. Therefore, it was necessary to know how many of the cells in the population were behaving normally. The Amersham cell proliferation assay kit (Amersham Corporation, section 2.3.21) provides a means of testing this question *in situ*. The principle of the kit is to immunohistochemically stain those cells which are incorporating a thymidine analogue, 5-bromo-2'-deoxyuridine (BrdU) into replicating DNA. We identified those cells which were proliferating by examination of cell monolayers following staining with the cell proliferation assay kit by light microscopy (Plate 5.2 b-d)

5.2.5 Transglutaminase Activity Assay

The principle of the transglutaminase activity assay relies on the ability of the enzyme to catalyse the incorporation of a radiolabelled primary amine into a protein acceptor substrate (Lorand *et al* 1972, Chomczynski *et al* 1987). A modification of this method is described in section 2.3.7.2. The differences between butyrate-treated and control cultures continued to widen with time and a dose-dependent effect was evident in the butyrate-treated populations since the 2 mM-treated cultures had 1.5 to 2 times more transglutaminase activity than 1 mM-treated cultures (Figure 5.3).

Figure 5.2 Effect of sodium butyrate on DNA synthesis activity in VA13A. At the indicated times, cells were examined for *de novo* DNA synthesis by ^{3}H-methylthymidine incorporation as described in section 2.3.20. Cells were seeded as described previously in section 2.3.1.1.4, it was ensured that cell growth was within the exponential phase as calculated by analysis of population doubling times. Data represents the mean of 6 experiments, error bars mean ± standard error of mean..

Tritiated Thymidine Uptake in VA13a

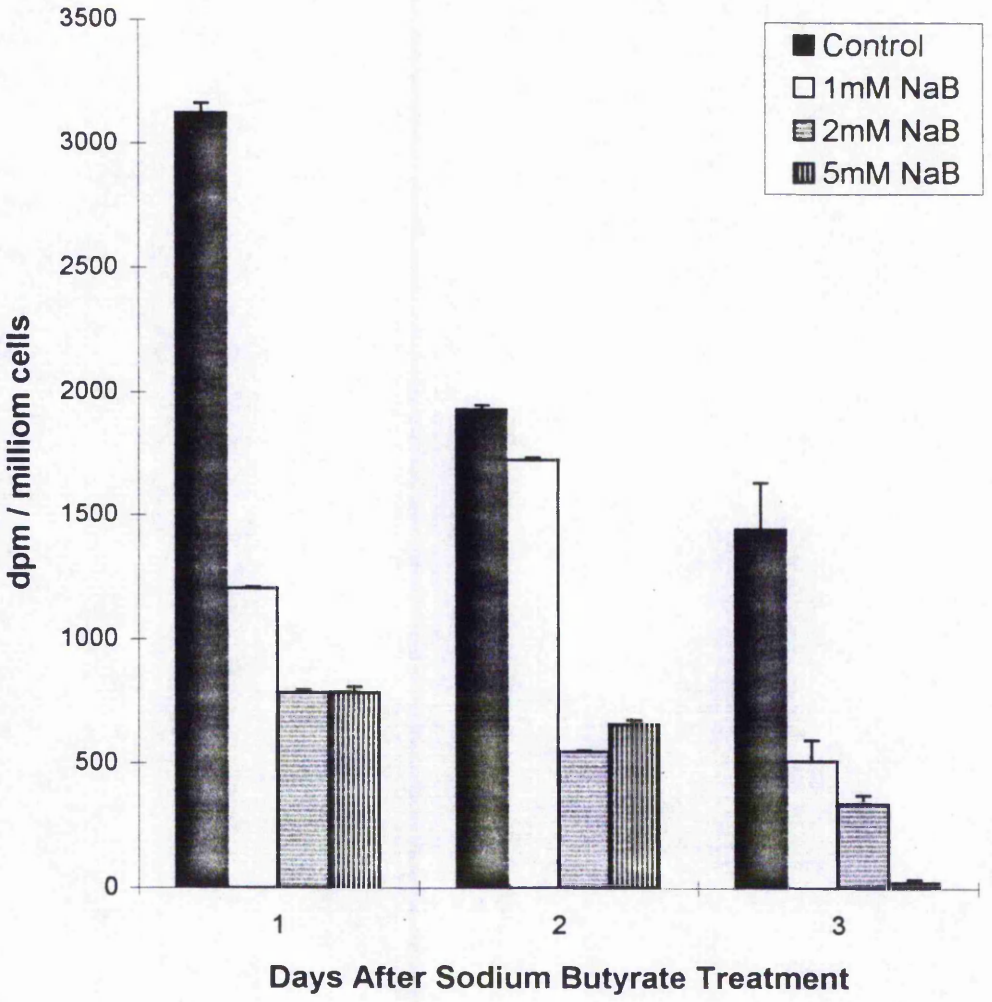

Plate 5.2 Analysis of cell proliferation following the effect of sodium butyrate on VA13A.

The cultures were maintained on the appropriate media for various time periods with complete medium changes every 48 h. At the indicated times, cells were examined for DNA synthesis and cell proliferation by bromodeoxyuridine incorporation, using the Amersham cell proliferation assay kit as described in section 2.3.21. Shown are the light micrographs of immunoperoxidase positive cells (control (B), 1mM NaB (C), 2mm NaB (D); inset plate (A) shows thymidine uptake as shown in Figure 5.2). Note that not all the cells in each photograph have taken up the peroxidase substrate. Also note that in the 2mM sodium butyrate (NaB) culture (plate D) those which have stained dark brown are predominantly larger than those in the other photographs.. Data represents the mean of 6 experiments, error bars mean ± standard error of mean. Magnification X 62.5 in all plates.

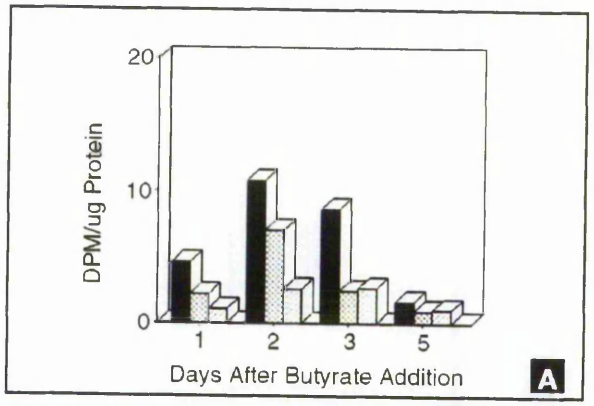
20
10
0
DPM/ug Protein
1
2
3
5
Days After Butyrate Addition
A

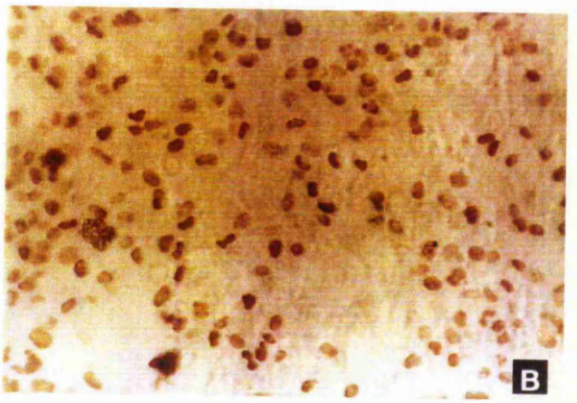
B

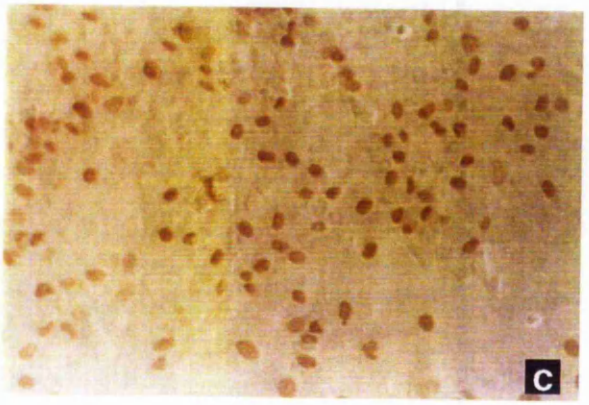
C

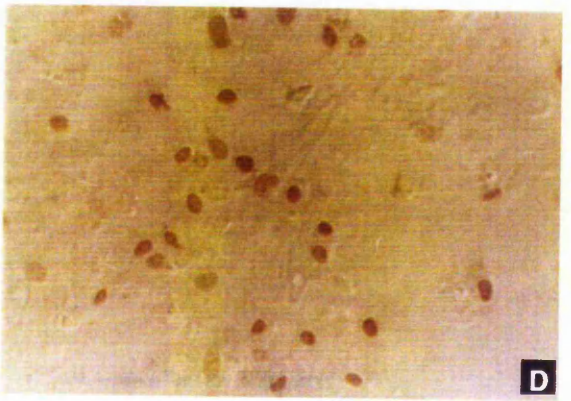
D

Figure 5.3 Transglutaminase activity of VA13A as effected by sodium butyrate. Cultures were inoculated at 30-40,000 cells/cm^2 and 48 h later exposed to various concentrations of sodium butyrate. The cultures were maintained on the appropriate media for various time periods with complete medium changes every 48 h. At the indicated times, cells were harvested and assayed for transglutaminase activity using the radiolabelled putrescine assay described in section 2.3.7.2. The induction of tTGase can be seen to be dose and time-dependent. Data represents the mean of 6 experiments, error bars mean ± standard error of mean..

Transglutaminase Activity of VA13a Following Sodium Butyrate Treatment

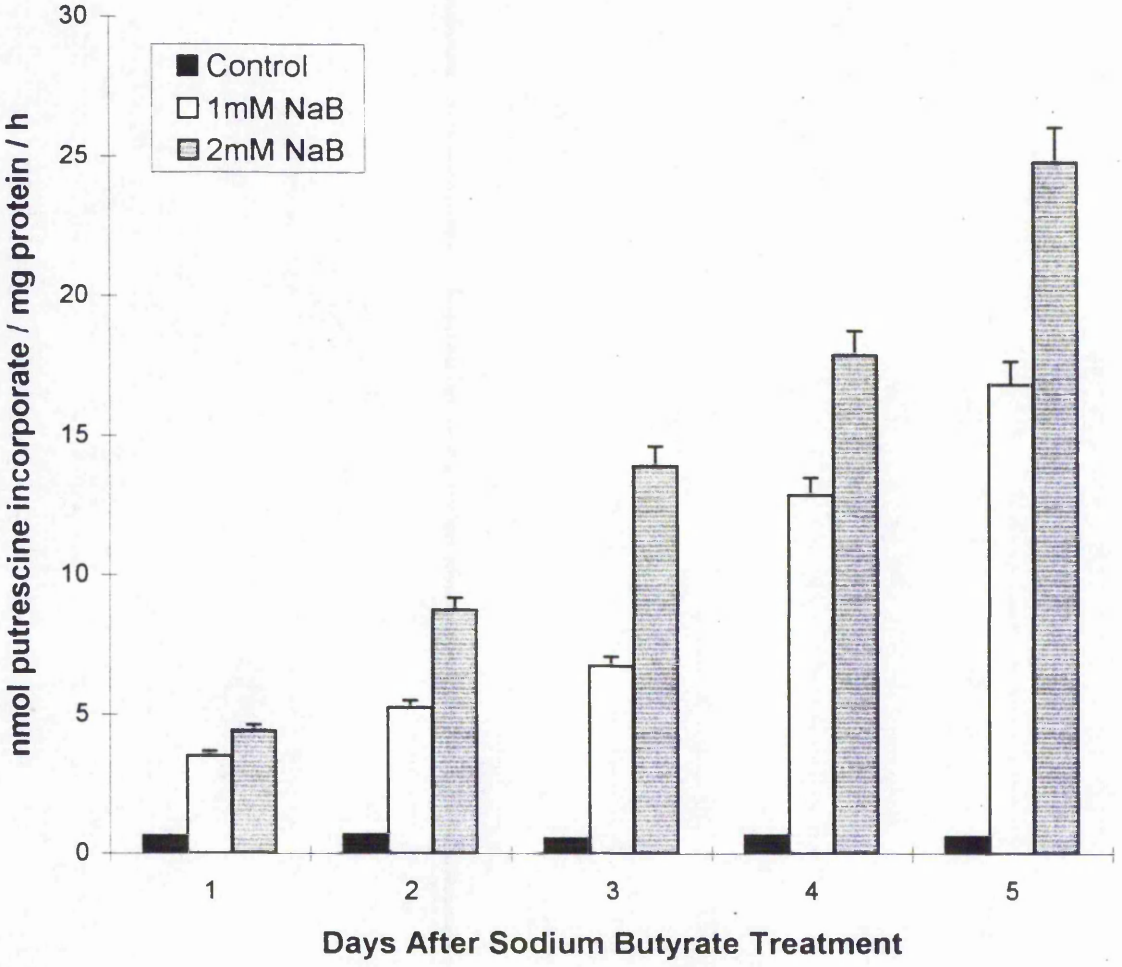

5.2.6 Transglutaminase Quantitation by Inhibition ELISA

Estimation of the amount of transglutaminase in the samples was carried out using an inhibition ELISA method developed in our laboratory (Lee *et al* 1987). Basically, the technique relies on the ability of the antigen present in the sample to combine with transglutaminase antibody CUB7401 (Birckbichler *et al* 1985) and effectively reduce the amount of antibody that is subsequently available to react with transglutaminase which is bound to a 96 well microtitre plate.(Section 2.3.8.2 & 2.3.8.3)

The amount of transglutaminase antigen increased 50 to 100-fold in the sodium butyrate treated samples when compared to the control cultures. The amount of immunoreactive material in the 2 mM sodium butyrate cultures was generally 1.5 to 2 times greater than that observed in the 1 mM sodium butyrate cultures. Transglutaminase activity and antigen were still increasing in the butyrate cultures after 5 days of exposure to the chemical, while both parameters remained relatively constant throughout this time period in the control cultures. Figure 5.4

5.2.7 Isolation and Quantitation of Apoptotic Envelopes

The apoptotic envelope is fully stabilised by the action of transglutaminase-mediated crosslinking, and in the process is rendered insoluble to chaotrophic agents (Fesus *et al* 1989) by utilising this physical property of insolubility apoptotic envelopes may be isolated from cells in culture, thereby giving an estimate of cell apoptosis which may be directly caused by tTGase-mediated reactions.

The number of apoptotic envelopes isolated from the both cultures and culture supernatants followed a slightly different pattern (Figure 5.5 and Figure 5.6 plate d). A significant elevation in the number of apoptotic envelopes was seen in butyrate-treated cultures within 1 day of butyrate addition. Envelope content continued to increase in the butyrate-treated cultures and reached a maximum level after 3 days. Thereafter, envelope quantity decreased and the levels in butyrate-treated cells was somewhat lower than the levels found in control cells on the same day. Once again the 2 mM sodium butyrate cultures had the highest level of apoptotic envelopes. No evidence of a second peak of apoptosis was seen at later time

Figure 5.4 Transglutaminase protein antigen of VA13A as effected by sodium butyrate. Cultures were inoculated at 30-40,000 cells/cm^2 and 48 h later exposed to various concentrations of sodium butyrate. The cultures were maintained on the appropriate media for various time periods with complete medium changes every 48 h. At the indicated times, cells were harvested and assayed for transglutaminase antigen using a monoclonal antibody in an inhibition ELISA assay (sections 2.3.8.2 and 2.3.8.3. The induction can be seen to be dose and time-dependent. Data represents the mean of 6 experiments, error bars mean ± standard error of mean..

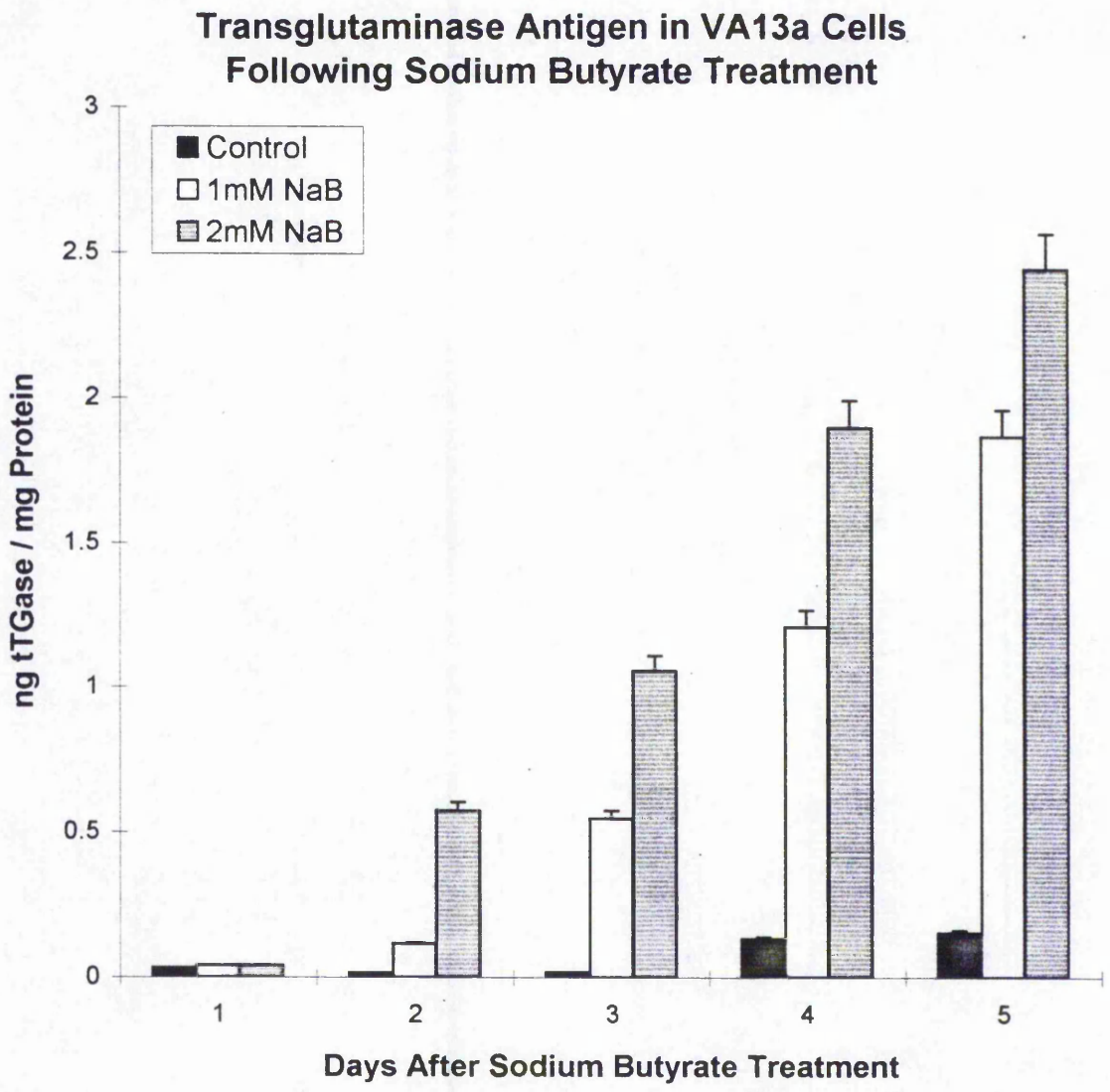
Transglutaminase Antigen in VA13a Cells
Following Sodium Butyrate Treatment
Control
1mM NaB
2mM NaB
ng tTGase / mg Protein
3
2.5
2
1.5
1
0.5
0
1
2
3
4
5
Days After Sodium Butyrate Treatment

Figure 5.5 Quantitation of SDS/insoluble apoptotic envelopes of VA13A as effected by sodium butyrate. Cultures were inoculated at 30-40,000 cells/cm^2 and 48 h later exposed to various concentrations of sodium butyrate. The cultures were maintained on the appropriate media for various time periods with complete medium changes every 48 h. At the indicated times, culture medium and adherent cell were harvested and envelopes isolated according to the method set out in section 2.3.11. "Sister" flasks were counted to ascertain the cell number. Clearly the apoptotic index of the butyrate treated cultures continues to rise until day three, after this point the numbers drop rapidly Data represents the mean of 6 experiments, error bars mean ± standard error of mean..

Apototic Envelope Index for VA13a Treated with Sodium Butyrate

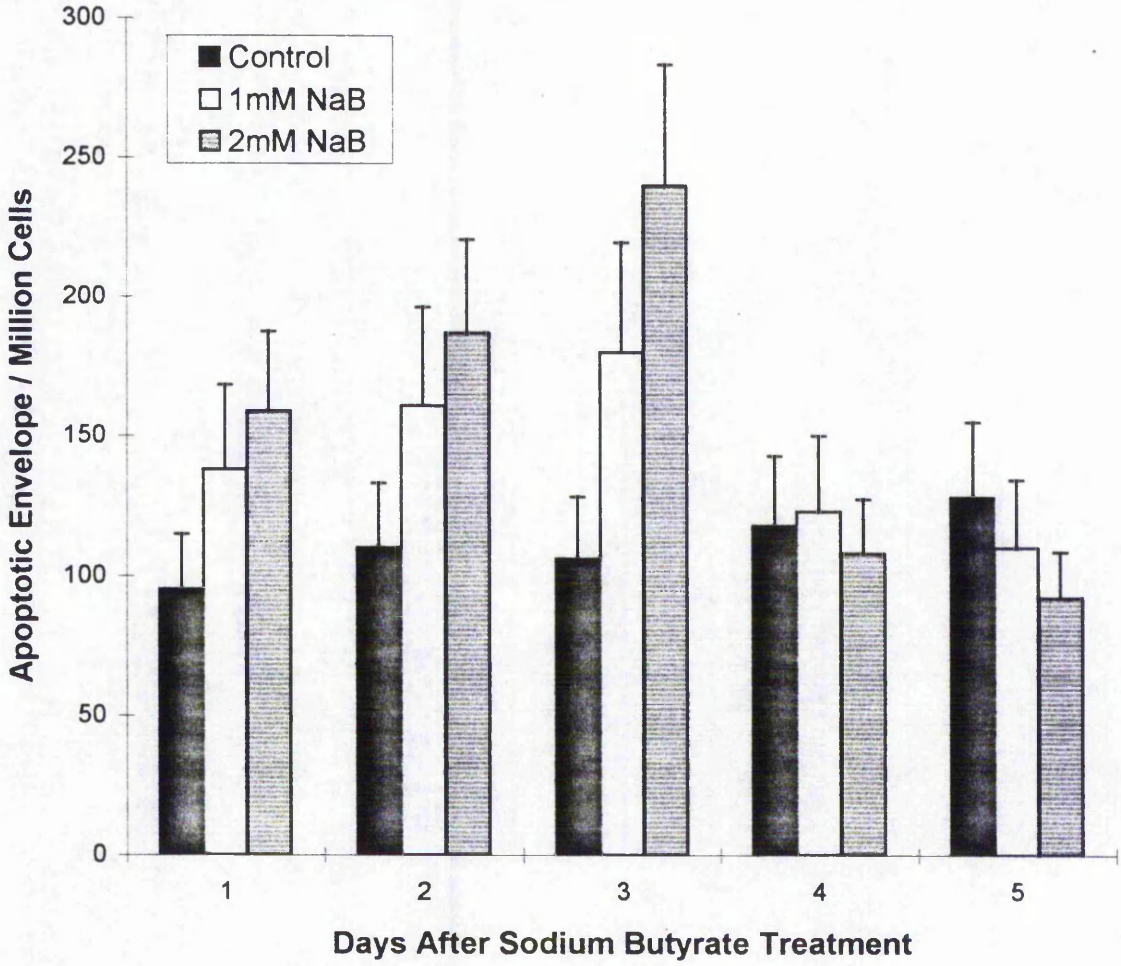

Figure 5.6 Composite figure summarising the effects of sodium butyrate treatment on VA13a with respect to : (A) tTGase activity, Figure 5.3; (B) tTGase antigen, Figure 5.4; (C) tTGase-mediated apoptotic envelope index, Figure 5.5 and plate (D) photomicrograph of an isolated apoptotic envelope. Magnification X 62.5.

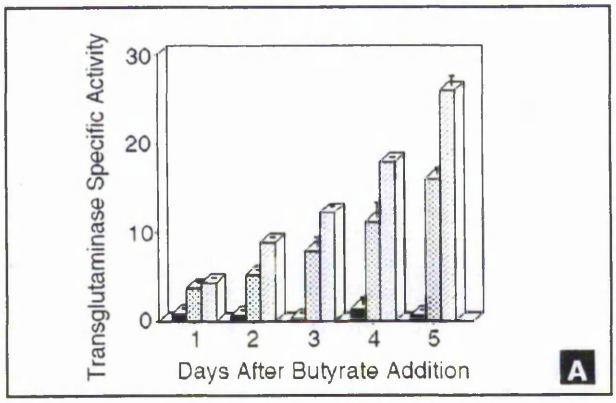
Transglutaminase Specific Activity
30
20
10
0
1 2 3 4 5
Days After Butyrate Addition
A

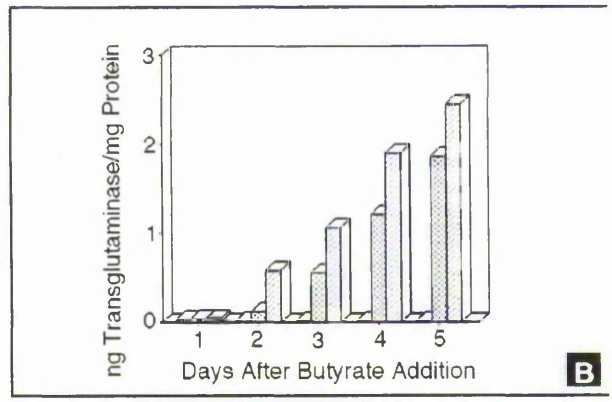
ng Transglutaminase/mg Protein
3
2
1
0
1 2 3 4 5
Days After Butyrate Addition
B

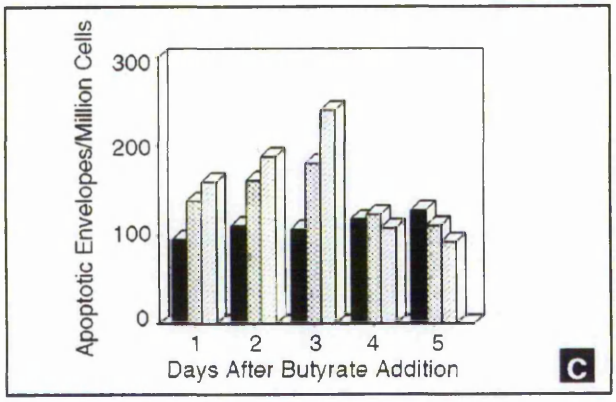
Apoptotic Envelopes/Million Cells
300
200
100
0
1 2 3 4 5
Days After Butyrate Addition
C

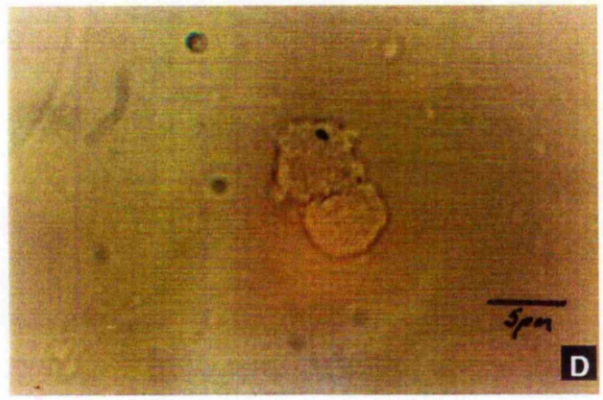
5μm
D

periods, although there is an increase in the number of giant cells with the greater amounts of DNA.

5.2.8 Indirect Immunofluorescence Studies on Cell Monolayers

Having previously made a polyclonal antibody raised to tTGase-mediated apoptotic envelopes (Sections 2.3.11 & 2.3.12 et seq) this was used inconjunction with the anti-tTGase monoclonal antibody CUB 7401 to undertake *in situ* visualisation and subsequent quantitation of immunopositive cells (section 2.3.14.3).

Immunofluorescence studies with monoclonal antibody to cellular transglutaminase confirmed the presence of more transglutaminase in cells which had been exposed to sodium butyrate (Plate 5.3 a-f) than control cells. Cells which by morphological examination were thought to be cells undergoing apoptosis, namely those cells which were round, dark and appeared to contain inclusion bodies, also stained positive with the antibody to transglutaminase. In certain instances these structures stained more intensely than the surrounding cells (Plate 5.3 d & e arrows). Non-immune hybridoma fluid gave no visible fluorescence (Plate 5.3 a) despite the presence of a large number of cells as seen in the phase contrast photograph (Plate 5.3 b).

Studies with a polyclonal antibody to apoptotic envelopes showed that the material which primarily stained with the antibody were the dark, pitted structures (Plate 5.4 a-f). It should be noted that not all suspected apoptotic cells stained with the antibody to transglutaminase. Control cultures also showed the presence of some immunoreactive material to antibody to apoptotic envelopes (Plate 5.4 a). However, the amount of staining was less than that seen in the butyrate-treated cultures which is consistent with the apoptotic envelope counts reported in Figure 5.5 Non-immune serum showed essentially no staining for apoptotic envelopes (Plate 5.4 a).

5.2.9 Effect of Sodium Butyrate on Cell Cycle Kinetics

Cells were stained with propidium iodide (Plate 5.5 b-d) and examined for distribution of the stain using a Fluorescent Automated Cell Sorter for up to 5 days after the addition of sodium butyrate. Analysis was carried out on a Becton Dickinson FACS Scan flow cytometer (section 2.3.19). A total of 20,000 excitation events were monitored and the data recorded. Post-run analyses were carried out using the CellFIT Cell-Cycle Program

Plate 5.3 Immunofluorescent staining for transglutaminase in VA13a as described in section 2.3.14.3.

Cultures were inoculated at 30-40,000 cells/cm^2 on chamber well slides and 48 h later exposed to various concentrations of sodium butyrate . The cultures were maintained on the appropriate media for various time periods with complete medium changes every 48 h (section 2.3.1.1.4). 72 h after treatment, cells were washed, fixed, permeabilised and stained with the monoclonal antibody CUB 7401 specific for transglutaminase or immunoglobulin isotype, control monoclonal antibody CUB 11. (A) control treated stained with CUB 11 - non-immune control; (B) 1mM NaB treated stained with CUB7401; (C) 2mM NaB treated stained with CUB7401; (D) control treated stained with CUB 7401 - immune control; (E) brightfield image for plate (B); bright field image for plate (C), An increase in the intensity of tTGase antibody staining can be observed, plate (C) showing the cytoplasmic and peri-nuclear distribution of the enzyme. The arrows indicate areas of suspected apoptotic cells. Magnification X 62.5 in all plates.

Plate 5.4 Immunofluorescent staining for transglutaminase-mediated apoptotic envelopes in VA13a as described in section 2.3.14.3.

Cultures were inoculated at 30-40,000 cells/cm^2 on chamber well slides and 48 h later exposed to various concentrations of sodium butyrate . The cultures were maintained on the appropriate media for various time periods with complete medium changes every 48 h (section 2.3.1.1.4). 72 h after treatment, cells were washed, fixed, permeabilised and stained with a polyclonal antibody specific for transglutaminase-mediated apoptotic envelopes (anti-envelope) or immunoglobulin isotype, control rabbit IgG. (A) control treated stained with - non-immune control; (B) 1mM NaB treated stained with anti-envelope; (C) 2mM NaB treated stained with anti-envelope; (D) control treated stained with anti-envelope - immune control; (E) brightfield image for plate (B); bright field image for plate (C), An increase in the number of irregular shaped cells, which have detached from the flask surface can be observed, plate (C) showing a cell with a number of definite membrane blebs. Cells with normal morphology which were still flattened and adhered to the flask surface can be seen in the matched brightfield images and can be seen not to stain with the anti-envelope antibody. The arrows indicate areas of suspected apoptotic cells. Magnification X 62.5 in all plates.

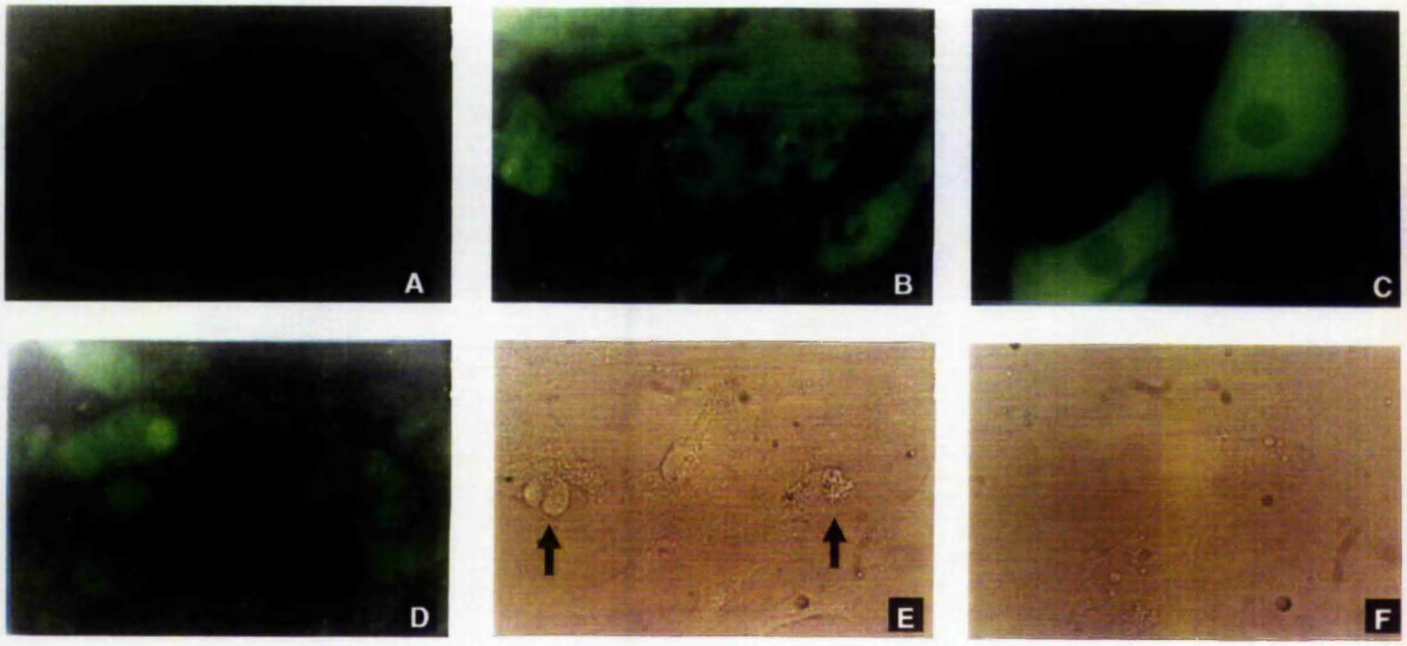
A
B
C
D
E
F

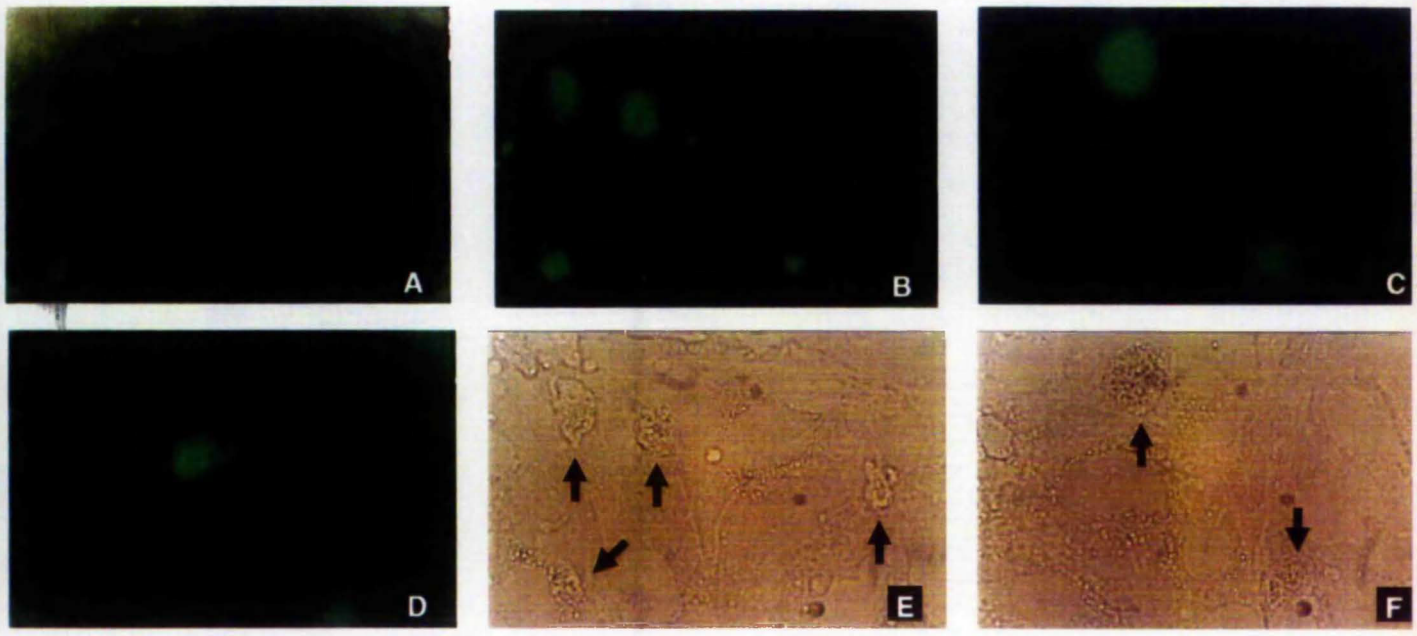
A
B
C
D
E
F

Plate 5.5 Inset (A) Table 5.2a- summary table for the distribution of population types following flow cytometry.

U.V. Photomicrographs of propidium iodide stained cells, taken under a rhodamine filter 620 nm. These are day 3 cells for each experimental condition a sample of which had been examined by flow cytometry (D) control, (C) 1 mM NaB and (B) 2 mM NaB.(as described in section 2.3.19). These photographs indicate that the cells examined by flow cytometry are indeed single-cells. Hence it confirms that those large cells which previously stained for bromodeoxyuridine (see Plate 5.2 b-d), did actually contain higher amounts of DNA, see cells after 2 mM NaB treatment plate (B). . Thus, the extra peak of DNA Staining appearing in the histograms (Figure 5.7 A-E) is legitimate and not cell artefacts or clumps. Magnification X 62.5 in all plates.

Sample	G_0/G_1	S	G_2/M	Other
Control				
Day 1	46.0	18.1	35.9	–
Day 2	49.5	20.7	29.8	–
Day 3	43.6	27.3	29.1	–
Day 4	53.0	19.5	27.5	–
Day 5	63.2	4.9	31.9	–
1 mM Butyrate				
Day 1	54.3	11.0	34.7	–
Day 2	56.1	15.1	28.8	–
Day 3	51.4	13.1	35.5	–
Day 4	60.7	14.7	23.1	1.5
Day 5	31.3	19.8	44.8	4.1
2 mM Butyrate				
Day 1	49.5	8.1	42.4	–
Day 2	31.9	9.3	58.8	–
Day 3	13.9	10.0	53.8	22.3
Day 4	21.5	3.7	37.4	37.4
Day 5	24.9	10.6	33.1	31.4

A

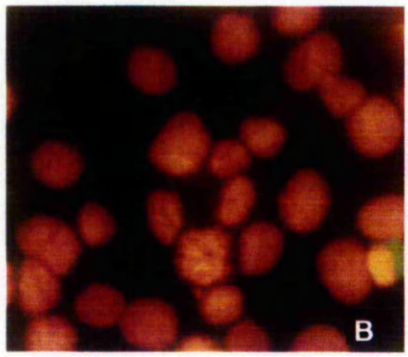

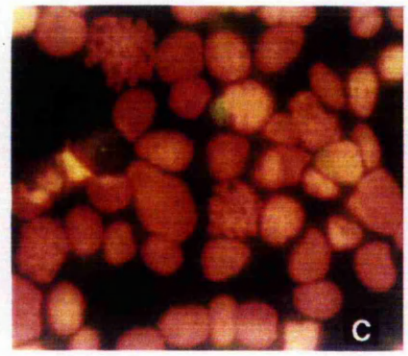

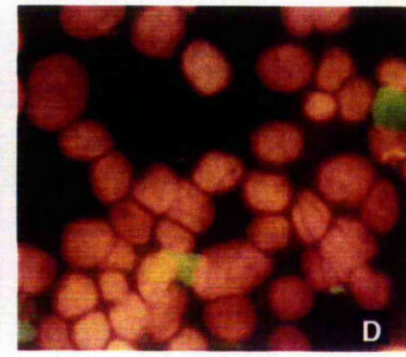

from Becton Dickinson Version 2.01.2. Cell cycle distribution histograms of the control populations and populations treated with the sodium butyrate were compared. A portion of the cells was visualised by examination on the fluorescent microscope.

Initially classical histograms of DNA distribution were observed in the control populations, i.e. the concentration of propidium iodide incorporated by G0/G1 cells was half that incorporated by mitotic cells (Table 5.1 a). Cell cultures treated with 1 mM sodium butyrate closely mimicked the control population for percentages of cells in G0/G1, S and G2/M phase, but the histograms from the 2 mM sodium butyrate-treated cells showed an extra peak of DNA staining by day 3 after sodium butyrate addition. This peak became more prominent with time accounting for as much as 38% of the total cells after 5 days exposure to sodium butyrate (Table 5.1 a). There is evidence of a similar population beginning to appear in the 1 mM sodium butyrate cultures on days 4 and 5 (Table 5.1 a).

However, closer examination of the data suggested that the cell population may becoming synchronised in the G2/M phase (control 32 %, 1mM NaB 33% and 2mM NaB 53%). Examination of replicate aliquots of the samples remaining after flow cytometric analysis by fluorescent microscopy showed that some of the cells treated with 2 mM NaB appeared larger and had larger nuclei than those of the 1 mM group which in turn appeared larger than those of the control group (Table 5.1 a). This provides additional evidence that there was a sub-population of cells in the butyrate-treated cultures which continued to synthesise DNA but did not undergo mitosis. There were cells visible in the photographs which showed chromosomes pairing-up and separating out, but these cells did not have defined chiasmata or spindle poles (Plate 5.5 b-d). To aid discussion of the flow cytometric data the percentages from each histogram have been summarised in Table 5.1 a. As conformation of the DNA status and to re-confirm apoptosis acridine orange staining of nuclear DNA was carried out, the typical fragmentation of the DNA as seen in apoptosis can be seen in Plate 5.6.

In a separate experiment, the cell cultures were examined using an algorithm for both diploid and aneuploid cell populations. This analysis showed the presence of both diploid and aneuploid populations in the cell culture (Table 5.1 b). The percentage of diploid cells entering the G2/M mitotic phase of the cell cycle decreased in the sodium butyrate-treated cultures (control 18.1%; 1 mM sodium butyrate 5.4%; 2 mM sodium butyrate, 10.8%), whereas the percentage o aneuploid cells entering G2/M following sodium butyrate

Table 5.1 a Percentage Of VA13a Cells In Each Phase Of Cell Cycle Following Sodium Butyrate Treatments Over Five Days. - Single Population Analysis.

Table 5.1 b Percentage Of VA13a Cells In Each Phase Of Cell Cycle Following Five Days Sodium Butyrate Treatments. - Double Population Analysis.

Tabulation of the flow cytometric analysis on VA13A. The cells were cultured in the presence or absence of sodium butyrate (section 2.3.1.1.4), cellular DNA was stained with propidium iodide, and the stain distribution examined using a fluorescent cell sorter (section 2.3.19). (1a) These values represent the percentage of the cells in the population in a particular phase of the cell cycle as determined by a single population algorithm for diploid cells. The column headed "Other" indicates that these populations of cells contained more DNA compared to the cells in G_0/G_1, S or G_2/M phases. (1b) Extended analysis, to examined those cells labelled "Other" in table 5.1a. A double population algorithm for aneuploid cells has been used. Example given is for data samples 72 h (5 days) after treatment.

Table 5.1 a Percentage Of Va13a Cells In Each Phase Of Cell Cycle Following Sodium Butyrate Treatments Over Five Days. - Single Population Analysis.

	Percent Diploid			
SAMPLE	G_o / G_1	*S*	G_2M	*Other*
CONTROL				
DAY 1	46.0	18.1	35.9	
DAY2	49.5	20.7	29.8	
DAY3	43.6	27.3	29.1	
DAY4	53.0	19.5	27.5	
DAY5	63.2	4.9	31.9	
1mM BUTYRATE				
DAY1	54.3	11.0	34.7	
DAY2	56.1	15.1	28.8	
DAY3	51.4	13.1	35.5	
DAY4	60.7	14.7	23.1	1.5
DAY5	31.3	19.8	44.8	4.1
2mM BUTYRATE				
DAY1	49.5	8.1	42.4	
DAY2	31.9	9.3	58.8	
DAY3	13.9	10.0	53.8	22.3
DAY4	21.5	3.7	37.4	37.4
DAY5	24.9	10.6	33.1	31.4

Table 5.1 b Percentage Of Va13a Cells In Each Phase Of Cell Cycle Following Five Days Sodium Butyrate Treatments. - Double Population Analysis.

Sample	*Percent Diploid*			*Percent Aneuploid*		
	G0/G1	*S*	*G2/M*	*G0/G1*	*S*	*G2/M*
Control	16 ± 5	35 ± 12	18 ± 6	17 ± 6	13 ± 5	1 ± 1
1mM Sodium butyrate	32 ± 1	25 ± 3	6 ± 3	22 ± 2	13 ± 3	2 ± 1
2mM Sodium butyrate	23 ± 4	21 ± 1	11 ± 2	25 ± 4	16 ± 3	4 ± 2

Plate 5.6 U.V. Photomicrographs of acridine orange stained cells, taken under an FITC filter 517 nm excitation.

These are day 5 cells for each experimental condition isolated from the cell supernatant. The evident fragmentation of the cellular DNA as seen in these photographs confirms the presence of apoptosis, in the cultures following the sodium butyrate treatment. Magnification X 62.5 in all plates. NB. The condition of the cells in these plates are poor due to excessive handling prior to microscopy.

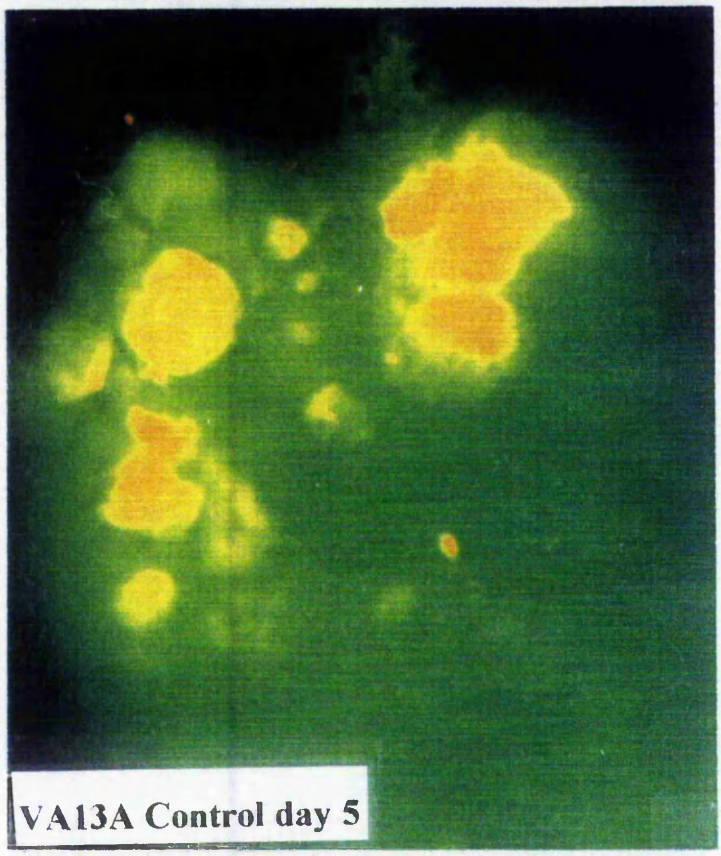
VA13A Control day 5

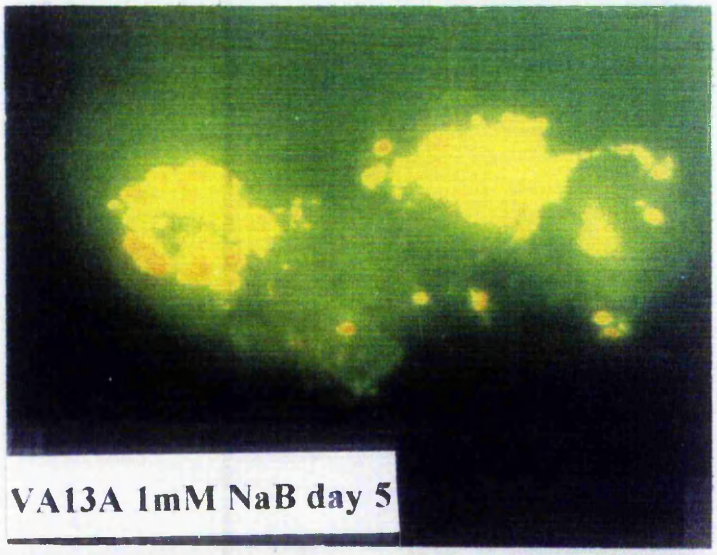
VA13A 1mM NaB day 5

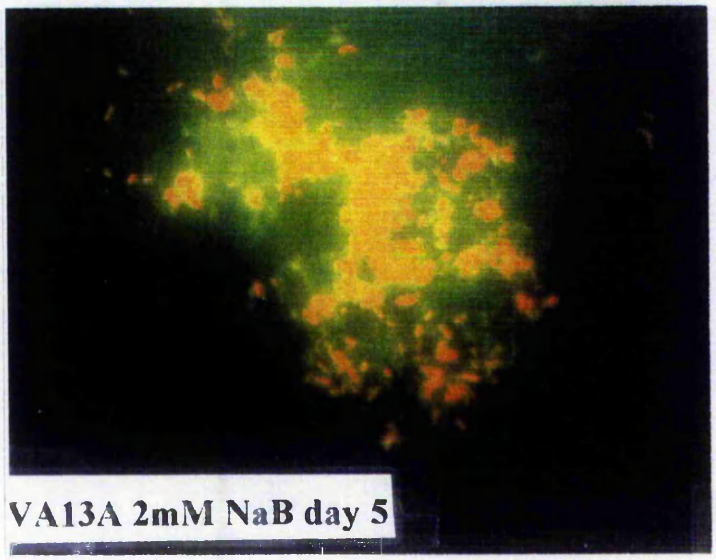
VA13A 2mM NaB day 5

Figure 5.7 A-C Flow cytometry histograms for the example population given in Table 5.1b. The histograms show (A) control; (B) 1mM NaB and (C) 2mM NaB analysed with the diploid / single cell population algorithm. While (D) and (E) show the histograms (B) and (C) reanalysed with the double / aneuploid cell population analysis of VA13a following 72 h topical treatment with sodium butyrate.

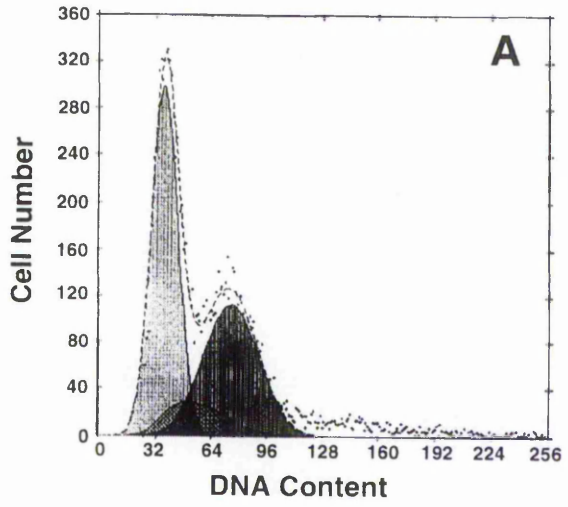
A
Cell Number
360
320
280
240
200
160
120
80
40
0
0
32
64
96
128
160
192
224
256
DNA Content

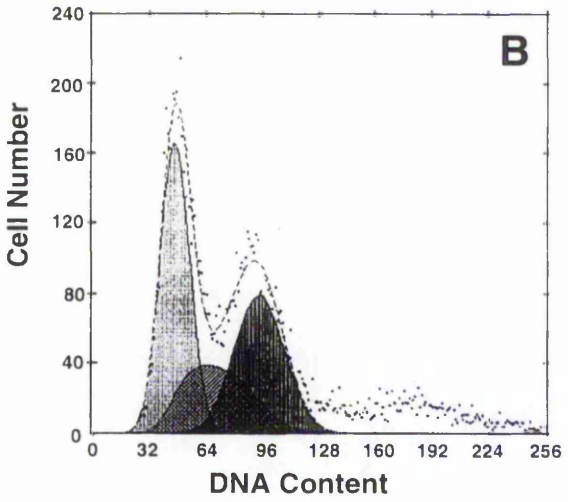
B
Cell Number
240
200
160
120
80
40
0
0
32
64
96
128
160
192
224
256
DNA Content

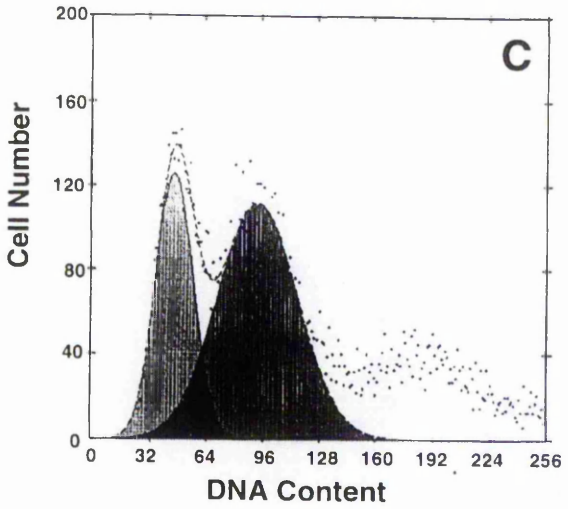
C
Cell Number
200
160
120
80
40
0
0
32
64
96
128
160
192
224
256
DNA Content

Figure 5.7 D & E Flow cytometry histograms for the example population given in Table 5.1b. While (D) and (E) show the histograms (B) and (C) reanalysed with the double / aneuploid cell population analysis of VA13a following 72 h topical treatment with sodium butyrate.

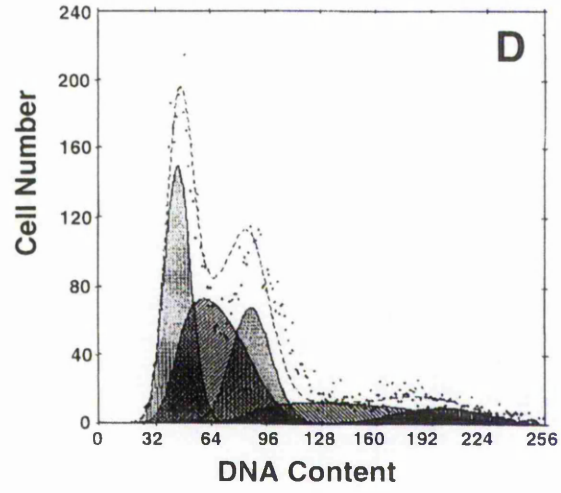
D
Cell Number
240
200
160
120
80
40
0
0
32
64
96
128
160
192
224
256
DNA Content

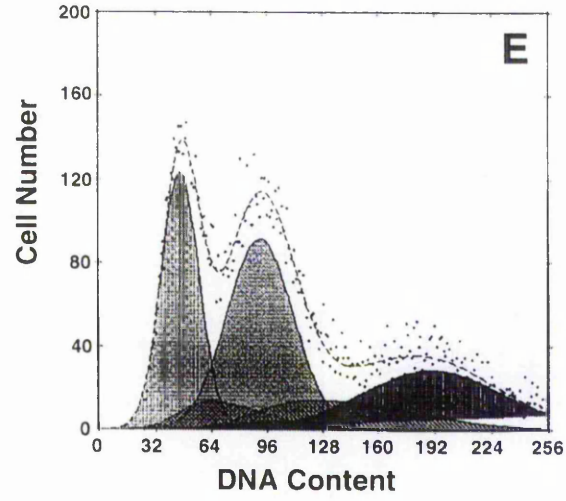
E
Cell Number
200
160
120
80
40
0
0
32
64
96
128
160
192
224
256
DNA Content

treatment increased (control 0.7%; 1 mM sodium butyrate, 2.0%; 2 mM sodium butyrate 3.6%). The distribution of both diploid and aneuploid cell populations following sodium butyrate treatment may been seen more clearly in representative flow cytometry histograms in Figure 5.7 a-e.

5.3 Discussion

A dose- and time-dependent induction of tissue transglutaminase and apoptosis and a decrease in cell number in VA13A cells following treatment with sodium butyrate was observed. The mode of action of sodium butyrate seemed to be one of terminal cell differentiation resulting in a change in the normal cell cycle kinetics of the total cell population.

Flow cytometric analyses showed that sodium butyrate altered the normal cell cycle kinetics of the VA13A cell. Control cultures showed a typical distribution of cells in all phases of the cell cycle throughout the course of these experiments, whereas sodium butyrate-treated cultures showed a multiple response. By day 3, the cells in the 2 mM butyrate populations showed some degree of synchrony of cells in G2/M phase, but the histograms also contained an extra peak of DNA staining (Figure 5.7 .a-e). To analyse the data correctly, it was necessary to use a second program to curve-fit the data. The new analysis suggested that there were at least three sub-populations of cells within the butyrate-treated cultures. One sub-population of cells was traversing the cell cycle normally, a second sub-population was undergoing apoptosis and a third sub-population of cells was not traversing the cell cycle or traversing it slowly. This third sub-population of cells was generally larger in size than the normal cycling cells, and appeared to incorporate more propidium iodide indicating that they contained greater quantities of DNA. Examination of these cells by fluorescent microscopy confirmed that they were bigger (Plate 5.5). These cells may have actually been ready to go through the cell cycle but were interrupted in S phase and continued to synthesise new DNA. Mian *et al* (1993) showed that metastatic hamster fibrosarcoma cells, transfected with cDNA encoding for expression of tTGase could be synchronised at the transition point between S and G2/M phases of the cell cycle. Other laboratories have reported that sodium butyrate does create giant cells which are removed from the cell cycle, but which continue to produce DNA, RNA, and proteins (Martin *et al* 1990). These populations of cells have not been reported to undergo apoptosis (Schwartzman and Cidlowski 1993, Kerr *et al* 1972, Wyllie *et al* 1980, Wyllie 1980, Wyllie 1981).

One of the reasons we believe that apoptotic envelope formation does not continue to increase in these butyrate-treated cells after 3 days even though transglutaminase is continuing to increase is that the remaining cells do not have the correct substrates for transglutaminase to "work on" for the apoptotic event. Results from the literature suggest

that a percentage of cells whether *in vitro* or *in vivo* are undergoing apoptosis at any given time (Wyllie 1981). In our study, when the sodium butyrate was added, it is possible only those cells in the population which were "primed" for apoptosis with the death gene proteins which would serve as substrates for transglutaminase during the apoptotic event responded and underwent apoptosis. The transglutaminase-mediated crosslinks were produced in these "primed" cells, the cells became reduced in size, , the phagocytic receptors were expressed and the ultimate outcome was the formation of the apoptotic envelope. In this study only a small number of cells were correctly "primed" and ready for the apoptotic process to be carried out. Once the "primed" cells were driven to apoptosis and removed from the system, two sub-populations of cells remained. Neither of these populations showed high levels of apoptosis. One of these populations was essentially cell cycle-arrested and consisted of large cells with extra DNA, while the other appeared to cycle in a normal manner, but was not "primed" for the apoptotic event. As a consequence, even though transglutaminase was increasing in amount and activity in the culture, apoptotic envelopes were not produced because the death genes were not being transcribed and end-product protein substrate(s) were not being translated. This idea is given credibility by the postulated action of apoptosis initiating genes discussed in the literature, e.g., c-myc, p53, c-fos and c-jun (Compton *et al* 1990, Mc.Conkey *et al* 1989, Mc.Conkey 1990, Ellis and Horovitz 1986, Buttyan *et al* 1988 and 1989, Yuh and Thompson 1989, Hockenberry *et al* 1990, Rubin *et al* 1991, Sentman *et al* 1991, Younish-Rouach *et al* 1991). Another controlling gene is bcl-2 which is thought to abrogate apoptosis by the production of its end-product protein in the inner-mitochondrial wall (Hockenberry *et al* 1990, 1991).

Evidence that transglutaminase does work on specific substrates when forming apoptotic end products can be found in the later work on transglutaminase substrates. Treatment of HT29 human colon cancer cells (Chapter 6 et seq), BHK-21 baby hamster fibroblasts, rat liver homogenates/slices and WI-38 human lung fibroblasts (the parent of the virally transformed VA13A cell used in these studies) with agents which induce transglutaminase e.g. retinoic acid or calcium ionophore A23187, induced the formation of an apoptotic-related transglutaminase-mediated product. Radiolabelling studies suggested that a 38 KDa and a 43 KDa protein contributed to the formation of this SDS-insoluble polymer (Knight *et al* 1993, Smethurst and Griffin 1996). Examination of Western blots with anti-polymer antibody confirmed an increase in stain of SDS-insoluble polymer at the top of the gel while the staining of the 38 KDa and 43 KDa protein regions in the gel decreased, adding further support to the idea that these two proteins were used by transglutaminase as substrates for

the polymer (This has now been confirmed by the work of Fesus *et al* 1997). Specific antibodies to the two suspected transglutaminase substrates would be beneficial in resolving this question. Similarities in the amino acid composition of the high molecular weight product described above and apoptotic envelopes isolated from provides additional evidence that these two materials are closely related (Knight *et al* 1993).

It is also possible that the large cells that were produced and did not appear to divide were the cells which continued to produce more and more transglutaminase leading to an overall increase in the transglutaminase levels. A feature shown to be possible in cells with high expression of tTGase, following transfection with cDNA for tTGase (Mian *et al* 1993). Within the scope of these experiments, we were unable to determine if this was the case.

The fact that not all suspected apoptotic cells stained with the antibody to transglutaminase suggests that there may be stages in the apoptotic process where the epitope for transglutaminase is unavailable to the antibody. It is also possible that transglutaminase has been altered either by crosslinking to another protein(s) or to itself (Birckbichler and Patterson 1990) thus changing its antigenicity such that the antibody no longer recognises the protein. Or the role of tTGase within the apoptosis seen here is purely a coincidental one.

Recently, several reports have shown that the induction of apoptosis is closely related to topical sodium butyrate treatment (Scheppach *et al* 1992, Kruth 1982, Kruth *et al* 1992, Pouillart *et al* 1992, D'Argenio *et al* 1992). In cases of ulcerative colitis or acute colitis, the cells of the intestinal lumen are highly inflamed, but following treatment with sodium butyrate enemas the patients respond and the inflammation is reduced (Hague *et al* 1993, D'Argenio *et al* 1992). In addition, cells taken from the intestinal lumen or colonic cancer cells grown *in vitro* have been shown to be induced into apoptosis following topical sodium butyrate treatment (Calabresse *et al* 1993, Scheppach *et al* 1992, Kruth *et al* 1992). In these studies, it has been shown that a dose-dependent and time-dependent induction of transglutaminase and apoptosis in VA13A cells following exposure to sodium butyrate takes place. This correlates well with reported increases of transglutaminase in the final stages of apoptosis (Fesus *et al* 1987,1989, Knight *et al* 1991, 1993). Reports from two independent labs support our findings of apoptosis induction following sodium butyrate treatment (Arundel *et al* 1986, Chung *et al* 1985). In summary, these results suggest a mode of action for the therapeutic effects of sodium butyrate as seen in the topical

treatment of reversal of symptoms in ulcerative colitis and neoplastic growth; namely the induction of apoptosis and transglutaminase. The biochemical and molecular mechanism(s) or pathway(s) by which sodium butyrate orchestrates this response remains to be elucidated and is currently under investigation. In any event, the induction of apoptosis or differentiation in a malignant tumour would appear beneficial to the patient. Whether one or both mechanisms occurred, tumour progression would be expected to be slowed and this might allow for better results with standard therapeutic approaches.

In summary, the flow cytometry analysis showed that the starting culture of transformed WI-38 VA13a was a mixed population of both diploid and aneuploid cells. The diploid cells appeared to have a normal cell cycle distribution. Following treatment with sodium butyrate, total cell numbers decreased, but the percentage of aneuploid cells in the culture increased. Thymidine uptake and bromodeoxyuridine (BrdU) proliferation assays demonstrated that the sodium butyrate-treated cultures were not experiencing cytotoxic effects at the stated concentrations of the topical agent. This data suggests that some cells were traversing the cell cycle more slowly or possibly undergoing cell cycle arrest while continuing to synthesise DNA I suggest that in addition to inducing apoptosis, sodium butyrate inhibited cell proliferation and altered cell morphology consistent with cell differentiation (Dyson *et al* 1992, Kamech *et al* 1986, Kim *et al* 1980, Kruth 1982, Scheppach *et al* 1992). The reason for the dual pathways of apoptosis and differentiation being the possible basis for future studies. The fact that in previous studies transglutaminase activity remained elevated for 5-7 days in the sodium butyrate-treated cells (Birckbichler *et al* 1983, Lee *et al* 1985, Thomas *et al* 1994) suggests that transglutaminase also plays a role in cells suspected of undergoing differentiation. It cannot be ruled out from these studies that the cells that became enlarged will not undergo apoptosis at a later time.

In the studies reported here, I have shown an induction of apoptosis in VA13A cells following exposure to sodium butyrate. This induction correlates with reported increases of transglutaminase in the final stages of apoptosis (El-Alaoui *et al* 1992, Fesus *et al* 1987, 1989, Knight *et al* 1983, Knight *et al* 1991, Piacentini *et al* 1991, Schwartzman and Cidlowski 1993). Reports have shown induction of apoptosis is closely related to topical sodium butyrate treatment (Calabresse *et al* 1993, Hague *et al* 1993). In cases of ulcerative or acute colitis, the cells of the intestinal lumen are highly inflamed. Following treatment with sodium butyrate enemas, the patients responded and the inflammation was reduced (Rowe and Bayliss 1992, Scheppach *et al* 1992, Scheppach 1994). Independent studies

have shown that transglutaminase and sodium butyrate play a role in ulcer healing in rats suffering from ulcerative colitis (D'Argenio *et al* 1992, 1994). Cells taken from the intestinal lumen or colonic cancer cells grown in vitro showed morphological and biochemical characteristics typical of apoptosis following topical sodium butyrate treatment (Hague *et al* 1993, Kim *et al* 1980, Lu *et al* 1992, Nathan *et al* 1990, Rowe and Bayliss 1992).

The objective of this study to investigate the topical action of sodium butyrate on VA13a, thereby analysing the induction of tTGase activity and antigen; has produced data which indicates how sodium butyrate might be used to alleviate diseased tissues by inducing apoptosis or differentiation. Evidence for transglutaminase involvement in the current study included isolation of increased amounts of apoptotic envelopes (Figure 5.5 & 5.6 plate d) and immunofluorescent staining with antibody to apoptotic envelopes (Plate 5.4 a-f). In an effort to further delineate the contribution of transglutaminase to the apoptosis pathway, transfection of VA13A cells with cDNA for transglutaminase and proto-oncogenes involved in apoptosis (e.g. bcl_2) are currently in progress in the laboratories at Nottingham Trent University. One of the reported results of treatment of VA13A cells with sodium butyrate is an increased expression of SV40 large-T and small-T antigens and down regulation of p53 (Goldberg *et al* 1992). These events occur early after addition of sodium butyrate and their relationship to the induction of apoptosis or transglutaminase in these cells must await further experimentation.

In conclusion, these results suggest a mode of action for the therapeutic effects of sodium butyrate seen in the topical treatment and reversal of symptoms in ulcerative colitis and neoplastic growth. The biochemical and molecular mechanism(s) by which sodium butyrate orchestrates this response is currently under investigation. The human *in vitro* cell culture system studied here offers a model system not only to study the efficacy of sodium butyrate as a chemotherapeutic agent, but it also offers the potential to identify biomarkers for apoptosis and possibly differentiation in response to sodium butyrate. Such studies could lead to beneficial therapeutic treatment not only in inflammatory bowel disease but also in prostate and other types of cancer.

6.0 Induction of Tissue Transglutaminase During All-Trans Retinoic Acid-Induced Apoptosis of HT29 Human Colon Cancer Cells : Novel Identification of Apoptotic Cells by Confocal Laser Microscopy.

6.1 Introduction.

6.2 Results.

6.2.1 Cell Culture of HT29.

6.2.2 Effect of Retinoic Acid on Cell Growth and Transglutaminase Activity.

6.2.3 Effect of Retinoic Acid on Levels of Transglutaminase Protein and mRNA.

6.2.4 Quantitation of TGase-Mediated SDS-Insoluble Polymer by ELISA.

6.2.5 Effect of R.A. on DNA Degradation.

6.2.6 Effect of R.A. on Isopeptide Levels.

6.2.7 Effect of R.A. on Apoptotic Index.

6.2.8 Use of Percoll Density Gradients to Concentrate Populations of Apoptosing Cells and Subsequent Microscopic Analysis.

6.3 Discussion.

6.1 Introduction

In the previous chapter the ability of sodium butyrate, to induce the enzymic activity of tTGase, when applied topically to a culture of WI38 VA13a cells was discussed. Both a time- and dose-dependent increase in the tTGase activity and the amount of antigenic protein were detected. It was found that those cells which expressed an increased level of the enzyme underwent changes in morphology consistent with apoptosis and growth characteristics. In order to establish whether these observations were cell type specific, sodium butyrate specific or indeed as a consequence of the elevated levels of tTGase; a second pharmacological cell culture experimental system was developed.

Consistent with the choice of VA13a, a second neoplastic Human cell line was chosen. HT29 (Fogh and Trempe 1975) is an epithelial-like cell isolated from an adenocarcinoma of the colon, explanted from a primary tumour mass found in a 44 year-old Caucasian woman in 1964 by Fogh. The topically applied pharmacological agent chosen was all-trans-retinoic acid (RA). Which had previously been shown to induce the gene expression of tTGase in a number of cell types (Davies *et al* 1985, Chiocca *et al* 1988, Piacentini *et al* 1993).Thus, if the hypothesis, that tTGase was responsible for the apoptosis and cellular differentiation observed in VA13a, were to be correct then HT29 should respond in a similar manner when treated topically with RA. Retinoic acid acts as a transcriptional regulator of tTGase expression, the effects are mediated by at least two classes of nuclear receptors, retinoic acid receptors (RAR's) that bind all-trans-retinoic acid and retinoid X receptors (RXR's) that bind 9-cis-retinoic acid. Each class consists of three subtypes (α, β & γ) which show characteristic spatial and temporal distribution in both embryonic and adult tissues. RAR's and RXR's can mediate ligand-dependent gene expression either by forming heterodimer (RAR / RXR) or homodimer (RXR / RXR) complexes that bind to their respective response elements and confer ligand-activated transcriptional control.

The pattern of experiments which were carried out followed the original scheme as for sodium butyrate on VA13a. Cell growth and morphology in the presence of RA, tTGase activity, antigen, and mRNA levels were monitored, also levels of the tTGase-mediated cell products, the ε(γ-glutamyl) lysine isodipeptide crosslink, the apoptotic envelope and the SDS-insoluble high molecular weight polymer. Apoptosis was assessed by DNA laddering and morphological examination of cell extracts.

6.2 Results

6.2.1 Cell Culture of HT29.

Cultures of HT29 were maintained as described in section 2.3.1.1.3. Non-confluent populations of cells were studied in the presence and absence of all-trans retinoic acid.

6.2.2 Effect of Retinoic Acid on Cell Growth and Transglutaminase Activity..

The action of retinoic acid to inhibit growth of HT29 in culture can be seen in Figure 6.1, cell number decreasing 1.88 fold in the 50μM treated flask after 5 days RA treatment when compared to the control culture. A dose-dependant and time-dependant induction of transglutaminase activity with retinoic acid in HT29 can be seen in Figure 6.2; there is a 1.96 fold increase in the activity of the 50 μM RA treated culture after 5 days when compared to the control untreated culture, indicating that those cells remaining in culture after five days exposure to R.A. had a significantly higher endogenous transglutaminase activity.

6.2.3 Effect of Retinoic Acid on Levels of Transglutaminase Protein and mRNA.

Figure 6.3 shows the results of Western immuno-probing of SDS/PAGE electrophoresis and Northern hybridisation (Figure 6.4) of HT29 cell extracts. These results confirm the action of R.A. to induce transglutaminase with time in a dose-dependent fashion. They expand the pervious result of increased tTGase activity and indicate that new message for the protein has been transcribed and translated into new catalytically active enzyme.

Figure 6.1 Effect of RA on the cell growth of HT29. Cells were grown in Mc.Coy's 5a Medium supplemented with 10% (v/v) foetal bovine serum and 48 h later exposed to various concentrations of RA (section 2.3.11.3). At the indicated times cell numbers were examined. Cell numbers were quantitated using the citric acid / crystal violet method for nuclei (section 2.3.1.3). A dose- and time-dependent decrease in cell number can be observed following the RA treatment. Values shown are the mean of n=6 experiments ± S.E.M.

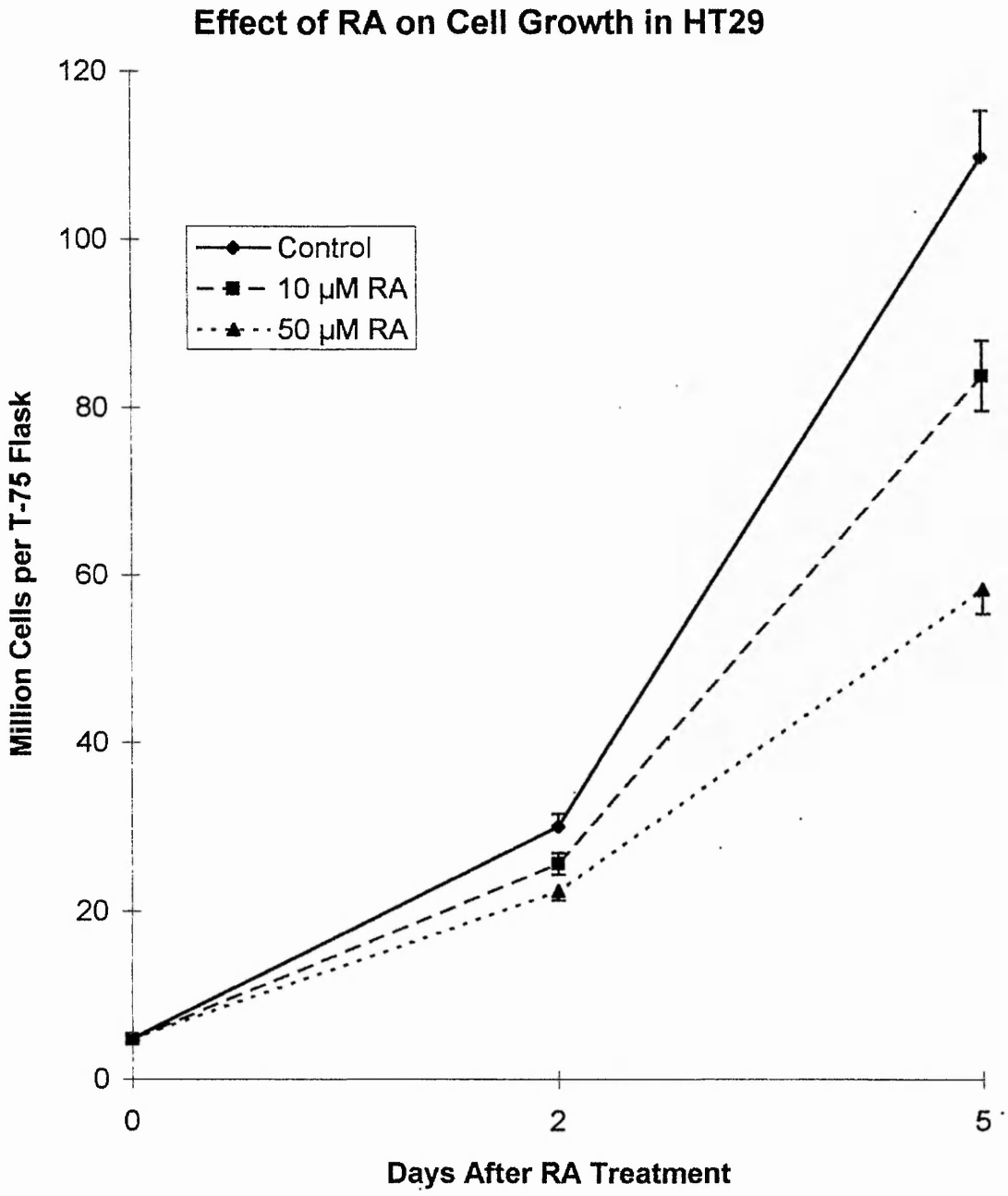
Effect of RA on Cell Growth in HT29
120
100
80
60
40
20
0
Million Cells per T-75 Flask
Control
10 µM RA
50 µM RA
0
2
5
Days After RA Treatment

Figure 6.2 Effect of RA on Transglutaminase Catalytic Activity in HT29. For the tTGase activity assay the methods of sections 2.3.1.2; 2.3.4; 2.3.7.2 were used. Briefly, , cells were washed with calcium-free Earle's solution, scraped into TBS-EDTA solution, sonicated for 5 s and then tTGase activity was measured by the incorporation of [^{14}C] putrescine into N,N' - dimethylcasein. One unit of enzyme activity was defined as 1 nmol of putrescine incorporated in 1 min per mg of protein at 37°C. A dose- and time-dependent increase in tTGase activity can be observed following the RA treatment. Values shown are the mean of n=6 experiments ± S.E.M.

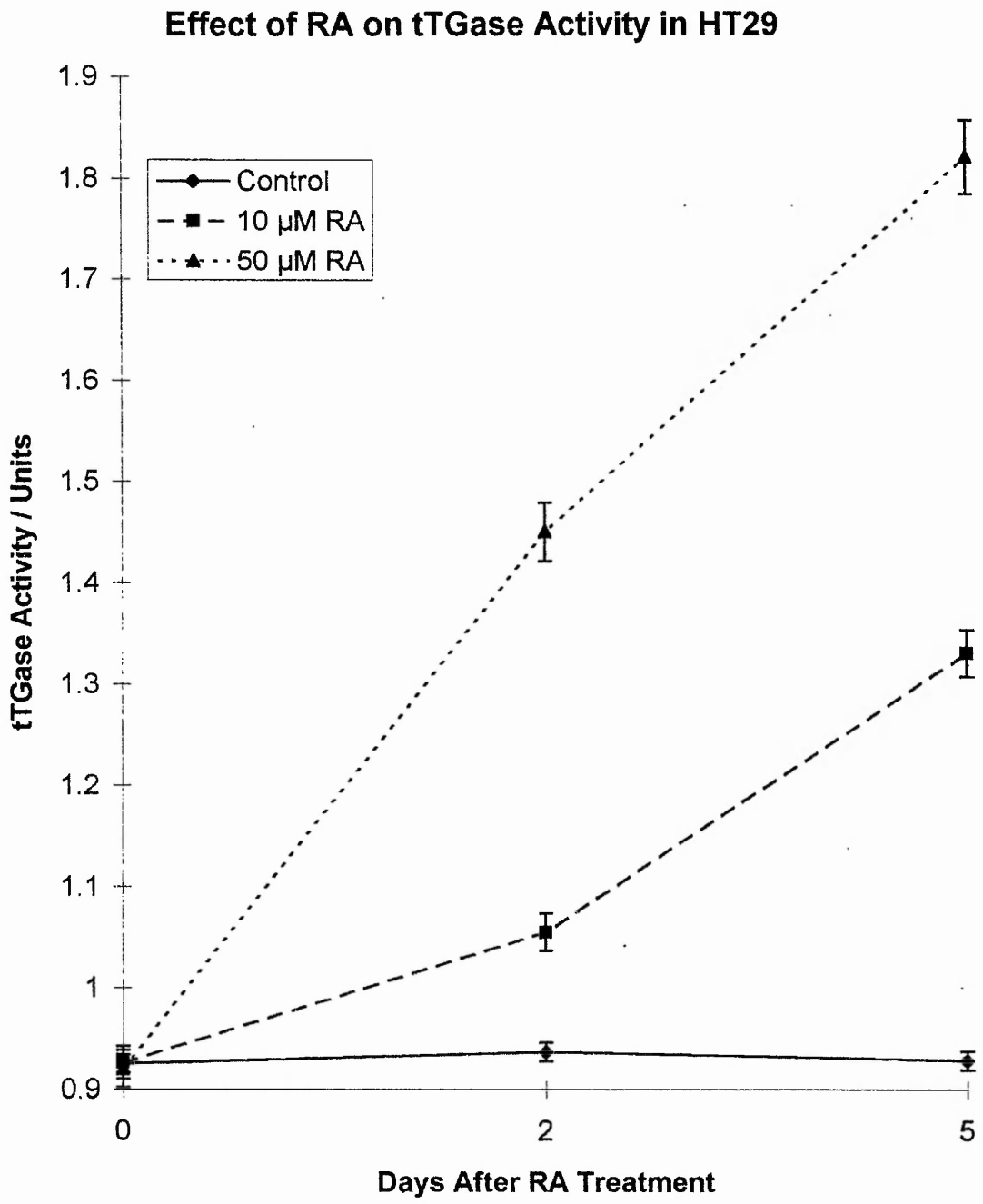
Effect of RA on tTGase Activity in HT29
1.9
1.8
1.7
1.6
1.5
1.4
1.3
1.2
1.1
1
0.9
tTGase Activity / Units
Control
10 µM RA
50 µM RA
0
2
5
Days After RA Treatment

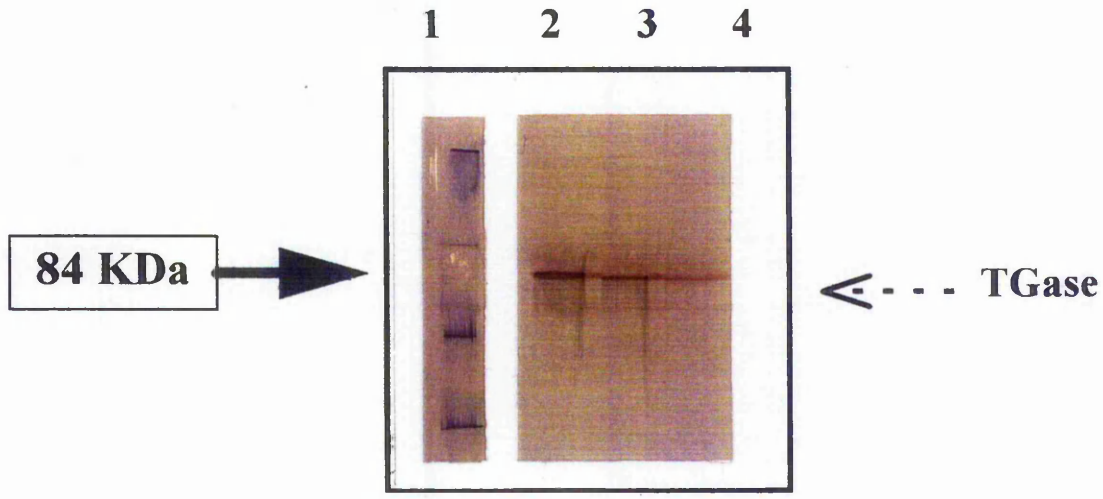

Figure 6.3 Effect of RA treatment on tTGase protein in HT29. Each lane of a 10% SDS / PAGE gel was loaded with 100 µg of cell homogenate proteins according to section 2.3.22. After resolution of the gel it was electroblotted (section 2.3.23) on to nitrocellulose membrane ready for Western blotting (section 2.3.23.2). The membrane was probed with a 1:100 dilution (4.5 µg / µl protein IgG) of the CUB74 monoclonal antibody raised to tTGase. The molecular weight standards are shown in Lane 1, 84KDa standard indicted by the bold arrow. Lane 2, HT29 treated with 50 µM RA. Lane 3, HT29 treated with 10 µM RA. Lane 4, HT29 controls treated with ethanol RA vehicle only. A single band can be seen in each lane corresponding to the 85KDa molecular weight of tTGase. Those cells treated with RA giving a stronger immunostaining indicating a greater amount of the tTGase protein to be present.

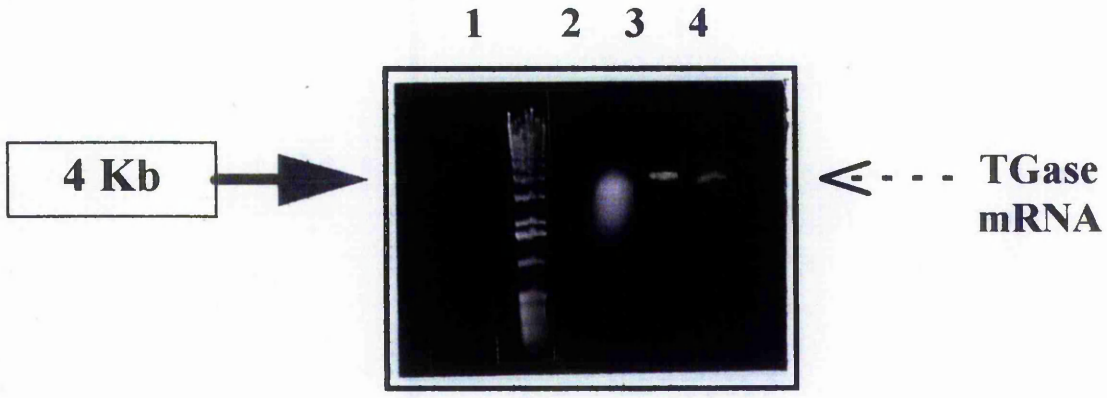

Figure 6.4 Effect of RA treatment on tTGase mRNA in HT29. Each lane of a 4% denaturing agarose gel was loaded with 3 µg of polyadenylated mRNA according to section 2.3.24. After resolution of the gel it was capillary blotted (section 2.3.23) on to a nylon membrane ready for Northern blotting (section 2.3.25.6). The membrane was probed with a radiolabelled cDNA probe specific for endothelial tTGase . The molecular weight standards are shown in Lane 1, 4 Kb standard indicted by the arrow. Lane 2, HT29 treated with 50 µM RA. Lane 3, HT29 treated with 10 µM RA. Lane 4, HT29 controls treated with ethanol RA vehicle only. A single band can be seen in each lane corresponding to the 4 Kb transcription fragment size of tTGase. Those cells treated with RA giving a stronger immunostaining indicating a greater amount of the tTGase message to be present.

6.2.4 Quantitation of TGase-Mediated SDS-Insoluble Polymer by ELISA.

Using a standard method for an indirect ELISA the amount of transglutaminase-mediated SDS/insoluble polymer involved with apoptotic envelope formation; was determined in control and retinoic acid treated cells. Final readings of polymer concentration were calculated from the calibration graph shown in Figure 6.5. The results are tabulated in Table 6.1 (examples of the calculation used are shown) from this table it can be seen that those cells treated with 50μM R.A. for four days have 2.32 times the amount of tTGase-mediated apoptotic polymer per cell than the corresponding control cells.

The polyclonal antisera used in the above ELISA to quantitate amounts of transglutaminase-mediated SDS / insoluble polymer was raised against apoptotic envelopes isolated form hamster fibroblasts in culture. Plate 3.1 part c shown previously indicates the immunoreactivity of this antiserum to intact isolated apoptotic envelopes. Using the kind gift from Dr.S.El-Alaoui of a monoclonal antiserum raised to the transglutaminase product of ε(γ-Glutamyl) lysine isodipeptide (El-Alaoui *et al* 1991, Roch *et al* 1991) (Plate 3.1 part d), we were able to confirm that the apoptotic envelope itself is truly a transglutaminase-mediated product. Hence, using this knowledge we can infer that the polymer isolated from the HT29 cells and reacting with the anti-apoptotic envelope antisera may in fact be precursor constituents of apoptotic envelopes. Figure 6.6 shows an SDS/PAGE gel of control and R.A. treated cell homogenates. There is seen an accumulation of high molecular weight SDS-insoluble polymer at the stacking / resolving gel interface and left in the loading wells. Here, the visualisation of increased amounts of high-molecular weight polymers following R.A. treatment, confirm the results of the ELISA.

Figure 6.5 Calibration graph for the SDS / insoluble polymer ELISA. Purified amounts of the SDS / insoluble polymer isolated from rat liver (section 2.3.10) and of apoptotic envelope polymer isolated from BHK-21 cells (2.3.11) was used to calibrate the immunoreactivity of the two antisera (section 2.3.13). This graph was used to calculate the amounts of each polymer found in the preparations of HT29 following RA treatment.

Calibration of Antigen ELISA

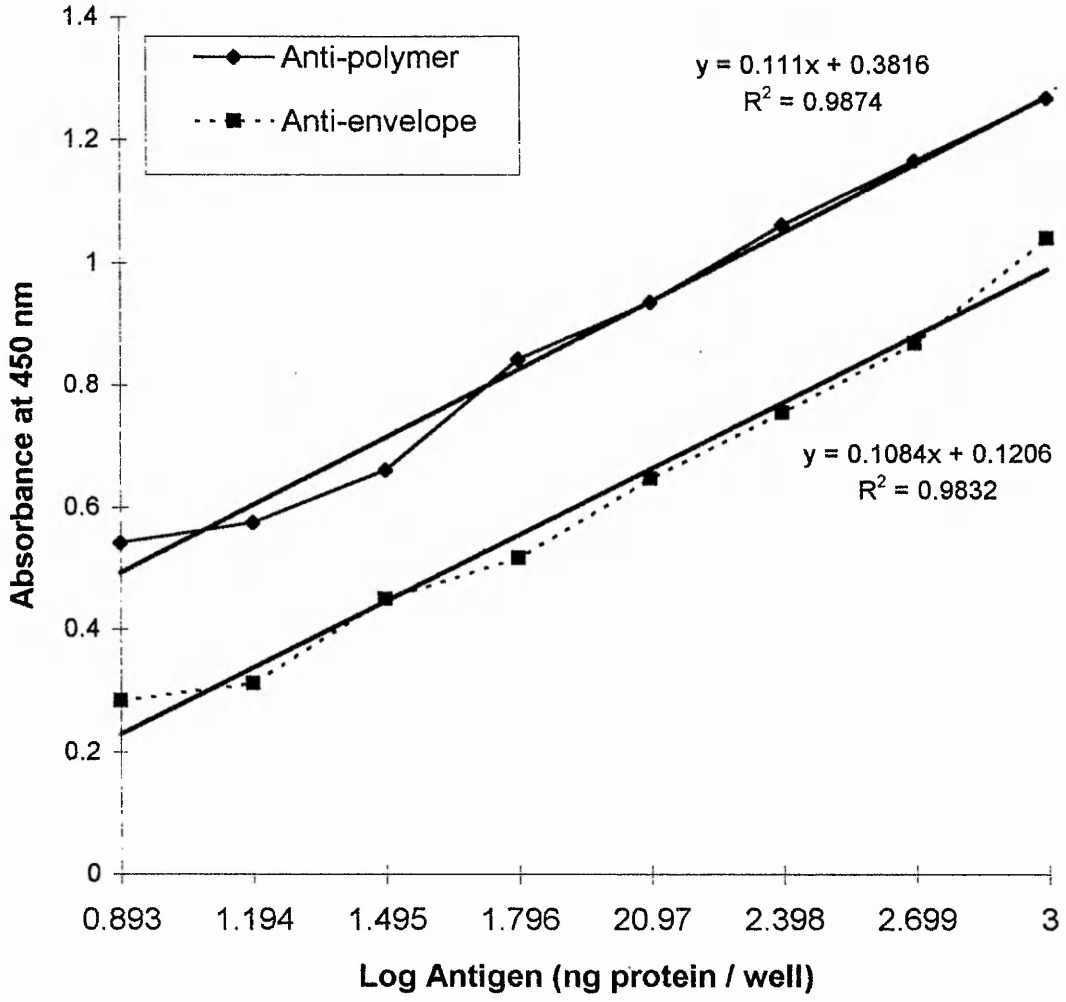

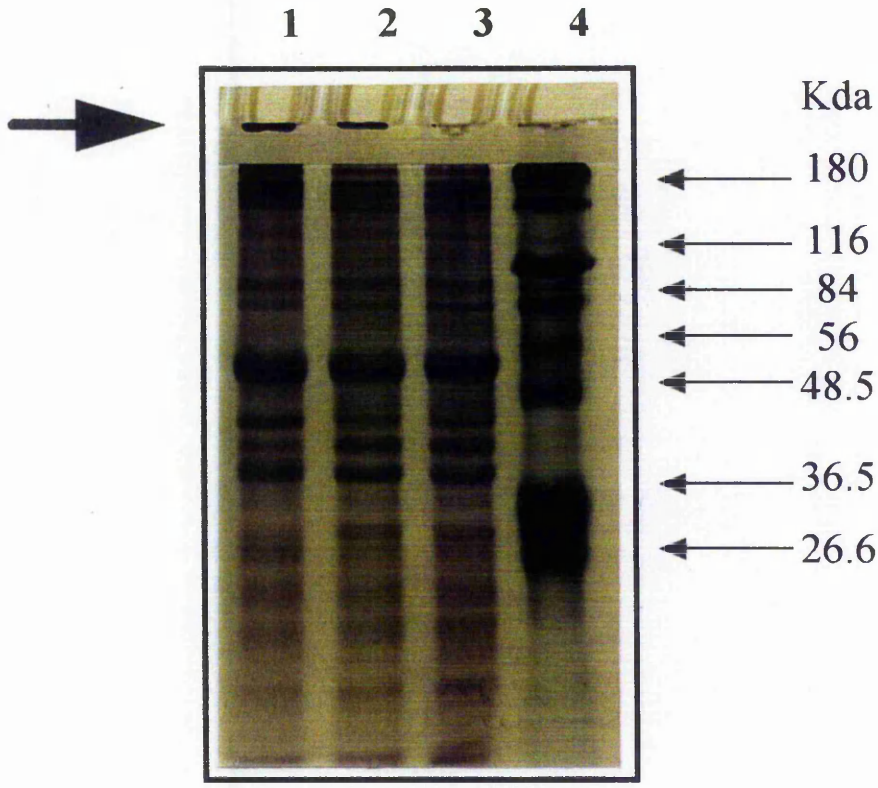

Figure 6.6 Effect of RA treatment on the formation of tTGase- mediated high molecular weight protein polymers in HT29. Each lane of a 10% SDS / PAGE gel was loaded with 100 µg of cell homogenate proteins according to section 2.3.22. After resolution the gel was stained with Comassie brilliant blue dye according to section 2.3.22.1. The molecular weight standards are shown in Lane 4,. Lane 1, HT29 treated with 50 µM RA. Lane 2, HT29 treated with 10 µM RA. Lane 3, HT29 controls treated with ethanol RA vehicle only. Protein staining can be seen of a large molecular weight material which remains in the wells of lanes 1 and 2. It can also be seen at the stacking and resolving gel interface. Those cells treated with RA giving stronger protein staining for this high molecular weight material indicating the possibility of greater amounts of crosslinked tTGase-mediated proteins to be present.

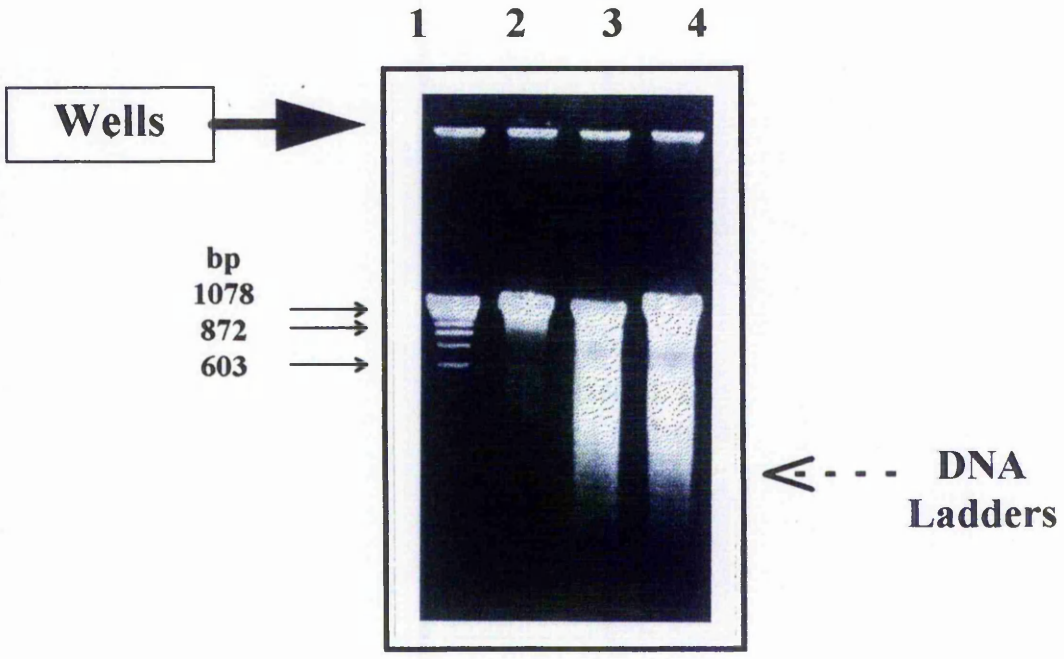

Figure 6.7 Effect of RA on the DNA degradation of HT29 cells. Cells were treated with 10 or 50 μM RA for four days and both floating and attached cells were harvested (section 2.3.25.1). The DNA degradation by endonucleases was analaysed by agarose gel electrophoresis (section 2.3.25.5). Lane 1, molecular weight markers (X174RF DNA / HaeIII Fragments); Lane 2, control culture of HT29; Lane 3, 10 μM RA treated HT29 and Lane 4, 50 μM RA treated HT29. DNA degradation typical of the nudonuclease laddering associated with apoptosis can be seen only in the RA treated preparations.

Table 6.1 Quantitation of absorbance data for the ELISA in Figure 5.5. To determine the protein concentration of apoptotic SDS / insoluble polymer found in RA treated cultures of HT29. Shown is an example of the calculations used.

Table 6.1 Absorbance Data for ELISA on HT29 Cells, to determine the Protein Concentration of Apoptotic Material using the Anti-Apoptotic Envelope Antisera.

	Protein Standards in μg/ml SDS Apoptotic Polymer					*HT29 Control 1:10*	*HT29 R.A. 1:10*
	112.9	***56.45***	***37.63***	***28.23***	***22.58***		
	0.232	*0.189*	*0.163*	*0.192*	*0.123*	0.171	0.163
	0.240	*0.185*	*0.163*	*0.192*	*0.123*	0.156	0.160
	0.247	*0.191*	*0.171*	*0.189*	*0.169*	0.175	0.174
	0.249	*0.189*	*0.180*	*0.129*	*0.209*	0.167	0.166
	0.268	*0.185*	*0.183*	*0.164*	*0.130*	0.171	0.164
TOTAL	***1.236***	***0.939***	***0.852***	***0.806***	***0.755***	**0.840**	**0.827**
MEAN	***0.2472***	***0.1878***	***0.1704***	***0.1612***	***0.1510***	**0.1680**	**0.1654**
S.D.	***0.0134***	***0.0027***	***0.0117***	***0.0301***	***0.0376***	**0.0073**	**0.0053**

(All absorbance readings were taken at 405nm following 60 minute incubations at 27°C).

	Control Serum Readings for Standards					*HT29 Control 1:10*	*HT29 R.A. 1:10*
	112.9	***56.45***	***37.63***	***28.23***	***22.58***		
	0.105	*0.100*	*0.098*	*0.101*	*0.099*	0.111	0.111
	0.111	*0.102*	*0.106*	*0.098*	*0.101*	0.113	0.105
TOTAL	***0.216***	***0.202***	***0.204***	***0.199***	***0.200***	**0.224**	**0.216**
MEAN	***0.108***	***0.101***	***0.102***	***0.0995***	***0.100***	**0.112**	**0.108**
S.D.	***0.0042***	***0.0014***	***0.0057***	***0.0021***	***0.0014***	**0.0014**	**0.0042**

(All absorbance readings were taken at 405nm following 60 minute incubations at 27°C).

Calculation of protein values for the cell samples :

CONTROL

Number of cells in the culture	14,985,000	cells
Protein reading μg/ml from calibration data curve.	36.62	μg/ml
Protein concentration multiplied by dilution factor (1:10)	366.18	μg prot/50μl
Protein concentration corrected to 1ml.	7323.60	μg prot/ml
Correction per cell (7323.6/14985000)	0.000488	μg prot/cell
Multiply by 1000 to give **ng APOPTOTIC PROTEIN per Cell.**	**0.4887**	**ng prot/cell**

50μM RETINOIC ACID

Number of cells in the culture	5,994,000	cells
Protein reading μg/ml from calibration data curve.	34.11	μg/ml
Protein concentration multiplied by dilution factor (1:10)	341.10	μg prot/50μl
Protein concentration corrected to 1ml.	6822.00	μg prot/ml
Correction per cell (6822.0/5994000)	0.001138	μg prot/cell
Multiply by 1000 to give **ng APOPTOTIC PROTEIN per Cell.**	**1.1381**	**ng prot/cell**

6.2.5 Effect of R.A. on DNA Degradation.

One of the standard methods for confirming apoptosis in cell cultures is to prove the action of calcium and magnesium-dependent endonucleases on cellular DNA. If such endonucleases are active then cleavage of genomic DNA will occur leaving fragments of approximately 180 base pairs - "DNA ladders". The ethidium bromide stained agarose gel seen in Figure 6.7 clearly shows the production of a DNA ladder after the treatment of R.A. Thus indicating the induction endonucleases associated with the initiation of apoptosis.

6.2.6 Effect of R.A. on Isopeptide Levels.

Having previously shown that those cells treated with R.A. have an induction of catalytic activity, antigenic protein and message for the enzyme tissue transglutaminase, to complete the proof it was necessary to look for TGase product. Table 6.2 shows the results of analysis for the ε(γ-Glutamyl) lysine isodipeptide; those cells treated with R.A. having 34.3 times greater levels of isopeptide than control cells.

6.2.7 Effect of R.A. on Apoptotic Index.

Knowing that a possible link could exists between tissue transglutaminase and the formation of apoptotic envelopes, it was necessary to investigate whether the tTGase-mediated envelopes as seen in Plate 3.1 part a; could be found in the HT29 / retinoic acid experimental system. If production of apoptotic envelopes also increased in the R.A. treated cells; it suggests that retinoic acid induction of tTGase could mediate the induction of apoptosis in the HT29 culture; in a similar way to the action of sodium butyrate on the VA13a cells.

Table 6.2 Effect of RA on tTGase Activity, Apoptotic Index and Level of ε-γ(gultamyl) lysine crosslinks in HT29 Cells. Summary table show the effect of five days administration of 50 μM RA on HT29 compared to the control culture. In each parameter tested there has been an increase following the RA treatment.

Table 6.2 Effect of RA on tTGase Activity, Apoptotic Index and Level of ε-γ(gultamyl) lysine crosslinks in HT29 Cells

PARAMETER TESTED	*CONTROL*	*50 μm RETINOIC ACID*
tTGase Activity / (nmol / min / mg protein)	0.92 ± 0.21	1.77 ± 0.19
Apoptotic Index Percentage of total cell count	3.38 ± 0.32	9.98 ± 0.53
ε-γ(gultamyl) lysine crosslinks (pmol / ARB's from 10^6 cells)	0.511 ± 0.015	2.26 ± 0.31
ε-γ(gultamyl) lysine crosslinks (pmol / 10^6 intact cells)	0.755 ± 0.023	25.90 ± 0.810

This was investigated by microscopically examining large numbers of control and R.A. treated cells. Following harvesting from the culture slides were prepared of the HT29 cells using a bench-top cytospin (section 2.3.1.2), Ten random fields of the slides were examined and all cells counted and scored for their appearance. Those cells which looked smooth with no cell surface blebbing were scored normal, while those which contained "highly light refractive" bodies and evident cell surfacing blebbing were scored apoptotic. To ensure that we were not counting necrotic cells trypan blue viability assays were carried out prior to slide preparation. Plate 6.1 part (A) shows a light micrograph of washed HT29 cells following induction with RA (the cells have been stained with methylene blue to highlight the nuclei). Plate 6.1 part (B) shows a high power magnification of an isolated apoptotic envelope from the RA treated HT29 cells.

A total of 740 control cells were counted in ten fields of these 25 were apoptotic (3.38%) and 451 cells were counted in ten fields of the R.A. treated cells of these 45 were scored apoptotic (9.98%) an increase of 2.95 times. Table 6.3 shows a summary of the cell counting.

The distinctive appearance of the apoptotic cells with the high number of small highly light refractive apoptotic bodies can be seen in both Plate 6.1 (A) and 6.1 (B). These bodies have been given the abbreviation "ARB's - apoptotic refractive bodies". Using the traditional method of chaotrophic agents to isolate SDS / insoluble apoptotic envelopes from the R.A. treated HT29 culture also isolated very high numbers of ARB's (see Plate 6.2 parts A & B). Further, more stringent washing of these bodies with 6M guanidine hydrochloride highlighted both an high insolubility and the light refractive properties (Plate 6.3 parts C & D). Indicating that these too may be highly crosslinked products of

Plate 6.1 Effect of RA treatment on the morphology of HT29. (A) shows a bright field light micrograph of isolated HT29 cells from the pellet of a Percoll gradient (section 2.3.18) stained with methylene blue. Clearly visible in the cells are the light refractive apoptotic bodies (ARB's). Magnification X 100. Plate (B) shows an SDS/ insoluble apoptotic envelope prepared from a sample of cells shown in (A) according to the method of section 2.3.11. Again clearly visible are the ARB's magnification X 400.

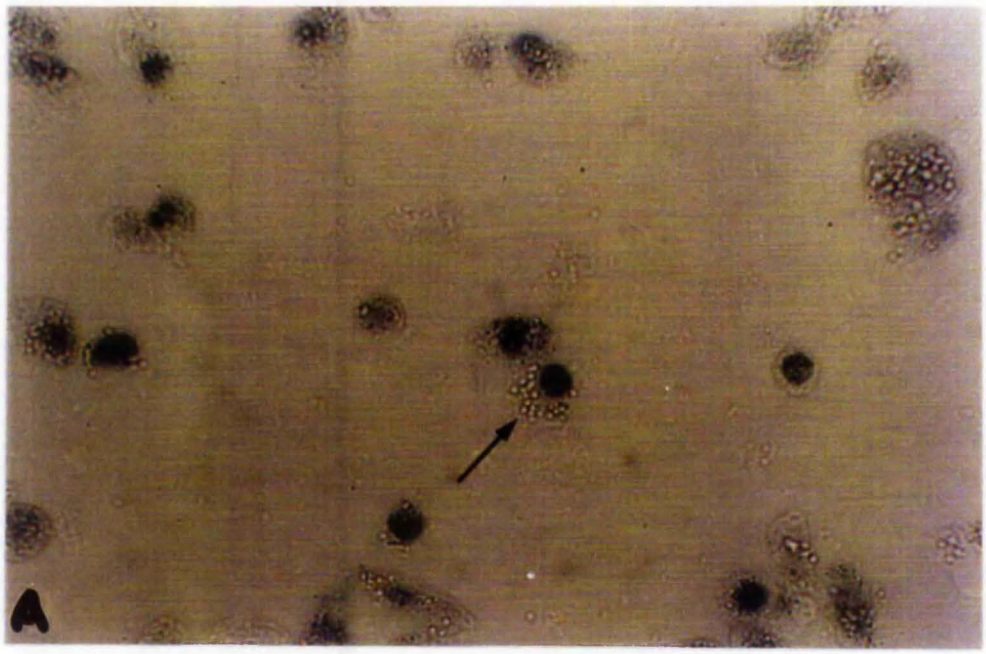
A

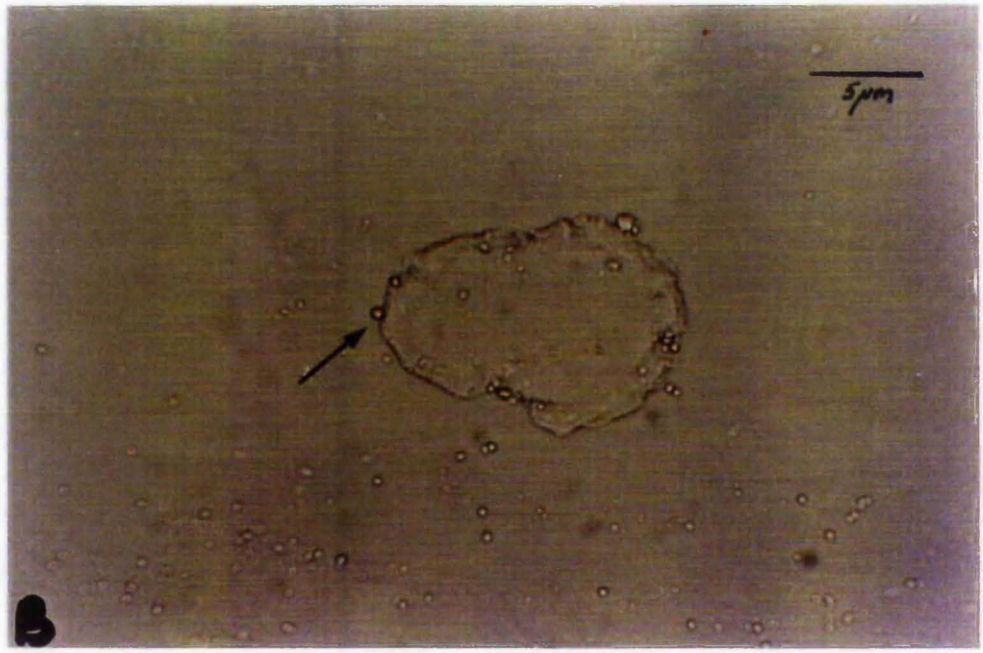
5μm
B

Table 6.3 Scoring of image analysis of apoptosing HT29 Cells using the ACAS 570 Confocal Laser Cytometer. Tables summarising the counts of total cell number, apoptotic cells, ARB's and fluorescence scores for both control and 50 μM RA cultures after five days treatment.

Table 6.3 Image Analysis of Apoptosing HT29 Cells using the ACAS 570 Confocal Laser Cytometer.

HT29 CONTROL - Mean percentage of APOPTOTIC CELLS counted per field = 3.38%

CELLS / FIELD	*APOPTOTIC CELLS*	*APOPTOTIC REFRCTIVE BODIES*	*FLUORESCENT SCORE / FIELD*	*FLUORESCENT SCORE / CELL*
75	3	1	44	0.59
77	4	1	51	0.66
81	6	1	53	0.65
94	4	1	53	0.56
91	6	1	52	0.57
62	0	-	30	0.48
64	0	-	33	0.52
61	1	1	32	0.52
65	1	1	32	0.49
70	0	-	34	0.49
TOTAL 740	**25**	**7**	**414.0**	**5.53**
MEAN 74.00	**2.50**	**0.70**	**41.40**	**0.55**
S.D. 11.82	**2.42**	**0.48**	**10.07**	**0.06**

HT29 50μM RETINOIC ACID - Mean percentage APOPTOTIC CELLS per field = 9.98%

CELLS / FIELD	*APOPTOTIC CELLS*	*APOPTOTIC REFRCTIVE BODIES*	*FLUORESCENT SCORE / FIELD*	*FLUORESCENT SCORE / CELL*
41	5	1	49	1.20
40	4	1	51	1.28
48	6	1	57	1.19
38	1	1	42	1.11
49	4	1	48	0.98
42	4	1	47	1.12
47	2	1	48	1.02
49	8	1	44	0.90
45	4	1	53	1.18
52	7	1	74	1.42
00	-	-	39	0.00
TOTAL 451	**45**	**10**	**552.0**	**11.40**
MEAN 41.00	**4.09**	**0.91**	**50.18**	**1.04**
S.D. 14.29	**2.43**	**0.30**	**9.35**	**0.37**

Plate 6.2 Isolated apoptotic refractive bodies (ARB's). Obtained by the action by boiling in 20%(w/v) SDS, (section 2.3.13) shown held together by DNA. These ARB's were extracted from a single T-75 flask of HT29 cells from each of the culture conditions, after five days treatment. (A = 50 μM retinoic acid treated, approximately 60 x 10^6 cells; B = control approximately 110 x 10^6 cells). These preparations were then further treated with 6 M guanidine hydrochloride (C = 50 μM retinoic acid treated; D = control). Thus proving the stability of the bodies and their resistance to chaotrophic digestion. The refractive nature of these bodies can now be seen clearly; the higher number extracted from a much reduced cell number in the R.A. treated flask indicates just how many there were per cell.

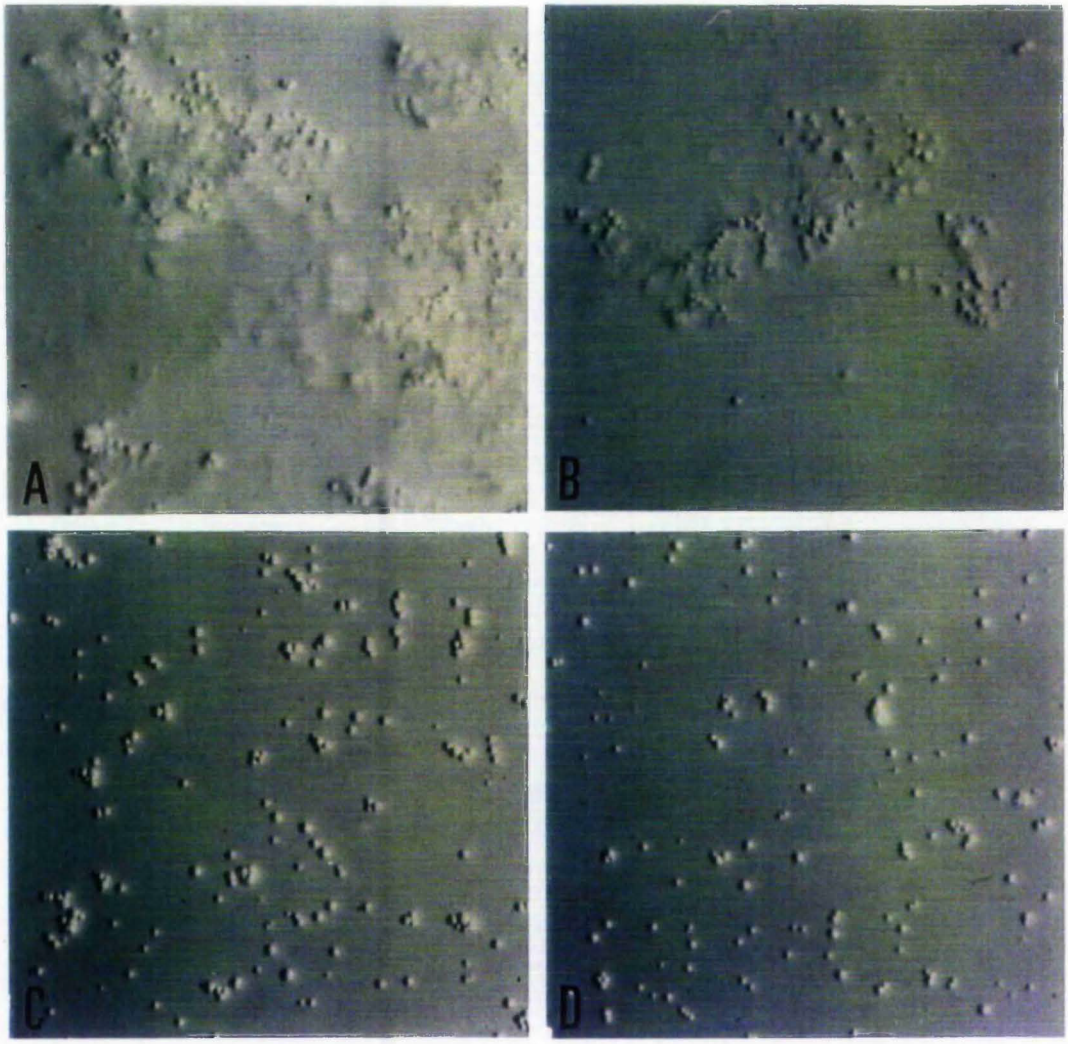
A
B
C
D

Plate 6.3 Normarski phase contrast photomicrographs of HT29 cells isolated from the top of the Percoll gradient. This population of cells generally represents the non-apoptotic cells; but due to clogging of the gradient some apoptotic cells can remain at the top of the gradient. (A), shows the retinoic acid (50μM) treated, with an apoptotic cell containing some apoptotic refractive bodies (ARB's) marked with an arrow. (B), shows the smooth appearance of the control cells.

Normarski phase contrast photomicrographs of HT29 cells isolated from the pellet found at the bottom of the Percoll gradient. This population of cells generally represents the apoptotic cells; but due to clogging of the gradient some non-apoptotic cells can remain at the top of the gradient. (C), shows the retinoic acid (50μM) treated, with an apoptotic cell containing many apoptotic refractive bodies (ARB's) marked with an arrow. (D), shows the smooth appearance of the control cells, with one marked with an arrow which is starting to show some small ARB's; this cell represents the endogenous apoptotic cells of the control population..

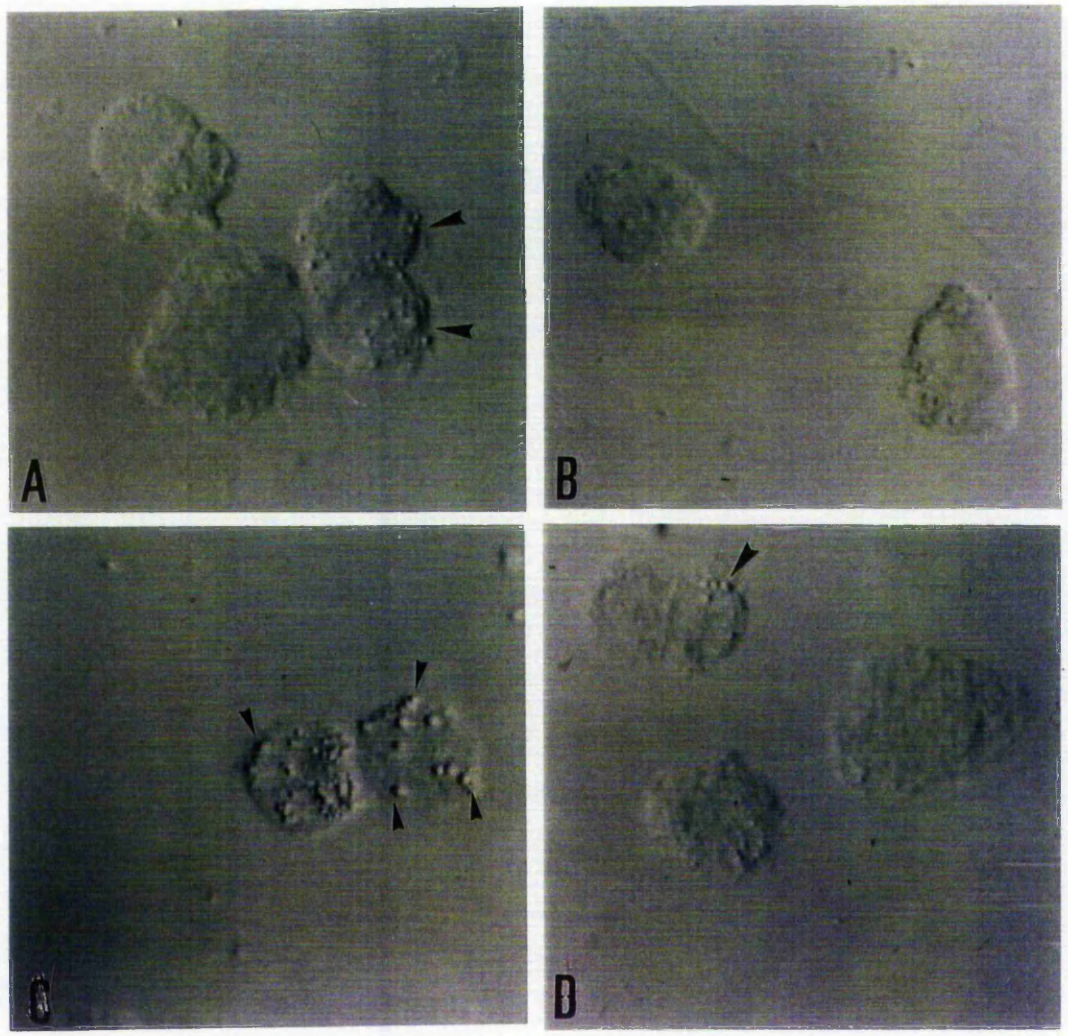
A
B
C
D

transglutaminase and high in ε-γ(gultamyl) lysine isodipeptide crosslinks, a result already suggested from the HPLC analysis of cell extracts for ε-γ(gultamyl) lysine crosslinks (Table 6.2) and by the high molecular weight polymer found on SDS/PAGE (Figure 6.6).

6.2.8 Use of Percoll Density Gradients to Concentrate Populations of Apoptosing Cells and Subsequent Microscopic Analysis.

The feature of apoptosing cells to remain viable until the point of phagocytosis and to shrink their size results in the increase of their inherent cell density. Thus by using the cell separation medium Percoll and density gradient centrifugation we were able to collect pellets of apoptosing cells. The Normarski phase contrast photomicrographs shown in Plate 6.3 parts A - D, show cells isolated form different regions of Percoll gradients. Photos 6.3 parts A & B show mixed populations of cells remaining at the top of Percoll gradients after centrifugation, the population treated with retinoic acid (Plate 6.3 part A) show blebbed cells and distinctive ARB's.

The isolated cell pellets of apoptosing cells from the two RA treated and control experimental conditions also clearly show the big difference. In the R.A. treated culture. these cells are smaller and contain a high number of very distinctive ARB's (Plate 6.3 part C). Chemical extraction of the ARB's can be performed with SDS as mention earlier (Plate 6.2 parts A & B) followed by 6M guanidine hydrochloride (Plate 6.2 parts C & D) proving that they are truly SDS / insoluble products; crosslink analysis of extracted ARB's found them to be rich in the ε(γ-Glutamyl) lysine isodipeptide indicating them to be a possible transglutaminase-mediated products Table 6.2.

Figure 6.8 Graph showing the correlation of fluorescent score per field with the total numbers of cells and apoptotic cells, in the control treated population, after five days.

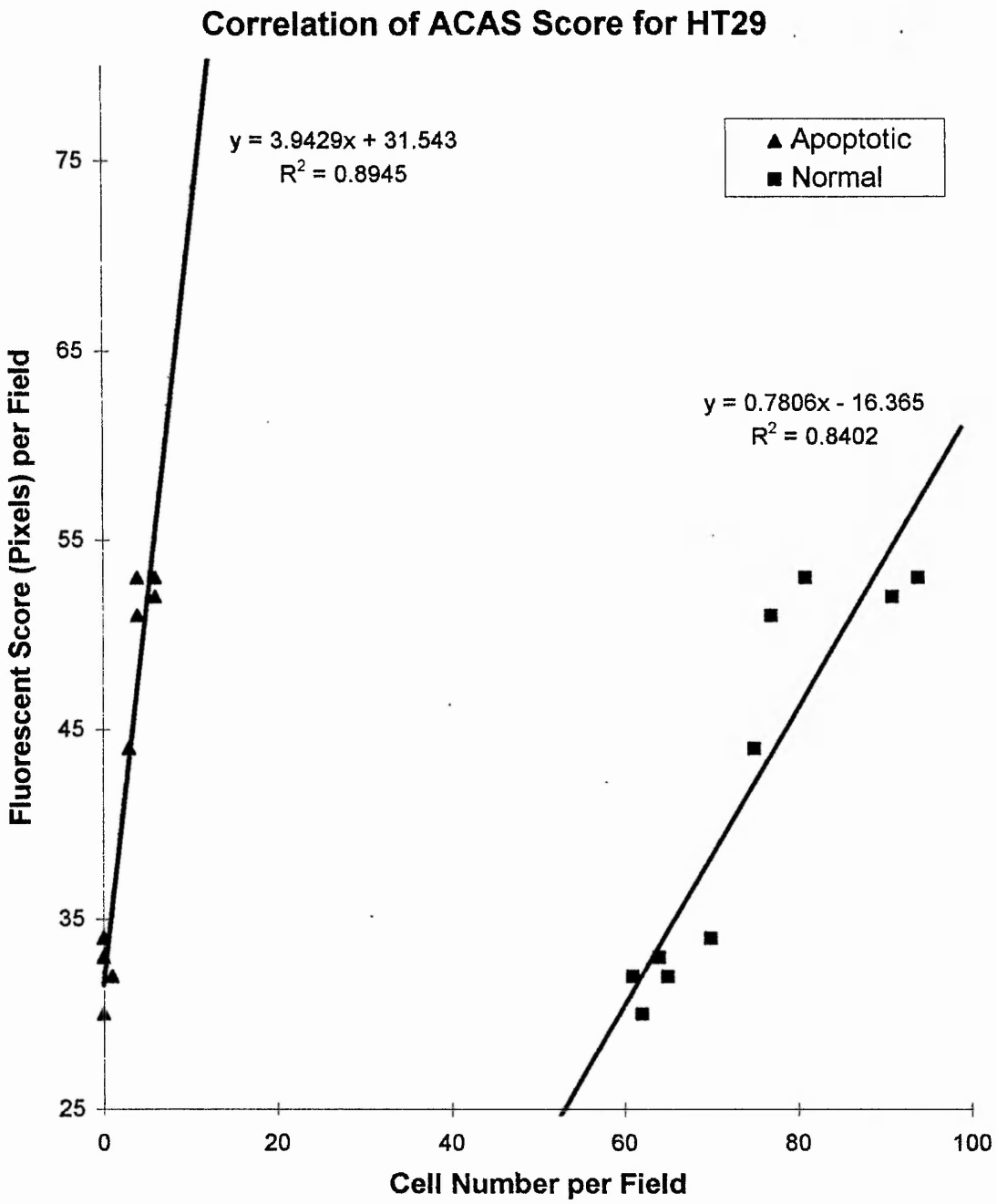
Correlation of ACAS Score for HT29
y = 3.9429x + 31.543
R2 = 0.8945
y = 0.7806x - 16.365
R2 = 0.8402
▲ Apoptotic
■ Normal
Fluorescent Score (Pixels) per Field
Cell Number per Field
25
35
45
55
65
75
0
20
40
60
80
100

Figure 6.9 Graph showing the correlation of fluorescent score per field with the total numbers of cells and apoptotic cells, in the retinoic acid treated population, after five days.

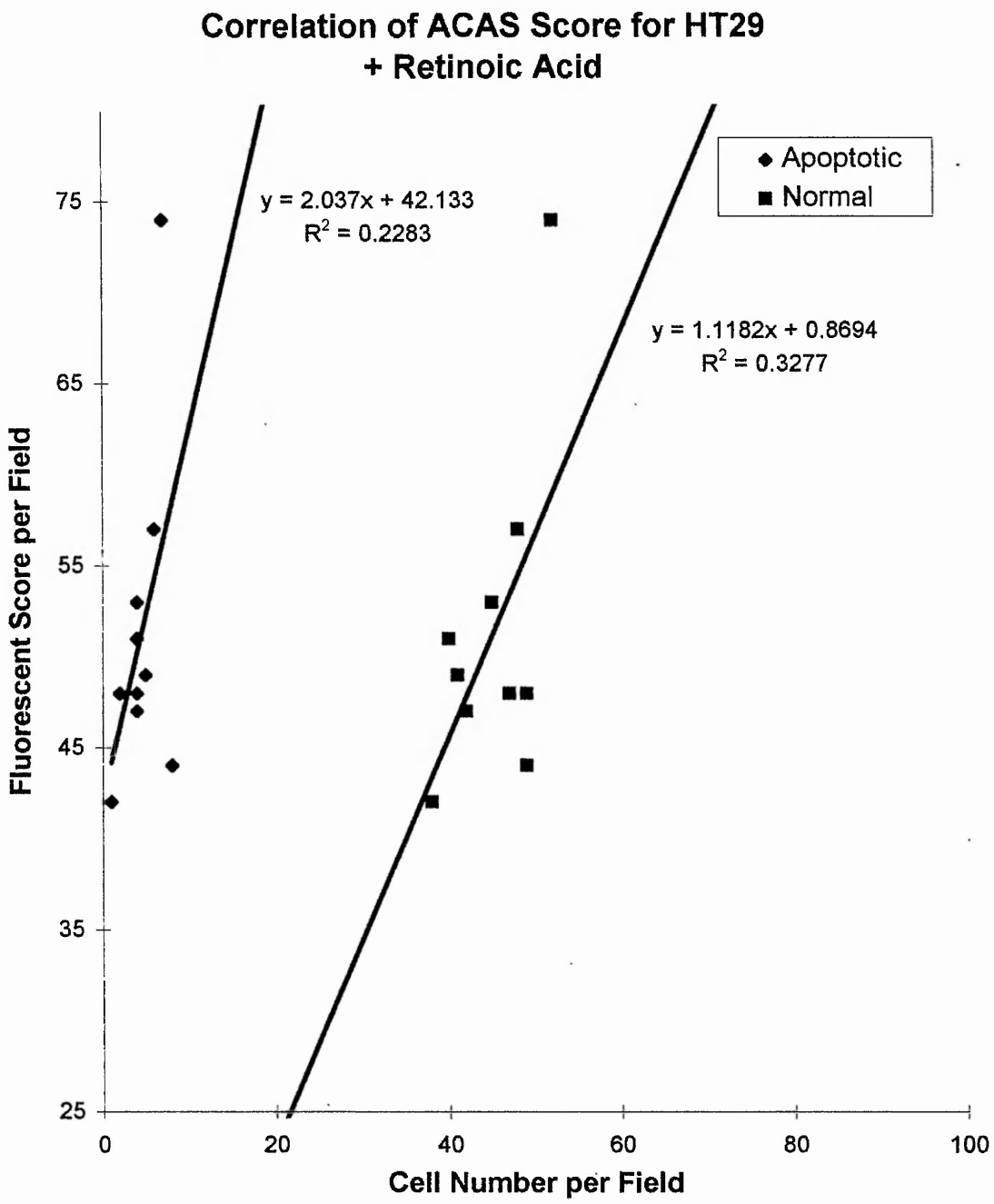
Correlation of ACAS Score for HT29
+ Retinoic Acid
Apoptotic
Normal
y = 2.037x + 42.133
R2 = 0.2283
y = 1.1182x + 0.8694
R2 = 0.3277
Fluorescent Score per Field
Cell Number per Field
75
65
55
45
35
25
0
20
40
60
80
100

The presence of the light refractive apoptotic bodies (ARB's) was further investigated by examination of cells on a confocal laser cytometer. Cell preparations were prepared as before and spun onto slides. When examined it became apparent that the ARB's caused the incident laser light to show a high degree of auto-fluorescence. Thus it was possible to quickly identify those cells which contained ARB's by scanning for areas of high fluorescence. Very high numbers of cells were scanned these included cells prepared from Percoll gradients; from both control and R.A. treated cultures. For each field of cells looked at the operator (GLT) visually counted the total numbers of cells, the total numbers of cells with evident blebs or ARB's (apoptotic cells) before scanning the same field with the argon laser. The analysis programme could then quantitate the total amount of fluorescence per field, thus the average amount of fluorescence per cells could be determined.

When analysed it was found that the retinoic acid treated cells gave higher readings for fluorescence, this corresponded to the fact that their were also higher numbers of apoptotic cells per field in this culture, as previously described. Table 6.3 shows the break down of the cell counts and fluorescent scores. This data is shown graphically in Figure 6.8 for control and Figure 6.9 for retinoic acid; the relationship between normal cells and apoptotic cells and the fluorescent score they give on the cytometer can be seen. Good correlations were found for the fluorescent score and the numbers of apoptotic cells following RA treatment Examination of the matched phase contrast and fluorescent scans for representative fields can be seen in the series of Plates 6.4 parts 1-4 (control) and Plates 6.5 parts 1-4 (retinoic acid). Apoptosing cells are marked on the phase scans and the subsequent fluorescent image they produce under the laser can be seen on the matched laser scans. Cells have been analysed from the gradient and pellets obtained after Percoll

Plate 6.4 This series of computer enhanced, false colour microscope scans are of the cells prepared from the control population of HT29 harvested at day 5. The scans are paired, one merge scan (1) - which shows a phase contrast image of a field of cells and following that the corresponding fluorescent scan (2) . Apoptotic cells are marked with arrows. The order of the scans being : **I). Control cells from the top of a Percoll gradient.**

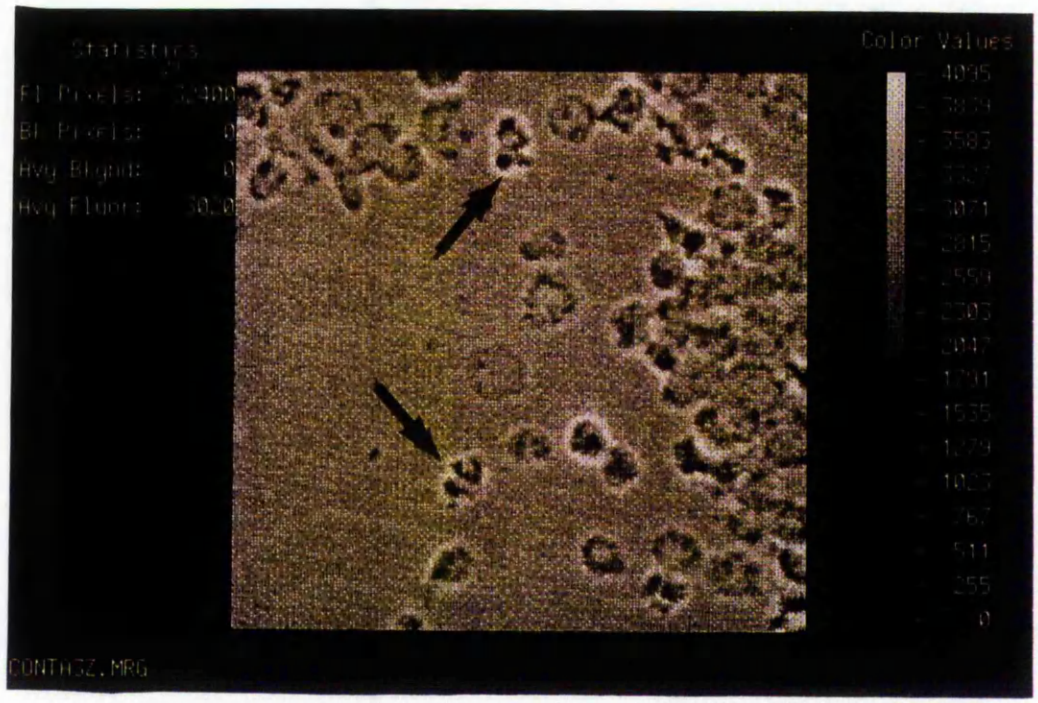
Statistics
Color Values
CONTH3Z.MRG

1

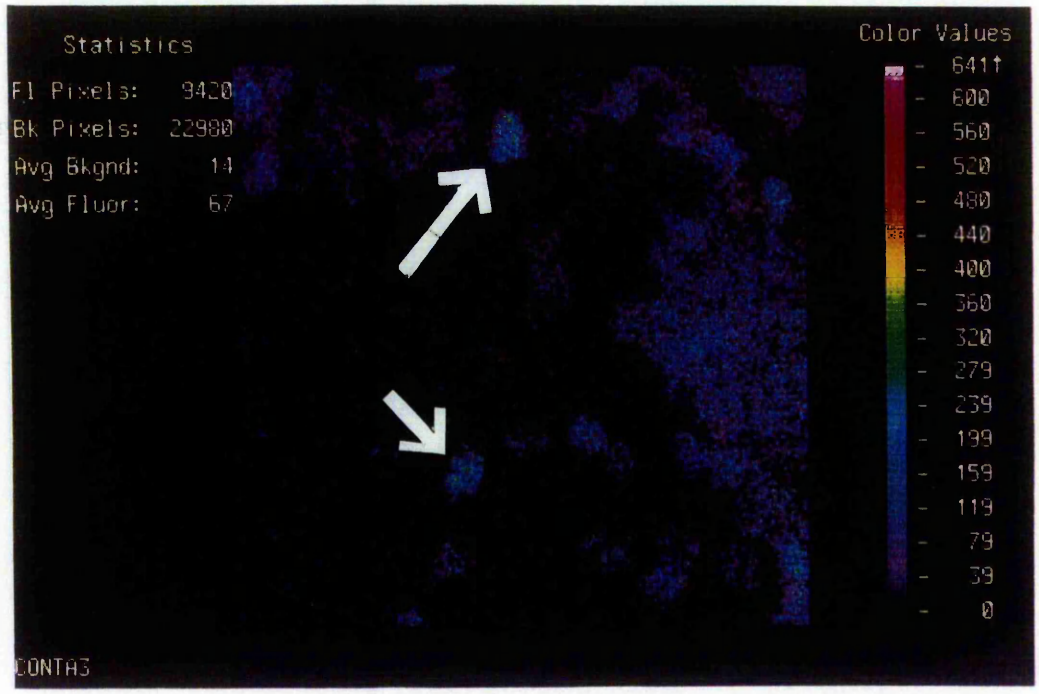
Statistics
Fl Pixels: 9420
Bk Pixels: 22980
Avg Bkgnd: 14
Avg Fluor: 67
Color Values
6411
600
560
520
480
440
400
360
320
279
239
199
159
119
79
39
0
CONTA3

2

Plate 6.4 This series of computer enhanced, false colour microscope scans are of the cells prepared from the control population of HT29 harvested at day 5. The scans are paired, one merge scan (1) - which shows a phase contrast image of a field of cells and following that the corresponding fluorescent scan (2) . Apoptotic cells are marked with arrows. The order of the scans being : **II). Control cells from the pellet of the Percoll gradient.**

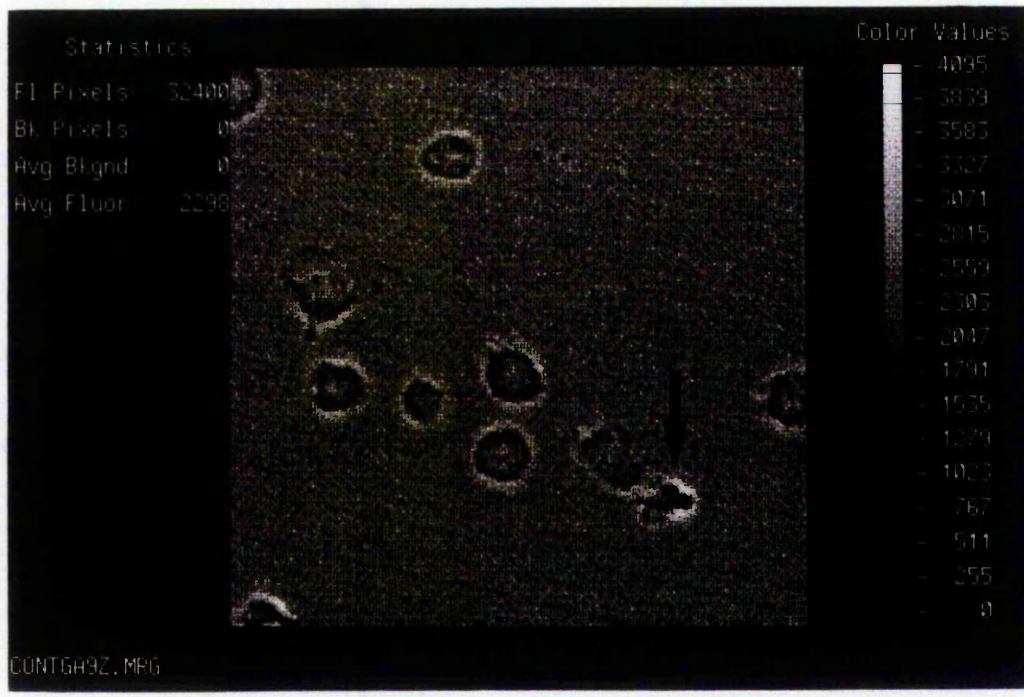
Statistics
Fl Pixels 32400
Bk Pixels 0
Avg Bkgnd 0
Avg Fluor 2298
Color Values
4035
3809
3583
3357
3071
2815
2559
2303
2047
1791
1535
1279
1023
767
511
255
0
CONTGA9Z.MRG

1

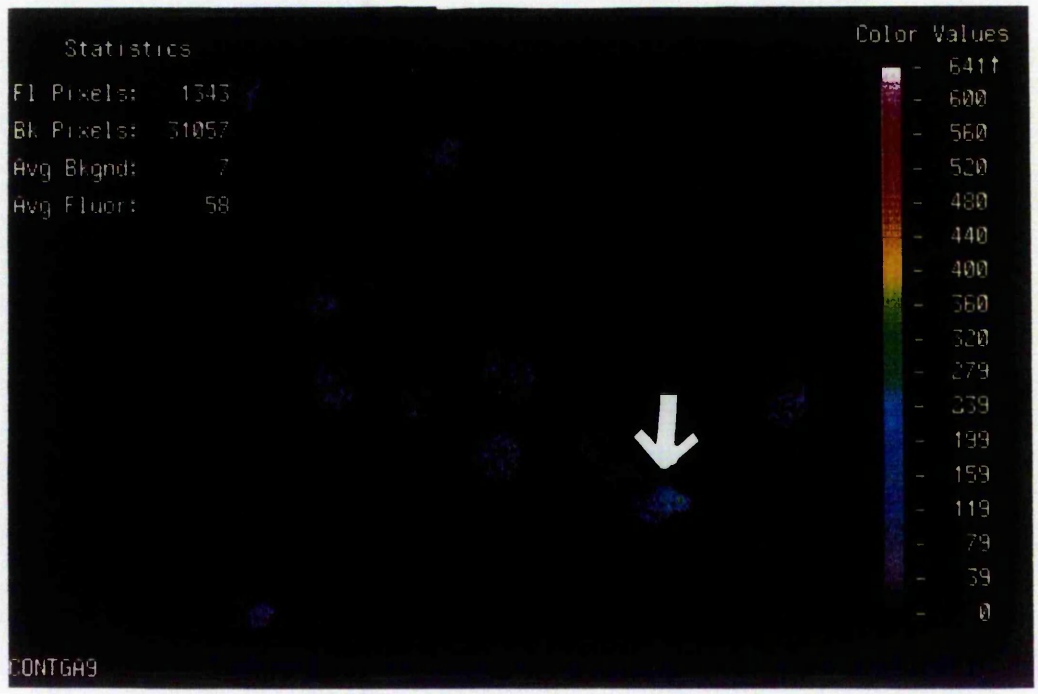
Statistics
Fl Pixels: 1343
Bk Pixels: 31057
Avg Bkgnd: 7
Avg Fluor: 58
Color Values
641f
600
560
520
480
440
400
360
320
279
239
199
159
119
79
39
0
CONTGA9

2

Plate 6.5 This series of computer enhanced, false colour microscope scans are of the cells prepared from the retinoic acid population of HT29 harvested at day 5. The scans are paired, one merge scan - which shows a phase contrast image of a field of cells and following that the corresponding fluorescent scan. Apoptotic cells are marked with arrows. The order of the scans being : **I). RA treated cells from the top of a Percoll gradient**

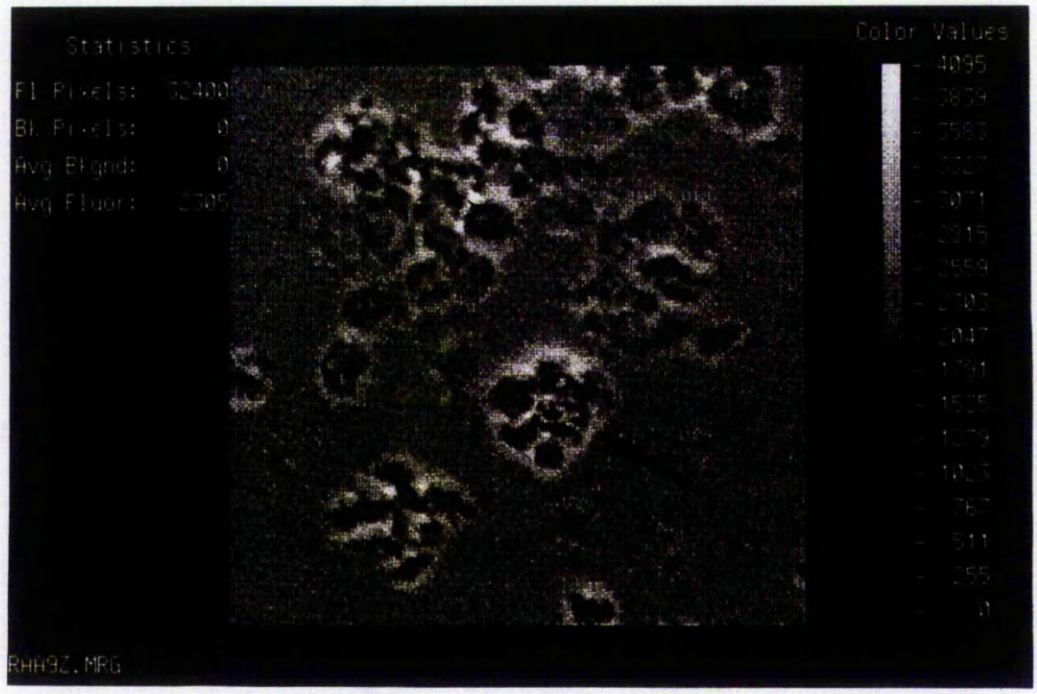
Statistics
Fl Pixels: 32400
Bk Pixels: 0
Avg Bkgnd: 0
Avg Fluor: 2305
Color Values
4095
RHA9Z.MRG

1

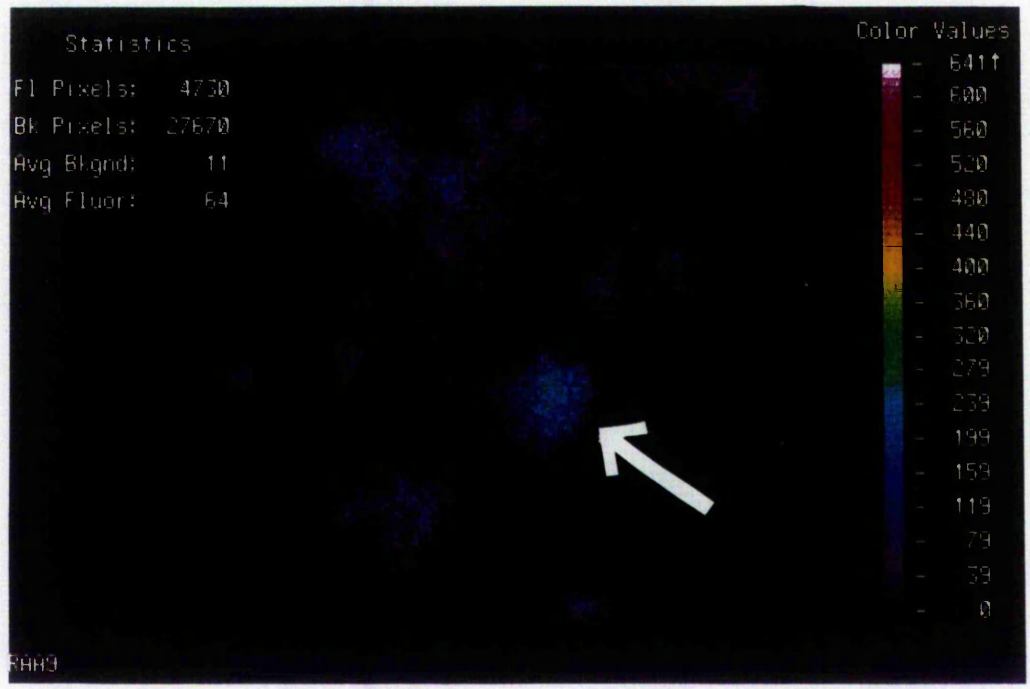
Statistics
Fl Pixels: 4730
Bk Pixels: 27670
Avg Bkgnd: 11
Avg Fluor: 64
Color Values
641↑
600
560
520
480
440
400
360
320
279
239
199
159
119
79
39
0
RHA9

2

Plate 6.5 This series of computer enhanced, false colour microscope scans are of the cells prepared from the retinoic acid population of HT29 harvested at day 5. The scans are paired, one merge scan - which shows a phase contrast image of a field of cells and following that the corresponding fluorescent scan. Apoptotic cells are marked with arrows. The order of the scans being : **II). RA treated cells from the pellet of the Percoll gradient.**

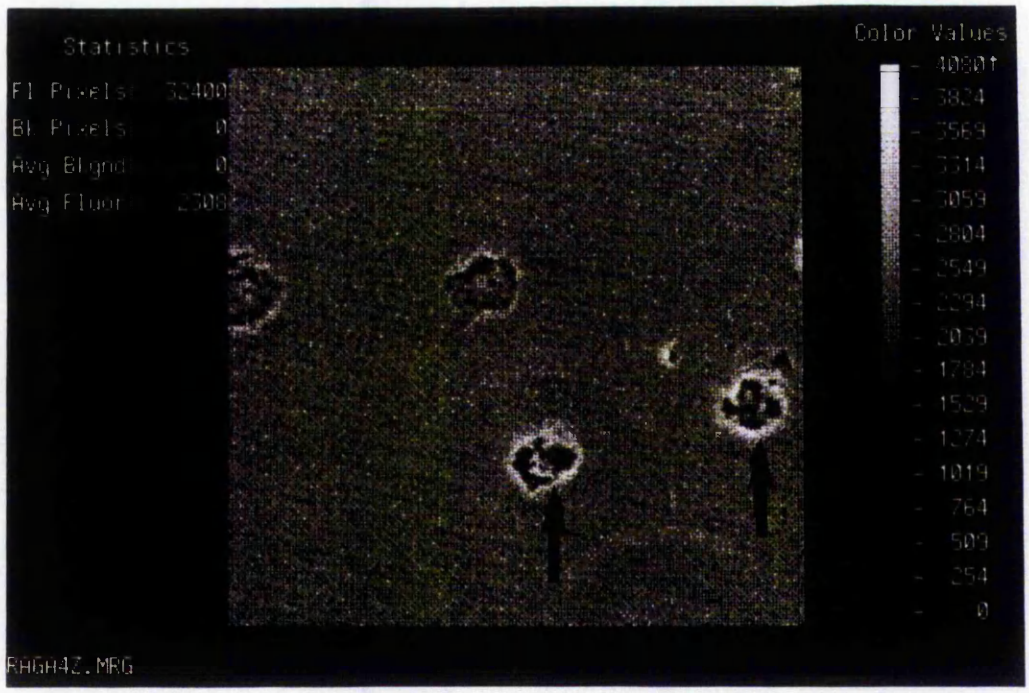
Statistics
Fl Pixels: 32400
Bk Pixels: 0
Avg Bkgnd: 0
Avg Fluor: 2508
Color Values
4080↑
3824
3569
3314
3059
2804
2549
2294
2039
1784
1529
1274
1019
764
509
254
0
RHGH4Z.MRG

1

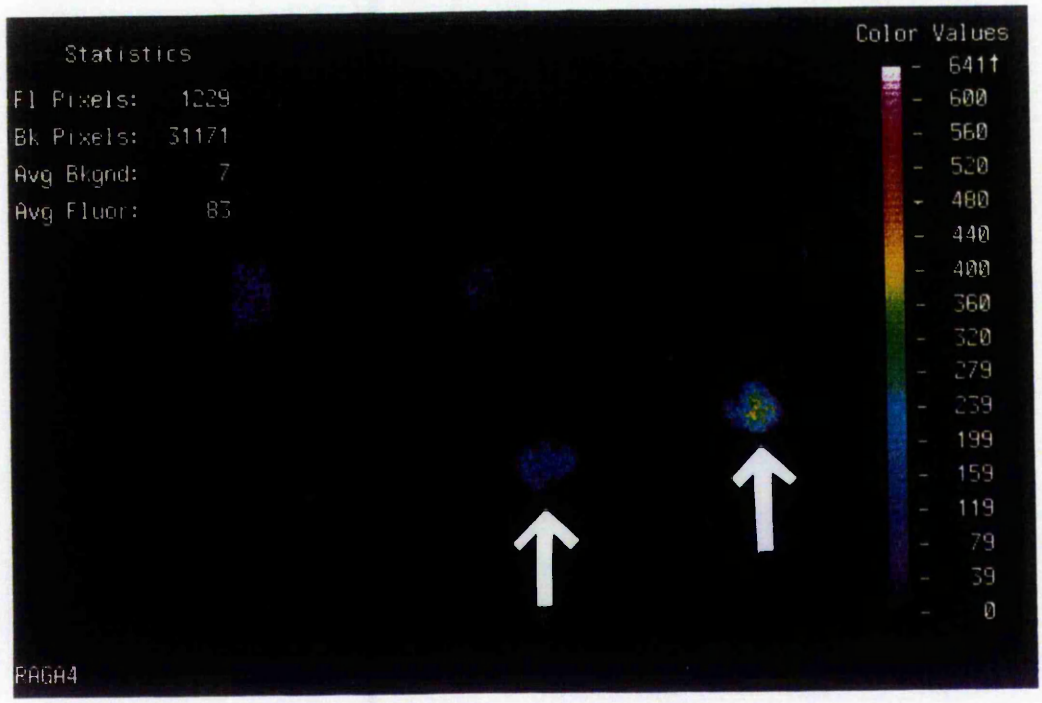
Statistics
Fl Pixels: 1229
Bk Pixels: 31171
Avg Bkgnd: 7
Avg Fluor: 83
Color Values
641↑
600
560
520
480
440
400
360
320
279
239
199
159
119
79
39
0
RAGH4

2

separation. Those cells containing ARB's and with abnormal morphology are clearly highlight by the auto-fluorescence.

A feature of the confocal laser cytometer that was used for this study was the ability to scan through individual cells with the laser in the z-axis. Using 0.4μM steps in the direction of the z-axis it was possible to score the auto-fluorescence present in an individual apoptotic cell of HT29 produced after 50μM R.A. treatment.

Examination of the series of confocal scans (Plate 6.6 parts 1-5) for this procedure showed how the ARB's are the sources of the auto-fluorescence in these apoptotic cells; also the plot of fluorescence distribution (Plate 6.6 part 5) shows fluorescence to be a linear relationship throughout the cell, this infers that the ARB's are wholly intracellular, and seen to have a spherical shape from the guanidine isolation photographs.. The presence and distinctive appearance of these light refractive apoptotic bodies (ARB's) in the culture of HT29 following retinoic acid treatment has enabled investigation of this new technique to quickly identify apoptotic cells

Acknowledgements

The authors thank Dr. Peter Davies for a gift of the human endothelial cDNA for transglutaminase and Dr. Chandra Franklin for helping with the Normarski photomicroscopy.

Plate 6.6 This is a composite figure of sequential confocal microscopic scans (1-4) through an individual apoptotic HT29 human colon carcinoma cell, induced into apoptosis by retinoic acid. The false colour images are point scanning the same field in the z-axis. Cutting 0.4μm lower each time. The more the colour of the cell moves to the red end of the scale; the higher the intensity of auto-fluorescence. Normal light microscopic examination of this same field has shown that the red spot areas correspond to the apoptotic refractive bodies - ARB's. The final plate (5) in this series indicates the distribution of fluorescence to be linear and wholly inside the cell, confirming the ARB's to be intracellular structures , rather than protruding surface blebbing.

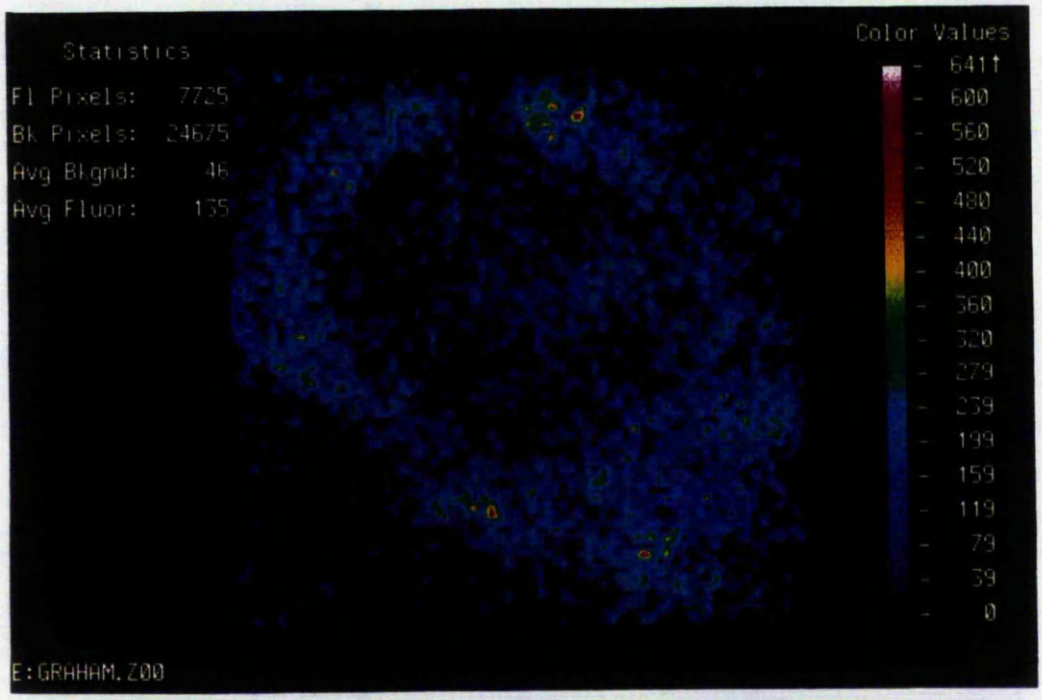
Statistics
Fl Pixels: 7725
Bk Pixels: 24675
Avg Bkgnd: 46
Avg Fluor: 135
Color Values
641↑
600
560
520
480
440
400
360
320
279
239
199
159
119
79
39
0
E:GRAHAM.Z00

1

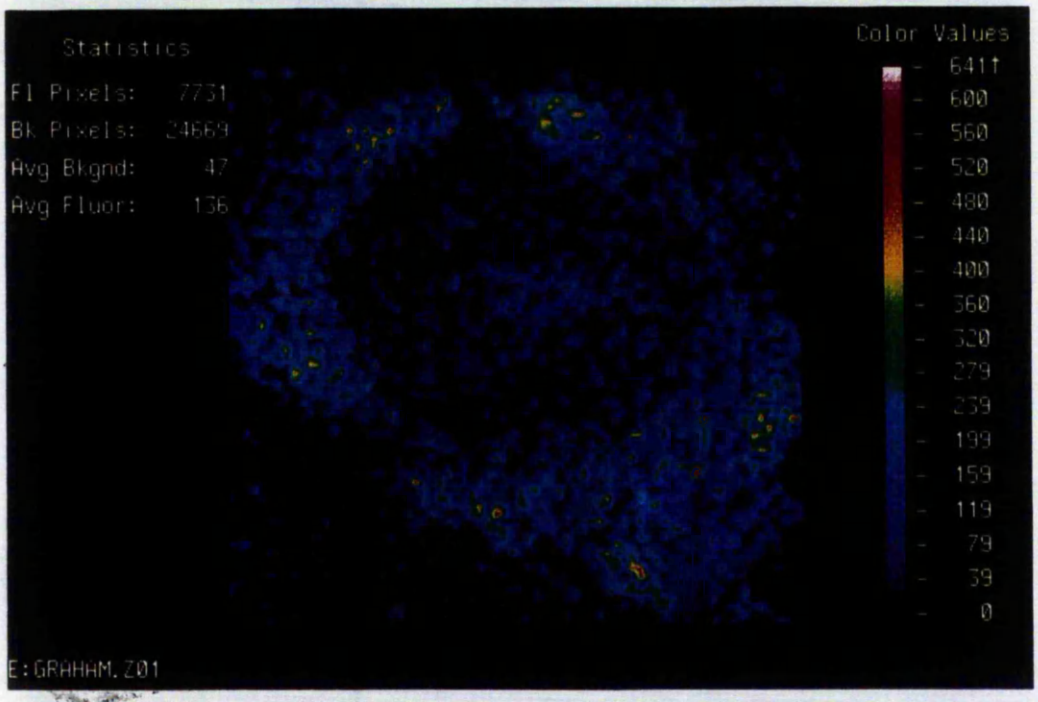
Statistics
Fl Pixels: 7731
Bk Pixels: 24669
Avg Bkgnd: 47
Avg Fluor: 136
Color Values
641↑
600
560
520
480
440
400
360
320
279
239
199
159
119
79
39
0
E:GRAHAM.Z01

2

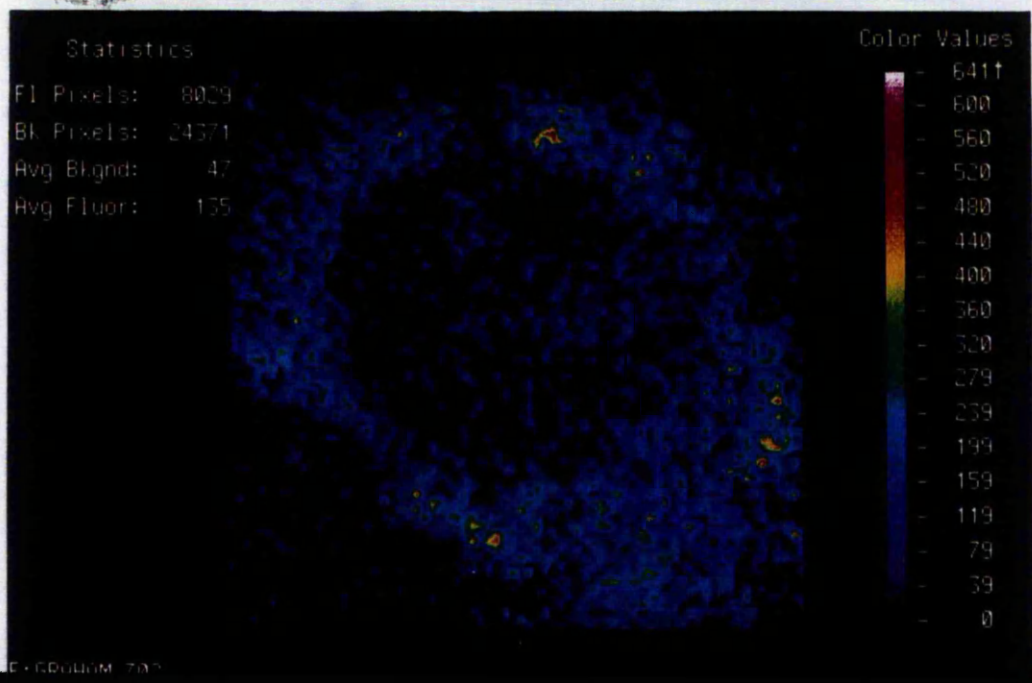
Statistics
Fl Pixels: 8029
Bk Pixels: 24371
Avg Bkgnd: 47
Avg Fluor: 135
Color Values
641↑
600
560
520
480
440
400
360
320
279
239
199
159
119
79
39
0

3

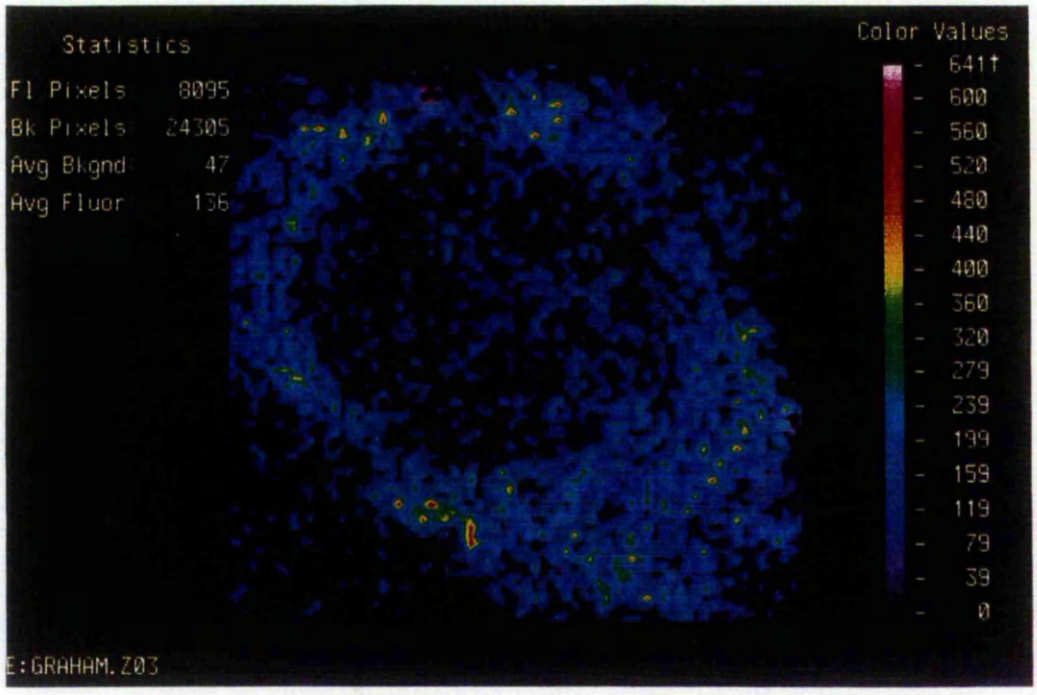
Statistics
Fl Pixels 8095
Bk Pixels 24305
Avg Bkgnd 47
Avg Fluor 136
Color Values
641↑
600
560
520
480
440
400
360
320
279
239
199
159
119
79
39
0
E:GRAHAM.Z03

4

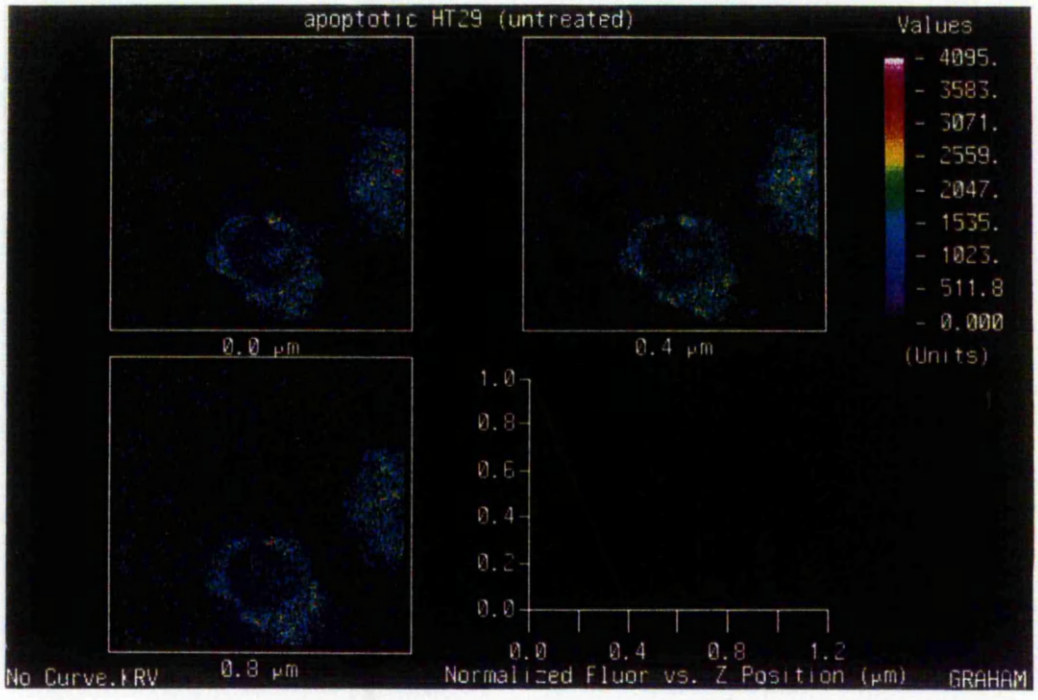
apoptotic HT29 (untreated)
Values
4095.
3583.
3071.
2559.
2047.
1535.
1023.
511.8
0.000
(Units)
0.0 µm
0.4 µm
0.8 µm
1.0
0.8
0.6
0.4
0.2
0.0
0.0
0.4
0.8
1.2
Normalized Fluor vs. Z Position (µm)
No Curve.KRV
GRAHAM

5

6.3 Discussion and Conclusions.

In this study the action of retinoic acid to induce the message, protein and activity of tissue transglutaminase has been confirmed. Furthermore, inconjunction with the induction of transglutaminase the cell culture has been induced into a high degree of apoptosis. Conventional, methods of measuring apoptosis, have been employed, namely DNA ladders and physical appearance of the cells.

In addition to this the availability of a confocal laser cytometer, made it possible to examine the apoptotic cells in more detail. Noticeable immediately in the retinoic acid treated cells was the presence of a large number of small, light refractive bodies. These have been termed Apoptotic Refractive Bodies (ARB's). They have been isolated by the action of detergents and chaotrophic agents, reverse phase HPLC analysis has shown them to be abundant in the transglutaminase-mediated crosslink.

As with the other models of transglutaminase induction, which have been used in this study to monitor apoptosis both *in vivo* and *in vitro*; it has not been possible to detect whether the enzyme is actually controlling the programmed cell death. What has been made clear is that through the models used there has been a consistent finding the increased transglutaminase activity during the production of apoptotic material. Transglutaminase may not therefore, be the essential controlling enzyme of programmed cell death; but it is actively involved in the biophysical changes associated with apoptosis. The recent work highlighting the possible signal transduction role of transglutaminase may hold the key to solving the question of transglutaminases' role in apoptosis. Incomplete signalling, may be a necessary trigger for expression of the death genes which together with the endonucleases and transglutaminase, drive the cell through the apoptotic pathway. The actions of

acetylaminofluorene, sodium butyrate and retinoic acid; as pharmacologically active compounds may indeed cause changes in the concentration of the messengers making up the signal transduction pathway in which transglutaminase is involved.

Understanding of programmed cell death is now a very important principle being employed in biological laboratories. It holds the potential to reverse or inhibit both neoplastic growth and the spread of malignant disease. The understandings learnt in this project of the role that transglutaminase plays in apoptosis, will help to formulate part of the complete picture.

Although tTGase is essentially an intracellular enzyme, there is now increasing evidence to suggest that it has the ability to act at the cell surface, which may be important in both cell adhesion (Gentile *et al* 1992) and stabilisation of the extracellular matrix Aeschilmann *et al* 1993 and Johnson *et al* 1997). If tTGase is active at the cell surface it is necessary to investigate which components of the extracellular matrix act as substrates, being crosslinked into large polymeric matrices which resist degradation and initially assist in the wound healing process but if persistent may exacerbate scarring. Secondly, are the same substrates components of both the SDS-insoluble polymer and apoptotic envelope? Therefore, the next chapter investigates specifically substrates of tTGase which are implicated in the formation of these two tTGase-mediated apoptotic structures.

7.0 Investigation of Transglutaminase Substrates in Cells using Cell Permeabilisation and Substrate Labelling Techniques.

7.1 Introduction.

7.2 Results.

7.2.1 Time-dependent incorporation of BTC into rat liver homogenates.

7.2.2 Effect of Ca^{2+} ionophore A23187 on the incorporation of BTC into BHK21.

7.2.3 Optimisation of electropermeabilisation settings for the incorporation of BTC into HT29, VA13a and ECV304 cell lines.

7.2.4 Specific incorporation of BTC into a low molecular weight protein found in HT29 cell line following RA treatment.

7.3 Discussion.

7.1 Introduction.

Having now established that each of the following cell lines, WI38 VA13a and HT29 can be induced into apoptosis by the topical action of sodium butyrate and retinoic acid respectively. Moreover that in each case tTGase message, antigen and catalytic activity is seen to increase in a time- and dose-dependent manner in response to these topical agents. These two *in vitro* models will be used to investigate substrates of tTGase implicated in stabilisation of the ECM; via an *in vitro* cell labelling method.

In addition to its protein crosslinking activity, tTGase is a GTP-binding protein (Achyuthan and Greenberg 1993 and Nakaoka *et al* 1994) with GTPase activity (Lee *et al* 1989), which also may be important in transducing extracellular signals via the α1-adrenergic receptor to phospholipase C (Nakaoka *et al* 1994). Studies with purified tTGase indicate that GTP, and to a lesser extent ATP, are capable of inhibiting its Ca^{2+} -dependent cross-linking activity by altering the conformation of the enzyme and decreasing its affinity for Ca^{2+} (Achyuthan and Greenberg 1993 and Bergamini 1994). It has been suggested that this regulation by GTP may be one way of modulating its cellular activity, such that the intracellular role of tTGase would be limited to that of a GTP-binding protein. Any cross-linking role for the enzyme would then be limited to cell-surface interactions; where nucleotides are absent and Ca^{2+} ions are plentiful : or in the dying cell, where ATP is lower and higher intracellular Ca^{2+} concentrations are established (Wyllie 1987).

However, the previous tTGase substrate studies, like those carried out by Achyuthan, Bergamini, Aeschilmann and Paulsson *et al* were conducted with fixed Ca^{2+} ion concentrations of 100μM or above with purified reagents and enzyme extracts. All of these factors are set to give the control of a test-tube experiment and so may behave differently to the intracellular environment, where the association of tTGase with other cellular factors may also exert an effect on its activity. Examples of such interactions would be those of tTGase with a particulate-associated inhibitory factor found in endothelial cells (Korner *et al* 1989), or with calmodulin (Takeuchi *et al* 1992) which may affect the enzyme when responding to nucleotides or Ca^{2+} . In order to observe tTGase activity on native substrates under cytosolic conditions the method of electropermeabilised cells will used.

The initial method chosen for the study of tTGase substrate labelling was either tissue or cellular homogenisation. Direct comparison of the two methods will be made in order to

establish the validity of using the permeabilisation method, which is the preferred method as it maintains much of the cellular integrity and spatial organisation of intracellular constituents (Swezey and Epel 1992).

Briefly, a biotinylated polyamine, biotin-X-cadaverine (BTC) will be used as the labelling substrate (section 2.3.17). It will be incubated under fixed calcium ion concentrations of 5 μM under the conditions of the tTGase activity assay (section 2.3.7.1). Both cellular homogenates (2.3.3) and electropermeabilised cell preparations (section 2.3.16) will be examined. After incubation the reactions will be stopped by the addition of the non-specific tTGase inhibitor - iodoacetamide. Samples will then be prepared for SDS / PAGE electrophoresis (section 2.3.22). Using the principle of Streptavidin / biotin interaction those proteins which have incorporated the donor substrate will then be visualised by Western blotting (section 2.3.23).

Those preparations investigate will include fresh rat liver homogenates, chosen because of the high endogenous levels of tTGase activity. VA13a cells treated with 2 mM sodium butyrate for 4 days and HT29 treated with 10 μM retinoic acid for 4 days. As shown previously both of these conditions lead to an induction of tTGase and reduction in overall cell number by a possible apoptotic / physiological programmed cell death. Ideally, all testing of substrate availability should be carried out on separated population of "normal" and "apoptotic" cell. However, due to the very large numbers of cells which would have to be grown for adequate protein loading of gels this was not possible. Hence, incubations with BTC were carried out on mixed population of cells harvested both from the monolayer and culture supernatant; thus ensuring that those cells of possible apoptotic morphology were incorporated in the study.

The aim of the work in this chapter was to identify any proteins which are amine acceptor substrates, common to all these cells types. Having established which acceptor proteins were of interest it was then hoped to purify one of these to homogeneity and attempt amino acid sequencing to try and gain an identification. Though, I was able to consistently show that a protein of 41-43kda was a common amine acceptor substrate of tTGase catalysed incorporation of BTC attempts to obtain amino acid sequence data were unsuccessful due to N-terminal blockade. Therefore, this data has not been shown.

7.2 Results.

7.2.1 Time-dependent incorporation of BTC into rat liver homogenates.

Fresh rat liver homogenates (20% (v/v) were prepared according to the method of section 2.3.3. The preparation was kept on ice at all times and split into two fractions. One was treated as the catalytic fraction, to this was added Ca^{2+} ions at 5 µM concentration and DTT at 2.5 mM both according to the tTGase activity assay (section 2.3.7). The total reaction volume was kept to a maximum of 500 µl. The second fraction was treated as a reaction control, in this fraction the calcium ions were replaced by 5 mM EGTA to prevent the activation of any endogenous tTGase. To both fractions 10 µl of a stock solution of biotinylated-X-cadaverine (BTC) was added to give a final concentration of 230 µM. Finally, both fractions were mixed and incubated at 37°C for 15 minutes. At 5 minute intervals from time (t = 0) 50 µl volumes were removed and prepared for SDS / PAGE (section 2.3.22) and Western Blotting (section 2.3.23).

[Please note that the Western blots are to be used only as qualitative evidence of BTC incorporation by the catalytic activity of tTGase. Some of the 4-chloronathol bands were not captured on the photographs well and have been enhanced at the time of photographing only for the purposes of clarity.]

Plate 7.1 shows the nitro-cellulose membrane after immunoprobing with streptavidin-peroxidase and colour development with 4-chloronapthol. The blot is split into two halves, on the left are the samples removed at each time interval from the control fraction. No staining can be seen. While on the right are the samples removed from the calcium activated fraction. Here incorporation of the BTC can be clearly seen into a protein of 41-43 KDa. Marked with the bold arrow. The staining pattern also shows that this incorporation was time-dependent.

Also seen on Plate 7.1 and marked with the broken arrow is the position of the stacking gel / resolving gel interface. Here it can be seen that there was formation of a high molecular weight polymer, which also incorporate some of the BTC. The amount of polymer formed was also seen to increase with the incubation time. This finding confirms the earlier result of section 5 where a high molecular weight tTGase-mediated polymer was obtained from the RA treatment of HT29.

Plate 7.1 Incubation of rat liver homogenates with biotin-x-cadaverine. Fresh 20% (w/v) rat liver homogenates (section 2.3.3) were incubated with 230 μM BTC for 15 minutes at 37°C (section 2.3.17). Samples were removed at 5 minute intervals and prepared for SDS / PAGE (section 2.3.22). This photograph of the nitro-cellulose membrane showing the Western blot probed with streptavidin-peroxidase and developed with 4-chloronaphtol (section 2.3.23). The large bold arrow show the relative position of the 44KDa standard and indicates a protein acceptor substrate for the tTGase-mediated incorporation of BTC. The small broken arrow indicates the increasing amount of high molecular weight polymer which has also had BTC incorporated. Where calcium was replaced by EGTA no staining was seen. The lanes were loaded as follows :

Lane 1, prestained molecular weight standards, BioRad;

Lane 2, 15 min incubation with BTC 230 μM and EGTA 5 mM;

Lane 3, 10 min incubation with BTC 230 μM and EGTA 5 mM;

Lane 4, 5 min incubation with BTC 230 μM and EGTA 5 mM;

Lane 5, 0 min incubation with BTC 230 μM and EGTA 5 mM;

Lane 6, 15 min incubation with BTC 230 μM and $CaCl_2$ 5 μM;

Lane 7, 10 min incubation with BTC 230 μM and $CaCl_2$ 5 μM;

Lane 8, 5 min incubation with BTC 230 μM and $CaCl_2$ 5 μM;

Lane 9, 0 min incubation with BTC 230 μM and $CaCl_2$ 5 μM;

Lane 10, Rainbow prestained molecular weight standards, Amersham.

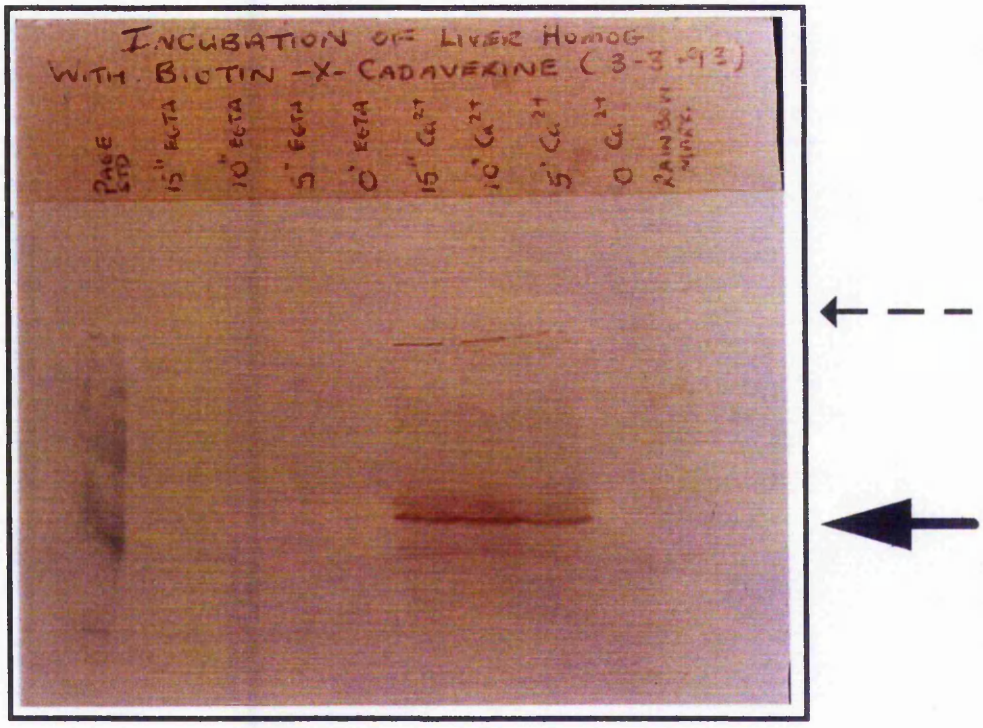

1 2 3 4 5 6 7 8 9 10

By showing that the high molecular weight polymer can act as an acceptor for tTGase-mediated incorporation of the polyamine BTC it gives further evidence that this polymeric material found in tumours and its related structure of the apoptotic envelope are formed and / or stabilised by the catalytic cross-linking action of tTGase.

7.2.2 Effect of Ca^{2+} ionophore A23187 on the incorporation of BTC into BHK-21 cell homogenates.

One of the major limitations of using cellular homogenates for the study of enzyme substrates is that the disruption of the cell creates an abnormal physical condition. A critical feature of tTGase is that the intracellular Ca^{2+} ion concentration of healthy cells is thought to be too low for the catalytic activation of tTGase. This makes a great deal of sense because it would be undesirable for uncontrolled cross-linking to occur in healthy cells. However, when the integrity of the cell is compromised there is availability of the extracellular calcium to influx into the cell providing the correct conditions for tTGase activation.

To test this the divalent cation ionophore A23187 was selected to recreate the conditions of controlled membrane rupture in BHK-21 cells. The action of the ionophore is to open calcium ion channels on the cell surface thus allowing the influx of extracellular ion into the cell. If tTGase is activated by this influx of Ca^{2+} ions then it should still be able to incorporate BTC into acceptor proteins. Five identical T-75 flasks were seeded with BHK-21 cells and allowed to grow to an 80% confluent monolayer. To these were added 100 µl volumes of varying concentrations of A23187 or vehicle as control (0 - 2.0 µM A23187 in 100% (v/v) ethanol vehicle) and a fixed concentration of BTC at 230 µM. These flasks were left to incubate for 1 hour at 37°C. The monolayers were then washed and the cells collected and prepared for SDS / Page and Western blotting as described previously (sections 2.3.22 and 2.3.23).

Plate 7.2 shows the resulting Western blot membrane, faint bands (enhanced) of staining can be seen for the incorporation of BTC into the 41 - 43 KDa acceptor protein when 0.5, 1.0 and 1.5 µM concentrations of A23187 are used. No incorporation can be seen in the control or 2 µM concentration (this concentration was thought to be cytotoxic to the cells). The degree of BTC substrate incorporation is low, but does confirm that only when extracellular Ca^{2+} ions are brought inside the cell is tTGase activated. The low level of substrate incorporation here is probably due to the poor permeabilisation of the cell membrane thus reducing movement of the BTC inside the cells, but allowing free Ca^{2+} ion movement. To over come this problem the degree of cell membrane permeabilisation was standardised using the method of electropermeabilisation.

Plate 7.2 Effect of Ca^{2+} ionophore A23187 on the incubation of BHK-21 cell monolayers with biotin-x-cadaverine. Sub-confluent monolayers of BHK-21 (section 2.3.1) were incubated with 230 µM BTC for 60 minutes at 37°C (section 2.3.17). Samples were removed and prepared for SDS / PAGE (section 2.3.22). This photograph of the nitro-cellulose membrane showing the Western blot, probed with streptavidin-peroxidase and developed with 4-chloronaphtol (section 2.3.23) (enhanced bands). The large bold arrow show the relative position of the 44KDa standard and indicates a protein acceptor substrate for the tTGase-mediated incorporation of BTC. Where no calcium ionophore was present no staining was seen. The lanes were loaded as follows :

Lane 1, biotinylated molecular weight standards, BioRad;

Lane 2, 60 min incubation of BHK-21 with BTC 230 µM and 2.0 µM A23187;

Lane 3, 60 min incubation of BHK-21 with BTC 230 µM and 1.5 µM A23187;

Lane 4, 60 min incubation of BHK-21 with BTC 230 µM and 1.0 µM A23187;

Lane 5, 60 min incubation of BHK-21 with BTC 230 µM and 0.5 µM A23187;

Lane 6, 60 min incubation of BHK-21 with BTC 230 µM and 0.0 µM A23187;

Lane 7, prestained molecular weight standards, BioRad.

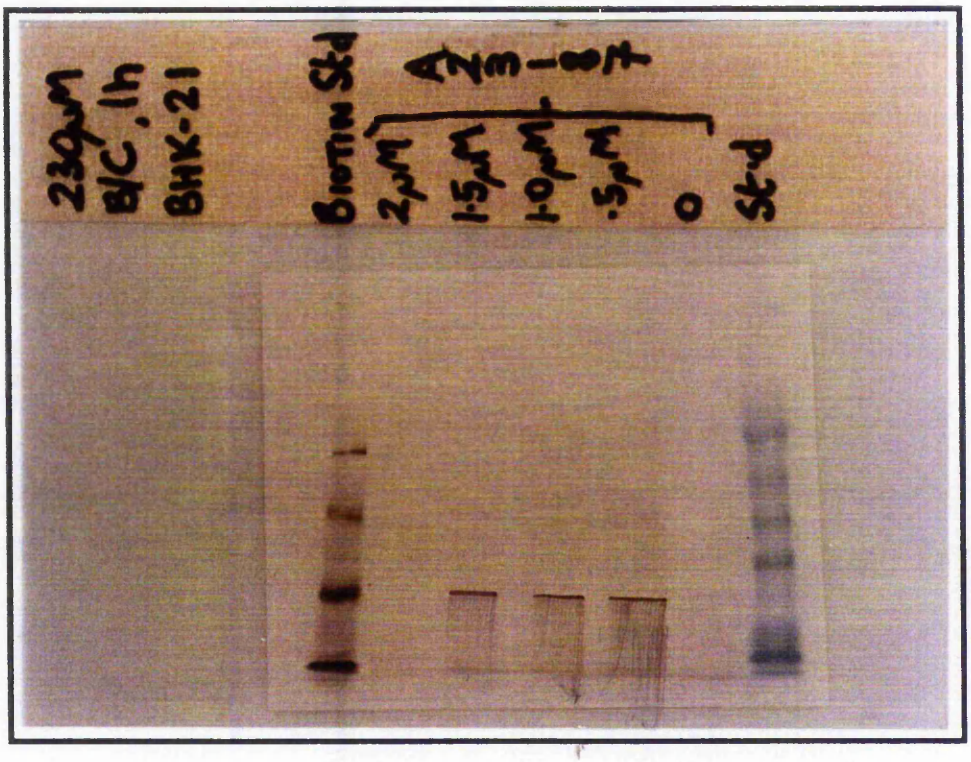

1 2 3 4 5 6 7

7.2.3 Optimisation of electropermeabilisation settings for the incorporation of BTC into HT29, VA13a and ECV304 cell lines.

Electropermeabilisation consists of applying a short wave pulse of high voltage electricity across a suspension of single cells in a special metal sided cuvette (section 2.3.16) . The electric field strength produced "punches" holes into the cell membrane as it enters and exits the cells. These holes are temporary and are of a consistent size and number. Thus the cell becomes permeabilised within the minimum disruption of its normal physical structure. This allows the free movement of ions and labelled probes across the cell membrane. The size of the holes are regulated by varying the voltage (this will alter the amplitude of the wave), the aim is to permeabilise the cell but not to destroy its integrity. The degree of permeabilisation is checked by trypan blue dye exclusion assays which give an estimate of the number of cells permeabilised (section 2.3.1.3). The capacitance is kept constant at 3 μF (this is to keep the frequency of the wave constant), cuvette width is kept constant at 0.4 cm and the pulse time is kept constant at 5 cycles of 0.2 seconds each with 5 seconds cooling between each pulse to re-agitate the cell suspension.

Suspensions of each cell culture (1.0 to 1.5 X 10^5 / ml) were prepared in permeabilisation buffer according to the method of section 2.3.16. After electropermeabilisation the cell suspensions were quickly pelletted by centrifugation then re-suspended in the incubation buffer containing Ca^{2+} ions and BTC as described earlier (section 2.3.17). These reactions were allowed to incubate at 37°C for 30 minutes. After which they were prepared for SDS / PAGE and Western blotting as described earlier.

Figures 7.1, 7.2 and 7.3 show the effect of varying voltage on the percentage permeabilisation of HT29, VA13a and ECV304 respectively. Each of the cell types behaved in a similar fashion giving maximum percentage of permeabilisation when the voltage ranged from 0.48-0.76 kV. However, the standard errors of the mean counts shown in Figures 7.1, 7.2 and 7.3 was high in each case. This may be due to clumping of the cells or precipitation in the cuvette.

Plate 7.3 A shows the Commassie brilliant blue staining of a 10 % SDS / PAGE gel indicating the constant protein loading per lane of cell incubations of HT29, VA13a and ECV304 following incubation with BTC. Corresponding to this gel is shown the resultant Western blot for biotin-labelled probe (Plate 7.3 B). Bands of incorporation (enhanced) can

Figure 7.1 Effect of varying voltage on electropermeabilisation of HT29. Single cell suspensions of HT29 cells grown in 10 μM retinoic acid for 4 days were harvested according to section 2.3.1. The cells were re-suspended in poration buffer and exposed to five cycles of a 0.2 second pulsed electric field at varying voltages (section 2.3.16). After electroporation the cells were washed and stained with trypan blue vital exclusion dye (section 2.3.13). The percentage permeabilised cells were those which excluded the vital dye. The voltage which produced the maximum permeabilisation was selected for future experiments. Values shown are the mean of 4 experiments + /- standard error of the mean.

Effect of Varying Voltage on Electropremeabilsation of HT29

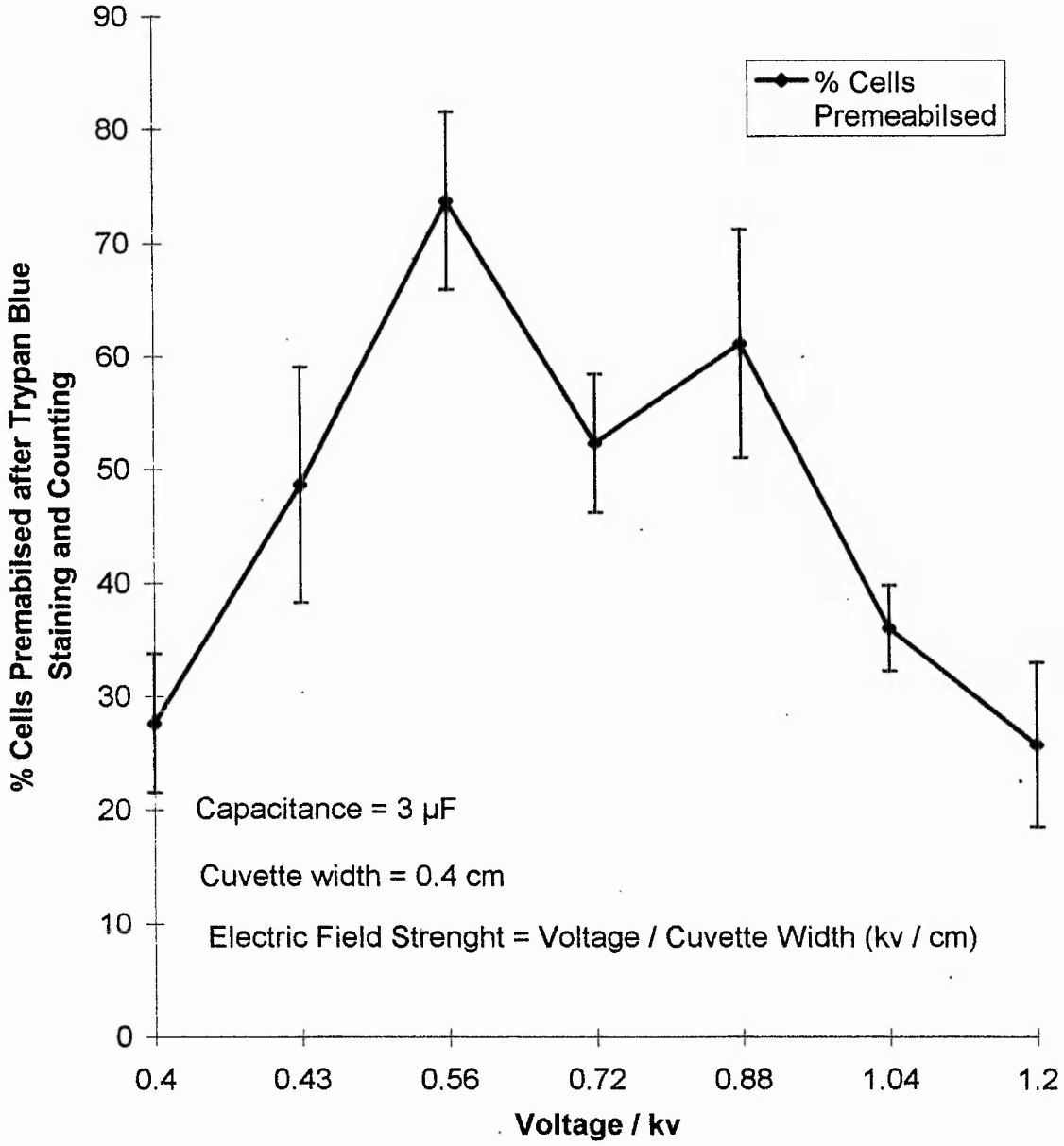

Figure 7.2 Effect of varying voltage on electropermeabilisation of VA13a. Single cell suspensions of VA13a cells grown in 2 mM sodium butyrate for 4 days were harvested according to section 2.3.1. The cells were re-suspended in poration buffer and exposed to five cycles of a 0.2 second pulsed electric field at varying voltages (section 2.3.16). After electroporation the cells were washed and stained with trypan blue vital exclusion dye (section 2.3.13). The percentage permeabilised cells were those which excluded the vital dye. The voltage which produced the maximum permeabilisation was selected for future experiments. Values shown are the mean of 4 experiments + /- standard error of the mean.

Effect of Varying Voltage on Electropremeabilsation of VA13a

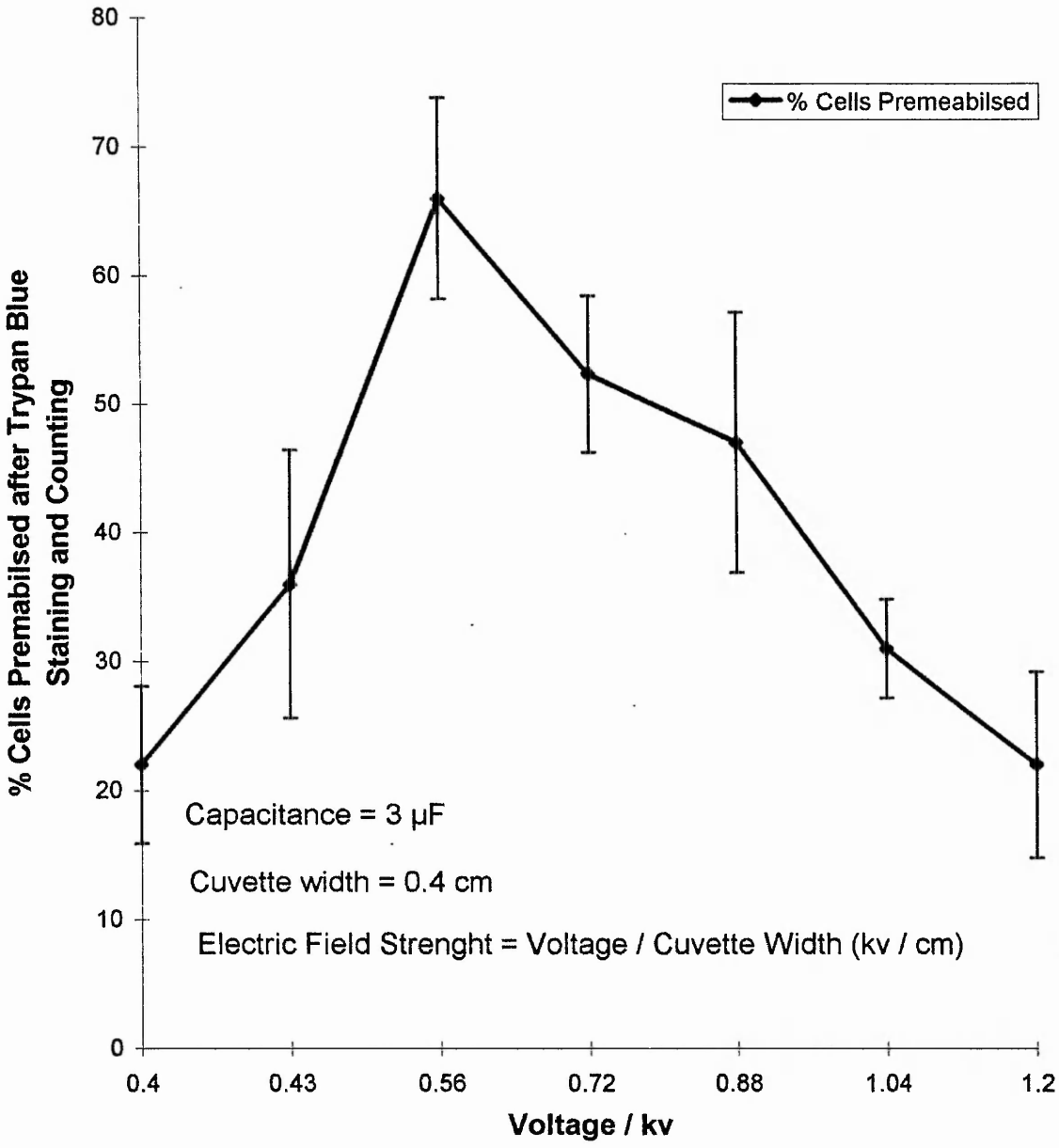

Figure 7.3 Effect of varying voltage on electropermeabilisation of ECV304. Single cell suspensions of ECV304 cells grown for 4 days were harvested according to section 2.3.1. The cells were re-suspended in poration buffer and exposed to five cycles of a 0.2 second pulsed electric field at varying voltages (section 2.3.16). After electroporation the cells were washed and stained with trypan blue vital exclusion dye (section 2.3.13). The percentage permeabilised cells were those which excluded the vital dye. The voltage which produced the maximum permeabilisation was selected for future experiments. Values shown are the mean of 4 experiments + /- standard error of the mean.

Effect of Varying Voltage on Electropremeabilsation of ECV 304

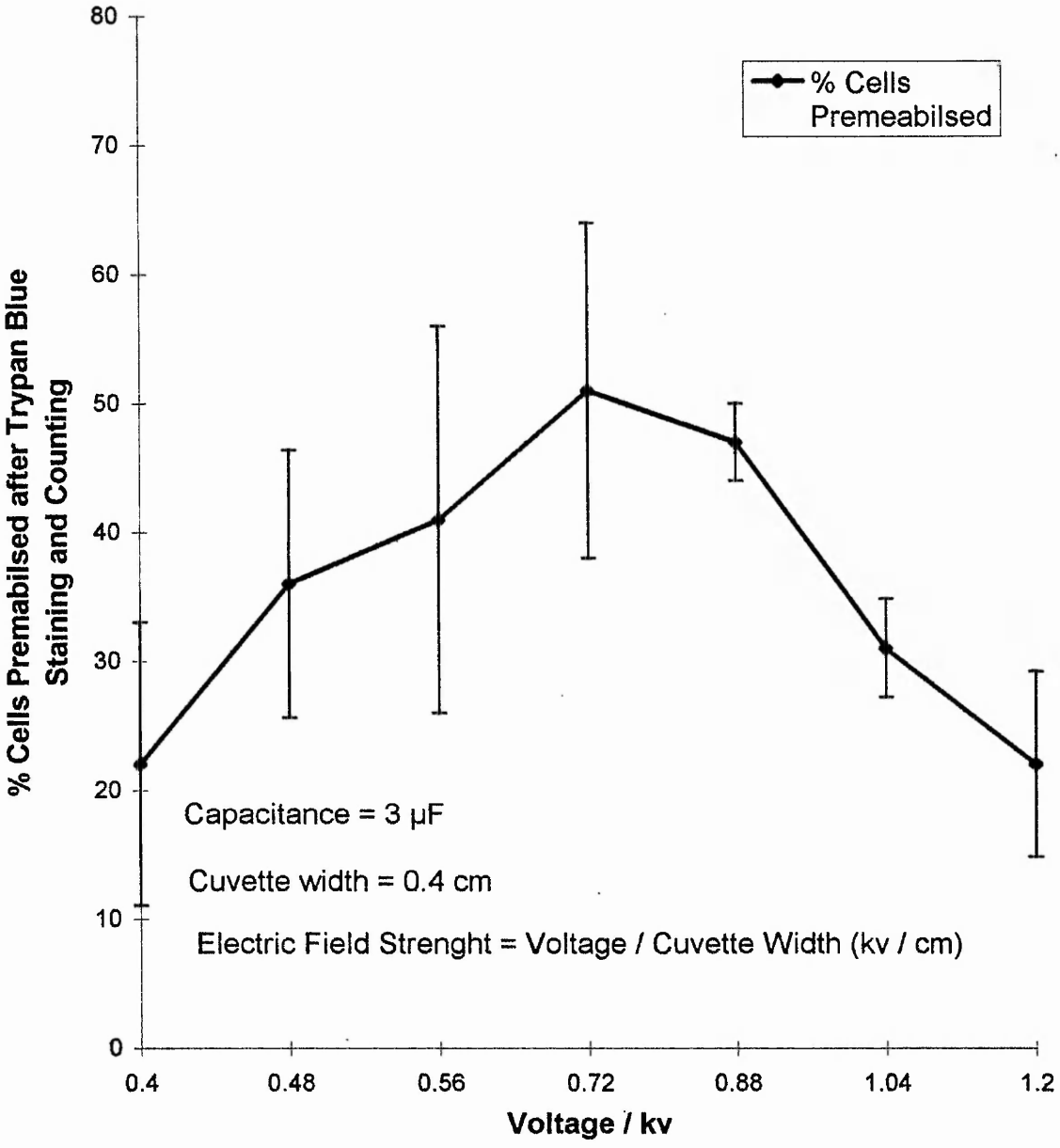

Plate 7.3 A & B Optimisation of electropermeabilisation conditions for the incorporation of biotin cadaverine. Single cell suspensions of HT29, VA13a and ECV304 (section 2.3.1) approx. 140,000 cells per ml of poration buffer were electropermeabilised according to the method of section 2.3.16. Various voltages were used to alter the electric field strength. Following permeabilisation the samples were incubated with 230 μM BTC for 30 minutes at 37°C (section 2.3.17). Samples were removed and prepared for SDS / PAGE (section 2.3.22). Plate A shows the loading pattern of the SDS / PAGE gel after Commassie blue staining. B is a photograph of the nitro-cellulose membrane showing the Western blot probed with streptavidin-peroxidase and developed with 4-chloronaphtol (section 2.3.23) (enhanced bands). The large bold arrow show the relative position of the 44KDa standard and indicates a protein acceptor substrate for the tTGase-mediated incorporation of BTC. No staining was seen in the ECV304 cell samples, possibly due to the low endogenous tTGase activity. However, both the HT29 (10 μM RA induced for 4 days) and VA13a (2 mM sodium butyrate induced for 4 days) cells showed incorporation of BTC by the action of tTGase. The lanes were loaded as follows :

Lane 1, HT29 cells incubated with 230 μM BTC, poration voltage 0.56 kV;
Lane 2, HT29 cells incubated with 230 μM BTC, poration voltage 0.48 kV;
Lane 3, VA13a cells incubated with 230 μM BTC, poration voltage 0.56 kV;
Lane 4, VA13a cells incubated with 230 μM BTC, poration voltage 0.48 kV;
Lane 5, ECV304 cells incubated with 230 μM BTC, poration voltage 0.56 kV;
Lane 6, ECV304 cells incubated with 230 μM BTC, poration voltage 0.48 kV;
Lane 7, prestained molecular weight standards, BioRad.

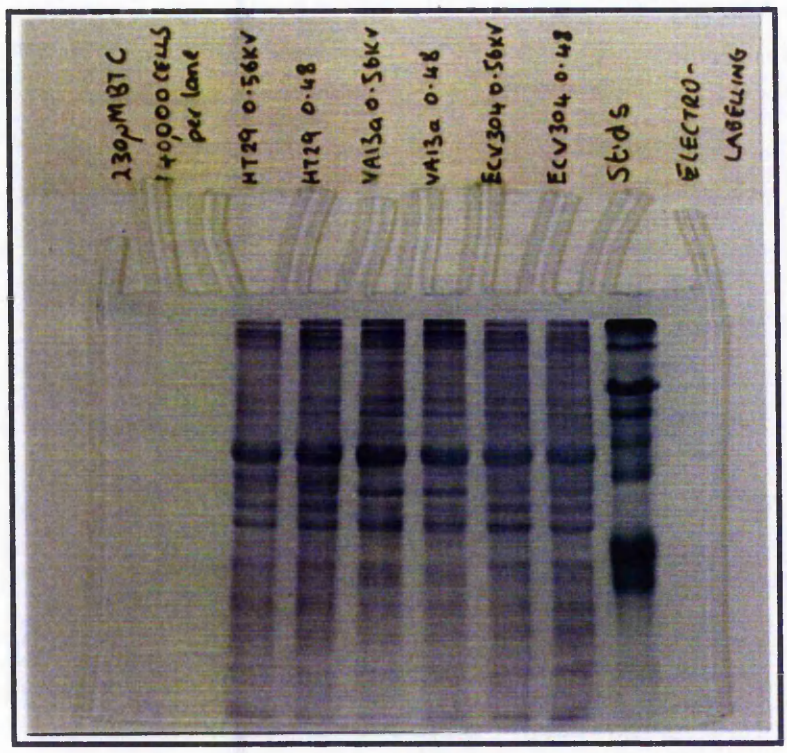

A

1 2 3 4 5 6 7

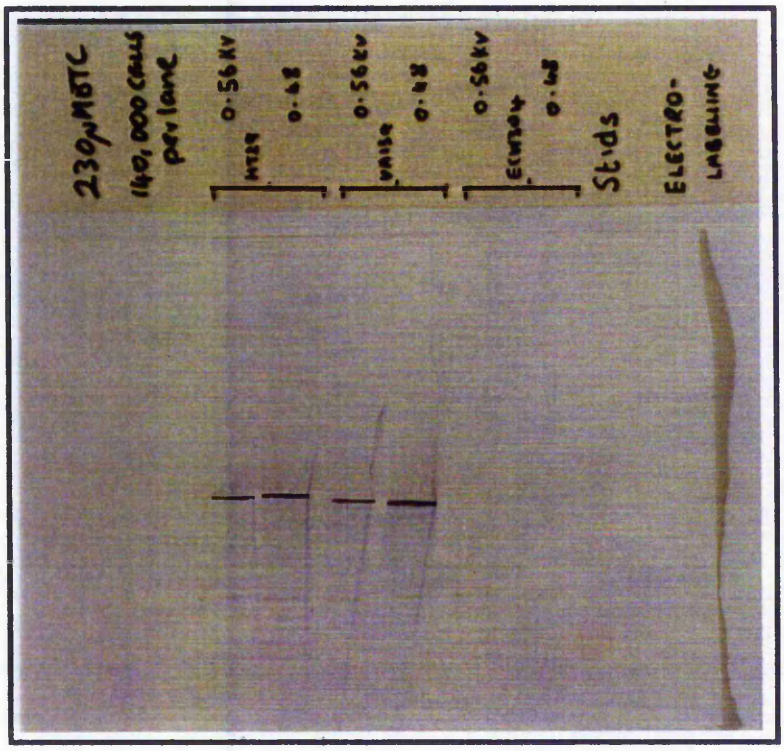

B

1 2 3 4 5 6 7

be seen for HT29 and VA13a at both 0.48 and 0.56 kV but not for the preparation of ECV304. This was expected as the endogenous level of tTGase activity in the ECV304 is 20 fold lower than in the other two cell lines, which have been treated with retinoic acid (10 μM) and sodium butyrate (2 mM) respectively to induce tTGase activity.

7.2.4 Specific incorporation of BTC into a low molecular weight protein found in HT29 cell line following RA treatment.

Selecting HT29 with retinoic acid treatment as it has the highest level of tTGase activity after 4 days of treatment the specific incorporation of BTC into the 41-43 KDa was examined. For this experiment the number of cells used was increased 100 fold, hence the electro permeabilisation conditions were adapted to maintain the percentage permeability to a maximal level.

Following electropermeabilisation at varying voltages (0.56 -1.04 kV) the cell suspensions were again separated into two fractions. Calcium was maintained at 5 μM in all fractions but half were incubated in the absence of BTC. One sample of HT29 cells was not electropermeabilised and acted as a control. By maintaining the calcium concentration at a level which would activate the endogenous tTGase the non-specific cross-reactivity of the streptavidin complex could be investigated.

Plate 7.4 A shows the shows the Commassie brilliant blue staining of a 10 % SDS / PAGE gel indicating the constant protein loading per lane of cell incubations of HT29, following incubation with BTC or without BTC at 230 μM Corresponding to this gel is shown the resultant Western blot for biotin-labelled probe (Plate 7.4 B). Bands of incorporation can in the 41 - 43 KDa only in those lanes where BTC had been added. Very little non-specific binding of the streptavidin-peroxidase reagent can be seen, but this does not occur in the corresponding molecular weight range of the specifically labelled protein. Those cells which had not been electropermeabilised did not show specific BTC incorporation, only a no-specific band at approximately 66 KDa in a similar fashion to the lanes where BTC had been omitted. This finding indicates the intracellular nature of tTGase.

Plate 7.4 A & B Electropermeabilisation conditions for the incorporation of biotin cadaverine into HT29. Single cell suspensions of HT29, (section 2.3.1) approx. 10,000,000 cells per ml of poration buffer were electropermeabilised according to the method of section 2.3.16. Various voltages were used to alter the electric field strength. Following permeabilisation the samples were incubated either with or without 230 μM BTC for 30 minutes at 37°C (section 2.3.17). Samples were removed and prepared for SDS / PAGE (section 2.3.22). Plate A shows the loading pattern of the SDS / PAGE gel after Commassie blue staining. B is a photograph of the nitro-cellulose membrane showing the Western blot probed with streptavidin-peroxidase and developed with 4-chloronaphtol (section 2.3.23). The large bold arrow show the relative position of the 44KDa standard and indicates a protein acceptor substrate for the tTGase-mediated incorporation of BTC. No staining was seen in the cell samples, where no BTC was added indicating that all other staining was specific. No staining was seen in the unpermeabilised cell sample inferring that the reactions were intracellular.. The lanes were loaded as follows :

Lane 1, prestained molecular weight standards, BioRad;
Lane 2, HT29 cells incubated with 230 μM BTC, poration voltage 0.56 kV;
Lane 3, HT29 cells incubated with no BTC, poration voltage 0.56 kV;
Lane 4, HT29 cells incubated with 230 μM BTC, poration voltage 0.72 kV;
Lane 5, HT29 cells incubated with no BTC, poration voltage 0.72 kV;
Lane 6, HT29 cells incubated with 230 μM BTC, poration voltage 0.88 kV;
Lane 7, HT29 cells incubated with no BTC, poration voltage 0.88 kV;
Lane 8, HT29 cells incubated with 230 μM BTC, poration voltage 1.04 kV;
Lane 9, HT29 cells incubated with no BTC, poration voltage 1.04 kV;
Lane 10, HT29 cells incubated with 230 μM BTC, no permeabilisation.

[Please note the order of the lanes is reversed for the Western blot.]

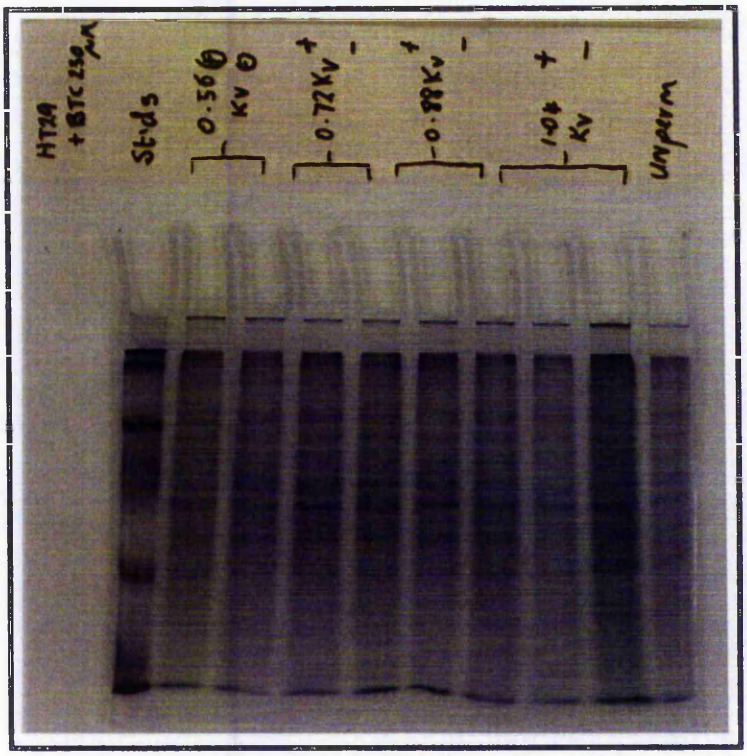

A

1 2 3 4 5 6 7 8 9 10

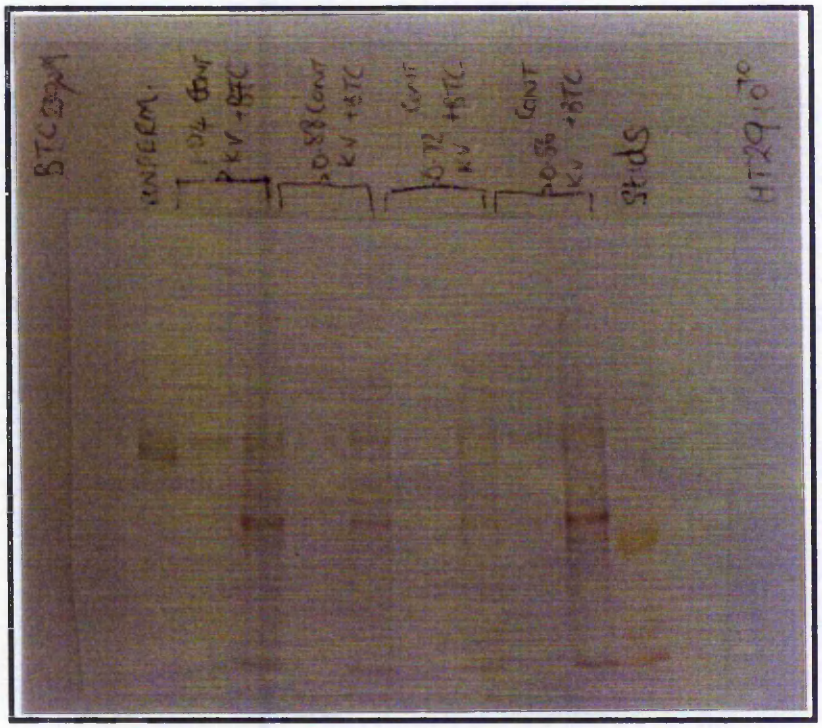

B

10 9 8 7 6 5 4 3 2 1

7.3 Discussion.

The data collected in this study uses a novel assay system utilising electropermeabilised cell and cellular homogenates to investigate the activation of tTGase activity in the intracellular and extracellular environment. In addition, it allows the identification of endogenous intracellular gamma-glutamyl- containing substrates under these conditions by visualising those proteins which incorporate the biotinylated polyamine probe, cadaverine. The choice of electropremeabilisation meant that the reaction conditions could be controlled without the loss of cell integrity.

With cell permeabilisation, the cytosolic solutes are dialysed into the surrounding medium and vice versa with no significant loss to the extracellular environment of tTGase or possible protein substrates (Smethurst and Griffin 1996). This is markedly different from detergent permeabilisation and homogenisation when mixing of cytosolic component and solutes of the extracellular environment occurs and continues unchecked, allowing tTGase to leak out and bind to components of the extracellular matrix e.g. fibronectin (Upchurch *et al* 1991).

In the cytoplasm of a resting energy-rich cell, the ATP levels may be as high as 8-11 nM and GTP levels between 50 and 300 μM (Smethurst and Griffin 1996, and references therein). With a proportion of each being bound to cytosolic proteins, giving lower free nucleotide concentrations. Similarly, in the resting cell the free Ca^{2+} ion concentration is 100 - 200 nM, under these conditions it is suggested that tTGase is inactive. A finding which is supported by the data in this chapter which showed no BTC incorporation in BHK-21 cells in the absence of ionophore A23187 (section 7.2.2). Also the negative result for incorporation of BTC when no extracellular Ca^{2+} was added to the systems.

Given this finding it is feasible that tTGase is activated at times of stress in the cell or when the cell membrane has been compromised. This is the hypothesis for the role of tTGase in wound healing (Upchurch *et al* 1991). tTGase could clearly be activated during the terminal stages of cell death or scarring, resulting from either necrosis or apoptosis, where intracellular Ca^{2+} ion concentrations increase and the cell becomes energy depleted lowering levels of inhibitory free nucleotides. This would fit in with the suggested role for tTGase in programmed cell death (apoptosis), where the formation of a fully crosslinked apoptotic envelope is only formed when the cell is destined to die.

The data in this chapter has highlighted a 41-43 KDa protein as being one of target the components of the apoptotic envelope. At 41KDa it is possible that this is actin, shown in chapter 3 to be immunologically reactive in the high molecular weight SDS / insoluble polymer isolated from rat liver. Also as the polymer and the apoptotic envelope have 80 % amino acid content homology (Hand *et al* 1991) it would follow that those proteins crosslinked together in these insoluble structures are made-up of similar component parts.

There is now mounting evidence that tTGase can act at the cell surface and may play a role in cell adhesion and extracellular matrix modifications resulting from scarring and fibrosis (Johnson *et al* 1997). This is certainly possible when membrane integrity is lost and the enzyme is freely available to activation by the high extracellular Ca^{2+}.

The availability of substrate of tTGase which are crosslinked together in the intact cell will not be significant if the free Ca^{2+} ion concentrations is too low. Thus in the "true" apoptotic cell where cells shrink and membrane integrity is preserved there should be no sudden rise in the intracellular concentrations of Ca^{2+}. Therefore, you would not expect to find structures such as the apoptotic envelope to be isolated from tissues.

This is infact the case in tissues *in vivo* the usual fate of the apoptotic cell is to be removed from the system by phagocytosis. This being carried out by wandering macrophages and commonly by neighbouring cells. Thus it would not be beneficial to such an efficient physiological cell death system for the target cell to be highly crosslinked and impossible to lyse by phagocytosis if it were full of tTGase-mediated ε-γ(gultamyl) lysine crosslinks. The apoptotic envelope is a consequence of the *in vitro* cell culture systems. These systems have homogenous populations of cells, no macrophages are present. The phagocytic capacity of the culture is finite and is set by the growth characteristics of the culture *in vitro*, taking into account the growth medium, availability of nutrients, contact inhibition and type of cell. Because removal of cells which have initiated into the apoptotic pathway is an energy consuming process I believe that the fate of the apoptotic cell *in vitro* is to become fully crosslinked by tTGase thus forming the apoptotic envelope. This will be discussed more fully in the next chapter.

8.0 Discussion.

From the evidence presented within the body of this report it has become clear that tissue transglutaminase is not the controlling factor, nor initiating factor in the apoptotic event. However, the physiological changes that can be evoked in apoptotic cells via the catalytic activity of tTGase to produce ε-γ(gultamyl) lysine crosslinks, between two proteins or free polyamines and structural proteins, of the cell, is not in doubt. Good evidence has been given for the production of transglutaminase-mediated products during he apoptotic event both *in vitro* and *in vivo*; namely the SDS-insoluble **apoptotic envelope** and the large molecular weight **SDS-insoluble polymer**. Both of which can be found, isolated and quantified in healthy, neoplastic and diseased tissues or within normal, neoplastic, metastatic or transformed cell lines.

This conclusion has been reach via the observation that no constant correlation exists between the level of tissue transglutaminase activity, amount of tissue transglutaminase antigen, amount of crosslinked catalytic product and the degree of damage within the experimental tissue / cell line under examination; whether this be solid hepatocellular carcinoma (AAF model), breast carcinoma (MCF-7), bone sarcoma (P8), hamster fibrosarcoma (MET clones), or continuous tissue cultures of Human colon carcinoma (HT29), transformed human endothelial cells (ECV307), malignant metastatic melanoma (A375) or SV40 virus transformed fibrosarcomas (WI38 VA13a).

The experimental strategies to evaluate the continuous tissue culture models have shown a number of pharmacological ways in which the catalytic activity of tissue transglutaminase my be induced within the cell. The topical application of all-trans retinoic acid, sodium butyrate and in the work from Knight *et al* 1991 and Johnson *et al* 1994 dexamethasone have all been shown to produce a dose- and time-dependent induction of tTGase messenger RNA and catalytically active protein, in the cell lines mentioned above.

However, a central paradox remains unsolved in the link between the presence of increased tTGase detected in tissues and cells; namely the correlation with detectable amounts of the catalytic end-product- ε-γ(gultamyl) lysine crosslinks. This paradox is central to this study and it was investigated by using the antisera produced during the course of experimental

work raised to react with the two tTGase-mediated products (anti apoptotic envelope antibody and anti-SDS-insoluble polymer antibody), both thought to be associated with apoptosis, the levels and distribution of both structures was investigated. Together with further analyses using antisera raised to tTGase and a monoclonal antibody to ε-γ(gultamyl) lysine crosslinks were the basis of investigating the role of tTGase in programmed cell death- apoptosis. The presence and relative amounts of each of these parameters was detailed in experimental systems both *in vivo* and *in vitro*.

The findings in this study which produced data showing a link between the incidence of apoptosis in tissues and cells and the co-incidence increased activation of the tTGase enzyme, have not fully explained this paradox. Apoptosis could still be quantified in the control experimental systems when there was little or no tTGase activity; thus indicating that programmed cell death can occur completely independently of tTGase activity. Therefore the original idea that tTGase activity causes the formation of the apoptotic envelope and hence the stabilisation of the apoptotic cell, is no longer valid. Though an associative link does remain.

The associative link shown by the data in this study hinges around two principles. Firstly, for the tTGase to become catalytically active the concentration of available free calcium ions (Ca^{2+}) must be at a minimum of 1-5 μM (Smethurst and Griffin 1996), this concentration is upto fifty times higher than the normal intracellular range of 100 - 200 nM and is more inline with the normal extracellular bathing concentration for calcium. For a cell to increase its intracellular calcium concentration to this level it would normally have undergone a trauma sufficient to begin cellular necrosis, not apoptosis. The most obvious insult being loss of membrane integrity to allow immediate and rapid cross-membrane flux of the high extracellular calcium ion load into the cell.

Secondly, as tTGase is not transcribed with a secretory leader sequence for export out of an intact cell via the Golgi, such a rupture of the cell membrane would allow contra-flow traffic of catalytically active tTGase out of the cell and onto the ECM (Upchurch *et al* 1992). This pattern of events is what best describes the wound healing role of tTGase. Immediately, at the site of an injury the actions of plasma transglutaminase (Factor XIIIa), begin to stabilise the blood clot thus "plugging" the wound. Those, cells punctured or damaged by the force of the trauma lose homeostatic calcium ion control, the concentration

of Ca^{2+} ions equilibrates in both intracellular and extracellular compartments of the cell. tTGase now intermixed between intra- and extracellular compartments becomes catalytically active and begins to form stable insoluble ε-γ(gultamyl) lysine crosslinks between protein substrates of the ECM, resulting in further stabilisation of the wound site and the formation of protective scar tissue which assists in the wound healing process.

The sequence of events outlined above are not associated with apoptosis; the damage incurred by cells and tissues receiving such an insult would certainly results in necrosis and the dispersal of local immune complexes (histamine, bradykin, prostglandins, prostacyclins, cytokines, chemokines and the complement cascade) and activation within the blood system of distant immunological factors and cell types drawn to this area in an attempt to minimise infection and inflammation. Localised apoptosis would maintain cellular integrity and minimise these effects. Where apoptosis dose play a part in the wound healing process is during the secondary stage of healing when the initial trauma is contained. The massive influx of inflammatory cells and increased proliferation of resident cells at the wound site now has to be restored to homeostatic levels, scar tissue is initially beneficial but if allowed to persist can exacerbate healing. Thus, controlled removal of cells which are now surplus to requirements can begin and it is apoptosis which provides the most efficient mechanism of cell deletion with the minimum amount of further immunological damage (Savill *et al* 1996).

The presence of large amounts of ε-γ(gultamyl) lysine crosslinks would prove detrimental to the tissues making phagocytosis of apoptotic cells difficult, as there is no known enzyme present in the mammalian system able to breakdown the crosslinks once formed. An exception being the reported isolation of an inhibitor of tTGase from the saliva of the Leech - Tridegin (Personal communication from Dr. R Wallace of Biopharm, UK) and the controversial report from the Russian group of Baskova *et al* 1994 of Destabilase another enzyme also isolated from the saliva of the leech which has the ability to catalyse the breakdown of ε-γ(gultamyl) lysine crosslinks. Though, this second compound is thought to be an artefact isolated from the enteric bacteria held within the gut of the leech rather than secreted by the leech itself. Either way, fully formed large crosslinked protein matrices containing very high proportions of the ε-γ(gultamyl) lysine crosslinks will be very difficult to digest *in vivo* and remove from the wound site. Thus, the role of tTGase in wound

healing is primarily one of "damage limitation" and not fined tuned to the control or activation of apoptosis which removes excessive cellular material at the site of scar tissue.

An observation made within this study which would support the finding that excessive catalytic activity of tTGase at the site of trauma, to be detrimental; has been shown by the detection, isolation and comparison of the apoptotic envelopes from cell culture systems with the SDS-insoluble polymer isolated from damaged tissues.

In order to understand this observation it is first necessary to briefly describe the functional differences between an *in vitro* cell culture system and the conditions present *in vivo*. By far the most obvious and important difference is the number of cell types present locally and / or available for migration into the site of injury. Contained in the cell culture flask you have a single homogeneous cell type growing in "ambient" conditions of limited surface area, limited nutrients. Once confluence is achieved the cell density to surface area ratio abides by a strict equation of cell number to nutrient availability. This is a fine equilibrium which unless the cell number is reduced by passage dilution or cell proliferation inhibited by artificial intervention with cell cycle synchronising / blocking compounds; then all cells in the culture may become stressed and result in large scale necrosis. Prolonged exposure of the culture to periods of stress may also cause the cells to alter their normal quiescent state, spontaneous phenotypic changes may be observed e.g. diploidy changing to eupolidy as in the treatment of VA13a with sodium butyrate.

When compared to a tissue which may have a number of heterologous resident cell types with the potential to migrate either small distances within the tissue or greater distances through the vascular or lymphatic systems. Secondly, the available source of nutrients is potentially unlimited and continually "refreshed" via the vasculature, which also carries away from the wound waste products of metabolism, sources of changes in pH and infection. Thirdly, there is the potential for intrusion into the wound site by cells of the immune system, all "phagocytosis hungry" (macrophages, monocytes, neutorphils, T cells etc..) which enact as a first line of defence against damage and disease.

My observation of the actions of tTGase in the cell culture systems evaluated are that the catalytic production of ε-γ(gultamyl) lysine crosslinks is allowed to progress "unchecked". Resulting in the formation of the fully crosslinked apoptotic envelopes, a situation as

mentioned earlier undesirable *in vivo* due to the lack of necessary enzymes for the digestion of these crosslinks. While *in vivo* it was not possible to isolate intact envelopes, rather it was only possible to isolate large polymeric SDS-insoluble material shown in Chapter 3 to be the constituent parts of apoptotic envelopes. This polymeric material still contains high numbers of ε-γ(gultamyl) lysine crosslinks but its formation into envelopes is not fully complete and therefore may render it more accessible to degradation / and or incorporation into newly synthesised ECM.

Though, this ability of the tTGase-mediated SDS-insoluble polymer to be degraded and / or re-integrated into ECM has not been proven within this thesis it is reasonable to conclude that due to the differences in availability of Ca^{2+} ion concentrations, suitable tTGase substrates and variations in different cell types present; then the action of tTGase in cell culture is different to its role *in vivo*.

Namely, when activated in cell culture tTGase will strive to form as many ε-γ(gultamyl) lysine crosslinks as possible, controlled only by the numbers of damaged / stressed cells present, concentration of free Ca^{2+} ions and availability of substrates. Resulting in the formation of the atypical product - apoptotic envelopes. While, *in vivo* the action of tTGase is to assist in the stabilisation of those cells directly at the site of damage, transient fluctuations in the levels of Ca^{2+} ion concentration are rapidly restored to homeostatic levels with the concentration gradient between intracellular and extracellular concentrations re-established. Thus halting the "unchecked" production of ε-γ(gultamyl) lysine crosslinks, leaving the tissue stable and in a status favourable for phagocytosis, which will allow specific cell deletion for scar tissue removal and remodelling via apoptosis at a later time.

To possibly prove this hypothesis it would be necessary to follow the production and degradation of tTGase-mediated products (apoptotic envelopes and SDS-insoluble polymer) both *in vivo* and *in vitro.*

Hence, it was necessary for me to investigate the individual protein constituents of both structures. My aim was to identify proteins which act as either glutamine or lysine acceptor / donor substrates for tTGase and make up part of the overall structure of apoptotic envelopes and the SDS-insoluble polymer. Once, identified it was then envisaged to monitor the development and use of the substrates within one of the cell culture systems

under evaluation. The substrate of choice being uniquely identifiable by labelling with either biotin, digoxigenin or a radionucleotide e.g. ^{35}S methionine.. This part of the study proved unsuccessful. Though the incorporation of the biotinylated polyamine cadaverine was demonstrated repeatedly; into a 41 - 43 KDa protein efforts to identify this protein failed.

Corroborative evidence for the data in this study has been shown over many years, by the individual work of the leading transglutaminase laboratories, outside of Nottingham (Aeschilmann *et al* 1991, 1992, 1993, 1994, 1996; Birckbichler *et al* 1976, 1997, 1978, 1980, 1981, 1983, 1985; Davies *et al* 1980, 1985, 1993; Fesus *et al* 1987, 1989, 1997; Gentile *et al* 1991, 1994; Melino *et al* 1994; Piacentini *et al* 1988, 1991, 1993). Their work has dealt with many different tissue and primary cell culture experimental systems, looking at the both apoptosis and the substrates, activation, induction and inhibition of tissue transglutaminase, including liver tumour studies, retinoic acid and sodium butyrate induction. tTGase-mediated polymers, where formed have been isolated and shown to include several intracellular and membrane-bound proteins. Namely, actin, annexin II, vinculin, fibronectin and desmosomal proteins; also all previously shown to be tTGase substrates (and Paulson 1996 and cited references there in).

In conclusion, data has been presented in this study which have shown tTGase to be potentially one of the killer effector elements of the programmed cell death pathway. I suggest that tTGase activation leading to the catalytic production of ε-γ(gultamyl) lysine crosslinks between proteins, results in the formation of large molecular weight SDS / insoluble polymers; causing irreversible polymerisation of the cell. It is these polymers which modify cell organisation and determines those ultrastructural changes typical of cells undergoing apoptosis. In addition the tTGase-dependent protein polymerisation might prevent the release of harmful intracellular components into the extracellular space. Thus helping to explain why apoptosis is an immunologically silent event not associated with inflammation and scar formation in the surrounding tissues.

If tissue transglutaminase has a role in programmed cell death - apoptosis? This is to stabilise the dying cell to help facilitate its programmed physiological cell death with the minimum of immunological disruption to the surrounding tissues. This physiological programming used by apoptotic cells should be regarded as the true end point of a cells' life, it is "normal" cell death, as it strives to maintain homeostasis at all times; when compared to the local immunological chaos of - necrosis.

9.0 References.

Achyuthan, KE. and Greenberg, CS. (1987) Identification of a guanosine triphosphate-binding site on guinea pig liver transglutaminase. J Biol. Chem. 262 : 1901-1906.

Aeschilmann, D. and Paulson, M. (1991) Cross-linking of laminin-nidogen complexes by tissue transglutaminase: A novel mechanism for basement membrane stabilisation. J Biol. Chem. 266 : 15308-15317.

Aeschilmann, D., Paulson, M. and Mann, K. (1992) Identification of GLN^{276} in nidogen as the amine acceptor in transglutaminase-catalysed crosslinking of laminin-nidogen complexes. J Biol. Chem. 267 : 11316-11321.

Aeschilmann, D., Wetterwald, A., Fleisch, H. and Paulson, M (1993) Expression of tissue transglutaminase in skeletal tissues correlates with the events of terminal differentiation of chondrocytes. J Cell Biol. 120 : 1461-1470.

Aeschilmann, D and Paulson, M (1994) Transglutaminase-catalysed matrix cross-linking in differentiating cartilage : Identification of osteonectin as a major glutaminyl substrate. J Cell Biol. 129 : 881-892.

Aeschilmann, D. and Paulson, M (1996) Transglutaminases : Protein cross-linking enzymes in tissues and body fluids. Thromb. Haemost. 71 : 402-415.

Argarwal, ML., Argarwal, A., Taylor, WR. and Stark. GR. (1995). P53 controls both G2/M and the G1 cell-cycle checkpoints and mediates reversible growth arrest in human fibroblasts. Proc. Natl. Acad. Sci. (USA) 92, 18 : 8493-8497.

Alitalo, K., Schwab, M., Lin, CC., Varmus, HE. and Bishop, JM. (1983). Homogeneously staining chromosomal regions contain amplified copies of an abundantly expressed cellular oncogene (C-MYC) in malignant neuroendocrine cells from a Human-colon carcinoma. Proc. Natl. Acad. Sci. (USA) 80, 6 : 1707-1711.

Angel, P., Allegretto, EA., Okino, ST., Hattori, K., Boyle, WJ., Hunter, T. and Karim, M. (1988). Oncogene JUN encodes a sequence-specific trans-activator similar to AP-1. Nature 332, 6160 : 166-171.

Arends, MJ., Kerr, JHR. and Currie, AH. (1990) Apoptosis: Mechanisms and roles in pathology. Am. J. Pathol. 136 : 593-608.

Arndt, K. and Fink, GR. (1986). GCN4 protein, a positive transcription factor in yeast, binds general control promoters at all 5' TGACTC 3' sequences. Proc. Natl. Acad. Sci. (USA) 83, 22 : 8516-8520.

Arundel, CM., Kenney, SM., Leith, JT. and Glicksman, AS (1986) Contrasting effects of the differentiating agent sodium butyrate on recovery processes after X-irradiation in heterogenous human colon tumour cells. Int. J. Radiation Oncology Biol. Phys., 12 : 959-968.

Bargou, RC, Daniel, PT., Mapara, MY., Bommert, K., Wagener, C., Kallinich, B., Ryer, HD. and Dorker, B. (1995). Expression of the BCL-2 gene family in normal and malignant breast-tissue - low BAX-alpha expression in tumour cells correlates with resistance to apoptosis. Int. J. Cancer 60, 8 : 854-859.

Barsigian, C., Stern, AM. and Martinez, J. (1991) Tissue (Type II) transglutaminase covalently incorporates itself, fibrinogen, or fibronectin into high molecular weight complexes on the extracellular surface of hepatocytes. J Biol. Chem. 266 : 22501-22509.

Baskova, IP., Aguejouf, O., Azougagh-Oualane, F., Zavalova, LL., Basanova, AV. and Doutremeuich, C. (1994) Destabilase an e-g(gultamyl) lysine crosslinks isopeptidase from the medicinal leech. Thromobsis Research 74 : 241-244.

Bergamini, C. M. (1988) GTP Modulates calcium binding and cation-induced conformational changes in erythrocyte transglutaminase. FEBS Letts. 239 : 255-258.

Birckbichler, PJ., Orr, GR. and Patterson, MK., Jr. (1976) Differential transglutaminase distribution in normal rat liver and rat hepatoma. Cancer Res., 36 : 2911-2914.

Birckbichler, PJ., Orr, GR., Conway, E. and Patterson, MK., Jr. (1977) Transglutaminase activity in normal and transformed cells. Cancer Res., 37 : 1340-1344.

Birckbichler, PJ. and Patterson, MK., Jr. (1978) Cellular transglutaminase, Growth, and Transformation. Ann. N.Y. Acad. Sci., 312 : 354-365.

Birckbichler, PJ., Carter, HA., Orr, GR., Conway, E. and Patterson, MK., Jr. (1978) e(g-Glutamyl)lysine isopeptide bonds in normal and virus transformed human fibroblasts. Biochem. Biophys. Res. Commun., 84 : 232-237.

Birckbichler, PJ. and Patterson, MK. Jr. (1980) Transglutaminase and e(g-glutamyl)lysine isopeptide bonds in eukaryotic cells. Prog. Clin. Biol. Res., 41 : 845-855.

Birckbichler, PJ., Orr, GR., Patterson, MK., Jr., Conway, E. and Carter, HA. (1981) Increase in proliferative markers after inhibition of transglutaminase. Proc. Natl. Acad. Sci. USA, 78 : 5005-5008.

Birckbichler, PJ., Orr, GR., Patterson, MK., Jr., Conway, E., Carter, HA. and Maxwell, MD (1983) Enhanced transglutaminase activity in transformed human lung fibroblast cells after exposure to sodium butyrate. Biochim. Biophys. Acta 723 : 27-34.

Birckbichler, PJ., Upchurch, HF., Patterson, MK., Jr. and Conway, E. (1985) A Monoclonal Antibody to Cellular Transglutaminase. Hybridoma 4 : 179-186.

Bissonnette, RP., Mc.Gahon, A., Mahboubi, A. and Green, DR. (1994). Functional MYC-MAX heterodimer is required for activation-induced apoptosis in T-cell hybridomas. J. Exp. Med. 180, 6 : 2413-2418.

Bohmann, D., Bos, TJ., Admon, A., Nishimura, T., Vogt, PK. and Tjian, R. (1987). Human proto-oncogene C-JUN encodes a DNA-binding protein with structural and functional-properties of transcription factor-AP-1. Science, 238, 4832 : 1386-1392.

Boise, LH., Gonzales-Garcia, M., Postema, CE., Ding, LY., Lindstein, T., Turka, LA., Mao, XH., Nunez, G. and Thompson, CB. (1993). BCL-X, a BCL-2-related gene that functions as a dominant regulator of apoptotic cell-death. Cell 74, 4 : 597-608.

Boothe, JL. and Folk, JE. (1969) A reversible, calcium-dependent, copper-catalysed guinea pig liver transglutaminase. J Biol. Chem. 244 : 399-405. inactivation

Buttyan, R., Zakeri, Z., Lockshin, R. and Wolgemuth, D. (1988) Cascade induction of c-fos, c-myc and heat shock 70K transcripts during regression of the rat ventral prostate gland. Mol. Endocrinol., 2 : 650-657.

Buttyan, R., Olsson, C.A., Pintar, J., Chang, C., Bandyk, M., Ng, P-Y. and Sawczuk, IS. (1989) Induction of the TRPM-2 gene in cells undergoing programmed cell death. Mol. Cell. Biol., 9 : 3473-3481.

Caelles, C., Helmberg, A. and Karim, M. (1994). P53 dependent apoptosis in the absence of transcriptional activation of P53 target genes. Nature 370, 6486 : 220-223.

Cai, DB and DeLuca, LM. (1991) Retinoids induce tissue transglutaminase in NIH 3T3 cells. Biochem. Biophys. Res. Comm. 175 : 1119-1124.

Calabresse, C., Venturini, L., Ronco, G., Villa, P., Chomienne, C. and Belpomme, D. (1993) Butyric acid and its monosaccharide ester induce apoptosis in the HL-60 cell line. Biochem. Biophys. Res. Commun., 195 : 31-38.

Cascino, I., Fiucci, G., Papoff, G. and Ruberti, G. (1995). 3 Functional soluble forms of the Human apoptosis-inducing FAS molecule are produced by alternate splicing. J. Immunol 6 : 2706-2713.

Cerretti, DP, Kozlosky, CJ., Mosley, B., Nelson, N., Vanness, K., Greenstreet, TA., March, CJ., Kronheim, SR., Druck, T., Cannizzaro, LA., Huebner, K. and Black, RA. (1992). Molecular-cloning of the interleukin-1-beta converting enzyme. Science 256, 5053 : 97-100.

Chen, CY., Oliner, JD., Zhan, QM., Fornace, AJ., Vogelstein, B. and Kastan, MB. (1994) Interactions between P53 and MDM2 in a mammalian cell-cycle checkpoint pathway. Proc. Natl. Acad. Sci. USA 91, 7 : 2684-2688.

Chiocca EA., Davies, PJ. and Stein JP (1988) The molecular basis of retinoic acid action. J Biol Chem 263 : 11584 - 11589

Chittenden, T., Harrington, EA., O'Connor, R., Flemington, C., Lutz, RJ., Evan, GI. and Guild, BC. (1995). Induction of apoptosis by the BCL-2 homologue BAK. Nature 374, 6524 : 733-736.

Chomczynski, P. and Sacchi, N. (1987). Single-step method of RNA isolation by acid guanidinium thiocyanate-phenol-chloroform extraction. Anal. Biochem., 162 : 156-159.

Chung, SI. and Folk, JE. (1972). Transglutaminase from hair follicle of guinea pig. Proc Natl. Acad. Sci. USA 69, 2 : 303-307.

Chung, SI. (1975) Transglutaminases. In : Isoenzymes (Markert, C.C. ed.) Acad. Press N.Y. vol. 1, pp. 259-274.

Chung, YS., Song, IS., Erickson, RH., Sleisenger, MH. and Kim, YS. (1985) Effect of growth and sodium butyrate on brush border membrane-associated hydrolases in colorectal cancer cell lines. Cancer Res., 45 : 2976-2982, 1985.

Cifone, MG., De Maria, R., Roncaioli, P., Rippo, MR., Azuma, M., Lanier, LI., Santoni, A. and Testi, R. (1993). Apoptotic signalling through CD95 (FAS/APO I) activates an acidic sphingomyelinase. J. Exp. Med. 180, 4 :1547-1552.

Clarke, AR, Gledhill, S., Hooper, ML., Bird, CC. and Wyllie, AH. (1994). P53 dependence or early apoptotic and proliferative responses within the mouse intestinal epithelium following gamma-irradiation. Oncogene 9, 6 : 1767-1773.

Clarke, DD, Neidle, A., Sarkar, NK. and Waelsch, H. (1957) Transamidating enzymes. Arch. Biochem. Biophys. 71 : 277-279.

Clarke, DD, Mycek, MJ., Niedle, A. and Waelsch, H. (1959). The incorporation of amines into proteins. Arch. Biochem. Biophys. 79 : 338-354.

Cole. MD (1986). The MYC oncogene - its role in transformation and differentiation. Annu. Rev Gen. 20 : 361-384.

Compton, MM., Haskill, JS. and Cidlowski, JA. (1988) Analysis of gluco-corticoid actions on rat thymocyte deoxyribonucleic acid by fluorescence-activated flow cytometry. Endocrinology, 122 : 2158-2164.

Cotter, TG and Martin, SJ. (1990) Cell death via apoptosis and its relationship to growth development and differentiation of both tumour and normal cells. Anti-Cancer Res. 10 : 1153-1160.

D'Argenio, G., Sorrentini, I., Cosenza, V., Gatto, A., Iovino, P., D'Armiento, FP, Baldassarre, F. and Mazzacca, G. (1992) Serum and tissue transglutaminase correlates with the severity of inflammation in induced colitis in the rat. Scan. J. Gastroenterol., 27 : 111-114.

Datta, R., Manome, Y., Taneja, N., Boise, LH., Weichselbaum, R., Thompson, CB., Slapak, CA. and Kufe, D. (1995). Overexpression of BCL-X(L) by cytotoxic drug exposure confers resistance to ionising radiation-induced internucleosomal DNA fragmentation. Cell Growth Differ 6, 4 : 363-370.

Davies, PJA., Davies, DA., Levitzki, A., Maxfield, FR., Milhaud, P., Willingham, MC. and Pastan, IH. (1980) Transglutaminase is essential in receptor-mediated endocytosis of a_2-macroglobulin and polypeptide hormones. Nature, 283 : 162-167, 1980.

Davies, PJA., Murtaugh, MP, Moore, WT., Johnson, GS. and Lucas, D. (1985) Retinoic acid-induced expression of tissue transglutaminase in human promyelocytic leukaemia (HL60) cells. J. Biol. Chem. 260 : 5166-5174.

Davies, P.J.A., Nagy, L., Thomazy, V., Sobieski, M. and Chandraratna, R. (1993) Retinoid-regulated expression of tissue transglutaminase in apoptotic cells. Oral communication at The American Society for Cancer Research, Cell Death in Cancer and Development Meeting. Chatham, Massachusetts October 17-21, 1993.

De Caprio, JA., Ludlow, JW., Figge, J., Shew, JY., Huang, CM., Lee, WH., Marsilio, E., Paucha, E. and Livingston, DM. (1988). The JUN proto-oncogene is positively autoregulated by its product, JUN/AP-1. Cell 54, 2 : 275-283.

Dyson, JED., Daniel, J. and Surrey, CR. (1992) The effect of sodium butyrate on the growth characteristics of human cervix tumour cells. Br. J. Cancer, 65 : 803-808.

El-Alaoui, S., Mian, S., Lawry, J., Quash, G. and Griffin, M. (1992) Cell cycle kinetics, tissue transglutaminase and apoptosis. FEBS Lett. 331 : 2, 74-78.

El-Alaoui, S., Legastelois, S., Roch, A-M., Chantepie, J. and Quash, G. (1991) Transglutaminase activity and $N^{-e(g}$-glutamyl)lysine isopeptide levels during cell growth: An enzymatic and immunological study. Int. J. Cancer, 48 : 221-226.

El-Deiry, WS., Harper, JW., O'Connor, PM., Velculesco, VE., Canman, CE., Jackman, J., Pientenpol, JA., Burrel, M., Hill, DE., Wang, YS., Wiman, KG., Mercer, WE., Kastan, MB., Kohn, KW., Ellegdge, SJ., Kinzler, KW. and Vogelstein, B. (1994). WAF1/CIP1 is induced in P53-mediated G1 arrest and apoptosis. Cell 54, 5 : 1169-1174.

Ellis, HM and Horvitz, HR. (1986) Genetic control of programmed cell death in the nematode *C. elegans*. Cell, 44 : 817-829.

Ellis, RE, Yaun, JY. and Horvitz, HR. (1991). Mechanisms and functions of cell-death. Annu. Rev. Cell Biol. 7 : 663-698.

Estus, S., Zaks, WJ., Freeman, RS., Gruda, M., Bravo, R. and Johnson, EM. (1994). Altered gene-expression in neurones during programmed cell-death - identification of C-JUN as necessary for neuronal apoptosis. J. Cell Biol. 127, 6 part 1 :1717-1727.

Evan, GI, Wyllie, AH., Gilbert, CS., Littlewood, TD., Land, H., Brooks, M., Waters, CM., Penn, LZ. and Hancock, DC. (1992). Induction of apoptosis in fibroblasts by C-MYC protein. Cell 69, 1 : 119-128.

Evan, GI. (1994). Induction of apoptosis in fibroblasts by C-MYC protein. Philos. Trans. R. Soc. Lond. B. Biol. Sci. 345: 269-275.

Fan, SJ., El Dieiry, WS., Bae, I., Freeman, J., Jondle, D., Bhatia, K., Fornace, AJ., McGrath, I. and O'Connor, PM. (1994). P53 gene-mutations are associated with decreased sensitivity of Human lymphoma-cells to DNA-damaging agents. Cancer Res. 54, 22 : 5824-5830.

Fang, W., Rivard, JJ., Mueller, DL. and Behrens, TW. (1995). Cloning and molecular characterisation of mouse BCL-X in B-lymphocytes and T-lymphocytes. J. Immunol. 153, 10 : 4388-4398.

Farrow, SN., White, JHM, Martinou, I., Raven, T., Pun, KT., Gringham, CJ., Martinou, JC. and Brown, R. (1995). Cloning of the BCL-2 homologue by interaction with adenovirus E1B 19K. Nature 374, 6524 : 731-733.

Fernandes-Alnemri, T., Litwack, G. and Alnemri, ES. (1994). CPP32, a novel Human apoptotic protein with homology to *Caenorhabditis elegans* cell-death protein CED-3 and mammalian interleukin-1-beta-converting enzyme. J. Biol. Chem. 269, 49 : 30761-30764.

Fesus, L., Thomazy, V. and Falus, A. (1987) Induction and activation of tissue transglutaminase during programmed cell death. FEBS Lett., 224 : 104-108.

Fesus, L., Thomazy, V., Autuori, F., Ceru, MP, Traces, E. and Piacentini, M. (1989) Apoptotic hepatocytes become insoluble in detergents and chaotrophic agents as a result of transglutaminase action. FEBS Lett., 245 : 150-154.

Fesus, L., Madi, A., Balajthy, Z., Nemes, Z. and Szondy, Z. (1997) Transglutaminase induction by various cell death pathways. Experientia. 52 : 942-949.

Folk, JE. and Cole, PW. (1966)) Mechanism of action of guinea pig liver transglutaminase. Purification and properties of the enzyme; identification of a functional cysteine essential for activity. J Biol. Chem. 241 ; 5518-5525.

Folk, JE., Cole, PW. and Mullooly, JP. (1967) Mechanism of action of guinea pig liver transglutaminase. The metal-dependent hydrolysis of p-nitrophenyl acetate; further observations on the role of metal in enzyme activation. J Biol. Chem. 242 : 2615-2621.

Folk, JE and Finlayson, JE (1977) A general reaction and distribution of transglutaminases. Adv. Prot. Chem. 31 : 1-133

Folk, JE (1980) Transglutaminases . Annu. Rev. Biochem. 49 : 517-531.

Fraij, BM., Birckbichler, PJ., Patterson, MK., Lee, KN. and Gonzales, R.A. (1992) A retinoic acid-inducible mRNA from human erythroleukaemia cells encodes a novel tissue transglutaminase homologue. J. Biol. Chem., 267 : 22616-22623.

Gagliardini, V., Fernandez, PA., Lee, RKK., Drexler, HCA., Rotello, RJ., Fishman, MC. and Yuan, JY. (1994). Prevention of vertebrate neuronal death by the crmA gene. J. Biol. Chem. 263, 5148 : 826-828.

Gentile, V., Saydak, M., Chiocca, EA., Akande, N., Birckbichler, PJ., Lee, KN., Stein, JP and Davies, P.J.A. (1991) Isolation and characterisation of cDNA clones to mouse macrophage and human endothelial cell tissue transglutaminases. J. Biol. Chem. 266 : 478-483.

Gentile, V., Davies, PJA. and Baldini, A. (1994) The human tissue transglutaminase gene maps on chromosome 20q12 by in situ fluorescence hybridisation. Genomics. 20 (2) : 295-297.

Girardi, AJ, Weinstein, D. and Moorhead, PS (1966) SV_{40} Transformation of human diploid cells. Ann. Med. Expl. Biol. Fenniae Helsinki, 44 : 242-254.

Goldberg, YP., Learner, VD. and Parker, MI. (1992) Elevation of large T-antigen by sodium butyrate on SV40-transformed WI38 fibroblasts. J Cell Biochem. 49 : 74-81.

Gonzalez-Garcia, M., Perez-Ballestero, R., Ding, LY., Duan, L., Boise, LH., Thompson, CB. and Nunez, G. (1994). BCL-X(L) is the major BCL-X messenger-RNA form expressed during murine development and its product localises to mitochondria. Development 120, 10 : 3033-3042.

Gooding, LR., Ranheim, TS., Tollefson, AE., Aquino, L. Duerksen-Hughes, P., Horton, TM. and Wold, WSM. (1991). The 10,400-Dalton and 14,500-Dalton proteins encoded by region E3 of adenovirus function together to protect many but not all mouse-cell lines against lysis by tumour-necrosis-factor. J. Virol. 65, 8 : 4114-4123.

Gorman, JJ. and Folk, JE. (1984) Structural features of glutamine substrates for transglutaminases : Specificities of human plasma factor XIIIa and the guinea pig liver enzyme toward synthetic peptides. J Biol. Chem. 259 : 9007-9010.

Gotz, C. and Montenarh, M. (1995). P53 and its implication in apoptosis (review). Int. J. Oncology 6, 5 : 1129-1135.

Gotz, C. and Montenarh, M. (1996). P53 - DNA-damage, DNA-repair and apoptosis. Revs. Physiol. Biochem. and Pharmacol. 127 : 65-95.

Greenberg, M. and Ziff, E. (1984). Stimulation of 3T3 cells induces transcription of the C-FOS proto-oncogene. Nature 311 5985 : 433-438.

Griffin, M., Knight, C.R.L., Rees, RC and Elliott, BM. (1989). Transglutaminase, tumour growth and metastasis. Biochem. Soc. Trans. 17, 4 : 714-715.

Hague, A., Manning, A.M., Hanlon, KA., Huschtscha, LI., Hart, D. and Paraskeva, C. (1993) Sodium butyrate induces apoptosis in human colonic tumour cell lines in a p53-independent pathway: Implications for the possible role of dietary fibre in the prevention of large-bowel cancer. Int. J. Cancer, 55 : 498-505.

Haldar, S., Jena, N. and Croce, CM. (1995). Inactivation of BCL-2 by phosphorylation. Proc. Natl. Acad. Sci. (USA) 92, 10 : 4307-4511.

Halgunset, J., Lamvik, T. and Espevik, T. (1988) Butyrate effects on growth, morphology, and fibronectin production in PC-3 prostatic carcinoma cells. The Prostate, 12 : 65-77.

Hanada, M., Aimesempe, C., Sato, T. and Reed, JC. (1995). Structure-function analysis of BCL-2 protein identification of conserved domains important for homodimerization with BCL-2 and Heterodimerization with BAX. J. Biol. Chem. 270, 20 :11962-11969.

Hand, D., Elliott, BM., Rees, RC and Griffin, M. (1987) Correlation of changes in transglutaminase activity and polyamine content of neoplastic tissue during the metastatic process. Biochim. Biophys. Acta, 930 : 432-437.

Hand, D., Elliott, BM. and Griffin, M. (1988). Expression of cytosolic and particulate forms of transglutaminase during chemically-induced rat-liver carcinogenesis. Biochem. et Biophys. Acta 970, 2 : 137-145.

Hand, D., Knight, C.R.L. and Griffin, M. (1990) Characterisation of the cellular substrates for transglutaminase in normal liver and hepatocellular carcinoma. Biochim. Biophys. Acta, 1033 : 57-64.

Harper, JW, Adami, GR., Wei, N., Keyomarsi, K. and Elledge, SJ. (1993). The P21 cdk-interacting protein CIP1 is a potent inhibitor of G1 cyclin dependent kinases. Cell 75, 4 : 805-816.

Haupt, Y., Rowan, S., Shaulian, E., Vousden, KH. and Oren, S. (1995). Induction of apoptosis in HELA-cells by transactivation deficient P53. Genes Dev. 9, 17 : 2170-2183.

Hawkins, CJ and Vaux, DL. (1994). Analysis of the role of BCL-2 in apoptosis. Immunol. Rev. 142 :127-139.

Hayflick, L. and Moorhead, PS (1961) The serial cultivation of human diploid cell strains. Exp. Cell Res., 25 : 585-621.

Heyman, R.A., Cesario, R., McClurg, M. and Lamph, WW (1993) Retinoid receptors, ligand specificity and cell death. Poster communication (A-33) at The American Society for Cancer Research, Cell Death in Cancer and Development Meeting. Chatham, Massachusetts October 17-21, 1993.

Ho, KC., Quarmby, VE., French, FS. and Wilson, EM. (1992) Molecular cloning of rat prostate transglutaminase cDNA: The major androgen-regulating protein-DPI of rat dorsal prostate and coagulating gland. J Biol. Chem. 267 : 12660-12667.

Hockenberry, DM, Nunez, G., Milliman, C., Schreiber, RD and Korsmeyer, SJ (1990) Bcl-2 is an inner mitochondrial membrane protein that blocks programmed cell death. Nature, 348 : 334-336.

Hockenberry, DM, Zutter, M., Hickey, W., Nahm, M. and Korsmeyer, SJ (1991) Bcl-2 protein is topographically restricted in tissues characterised by apoptotic cell death. Proc. Natl. Acad. Sci. USA, 88, 16 : 6961-6965.

Ichinose, A., Hendricksen, LE., Fujikawa, K. and Davie, EW. (1986) Amino acid sequence of the a-subunit of human factor XIII. Biochemistry 25 : 6900-6906.

Ichinose, A., Bottenus, RE. and Davie, EW. (1990) Structure of transglutaminases. J Biol. Chem. 265 : 13411-13414.

Ikura, K., Nasu, T., Yokota, H., Tsuchiya, Y., Sasaki, R. and Chiba, H. (1988) Amino acid sequence of guinea pig liver transglutaminase from its cDNA sequence. Biochemistry 27 : 2898-2905.

Ikura, K., Yokota, H., Sasaki, R. and Chiba, H. (1989) Determination of amino and carboxyl-terminal sequences of guinea pig liver transglutaminase: Evidence for amino-terminal processing. Biochemistry 28 : 2344-2348.

Ikura, K., Tsuchiya, Y., Sasaki, R. and Chiba, H. (1990) Expression of guinea pig liver transglutaminase cDNA in E. coli : Amino-terminal N-acetyl group is not essential for catalytic function of transglutaminase. Eur. J Biochem. 187 : 705-711.

Itoh, N. and Nagata, S. (1993). A novel protein domain required for apoptosis - mutational analysis of Human FAS antigen. J. Biol. Chem. , 15 : 10932-10937.

Itoh, N., Yonehara, S., Ishi, A., Yonehara, M., Mizushima, S., Sameshima, M., Hase, A., Seto, Y. and Nagata, S. (1991). The polypeptide encoded by the cDNA for Human cell-surface antigen FAS can mediate apoptosis. Cell 66, 2 : 233-243.

Johnson, TS., Knight, CRL., El-Alaoui, S., Mian, S., Rees, RC., Gentile, V., Davies, PJA. and Griffin, M. (1994) Transfection of tissue transglutaminase into a highly malignant hamster fibrosarcoma leads to a reduced incidence of primary tumour growth. Oncogene 9 : 2935-2942.

Johnson, TS, Griffin, M, Thomas, GL, Yang, B, Skill, J, Cox, A, Nicholas, Birckbichler, PJ, B, Kubara, C, El Nahas, AM. (1997) The role of transglutaminase in the rat subtotal nephrectomy model of kidney fibrosis. J Clinical Investigation 99,12:2950-2960.

Kamech, N., Hill, A-M. and Seif, R. (1986) Butyrate converts rat 3T3 fibroblasts into giant cells. Exp. Cell Res. 162 : 326-334.

Kannagi, R., Teshigawara, K., Noro, N. and Masuda, T. (1982) Transglutaminase activity during the differentiation of macrophages. Biochem. Biophys. Res. Comm. 105 : 164-171.

Kaufmann, SH., Desnoyers, S., Ottaviano, Y., Davidson, NE. and Poirier, OF. (1993). Specific proteolytic cleavage of poly(ADP-ribose) polymerase - An early marker of chemotherapy-induced apoptosis. Cancer Res. 53, 17 : 3976-3985.

Kerr, JFR., Wyllie, AH. and Currie, AR (1972) Apoptosis: A basic biological phenomenon with wide ranging implications in tissue kinetics. Br. J. Cancer, 26 : 239.

Kiefer, MC, Brauer, MJ., Powers, VC., Wu, JJ., Umansky, SR., Tomei, LD. and Barr, PJ. (1995). Modulation of apoptosis by the widely distributed homologue BAK. Nature 374, 6524 : 736-739.

Kim, I-G., Gorman, JJ., Park, S-C., Chung, S-I. and Steinhart, PM. (1993) The deduced sequence of the novel protransglutaminase E (TGase 3) of human and mouse. J Biol. Chem. 268 : 12682-12690.

Kim, YS, Tsao, D., Siddiqui, B., Whitehead, JS, Arnstein, P., Bennett, J. and Hicks, J. (1980) Effects of sodium butyrate and dimethylsulfoxide on biochemical properties of human colon cancer cells. Cancer 45 : 1185-1192.

Knight, C.R.L., Rees, RC and Griffin, M. (1991) Apoptosis: a potential role for cytosolic transglutaminase and its importance in tumour progression. Biochim. Biophys. Acta, 1096 : 312-318.

Knight, C.R.L., Hand, D., Piacentini, M. and Griffin, M. (1993) Characterisation of the transglutaminase-mediated large molecular weight polymer from rat liver; its relationship to apoptosis. Eur. J. Cell Biology 60 : 210-216.

Kojima, S., Nara, K. and Rifkin, DB. (1993) Requirement for transglutaminase in the activation of latent transforming growth factor beta in bovine endothelial cells. J Cell Biol. 121 : 439-448.

Korsmeyer, SJ, Shutter, JR., Veis, DJ., Merry, DE. and Oltvai, ZN. (1993). BCL-2/BAX - A rheostat that regulates an antioxidant pathway and cell-death. Semin. Cancer Biol. 4, 6 : 327-332.

Kozopas, KM, Yang, T., Buchan, HL., Zhou, P. and Craig, RW. (1993). MCL1, A gene expressed in programmed myeloid-cell differentiation, has a sequence similar to BCL2. Proc. Natl. Acad. Sci. (USA) 90, 8 : 3516-3520.

Krajewski, S., Krajewska, M., Shabaik, A., Wang, HG., Irie, S., Fong, L. and Reed, JC. (1994). Immunohistochemical analysis of *in vivo* patterns of BCL-x expression. Cancer Res. 54, 21 : 5501-5507.

Kruh, J. (1982) Effects of sodium butyrate, a new pharmacological agent, on cells in culture. Mol. Cell. Biochem., 42 : 65-82.

Kruh, J., Defer, N. and Tichonicky, L. (1992) Action moleculaire et cellulaire du butyrate. C.R. Soc. Biol., 186 : 12-25.

Kumar, S., Kinoshita, M., Noda, M., Copeland, NG. and Jenkins, NA. (1994). Induction of apoptosis by the mouse NEDD2 gene, which encodes a protein similar to the product of the *C.elegans* cell-death gene CED-3 and the mammalian IL-1-beta-converting enzyme. Genes Dev. 8, 14 : 1613-1626.

Kyprianou, N., English, HF., Davidson, NE and Isaacs, JT. (1991) Programmed cell death during regression of the MCF-7 human breast cancer following oestrogen ablation. Cancer Res., 51 : 162-166.

Laemmli, U.K. (1970) Polyacrylamide gel electrophoresis of proteins. Nature 227 : 680-685.

Lane, DP and Crawford, LV, 1979. Cell cycle controls. Nature. 278: 261-263.

Larsen, CJ, Seite, P., Hillion, J., Dagay, MF. and Berger, R. (1993). Some recent aspects of the molecular biology of Human lymphoma. Nouvelle Revue Francaise D'Hematologie. 35, 1 : 37-40.

Lazebnik, YA., Kaufman, SH., Desnoyers, S., Poirier, GG. and Earnshaw, WC. (1994). Nature 371, 6495 : 346-347.

Le Gouy, E., DePinho, R., Zimmerman, K., Collum, R., Yancopoulos, G., Mitsock, L., Kriz, R. and Alt, FW. (1987). Structure and expression of the murine L-MYC gene. EMBO J. 6, 11 : 3359-3366.

Lee, KN., Birckbichler, PJ and Fesus, L. (1986) Purification of human erythrocyte transglutaminase by immunoaffinity chromatography. Prep. Biochem. 16 : 321-335.

Lee, KN., Birckbichler, PJ, Patterson, MK., Jr., Conway, E. and Maxwell, M. (1987) Induction of cellular transglutaminase biosynthesis by sodium butyrate. Biochim. Biophys. Acta 928 : 22-28.

Lee, KN., Birckbichler, PJ and Patterson, MK., Jnr. (1989) GTP hydrolysis by guinea pig liver transglutaminase. Biochem et Biophys. Res. Comm. 162, : 3, 1370-1375.

Lee, KN., Maxwell, MD, Patterson, MK., Jr., Birckbichler, PJ and Conway, E. (1992) Identification of Transglutaminase Substrates in HT29 Colon Cancer Cells : Use of 5-(Biotinamido)pentylamine as a Transglutaminase-specific Probe. Biochim. Biophys. Acta 1136 : l2-l6.

Lee, KN., Arnold, SA., Conway, E., Maxwell, MD, Patterson, MK., Jnr., Carter, H. and Birckbichler, PJ (1993) Site-directed mutagenesis of human tissue TGase cys-277 is essential for catalytic activity but not for GTPase activity. Biochem. et Biophys. Acta 1202 : 1-6.

Leu, RW, Herriott, MJ, Moore, PE, Orr, GR. and Birckbichler, PJ (1982) Enhanced transglutaminase activity associated with macrophage activation. Possible role in Fc-mediated phagocytosis. Exp. Cell Res., 141 : 191-199.

Lorand, L., Downey, J., Gotoh, T., Jacobson, A. and Tokura, S. (1968). The transpeptidase system which crosslinks fibrin by g-glutamyl-e-lysine bonds. Biochem et Biophys Res. Comm. 31, 2 : 222-230.

Lorand, L., Campbell-Wilkes, LK. and Cooperstein, L. (1972) A filter paper assay for transamidating enzymes using radioactive amine substrates. Anal. Biochem., 59 : 623-631.

Lorand, L. and Stenberg, P. (1976) In: Handbook of biochemistry and molecular biology (Fasman, GD. ed.) C.R.C. Press, Cleveland, vol. 2, pp 669-685.

Lorand, L. and Conrad, SM. (1984) Post-translation modifications of proteins. Mol. Cell Biochem. 58 : 9-35.

Lorand. L. (1988) Transglutaminase-mediated cross-linking of proteins and cell ageing: the erythrocyte and lens models. Adv. Expl. Med. Biol., 231 : 79-94.

Lowry, OH, Rosebrough, NJ., Farr, AL and Randall, RJ (1951) Protein measurement with the folin reagent. J. Biol Chem. 193 : 265-275.

Lu, X., Walker, T., MacManus, JP and Seligy, VL. (1992) Differentiation of HT-29 human colonic adenocarcinoma cells correlates with increased expression of mitochondrial RNA: Effects of trehalose on cell growth and maturation. Cancer Res., 52 : 3718-3725.

Lynch, DH, Watson, ML., Alderson, MR., Baum, PR., Miller, RE., Tough, T., Gibson, M., Davis-Smith, T., Smith, CA., Hunter, K., Baht, D., Din, W., Goodwin, RG. and Seldin, MF. (1994). The mouse FAS-ligand gene is mutated in GLD mice and is part of a TNF family gene-cluster. Immunity 1, 2 : 131-136.

Mc.Conkey, DJ, Nicotera, P., Hartzell, P., Bellomo, G., Wyllie, AH and Orrenius, S. (1989) Glucocorticoids activate a suicide process in thymocytes through an elevation of cytosolic Ca^{2+} concentration. Arch. Biochem. Biophys., 269 : 365-370.

Mc.Conkey, DJ, Orrenius, S. and Jondal, M. (1990) Cellular signalling in programmed cell death (apoptosis). Immunol. Today, 11 : 120-121.

Maddox, A.M. and Haddox, MK. (1988) Characteristics of cyclic AMP enhancement of retinoic acid induction of increased transglutaminase activity in HL60 cells. Expl. Cell Biol. 56 : 49-59.

Maniatis, T., Fritsch, E., and Sambrook, J. (1987) Molecular Cloning: A laboratory manual. 2nd. Edition. Cold Spring Harbor laboratory Press. pp 6.15.

Martin, SJ, Bonham, A.M. and Cotter, TG (1990) The involvement of RNA and protein synthesis in programmed cell death (apoptosis) in human leukaemia HL-60 cells. Biochem. Soc. Trans., 18 : 634-636.

Matacic, S. and Loewy, AG. (1968) Identification of isopeptide crosslinks in insoluble fibrin. Biochem. Biophys. Res. Commun. 30 : 356-362.

Mehta, K. (1990) Significance of transglutaminase-catalysed reactions in growth and development of filarial parasite *Brugia malagi*. Biochem et Biophys Res. Comm. 173 : 3, 1051-1057.

Melion, G., Annicchiarico-Petruzzelli, M., Piredda, L., Candi, E., Gentile, V., Davies, PJA. and Piacentini, M. (1994) Tissue transglutaminase and apoptosis: Sense and antisense transfection studies with human neuroblastoma cells. Molec. and cell Biol. 14 : 6584-6596.

Mian, S., El-Alaoui, S., Lawry, J., Gentile, V., Davies, PJA. and Griffin. (1995) The importance of the GTP-binding protein tissue transglutaminase in the regulation of cell cycle progression. FEBS Letts. 370 : 27-31.

Mitchell, PJ, Wang, C. and Tjian, R. (1987). Positive and negative regulation of transcription *in vitro* - enhancer-binding protein-AP-2 is inhibited by SV40 T-antigen. Cell 50, 6 : 847-861.

Miura, M., Zhu, H., Rotello, R., Hartwieg, EA. and Yuan, JY. (1993). Induction of apoptosis in fibroblasts by IL-1-beta-converting enzyme, a mammalian homologue of the *C.elegans* cell-death gene CED-3. Cell 75, 4 : 653-660.

Miyashita, T., Krajewski, S., Krajewska, M., Wang, HG., Lin, HK., Liebermann, DA., Hoffman, B. and Reed, JC. (1994). Tumour-suppressor P53 is a regulator of BCL-2 and BAX gene-expression *in vitro* and *in vivo*. Oncogene 9, 6 : 1799-1805.

Miyashita, T. and Reed, JC (1995). Tumour-suppressor P53 is a direct transcriptional activator of the Human BAX gene. Cell 80, 2 : 293-299.

Moore, WT., Murtaugh, MP. and Davies, PJA. (1984) A retinoic acid induced expression of tissue transglutaminase in mouse peritoneal macrophages. J. Biol. Chem. 259 : 12794-12804.

Muesch, A., Hartmann, E., Rohde, K., Rubartelli, A., Sitia, R. and Rapoport, TA. (1990) A novel pathway for secretory proteins? TIBS 15 : 86-88.

Muller. R. (1986). Cellular and viral FOS genes - Structure, regulation of expression and biological properties of their encoded products. Biochim. Biophys. Acta 823, 3 : 207-225.

Munday, NA., Vallincourt, JP., Ali, A., Casano, FJ., Miller, DK., Molineaux, SM., Yamin, TT., Yu, VL. and Nicholson, DW. (1995). Molecular-cloning and pro-apoptotic activity of ICE(REL)II and ICE(REL)III, members of the ICE/CED-3 family of cysteine proteases. J. Biol. Chem. 270, 26 : 15870-15876.

Mycek, MJ, Clarke, DD, Neidle, A. and Waelsch, H. (1959). Amine incorporation into insulin as catalysed by transglutaminase. Arch. Biochem. Biophys. 84, 2 : 528-540.

Nagy, L., Thomazy, V., Sobieski, M. Chandraratna, R. and Davies, P.A. (1993) Retinoid induced changes in gene expression during differentiation and apoptosis in human myeloid leukaemia cell line (HL60). Poster communication (A-25) at The American Society for Cancer Research, Cell Death in Cancer and Development Meeting. Chatham, Massachusetts October 17-21, 1993.

Nakanishi, K., Nara, K., Hagiwara, H., Aoyama, Y., Ueno, H. and Hirose, S. (1991) Cloning and sequence analysis of cDNA clones for bovine aortic-endothelial-cell transglutaminase. Eur. J Biochem. 202 : 15-21.

Nakaoka, H., Perez, DM, Baek, KJ., Das, T., Husain, A., Misono, K., Im, M-J. and Graham, RM. (1994) G_h : A GTP-binding protein with transglutaminase activity and receptor signalling function. Science 264 : 1593-1596.

Nara, K., Nakabishi, K., Hagiware, H., Wakita, KI., Kojima, .S. and Hirose, S. (1989) Retinol induced morphological changes of cultured bovine endothelial cells are accompanied by a marked increase in transglutaminase. J. Biol. Chem. 264 : 19308-19312.

Nathan, DF., Burkhart, S. R., and Morin, MJ (1990) Increased cell surface EGF receptor expression during the butyrate- induced differentiation of human HCT-116 colon tumour cell clones. Exp. Cell Res., 190 :76-84.

Nau, MM., Brooks, BJ., Battey, J., Sausville, E., Gazdar, AF., Kirsch, IR., Mc.Bride, OW., Bertness, V., Hollis, GF. and Minna, JD. (1985). L-MYC, a new MYC-related gene amplified and expressed in Human small cell lung cancer. Nature 318, 6041 : 69-73.

Niedle, A., Mycek, MJ, Clarke, DD and Waelsch, H. (1958). Enzymic exchange of protein amide groups. Arch. Biochem. Biophys. 77, 1 : 227-229.

Nisen, P D., Zimmerman, KA., Cotter, SV., Gilbert, F. and Alt, FW. (1986). Enhance expression of N-MYC gene in Wilms-tumours. Cancer Res. 46, 12 : 6217-6222.

Nonaka, A. (1992) Transglutaminase produced by *Streptoverticillium* sp. : Its characteristics and capability in protein crosslinking. Oral Communication 2nd. Int. Conference on Transglutaminase and Protein Crosslinking Reactions, Ardmore, Oklahoma, U.S.A. 7-10th. June 1992.

Nunez, G., Seto, M., Sermeretis, S., Ferrero, D., Grignani, F., Korsmeyer, SJ. and Dallafavera, R. (1989). Growth-promoting and tumour-promoting effects of deregulated BCL2 in Human lymphoblastoid cells. Proc. Natl. Acad. Sci. (USA) 86, 12: 4589-45931.

Oehm, A., Behrman, I., Falk, W., Pawlita, M., Maier, G., Klas, C., Liweber, M., Richards, S., Dhein, J., Trauth, BC., Ponstingl, H and Krammer, PH. (1992). Purification and molecular-cloning of the APO-1 cell-surface antigen, a member of the tumour-necrosis-factor nerve growth-factor receptor superfamily - sequence identity with the FAS antigen. J. Biol. Chem. 267, 15 : 1070910715.

Ogasawara, T. (1995) J. Exp. Med. 181 : 485.

Oltvai, ZN, Milliman, CL. and Korsmeyer, SJ. (1993). BCL-2 heterodimerizes *in vivo* with a conserved homologue, BAX, that accelerates programmed cell death. Cell 74, 4 : 609-619.

Oltvai, ZN and Korsmeyer, SJ. (1994). Checkpoints of duelling dimers foil death wishes. Cell 79, 2 : 189-192.

Patterson, MK., Jr., Maxwell, MD, Birckbichler, PJ, Conway, E. and Carter, HA. (1982) Putrescine as a regulator of e(g-glutamyl)lysine isopeptide production and the proliferative state. Cell Biol. Int. Rep., 6 : 46l-470.

Peitsch, MC, Polzar, B., Stephan, H., Muller, C., Mannherz, HG and Tschopp, J. (1993) Characterisation of the endonuclease involved in DNA degradation in apoptosis. First International Meeting of the Hungarian Biochemical Society, Debrecen, Hungary. August 29th. to September 1st. 1993.

Persson, H., Hennighausen, L., Taub, R., DeGrado, W. and Leder, P. (1984). Antibodies to Human C-MYC oncogene product - evidence of an evolutionarily conserved protein-induced during cell-proliferation. Science 225, 4663 : 687-693.

Peterson, LL and Wuepper, KD. (1984). Epidermal and hair follicle transglutaminases and crosslinking in skin. Mol. Cell Biochem. 58, 1-2 : 99-111.

Pezzella, F., Tse, AGD., Cordell, JL., Pulford, KAF., Gatter, KC. and Mason, DY. (1990). Expression of the BCL2 oncogene protein is not specific for the 14-18 chromosomal transformation. Am. J. Pathol. 137, 2 : 225-232.

Phillips, MA., Stewart, BE., Qin, Q., Chakravarty, R., Floyd, EE., Jetten, AM. and Rice, RH. (1990) Primary structure of keratinocyte transglutaminase. Proc. Natl. Acad. Sci. USA. 87 : 9333-9337.

Piacentini, M. and Beninati, S. (1988). Gamma glutamylamine derivatives in isolated rat hepatocyte proteins. Biochem J. 249, 3 : 813-817.

Piacentini, M., Fesus, L., Farrace, MG, Ghibelli, L., Piredda, L. and Melino, G. (1991) The expression of 'tissue' transglutaminase in two human cancer cell lines is related with the programmed cell death. Eur. J. Cell Biol., 54 : 246-254.

Piacentini, M., Fesus, L. and Melino, G. (1993) FEBS Lett 320 : 150 - 154

Poon, M-C., Russell, JA., Low, S., Sinclair., Jones, AR., Blahey, W., Ruether, BA. and Hoar, DL. (1989) Hemopoietic origin of factor XIII a-subunits in platelets, monocytes and plasma. Evidence from bone marrow transplantation studies. J Clin. Invest. 84 : 787-792.

Pouillart, P., Cerutti, I., Ronco, G., Villa, P. and Chany, C. (1992) Enhancement by stable butyrate derivatives of anti-tumour and anti-viral actions of interferon. Int. J. Cancer, 51 : 596-601.

Rauscher III, FJ., Cohen, DR., Curran, T., Bos, TJ., Vogt, PK., Bohmann, D., Tjian, R. and Franza, BR. (1988). FOS-associated protein P39 is the product of the JUN proto-oncogene. Science 240, 4855 : 1010-1016.

Reed, JC, Haldar, S., Croce, CM. and Cuddy, MP. (1990). Complementation by BCL2 and C-HA-RAS oncogenes in malignant transformation of rat embryo fibroblasts. Mol. Cell. Biol. 10, 9 : 4370-4374.

Reed, JC, Talwar, HS., Cuddy, M., Baffy, G., Willamson, J., Raff, UR. and Fisher, GJ. (1991). Mitochondrial protein P26 BCL2 reduces growth factor requirements of NIH3T3 fibroblasts. Exp. Cell. Res. 195, 2 : 277-283.

Rice, RH. and Green, H. (1978) Relation of protein synthesis and transglutaminase activity to formation of the cross-linked envelope during terminal differentiation of cultured human epidermal keratinocytes. J. Biol. Chem. 76 : 705-711.

Rice, RH. and Green, H. (1979). Presence in Human epidermal cells of a soluble protein precursor of the cross-linked envelope - activation of crosslinking by calcium ions. Cell 18, 3 : 681-694.

Rice, RAH., Rong, X. and Chakravarty, R. (1990) Proteolytic release of keratinocyte transglutaminase. Biochem J. 265 : 351-357.

Roberts, AB and Sporn, MB (1984) in "The Retinoids" Goodman, DS Ed. Academic Press, New York. vol 2, 210-286.

Rocchi, P., Ferreri, A.M., Simone, G., Granchi, D., Paolucci, P., and Paolucci, G. (1992) Growth inhibitory and differentiating effects of sodium butyrate on human neuroblastoma cells in culture. Anticancer Res., 12 : 917-920.

Roch, A-M., Noel, P., El-Alaoui, S., Charlot, C. and Quash, G. (1991) Differential expression of isopeptide bonds N^{e}(g-glutamyl)lysine in benign and malignant human breast lesions: An immunological study. Int. J. Cancer, 48 : 215-220.

Rouvier, E., Luciani, MF. and Goldstein, P. (1993). FAS involvement in Ca^{2+} - independent T-cell-mediated cytotoxicity. J. Exp. Med. 177, 1 :195-200.

Rowe, WA. and Bayless, TM (1992) Colonic short-chain fatty acids: Fuel from the lumen? Gastroenterology, 103 : 336-339.

Rubin, E., Kharbanda, S., Gunji, H. and Kufe, D. (1991) Activation of the c-jun proto-oncogene in human myeloid leukaemia cells treated with etoposide. Mol. Pharmacol., 39 : 697-901.

Sarkar, NK., Clarke, DD and Waelsch, H. (1957) Transamidating enzymes. Biochim. et Biophys. Acta 25 : 451-452.

Sassone-Corsi, P., Lamph, WW., Kamps, M. and Verma, IM. (l988). FOS -associated cellular P39 is related to nuclear transcription factor-AP-1. Cell 54, 4 : 553-560.

Savill. J, Fadok, V., Henson, P. and Haslett, C. (1993) Phagocyte recognition of cells undergoing apoptosis. Immunol. Today 14 : 131-136.

Savill, J., Mooney, A. and Hughes, J. (1996) Apoptosis and renal scarring. Kid. Int. 49 : suppl 54, 14-17.

Scheppach, W., Sommer, H., Kirchner, T., Paganelli, G-M., Bartram, P., Christi, S., Richter, F., Dusel, G. and Kasper, H. (1992) Effect of butyrate enemas on the colonic mucosa in distal ulcerative colitis. Gastroenterology, 103 : 51-56.

Schlingensiepen, KH, Wollnik, F., Kunst, M, Schlingensiepen, R., Herdegen, T. and Brysch, W. (1994). The role of JUN transcription factor expression and phosphorylation in neuronal differentiation, neuronal cell-death and plastic adaptations *in vivo*. Cell. Mol. Neurobiol. 14, 5 : 417-505.

Schroff, G., Neuman, C. and Sorg, C. (1981) Transglutaminase as a marker for subsets of murine macrophages. Eur. J. Immunol., 11 : 637-642.

Schwartzman, R.A. and Cidlowski, JA. (1993) Apoptosis: The biochemistry and molecular biology of programmed cell death. Endocrine. Rev., 14 : 133-151.

Seitz, J., Keppler, C., Rausch, U. and Aumuller, G. (1990) Immunohistochemistry of secretory transglutaminase from rodent prostate. Histochemistry 93 : 525-530.

Seitz, J., Keppler, C., Huntemann, S., Rausch, U. and Aumuller, G. (1991) Purification and characterisation of secretory transglutaminase from the coagulating gland of the rat. Biochim. Biophys. Acta 1078 : 139-146.

Selkoe, DJ, Abraham, C. and Ihara, Y. (1982) Brain transglutaminase: *In vitro* crosslinking of human neurofilament proteins into insoluble polymers. Proc. Natl. Acad. Sci. USA, 79 : 6070-6074.

Sentman, CL, Shutter, JR, Hockenberry, D., Kanagawa, O. and Korsmeyer, SJ (1991) Bcl-2 inhibits multiple forms of apoptosis but not negative selection in thymocytes. Cell, 67 : 879-888.

Shainoff, JR., Urbanic, DA. and Di Bello, PM. (1991) Immunoelectrophoretic characterisation of the cross-linking of fibronectin and fibrin by factor XIIIa and tissue transglutaminase. J Biol. Chem. 266 : 6429-6437.

Sheng, DQ., Vayessiere, JL., Petit, PX., Le Coeur, H., Spatz, A., Mignotte, B. and Feunteun, J. (1994). Apoptosis is antagonised by large T-antigens in the pathway to immortalization by poliomaviruses. Oncogene 9, 11 : 3345-3351.

Silverman, GA., Yang, E., Proffitt, JH., Zutter, M. and Korsmeyer, SJ. (1993). Genetic transfer and expression of reconstructed yeast artificial chromosomes (YACS) containing normal and translocated BCL-2. Mol. Cell. Biol. 13, 9 : 5469-5478.

Smethurst, PA. and Griffin, M. (1996) Measurement of tissue transglutaminase activity in a permeabilised cell system ; its regulation cy Ca^{2+} and nucleotides. Biochem. J 313 : 803-808.

Steinman, HM (1995). The BCL-2 oncoprotein functions as an prooxidant. J. Biol. Chem. 270, 8 : 3487-3490.

Strasser, A., Harris, AW., Jacks, T. and Cory, S. (1994). DNA-damage can induce apoptosis in proliferating lymphoid-cells via P53-independent mechanisms inhibited by BCL-2. Cell 79, 2 : 329-339.

Suda, T., Takahashi, T., Goldstein, P. and Nagata, S. (1993). Molecular-cloning and expression of the FAS ligand Cell 7, 6 : 1169-1178.

Suedhoff, T., Birckbichler, PJ, Lee, KN., Conway, E. and Patterson, MK., Jr. (1990) Differential Expression of Transglutaminase in Human Erythroleukaemia Cells in Response to Retinoic Acid. Cancer Res. 50 : 7830-7834.

Swezy, DE. and Epel, D. (1992) in Guide to electroporation and electrofusion. (Chang, DC., Chassy, BM., Saunders, JA. and Sowers, AE. eds.) pp. 347-362. Academic Press, London.

Takahashi, N., Takahashi, Y. and Putnam, FW. (1986) Primary structure of blood coagulation factor XIIIa (fibrinoligase, transglutaminase) from human placenta. Proc. Natl. Acad. Sci. USA. 83 : 8019-8023.

Takakashi, T., Tanaka, M., Brannan, CI., Jenkins, NA., Copeland, NG., Suda, T. and Nagata, S. (1994). Generalised lymphoproliferative disease in mice, caused by a point mutation in the FAS ligand. Cell 76, 6 : 969-976.

Takeuchi, Y., Birckbichler, PJ., Maxwell, MD., Howell, B., Carter, H. and Patterson, MK. (1992)

Tanaka, Y., Yoshihara, K., Itaya, A., Kamiya, T. and Koide, SS. (1984). Mechanism of the inhibition of Ca^{2+}, and Mg^{2+} - dependent endonuclease of bull seminal plasma induced by ADP-ribosylation. J. Biol. Chem. 259, 10 : 6579-6585.

Tanaka, M., Suda, T., Takahashi, T. and Nagata, S. (1995). Expression of the soluble form of the Human FAS ligand in activated lymphocytes. EMBO J. 14, 6 : 1129-1135.

Tartaglia, :LA., Ayres, TM., Wong, WHG. and Goeddel, DV. (1993).. A novel domain within the 55 KDa TNF receptor signal cell-death. Cell , 5 : 845-853.

Thomas, GL., Henley, A., Rowland, T., Sahai, A., Griffin, M. and Birckbichler, PJ. (1996) Enhanced apoptosis in tansformed human lung fibroblasts after exposure to sodium butyrate. In Vitro Dev. Cell Biol. - Animal 32 : 505-513.

Thornberry, NA, Bull, HG., Calaycay, JR., Chapman, KT., Howard, AD., Kostura, MJ., Miller, DK., Molineaux, SM., Weidner, JR., Aunins, J., Elliston, KO., Ayala, JM., Cascano, FJ., Chin, J., Ding, GJF., Egger, LA., Gaffney, EP., Limjuco, G., Palyha, OC., Raju, SM., Rolando, AM., Salley, JP., Yamin, TT., Lee, TD., Shively, JE., Maccross, M., Mumford, RA., Schimidt, JA. and Tocci, MJ. (1992). A novel heterodimeric cysteine protease is required for interleukin-1-beta processing in monocytes. Nature 356, 6372 : 768 : 774.

Trauth, BC, Klas, C., Peters, AMJ., Matzku, S., Moller, P., Falk, W., De Bath, KM. and Krammer, PH. (1989). Monoclonal-antibody - mediated tumour regression by induction of apoptosis. Science 245, 4915 : 301-305.

Tsujimoto, Y. (1989). Stress-resistance conferred by high-level BCL2 - alpha protein in Human lymphoblastoid cell. Oncogene 4, 11 :1331-1336.

Upchurch, HF., Conway, E., Patterson, MK. and Maxwell, MD. (1992) Localisation of cellular transglutaminase on the extracellular matrix after wounding : Characteristics of the matrix bound enzyme. Am J Cell Physiol. 149 : 375-382.

Vaux, DL (1993). Toward an understanding of the molecular mechanisms of physiological cell-death. Proc. Natl. Acad. Sci. (USA) 90, 3 : 786-789.

Vaux, DL. and Strasser, A. (1996). The molecular biology of apoptosis. Proc. Natl. Acad. Sci. (USA) 93, 6 : 2239-2244.

Verma, IM and Graham, WR. (1987). The FOS oncogene. Adv. Cancer Res. 49 : 29-52.

Verma, IM and Sassone-Corsi, P. (1987). Proto-oncogene FOS - Complex but versatile regulation. Cell 51, 4 : 513-514.

Verma, IM (1986). Proto-oncogene FOS -A multifaceted gene. Trends Genet. 2, 4 : 93-96.

Vogt, PK., Bos, TJ. and Doolittle, RF. (1987). Homology between the DNA-binding domain of the GCN4 regulatory protein of yeast and the carboxyl-terminal region of a protein coded for by the JUN oncogene. Proc. Natl. Acad. Sci. (USA) 84, 10 : 3316-3319.

Volm, M., Drings, P., Woodrich, W. and Vankaick, G. (1993). Expression of oncoproteins in primary Human nonsmall cell lung-cancer and incidence of metastases. Clin. Exp. Metastasis 11, 4 : 325-329.

Wagner, AJ, Small, MB. and Hay, N. (1993). MYC-mediated apoptosis is blocked by ectopic expression of BCL2. Mol. Cell. Biol. 13, 4 : 2432-2440.

Waldman, T., Kinzler, KW. and Vogelstein, B. (1995). P21 is necessary for P53-mediated G1 arrest in human cancer cells. Cancer Res. 54, 22 : 5187-5190.

Wang, L., Miura, M., Bergeron, L., Zhu, H. and Yuan, JY. (1994). ICH-1, an ICE/CED-3 related gene, encodes for both positive and negative regulators of programmed cell-death. Cell 78, 5 : 739-750.

Watanabe-Fukunaga, R., Brannan, CI., Itoh, N., Yonehara, S., Copeleand, NG., Jenkins, NA. and Nagata, S. (1992). The cDNA structure, expression and chromosomal assignment of the mouse FAS antigen. J. Immunol. 148, 4 : 1274-1279.

Weraarchakul-Boonmark, N., Jeong, JM., Murthy, SNP., Engel, JD. and Lorand, L. (1992) Cloning and expression of chicken erythrocyte transglutaminase. Proc. Natl. Acad. Sci. USA. 89 : 9804-9808.

Williams, GT. (1991) Programmed cell death: Apoptosis and oncogenesis. Cell 65 : 1097-1098.

Williams-Ashman, HG and Canellakis, ZN (1979) Transglutaminases in mammalian reproductive tissues and fluids. Perspect. Biol. Med. 22 : 421-453.

Williams-Ashman, HG, Beil, RE, Wilson, J., Hawkins, M., Grayhack, J., Zunamon, A. and Weinstein, NK. (1980) Transglutaminases in mammalian reproductive tissues and fluids: Relation to polyamine metabolism and semen coagulation. Adv. Enzyme Reg. 18 : 239-258.

Wilson, EM. and French, FS. (1980) Biochemical homology between rat dorsal prostate and coagulating gland. J Biol. Chem. 255 : 10946-10953,

Wiseberg, LJ., Shiu, DT., Conkling, PR. and Shuman, MA. (1987) Identification of normal peripheral blood monocytes and liver as sites of synthesis of coagulation factor XIII a-chain. Blood 70 : 579-582.

Wong, DWS., Batt, C.A. and Kinsella, JE (1991) Expression of the transglutaminase gene in *E.coli*. Int. J. Biochem. 23 : 9, 947-953.

Wyllie, AH (1980) Glucocorticoid-induced thymocyte apoptosis is associated with endogenous endonuclease activation. Nature, 284 : 555-556.

Wyllie, AH, Kerr, JFR and Currie, AR (1980) Cell death: The significance of apoptosis. Int. Rev. Cytol., 68 : 251-306.

Wyllie, AH (1981) Cell death: a new classification separating apoptosis from necrosis. In: ID Bowden and R.A. Lockshin (eds.), Cell Death in Biology and Pathology, pp 9-34. London: Chapman & Hall, 1981.

Wyllie, AH (1987) Apoptosis. Int. Rev. Cytol. 17 :755-785.

Xiong, Y., Hannon, GJ., Zhang, H., Casso, D., Kobayashi, R. and Beach. (1993) P21 is a universal inhibitor of cyclin kinases. Nature 366, 6456 : 701-770.

Yonehara, S., Ishi, A. and Yonehara, M. (1989). A cell-killing monoclonal antibody (Anti-FAS) to a cell-surface antigen co-downregulating with the receptor of tumour necrosis factor. J. Exp. Med. 169, 5 : 1747.

Yoshihara, K., Yoshinori, T. and Koide, SS. (1975). Evidence for adenosine diphosphate ribosylation of Ca^{2+} and Mg^{2+} - dependent endonuclease. Proc. Natl. Acad. Scl. (USA) 72, 1 : 289-293.

Younish-Rouach, E., Resnitzky, D., Loten, J., Sachs, L., Kimchi, A. and Oren, M. (1991) Wild-type p53 induces apoptosis of myeloid leukaemia cells that is inhibited by interleukin-6. Nature, 352 : 345-347.

Yuan, JY., Shaham, S., Le Doux, S., Ellis, HM. and Horvitz, HR. (1993). The *C. elegans* cell-death gene CED-3 encodes a protein similar to mammalian IL-1-beta-converting enzyme. Cell 75: 641-652.

Yuh, Y-S. and Thompson, EB. (1989) Gluco-corticoid effect on oncogene/growth gene expression in human T lymphoblastic cell line CCRF-CEM. Specific c-myc mRNA suppression by dexamethasone. J. Biol. Chem., 264 : 10904-10910.

In Vitro Cell. Dev. Biol.—Animal 32:505–513, September 1996

1071-2690/96 $05.00 + 0.00

ENHANCED APOPTOSIS IN TRANSFORMED HUMAN LUNG FIBROBLASTS AFTER EXPOSURE TO SODIUM BUTYRATE

GRAHAM L. THOMAS, ANNA HENLEY, TAMI C. ROWLAND, ANIMESH SAHAI, MARTIN GRIFFIN, AND PAUL J. BIRCKBICHLER[1]

Oklahoma Medical Research Foundation, Noble Center for Biomedical Research, 825 NE 13th Street, Oklahoma City, Oklahoma 73104 (A. H., T. C. R., A. S., P. J. B.); and Department of Life Sciences, The Nottingham Trent University, Nottingham, England, NG11 8NS, UK (G. L. T., M. J. G.)

(Received 18 August 1995; accepted 21 December 1995)

SUMMARY

Simian virus-transformed human cells, WI-38 VA13A, showed a dose-dependent induction of apoptosis and reduction in cell numbers after exposure to sodium butyrate. Apoptosis was confirmed by ApopTag staining, isolation of apoptotic envelopes, and immunofluorescent staining with an antibody specific for apoptotic envelopes. Examination of the cell cultures by phase contrast and fluorescent microscopy revealed the presence of enlarged cells that displayed a more flattened morphology and morphological changes in the nucleus of cells exposed to sodium butyrate. Cell proliferation assays showed control and sodium butyrate cultures were synthesizing DNA and excluded any cytotoxic effects of sodium butyrate. Flow cytometry results indicated an increase in the number of aneuploid cells following sodium butyrate treatment. There was a decrease in the percentage of cells in C2/M in the diploid populations, but an increase in the percentage of cells in G2/M in aneuploid populations. This human *in vitro* model system suggests a mode of action for the therapeutic effects of sodium butyrate, which have been observed in the topical treatment of neoplastic cells and reversal of symptoms in ulcerative colitis: namely, the induction of apoptosis.

Key words: transglutaminase; differentiation; cell cycle; human cells.

INTRODUCTION

Sodium butyrate is a naturally occurring four-carbon fatty acid found in the diet and is often produced in the colon by the anaerobic breakdown of carbohydrates (47). It has been implicated in numerous cellular phenomena including cell growth and differentiation (33,34), and is becoming important in clinical studies for inducing differentiation in tumor cells both *in vivo* and *in vitro* (1,41). Sodium butyrate produced modifications in human tumors from several tissues (9,11,15,20,23,24,29,37,39,41), but the molecular mechanism of sodium butyrate's effect on cells has not been clarified.

Previous work from this laboratory has shown that exposure of simian virus-transformed human cells to sodium butyrate *in vitro* resulted in a concentration- and time-dependent increase in the cytosolic enzyme transglutaminase (7,35). Transglutaminases are a family of enzymes that require Ca^{2+} and a thiol-reducing agent in order to catalyze an acyl transfer reaction between peptide-bound glutaminyl moieties and various primary amines (21). When the primary amine is the ε-amino group of peptide-bound lysine, intermolecular ε-(γ-glutamyl)lysine isopeptide crosslinks are produced. Examples of physiological transglutaminase catalysis include fibrin clot stabilization, keratinocyte differentiation, and vaginal plug formation in rodents (21). We have reported that tissue transglutaminase was low in malignant tissues and in a variety of cells maintained in culture following viral or chemical transformation (4,5). An inverse relationship was found between metastatic spread and the level of tissue transglutaminase activity (3,14,25,31).

The role of transglutaminase in programmed cell death (apoptosis) has been established (16–18,30,32,40,46). Cells undergoing late stage apoptosis are thought to be stabilized by envelope formation through transglutaminase-mediated crosslinking and formation of an apoptotic envelope. This stabilization ensures that intracellular contents are not lost as the cell dies and negates the necessity for an immune response (28,50). Apoptosis is an energy-requiring process (10), and synthesis of new protein(s) is likely to be required for cell death to occur. Sodium butyrate is an agent that increases synthesis of messenger RNA for transglutaminase, which subsequently raises the level of catalytically active transglutaminase protein (7,35). In the following studies, we report that treatment of WI-38 VA13A cells with sodium butyrate leads to the induction of apoptosis. This human *in vitro* cell culture system offers a model to identify biomarkers for apoptosis in response to sodium butyrate.

MATERIALS AND METHODS

Cell culture. WI-38 VA13A (VA13A) human embryonic lung fibroblasts, a gift from Dr. V. J. Cristafalo of the University of Pennsylvania, Philadelphia, were maintained in T-flasks (Corning, Corning, NY) or chamber slides (Nunc, Inc., Naperville, IL) using McCoy's Medium 5a (GIBCO BRL, Grand Island, NY) supplemented with 10% (vol/vol) fetal bovine serum (FBS, Intergen,

[1] To whom correspondence should be addressed at Department of Urology, University of Oklahoma Health Sciences Center, 920 Stanton L. Young Blvd. 5SP330, Oklahoma City, OK 73190..

Purchase, NY), treated with sodium butyrate and enumerated as described previously (7). Cultures were negative for *Mycoplasma* by monthly testing (2).

Apoptotic index. The percentage of cells undergoing apoptosis was determined using the ApopTag kit (Oncor, Gaithersburg, MD) on total cell pools obtained by combining nonadherent and adherent cells from T-75 flasks. Nonadherent cells were collected from the culture medium by centrifugation at 2000 rpm for 5 min. Adherent cells were treated with 5 ml 0.05% (wt/vol) pronase, collected by centrifugation at 2000 rpm for 5 min and added to the nonadherent cell pellet. The combined pool of cells was resuspended in phosphate-buffered saline (PBS, 120 m*M* NaCl, 2.7 m*M* KCl, 10 m*M* NaH_2PO_4, pH 7.4), the number of cells was determined by trypan blue exclusion analysis, and the percentage of cells in apoptosis determined. At least 300 cells were counted in random fields throughout the slide and slides were prepared in duplicate. Apoptotic envelopes were isolated according to the method of Schmidt et al. (45). Briefly, cells were scraped into the growth medium and centrifuged at 2000 rpm for 5 min. The cell pellet was resuspended in 500 μl of PBS and 50 μl of 20% (wt/vol) sodium dodecylsulfate (SDS) and 5 μl of 100 m*M* dithiothreitol was added. The suspension was boiled for 5 min then cooled; 10 μg of DNAse I was added to prevent envelope clumping. The suspension was incubated for 1 h at room temperature and centrifuged at 13 500 rpm for 5 min to sediment a pellet of apoptotic envelopes. The apoptotic envelopes were resuspended in PBS and counted using a hemocytometer and a light microscope.

Cell cycle analysis. Adherent cells were washed twice with calcium-free Earle's solution, incubated in 10 ml of 10 m*M* ethylenediaminetetraacetic acid (EDTA, pH 7.4) for 1 h at 37° C, and detached from the T-75 flask by shaking. The resultant cell suspension was made homogenous by aspiration five times with a 10 ml pipette. The cells were pelleted by centrifugation at 2000 rpm for 5 min and resuspended in 0.4 ml calcium-free Earle's solution. One ml of 70% (vol/vol) ethanol was added drop-wise as a fixative. The cell suspensions were stored at 4° C until propidium iodide staining could be performed. On the day of flow cytometry analysis, all cell preparations were centrifuged and resuspended as single cells in 1.0 ml of calcium-free Earle's solution. To remove contaminating RNA, 5 μl of a 5 mg/ml stock solution of RNAse I was added and the mixture was incubated for 30 min at 37° C. The cell suspension was treated with 2 μl of propidium iodide (1.8 mg/ml in calcium-free Earle's solution), and incubated on ice for 5 min prior to analysis. Analysis was carried out on a Becton Dickinson FACS Scan flow cytometer (single population analysis) or an Orthocyte bench top cytometer (dual population analysis). A total of 20 000 excitation events were monitored and the data recorded. Post-run analyses were carried out using the CellFIT Cell-Cycle Program from Becton (Mountain View, CA) Dickinson Version 2.01.2 for single population analysis and MULTICYCLE DNA program for dual population analysis. A portion of the cells was visualized by examination under the fluorescent microscope.

Fluorescence and light microscopy studies. Cells for indirect immunofluorescence microscopy were maintained in chamber slides and processed 72 h after the addition of sodium butyrate. The medium was removed, the cells were washed twice with PBS and fixed with 4% (wt/vol) paraformaldehyde for 15 min at room temperature. The paraformaldehyde was removed and the cells were washed twice with PBS and permeabilized by incubation with absolute methanol for 30 min at −20° C. The fixed cells were washed twice with PBS and rabbit polyclonal antibody raised to SDS insoluble apoptotic envelopes was added. After incubation at 4° C overnight, the primary antibody was removed, the cells were washed with PBS, and biotin-labeled goat anti-rabbit secondary antibody was added. After incubation for 45 min at room temperature, the secondary antibody was removed, the slides were washed with PBS, and streptavidin-FITC conjugate was added. Biotin secondary antibody and streptavidin-FITC conjugate were used according to the manufacturer's instructions. The slides were examined on a Leitz Ortholux II (Leitz, Wetzlar, FRG) or Nikon Microphot FXA (Nikon, Garden City, NY) ultraviolet microscope fitted with a camera and appropriate filters. Photographs were taken on Ilford Delta Professional DX film using an exposure time of 1 min. Phase contrast photomicroscopy was performed using an Olympus CK-2 inverted microscope (Olympus Corporation, Woodbury, NY) fitted with an Olympus DM-4T camera and automatic exposure.

Other methods and reagents. Proliferating cells were identified by thymidine labeling (6) and DNA was stained with bis-benzimide (27) using published procedures. Protein was determined by the method of Lowry et al. (36) using the BioRad protein assay kit (BioRad Laboratories, Hercules, CA). Statistical analyses were performed using Student's *t*-test. Pronase, dithiothreitol, biotin-labeled secondary antibodies, and streptavidin-FITC were purchased from Calbiochem (San Diego, CA); PBS, bis-benzimide (Hoechst No. 33342), EDTA, RNAse I, and propidium iodide were purchased from Sigma Chemical Co. (St. Louis, MO); SDS, DNase I from GIBCO; sodium butyrate, trypan blue from Matheson, Coleman and Bell (Norwood, OH); paraformaldehyde from Aldrich Chemical Co. (Milwaukee, WI); and methanol from Fisher Scientific Co. (Pittsburgh, PA).

Results and Discussion

Significant differences in cell numbers were seen between sodium butyrate-treated cells and control cells 48 h after the addition of sodium butyrate (Fig. 1 *A*). Cell numbers increased in control cultures during this time while cell numbers remained relatively constant in the butyrate-treated cultures. Over the next 72 h, the number of cells in the sodium butyrate-treated cultures increased except in cultures exposed to 5 m*M* sodium butyrate. Because of this differential growth behavior of the cultures, we concentrated our studies within 72 h of the addition of sodium butyrate. Cells exposed to sodium butyrate generally exhibited a more flattened and elongated appearance within 24 h of the addition of sodium butyrate (data not shown). This effect was concentration dependent.

DNA synthesis was evident in all cultures during the 72 h after the addition of sodium butyrate (Fig. 1 *B*). The incorporation of radiolabeled thymidine was lower in the butyrate-treated cells when compared to control cultures receiving no sodium butyrate at each time period studied. Thymidine incorporation decreased progressively in all cultures during the 72 h exposure to sodium butyrate, and the decrease was concentration dependent. Seventy-two hours after the addition of sodium butyrate, the thymidine incorporations were 46%, 16%, 11%, and 1% for control, 1 m*M*, 2 m*M*, and 5 m*M* sodium butyrate cultures compared to the 24 h control culture receiving no sodium butyrate. The thymidine incorporation data are consistent with the cell numbers reported in Fig. 1 *A*. The trend in cell proliferation evidenced by the incorporation of radiolabeled thymidine was confirmed using the Amersham (Arlington Heights, IL) Cell Proliferation kit (data not shown).

Seventy-two hours after the addition of sodium butyrate, the percentage of cells undergoing apoptosis was three to eight times higher in the butyrate-treated cultures when compared to control cultures (Table 1). The difference between butyrate and control cultures increased as the sodium butyrate concentration increased. The characteristic laddering of DNA arising as a consequence of endonuclease activity was evident in the nonadherent cell populations from butyrate-treated cultures, but DNA laddering was not seen in either adherent control or adherent sodium butyrate-treated cell populations (data not shown). Similar results have been reported by other investigators (22,23).

Butyrate-treated cells showed morphologic changes in the nucleus characteristic of apoptosis. More of the nuclei in sodium butyrate-treated cells were irregular in shape and larger than nuclei from control cells when examined microscopically after staining DNA with bis-benzimide (Fig. 2). The number of apoptotic envelopes was higher in butyrate-treated cultures than in cultures receiving no butyrate (Table 1). Both sodium butyrate-treated and control cells showed the presence of immunoreactive material to a polyclonal antibody raised against detergent insoluble apoptotic envelopes (Fig. 3 *A*). The number of cells staining with the antibody was less in control cultures compared to the butyrate-treated cultures. Cells with irregular shapes and dark, pitted structures stained with the antibody to apoptotic envelopes, but cells with normal morphology did not react

with the antibody (Fig. 3 *B*). Nonimmune serum showed no staining for apoptotic envelopes in either control cells or sodium butyrate-treated cells (data not shown). These observations are consistent with the greater number of apoptotic envelope counts seen in the butyrate-treated cells compared to control cultures (Table 1). The percentage of apoptotic envelopes was considerably lower than the percentage of cells observed undergoing apoptosis by the ApopTag method. One reason for this difference may be that in culture there is a range or window of progression of apoptosis. With ApopTag, we saw the complete range, whereas, with the apoptotic envelope counts, we only had one final endpoint: insolubility in SDS.

The apoptotic envelope is rendered insoluble to chaotrophic agents by the action of transglutaminase-mediated crosslinking (17). In previous studies, we observed an induction of transglutaminase in VA13A cells following treatment with sodium butyrate (7,35). In the current studies, transglutaminase activity was monitored in selected experiments and found to increase 20–30-fold in cultures exposed to sodium butyrate when compared to samples receiving no sodium butyrate (data not shown). The lower recovery of apoptotic envelopes compared to the values seen with ApopTag may thus reflect the degree of crosslink formation catalyzed by transglutaminase. It may be that only the terminal apoptotic bodies that would be phagocytized *in vivo* are the ones that resisted solubilization by SDS in this study. Nonetheless, the observation of fluorescent staining with apoptotic-specific antibody (Fig. 3 *A*) clearly shows the presence of apoptotic envelopes, a catalyzed product of transglutaminase in the cultures, and provides evidence for transglutaminase involvement in this system.

Initial analysis of the cells using the single population algorithm suggested that treatment with sodium butyrate synchronized the cell into G2/M (control, 32%; 1 m*M* sodium butyrate, 33%; 2 m*M* sodium butyrate, 57%). Microscopic examination of the cells and proliferation data (Fig. 1) did not confirm accumulation of cells into G2/M. In a separate experiment, the cell cultures were examined using an algorithm for both diploid and aneuploid cell populations. This analysis showed the presence of both diploid and aneuploid populations in the cell culture (Table 2). The percentage of diploid cells entering the G2/M mitotic phase of the cell cycle decreased in the sodium butyrate-treated cultures (control, 18.1%; 1 m*M* sodium butyrate, 5.4%; 2 m*M* sodium butyrate, 10.8%), whereas the percentage of aneuploid cells entering G2/M following sodium butyrate treatment increased (control, 0.7%; 1 m*M* sodium butyrate, 2.0%; 2 m*M* so-

TABLE 1

MEASURE OF APOPTOSIS IN VIRUS TRANSFORMED HUMAN FIBROBLAST CELLS AFTER A 72-H EXPOSURE TO SODIUM BUTYRATE

Sample	Percent Apoptotic Cells[a]	Apoptotic Envelopes per Million Cells[b]
Control	2.4 ± 0.3 (6)[c]	104 ± 4 (3)
1 m*M* Butyrate	7.3 ± 1.8 (4)[d]	160 ± 12 (3)[d]
2 m*M* Butyrate	13.5 ± 2.5 (6)[d]	195 ± 24 (3)[d]
5 m*M* Butyrate	18.4 ± 5.3 (5)[d]	N.D.[e]

[a] ApopTag kit.
[b] Counted manually with hemocytometer.
[c] Mean ± SEM with the number of determinations in parenthesis.
[d] Significantly different from control $P \leq 0.05$.
[e] Not determined.

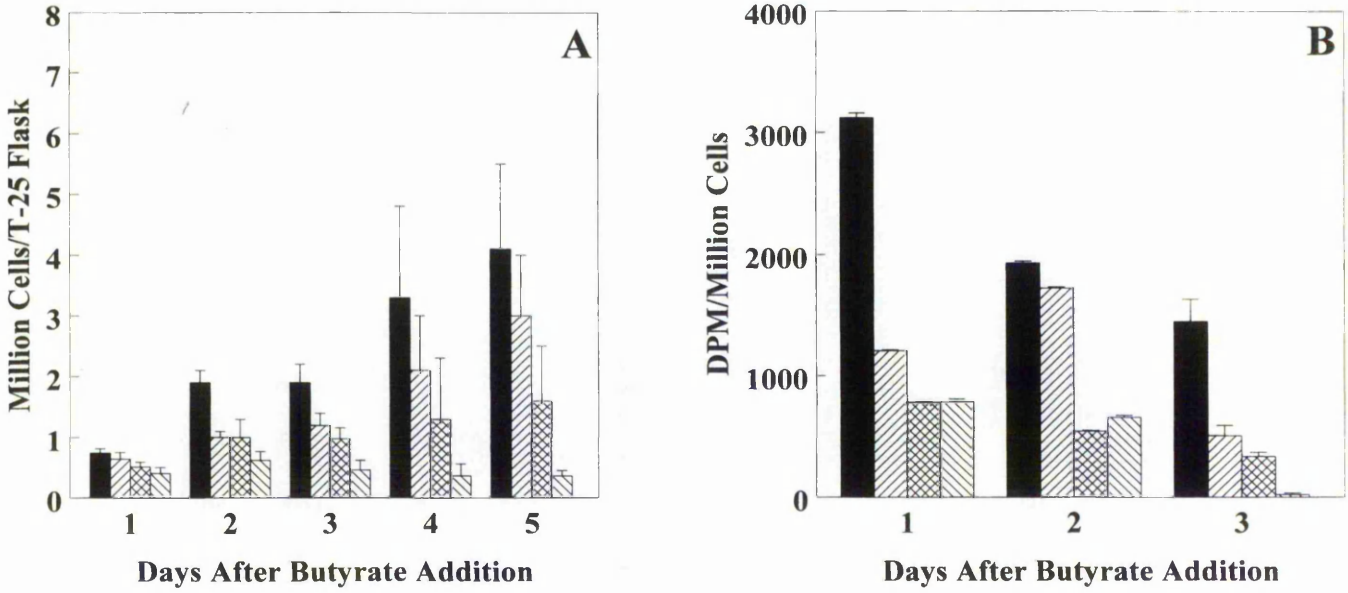

FIG. 1. Effect of sodium butyrate on cell growth and DNA synthesis in WI-38 VA13A cells. Cultures were inoculated at 30–40 000 cells/cm² and 48 h later exposed to various concentrations of sodium butyrate. The cultures were maintained on the appropriate mediums for various time periods with total medium replenishment occurring every 48 h. At the indicated times, cells were harvested for cell counts (*A*) or DNA synthesis by incorporation of thymidine (*B*) as described under "Materials and Methods." Control, no sodium butyrate (■), 1 m*M* sodium butyrate (▨), 2 m*M* sodium butyrate (▩), 5 m*M* sodium butyrate (▧). Data represent the means for three to six experiments with samples in duplicate. *Bars*, SEM.

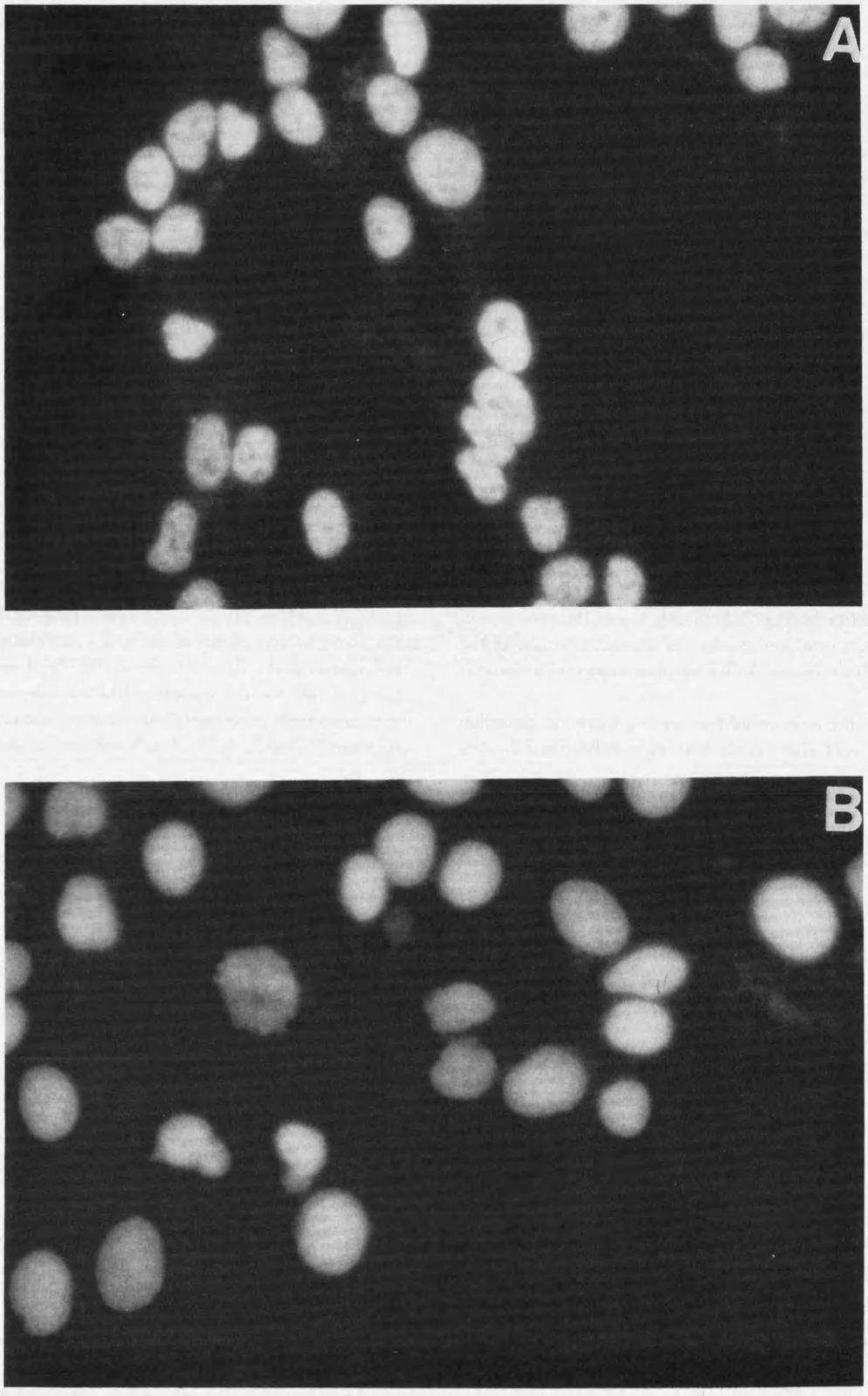

FIG. 2. Effect of sodium butyrate on morphology of nuclei in WI-38 VA13A cells. Cultures were inoculated at 30–40 000 cells/cm^2 and 48 h later exposed to various concentrations of sodium butyrate. The cultures were maintained on the appropriate mediums for 48 h and then stained with bis-benzimide as described under "Materials and Methods." *A*, control, no sodium butyrate; *B*, 2 m*M* sodium butyrate. Magnification = ×62.5.

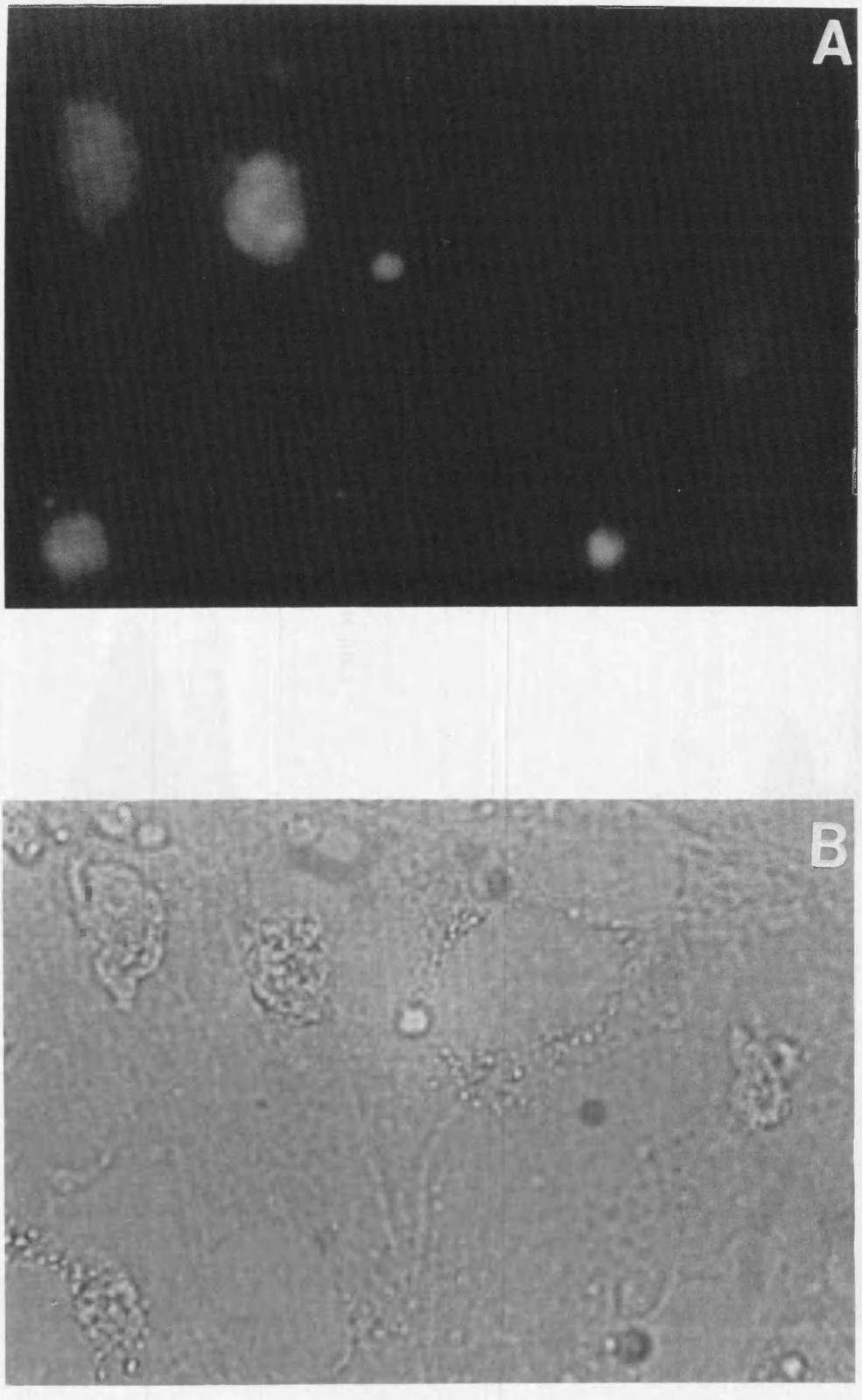

FIG. 3. Immunofluorescent staining for apoptotic envelopes in WI-38 VA13A cells. Cultures were inoculated at 30–40 000 cells/cm² and 48 h later exposed to various concentrations of sodium butyrate. The cultures were maintained on the appropriate mediums for 48 h and then processed for apoptotic envelopes by indirect immunofluorescence microscopy as described under "Materials and Methods." *A*, 2 m*M* sodium butyrate, rabbit anti-apoptotic envelope antibody; *B*, phase contrast photo of same field as *A*. Magnification = ×62.5.

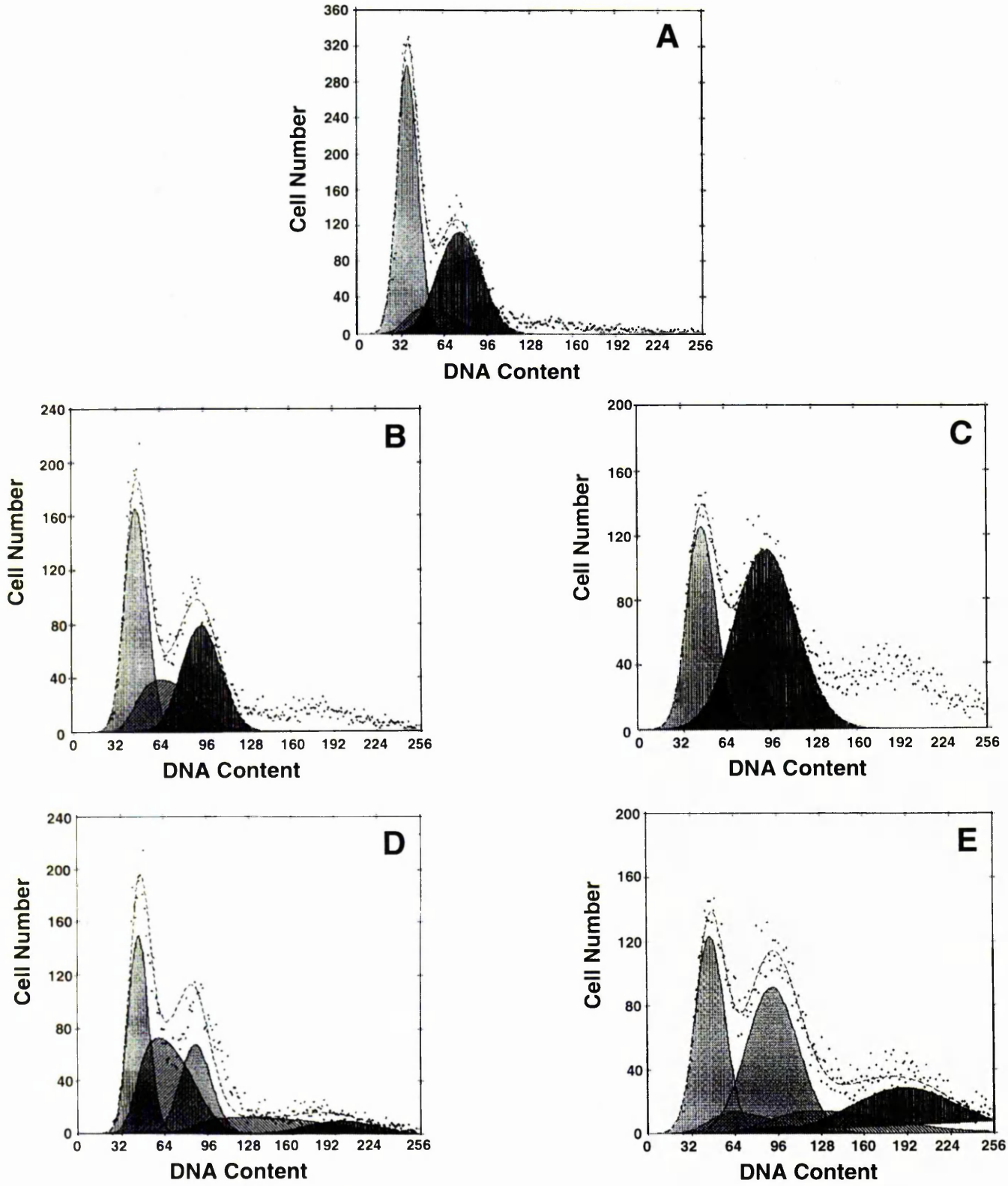

FIG. 4. DNA histogram of WI-38 VA13A cells. Cells were processed, stained with propidium iodide, and analyzed by flow cytometry as described under "Materials and Methods." *A*, Control, no sodium butyrate; *B*, 1 m*M* sodium butyrate, 72 h, analyzed by single population algorithm; *C*, 2 m*M* sodium butyrate, 72 h, analyzed by single population algorithm; *D*, 1 m*M* sodium butyrate, 72 h, analyzed by double population algorithm; *E*, 2 m*M* sodium butyrate, 72 h, analyzed by double population algorithm.

TABLE 2

CELL CYCLE ANALYSIS OF VIRUS TRANSFORMED HUMAN FIBROBLAST CELLS AFTER A 72-H EXPOSURE TO SODIUM BUTYRATE

	Percent Diploid			Percent Aneuploid		
Sample	G0/G1	S	G2/M	G0/G1	S	G2/M
Control	16 ± 5[a]	35 ± 12	18 ± 6	17 ± 6	13 ± 5	1 ± 1
1 m*M* Butyrate	32 ± 1	25 ± 3	6 ± 3	22 ± 2	13 ± 3	2 ± 1
2 m*M* Butyrate	23 ± 4	21 ± 1	11 ± 2	25 ± 4	16 ± 3	4 ± 2

[a] Mean ± SEM for three experiments.

dium butyrate, 3.6%). The distribution of diploid and aneuploid cells following sodium butyrate treatment can be seen more clearly in representative flow cytometry histograms (Fig. 4).

Other investigators have reported that sodium butyrate generated giant cells that were removed from the cell cycle, but that continued to produce DNA, RNA, and proteins (26,38,49). Furthermore, we have shown via (a) the ApopTag kit, (b) morphological changes in the nucleus, (c) isolation of apoptotic envelopes, and (d) immunofluorescent staining with an antibody specific for apoptotic envelopes that the percentage of cells undergoing apoptosis in the culture increased. From the current studies, we cannot tell whether the apoptotic cells came from the diploid populations, the aneuploid populations, or both. We show in this study that the nuclei of cultures treated with sodium butyrate were measurably larger than the nuclei of the control population (Fig. 2). DNA index values suggested that the aneuploid cells had twice the amount of DNA (control, 1.9; 1 m*M* sodium butyrate, 2.0; 2 m*M* sodium butyrate, 2.1): a finding consistent with the nuclei staining and cellular morphology. Staining did not show these larger cells were binucleate or undergoing mitosis (Fig. 2).

In summary, the flow cytometry analysis showed that the starting culture of transformed WI-38 VA13A was a mixed population of both diploid and aneuploid cells. The diploid cells appeared to have a normal cell cycle distribution. Following treatment with sodium butyrate, total cell numbers decreased, but the percentage of aneuploid cells in the culture increased. Thymidine uptake and bromodeoxyuridine (BrdU) proliferation assays demonstrated that the sodium butyrate-treated cultures were not experiencing cytotoxic effects at the stated concentrations of the topical agent. This data suggests to us that some cells were traversing the cell cycle more slowly or possibly undergoing cell cycle arrest while continuing to synthesize DNA.

We suggest that in addition to inducing apoptosis, sodium butyrate inhibited cell proliferation and altered cell morphology consistent with cell differentiation (15,26,29,33,44). The reason for the dual pathways of apoptosis and differentiation remains the basis for future studies. The fact that in previous studies transglutaminase activity remained elevated for 5–7 d in the sodium butyrate-treated cells (7,35,48) suggests that transglutaminase also plays a role in cells suspected of undergoing differentiation. It cannot be ruled out from these studies that the cells that became enlarged will not undergo apoptosis at a later time.

In the studies reported here, we have shown an induction of apoptosis in VA13A cells following exposure to sodium butyrate. This induction correlates with reported increases of transglutaminase in the final stages of apoptosis (16–18,30,32,40,46). Reports have shown induction of apoptosis is closely related to topical sodium butyrate treatment (8,23). In cases of ulcerative or acute colitis, the cells of the intestinal lumen are highly inflamed. Following treatment with sodium butyrate enemas, the patients responded and the inflammation was reduced (42,43,44). Independent studies have shown that transglutaminase and sodium butyrate play a role in ulcer healing in rats suffering from ulcerative colitis (12,13). Cells taken from the intestinal lumen or colonic cancer cells grown *in vitro* showed morphological and biochemical characteristics typical of apoptosis following topical sodium butyrate treatment (23,29,37,39,42).

The aim of this study was to show that sodium butyrate might be used to alleviate diseased tissues by inducing apoptosis or differentiation. Evidence for transglutaminase involvement in the current study included isolation of increased amounts of apoptotic envelopes (Table 1) and immunofluorescent staining with antibody to apoptotic envelopes (Fig. 3). In an effort to further delineate the contribution of transglutaminase to the apoptosis pathway, transfection of VA13A cells with cDNA for transglutaminase and protooncogenes involved in apoptosis (e.g., bcl_2) are currently in progress. One of the reported results of treatment of VA13A cells with sodium butyrate is an increased expression of SV40 large-T and small-T antigens and down-regulation of p53 (19). These events occur early after addition of sodium butyrate and their relationship to the induction of apoptosis or transglutaminase in these cells must await further experimentation.

In summary, our results suggest a mode of action for the therapeutic effects of sodium butyrate seen in the topical treatment and reversal of symptoms in ulcerative colitis and neoplastic growth. The biochemical and molecular mechanism(s) by which sodium butyrate orchestrates this response is currently under investigation. The human *in vitro* cell culture system studied here offers a model system not only to study the efficacy of sodium butyrate as a chemotherapeutic agent, but it also offers the potential to identify biomarkers for apoptosis and possibly differentiation in response to sodium butyrate. Such studies could lead to beneficial therapeutic treatment not only in inflammatory bowel disease but also in prostate and other types of cancer.

ACKNOWLEDGMENTS

The authors thank Ms. Viji Dandapani for her technical assistance with the flow cytometry, Dr. John Lawry for the dual population cell cycle analysis, Dr. C. R. L. Knight for providing the apoptotic envelope antibody, Dr. K. E. Achyuthan for critical review of the manuscript, and Ms. Laura Smith for